

Bio-based Crotonic Acid Production from Wastewater

Vahideh Elhami

Bio-based Crotonic Acid Production from Wastewater

PROEFSCHRIFT

Ter verkrijging van
de graad van doctor aan de Universiteit Twente,
op gezag van de rector magnificus,
Prof. dr. ir. A. Veldkamp,
volgens besluit van het College voor Promoties
in het openbaar te verdedigen
op vrijdag 14 April 2023 om 16:45 uur

door

Vahideh Elhami

Geboren op 06 September 1989
Marand, Iran

Dit proefschrift is goedgekeurd door:

de promotoren:

Prof. dr. ir. B. Schuur

Prof. dr. G.J. Vancso

Co-promotor:

dr. M.A. Hempenius

Cover design: Gildeprint B.V.

printed by: Gildeprint B.V.

ISBN: 978-90-365-5599-9

DOI: 10.3990/1.9789036555999

URL: <https://doi.org/10.3990/1.9789036555999>

Copyright © 2023 Vahideh Elhami, The Netherlands. All rights reserved. No part of this book maybe reproduced, stored in a retrieval system or transmitted in any form or by any means without permission of the author. Alle rechten voorbehouden. Niets uit deze uitgave mag worden vermenigvuldigd, in enige vorm of op enige wijze, zonder voorafgaande schriftelijke toestemming van de auteur.

Promotiecommissie:

Voorzitter:	prof.dr. J.L. Herek	Universiteit Twente
Promotor:	Prof.dr.ir. B. Schuur	Universiteit Twente
	Prof.dr. G.J. Vancso	Universiteit Twente
Co-Promotor:	dr. M.A. Hempenius	Universiteit Twente
Leden:	Prof.dr.ing. M.B. Franke	Universiteit Twente
	Prof.dr.ir. R.G.H. Lammertink	Universiteit Twente
	Prof.dr. R. Wickramasinghe	University of Arkansas
	Prof.dr.-Ing N. Kockmann	Technical University of Dortmund
	dr. J. Sousa	Paques Biomaterials B.V.

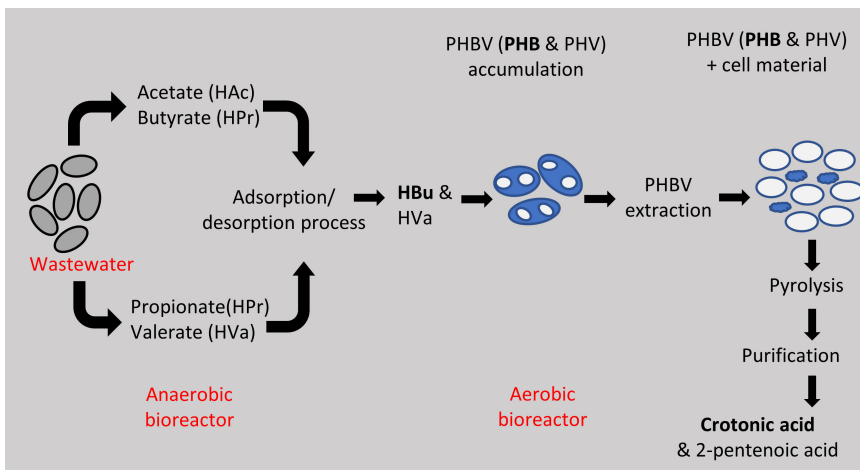
Dedicated to my beloved family

Contents

Chapter1: General Introduction and Literature Review.....	1
Chapter 2: Methacrylonitrile-based Adsorbents for Recovery of Volatile Fatty Acids from Fermentation Broth.....	39
Chapter 3: Recovery of Dilute (Bio-Based) Volatile Fatty Acids by Adsorption with Magnetic Hyperthermal Swing Desorption	59
Chapter 4: Extraction of Low Molecular Weight Polyhydroxyalkanoates from Mixed Microbial Cultures using Bio-based Solvents	97
Chapter 5: Crotonic Acid Production by Pyrolysis and Vapor Fractionation of Mixed Microbial Culture-based Poly(3-hydroxybutyrate-co-3-hydroxyvalerate)(PHBV).....	133
Chapter 6: Separation of Crotonic Acid and 2-Pentenoic Acid obtained by Pyrolysis of Bio-based Polyhydroxyalkanoates using a Spinning Band Distillation Column.....	161
Chapter 7: Conclusions and Prospective.....	191
Appendices	207

Chapter 1

General Introduction and Literature Review



A part of this chapter has been published:

Elhami, V.; Antunes, E.C.; Temmink, H.; Schuur, B., “*Recovery Techniques Enabling Circular Chemistry from Wastewater*”, **Molecules**, **2022**, 27.

1. Motivation

This thesis is about valorization of the chemicals in wastewater, thereby providing an approach for wastewater remediation and as well opening an avenue towards renewable chemicals. For me, this topic is of importance, because I grew up in Iran while witnessing its extreme struggles with global warming, water shortage, and environmental issues mainly associated to the waste/wastewater of the industries. Not only Iran, but many countries face these problems these days. To contribute to maintaining a habitable earth for the next generations, I am eager to contribute to any project aiming to develop sustainable and eco-friendly technology. During my master assignment, I worked on preparing a catalyst for wastewater treatment. For the PhD thesis, I was keen on functioning in this project which aims to utilize waste/wastewater and contribute to developing a circular economy value chain. The value chain addressed in this thesis is producing Polyhydroxyalkanoates (PHAs), trans-crotonic acid (CA) and 2-pentenoic acid (2-PA), PHAs being bio-plastics and CA and 2-PA being monomers for bio-based plastics.

Currently, there is a remarkable growing demand for renewable and environmentally sustainable chemical production pathways, due to the limited supply of the fossil fuel-based materials and their associated environmental issues. Figure 1-1 illustrates the linear and circular economy approaches to produce the fossil based plastics in general. CO₂ emission is one of the main challenges in production and incineration of the oil-based plastics and, it is estimated to reach 56 billion tons of CO₂ per year in 2050 [1]. Although recycling of the plastic can reduce CO₂ emission to some extent, this approach is in its early stages tackling the difficulties due to the

complexity of the plastic waste. Therefore, developing bio-based pathways towards bio-plastics is being investigated in parallel with plastic recycling. This approach can go through two routes. One is to obtain raw materials from the renewable and bio-based sources which is expressed as “Bio-refinery”. Another one is to replace the petrochemical-based plastics with bio-plastics with similar properties.

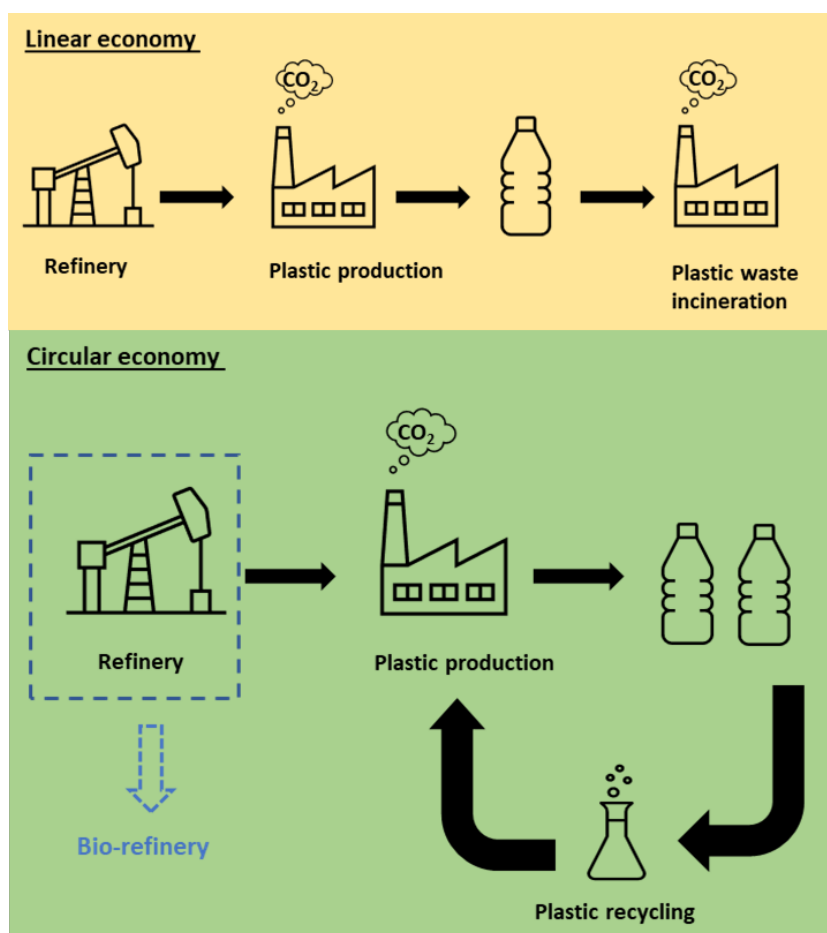


Figure 1-1. Schematic view of linear and circular economy approaches for plastic production

PHAs are one of the well-studied bio-polymers which can be produced from vegetable oil, starch proteins and different types of biomass [2]. Poly(3-hydroxybutyrate-co-3-hydroxyvalerate) (PHBV) co-polymer is the predominant type of PHA which can be obtained through waste fermentation. It consists of two monomers namely hydroxybutyrate (HB) and hydroxyvalerate (HV) [3]. Polymers with a low HV content < 10% are hard and brittle resembling unplasticized polyvinyl chloride (PVC), mid range HV content(10-25%) materials maintain a good balance of toughness and resemble polypropylene (PP), whilst high HV content (25-40%) PHBVs are soft and tough having a polyethylene (PE) like feel [4].

Next to the use of PHA, an alternative route towards value-added chemicals is through the pyrolysis of the PHAs, which results in 2-alkenoic acids. For instance, trans-2-butenoic acid or CA and 2-PA can be produced by depolymerization of PHBV. CA and its esters have a wide range of application in various industries [5]. However, its current production pathway is neither straightforward nor renewable which includes many synthesis and purification steps. Therefore, providing sustainable and renewable pathways is essential to enhance the market of these platform chemicals and reduce CO₂ emission associated to their petrochemical production routes.

Figure 1-2 represents an overview of the entire project, starting with waste/wastewater towards CA and 2-PA production. It is a multistep process, including anaerobic digestion of waste/wastewater to produce VFAs, followed by recovery of these VFAs from the fermentation broth using an adsorption-desorption technique. Afterwards, the VFAs are fed into an aerobic bio-reactor in which the microorganisms convert them into PHBV.

The intracellular PHBV is afterwards extracted by a solvent extraction approach and pyrolyzed towards CA and 2-PA.



Figure 1-2. An overview of the process to produce CA from waste/wastewater

In this chapter, the general introduction and literature review for each individual step is given as following sections:

2. Volatile fatty acids (VFAs) from wastewater

Short-chain carboxylic acids, so called VFAs are used in a wide range of industries producing products such as polymers, food, chemicals, and agriculture [6]. Figure 1-3 summarizes the application of the VFAs obtained by mixed microbial culture (MMC) using waste/wastewater as a feedstock [6-8]. VFAs are used as a building block in manufacturing pesticides, rubber, paint, plastics, and polymers, and can also be used as a preservative and

flavor in food and beverage industries [8,9]. Among them, acetic acid experienced a global market demand of about 15.924 kiloton in 2020 and it is estimated that the demand will increase with a compound annual growth rate (CAGR) of 5% from 2021 until 2026 [10]. 90% Of its global market is supplied by chemical synthesis from petroleum feedstocks which is mainly methanol carbonylation [11].

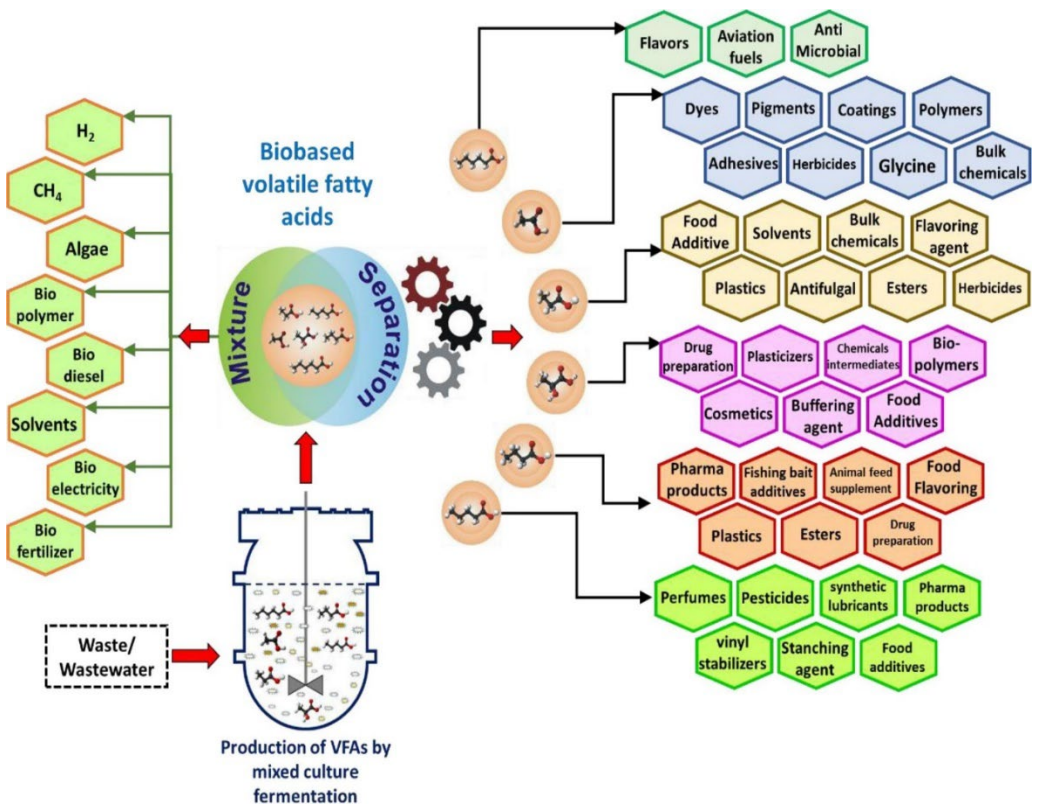


Figure 1-3. Scope and application of bio-based volatile fatty acids described in [6]

The bio-based VFAs can be obtained via the fermentation of a carbon source such as glucose, xylose, sucrose, etc. Fermentation can occur either in pure

cultures or in mixed cultures. The former requires sterile conditions to grow a mono-culture, containing a single species of microorganism which are then fed with pure substrates such as glucose. Therefore, this biological pathway cannot economically compete with the petrochemical routes due to its low productivity and high manufacturing cost [8]. To improve competitiveness, researchers have focused on providing an inexpensive bio-based alternative which is mainly fermentation of an organic-rich waste/wastewater using MMC [12-15].

MMC is preferred over the pure cultures as it does not require sterile conditions and enables to apply an inexpensive carbon-rich waste as a feedstock such as whey, biomass, food waste (FW), sewage sludge (SS) and organic fractions of municipal solid waste (OFMSW) [15,16]. SS from municipal wastewater treatment plant (WWTP) and FW are the most abundant organic wastes with an annual production of about 11×10^9 and 2×10^9 metric tons, respectively [17]. Due to their high organic content, they are the optimal candidates to be used as a carbon source for the microorganisms. Besides FW and SS, various solid and liquid wastes have been researched for VFA production including municipal solid waste, palm and olive oil, wood and paper mill effluent and dairy wastewater [12,16].

In MMC, the conversion of an organic substrate takes place gradually by different microorganisms which results in a complicated microbial ecosystem with a versatile metabolic capacity. Figure 1-4 illustrates the possible fermentation pathways that can occur in MMC. First, the hydrolytic microorganisms hydrolyze the complex biodegradable organics in the waste to their corresponding simple monomers, followed by acidogenic fermentation of these monomers into VFAs, called primary fermentation

[16]. Afterwards, the VFAs can either be separated from the fermentation broth or undergo several secondary fermentation pathways to produce methane, syngas, alcohol and medium chain carboxylic acids (MCCAs).

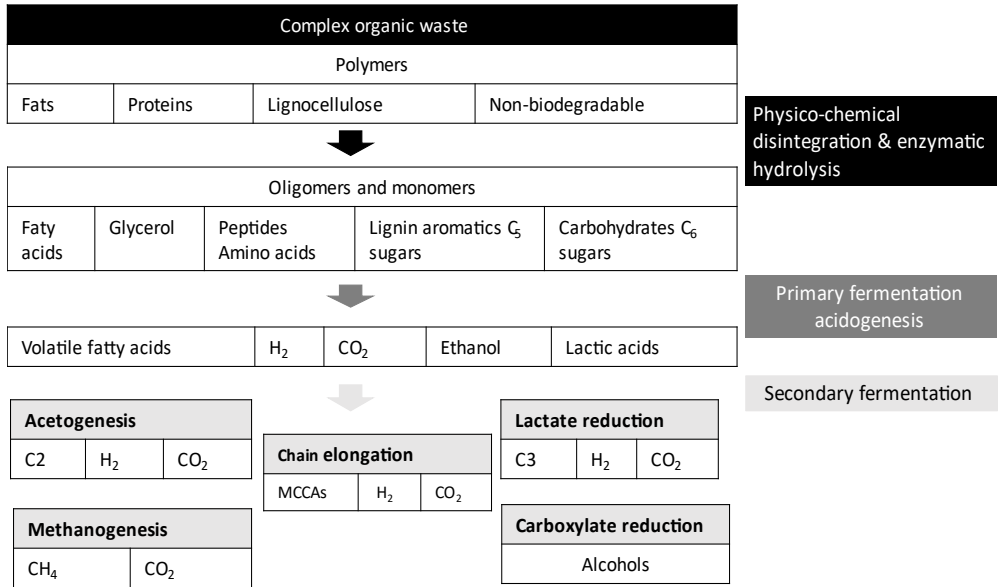


Figure 1-4. Possible fermentation pathways in mixed microbial culture (MMC) [18]

The acid content of the fermentation broth, obtained by waste digestion is reported to be about only 1 wt% as a result of the limited carbon content of waste/wastewater [19]. From an economic point of view, the separation method must thus be highly selective towards the acids over water. This selectivity can be achieved by affinity separation techniques which enable to recover a target compound from a relatively complex mixture. The main affinity separation techniques which have been applied to recover VFAs from the fermentation broth include liquid-liquid extraction [20-23], adsorption

[19,24,25] and membrane assisted separations [26-28]. Liquid-liquid extraction of the carboxylic acids from a fermentation broth is well studied [23], with traditional solvents [20], ionic liquids (ILs) [21] and, deep eutectic solvents [22,29]. ILs are preferred due to the higher distribution than traditional organic solvents at highly diluted acid streams. However, the regeneration of ILs is still challenging [30]. Alternatively, membrane-based separations are feasible techniques to concentrate the acids to some extent. These methods can even provide in-situ separation of the VFAs from the fermentation broth and prevent inhibitory impact of the VFAs on the metabolism of the microorganisms and increase the acid production yield [31]. However, each of these methods bears some limitations towards application as a stand-alone economically viable separation technique to recover VFAs. The main drawbacks associated with the various membranes are membrane fouling, high energy demand, and not being selective enough towards VFAs in the complex mixture of the fermentation effluent. Furthermore high cost of membrane maintenance and replacement hinders economy of operation [32].

Adsorption is one of the affinity separation methods which has shown great potential to effectively recover VFAs from dilute solutions [19,24,25]. Depending on the physicochemical nature of the adsorbent and fermentation effluent, a high selectivity towards VFAs in the complex solutions can be achieved by adsorption. Adsorption is a surface-based process involving the adhesion of a compound from a liquid or gas to a surface [8]. The efficiency of an adsorption process depends on the physicochemical properties of both the adsorbate and the adsorbent, as well as on the fluid phase properties. Surface chemistry, pore size and internal

surface area are the relevant characteristics of an adsorbent which directly influences its capacity. The adsorption potential of a VFA on a specific solid matrix is defined as the equilibrium VFA loading (q_{VFA}) on the resins as function of the equilibrium aqueous phase concentration, which is expressed as:

$$q_{VFA}[g_{VFA}/kg_{resin}] = f([VFA]_{eq}) \quad (1-1)$$

Where $[VFA]_{eq}$ is the concentration of the VFA in the aqueous phase at equilibrium. Depending on the concentration, q_{VFA} may be in the linear regime [33], but often multiparameter isotherms are applied to describe the loading as function of the concentration. Higher loadings indicate stronger interaction between the adsorbent and the solute. Various solid matrixes have been employed to recover VFAs from a dilute aqueous solution. Among them, non-functionalized styrene-divinylbenzene based copolymer with commercial name of Lewatit VP OC 1064 MD PH has shown a great potential to adsorb the VFAs from a complex mimicked fermentation broth [19,34]. It can attract undissociated carboxylic acids by physical interactions such as hydrophobic interaction between the acid hydrocarbon chain and solid matrix and hydrogen bond- interaction between their carboxyl groups and the aromatic ring of the adsorbent (see Figure 1-5) [19].

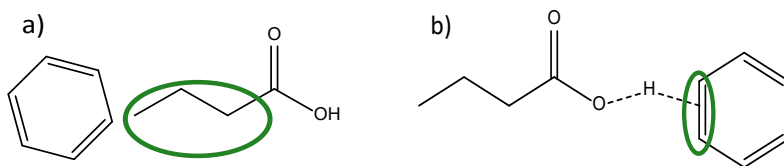


Figure 1-5. Possible interactions between a non-functionalized hydrophobic adsorbent and VFAs

A total VFA capacity of 76 g/kg is reported for non-functionalized styrene-divinylbenzene based adsorbent at an aqueous concentration of only 1 wt% total VFA loading [19]. This adsorbent is gaining more interest as it facilitates to selectively recover the acids in their undissociated form from a complex stream which contains mineral acids and salts as well. Moreover, a complete regeneration of the adsorbent is possible via thermal desorption without reducing the capacity of the adsorbent [19]. Reyhanitash et al. examined the application of a temperature program by hot nitrogen stripping, to directly fractionate the loaded acids during regeneration of the adsorbent [19]. It was found that indeed it is possible to recover the acids in high purity by applying a proper temperature profile based on the boiling point of the loaded components. The highest boiling of the VFAs in the mixture, butyric acid, was obtained in concentrations up to 90 wt% while its initial concentration in the feed was 0.25 wt%. Nonetheless, the quantity of the recovered acids in the most concentrated samples was not so high, because water physically fills the pores of the resin during adsorption and evaporates in earlier stages in thermal desorption due to its lower vapor pressure than the acids. The acid concentration in the condensed vapor recovered from the desorption continuously increases, meaning that it evaporates already partially in earlier stages. As a result, a large fraction of the acids has been co-desorbed during removal of water from the pores. Recently, Fufachev et al. [34] also applied non-functionalized PS-DVB resin to recover the volatile acids from the fermentation broth and convert them to ketones. The excess amount of water in the condensate deactivated the catalyst and decreased the efficiency of the ketonization reaction. Thus, to reduce the water content in the final condensate, they subjected the particles to a drying step at 70 °C

prior to thermal desorption. Although it facilitated to remove 80% of total water, up to 40% of the loaded acids were removed as well [34].

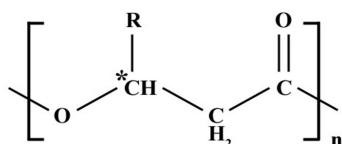
The current study aims at seeking other possible polymeric resins with acid loading capacities comparable to Lewatit VP OC 1064 MD PH. Furthermore, the main focus was on enhancement at the fractionation during thermal desorption to obtain larger amounts of acids with high concentrations. The heat diffuses from the surface of the resin into its core by hot nitrogen stripping. The heat-insulating character of polystyrene-based resins which results in a temperature gradient inside the particles that hinders sharper fractionation, because this gradient is in the opposite direction of the concentration gradients. In the present work, we describe the synthesis and application of new polymeric adsorbents, mainly a novel non-functionalized adsorbent that may heat particles from inside to facilitate separation of water and the acids during thermal desorption. Consequently, recovering the VFAs in highly concentrated form might be achieved.

3. Bio-based polyhydroxyalkanoates (PHAs)

PHAs are bio-polyesters that function as energy reserve, ensuring the long-term survival of the bacteria during nutrient scarce conditions [35,36]. The general structure of the PHA is shown in Figure 1-6. PHA consists of (R)-hydroxy fatty acids ranging between 600 - 35000 units length, where R is typically an unsaturated alkyl group [37]. Depending on the total carbon atoms within the monomer, they can be categorized into three groups. First being short chain length PHA (SCL-PHA) , consisting of 3-5 carbon atoms like C₄ poly(3-hydroxybutyrate) and C₅ poly(3-hydroxyvalerate). Second

being medium chain length PHA (MCL-PHA) which have between 6-14 carbon atoms, and long chain length PHA (LCL-PHA) which is the third and have more than 15 carbon atoms [38].

So far, over 150 types of PHA monomers have been discovered. Polyhydroxybutyrate (PHB) which is a SCL-PHA, is the most common type of PHAs, discovered by Lemoigne in 1926, whilst he observed the granules inside a gram-positive bacterium [39,40].



Poly(3-hydroxyalkanoate)

R group	Carbon no.	PHA polymer
methyl	C ₄	Poly(3-hydroxybutyrate)
ethyl	C ₅	Poly(3-hydroxyvalerate)
propyl	C ₆	Poly(3-hydroxyhexanoate)
butyl	C ₇	Poly(3-hydroxyheptanoate)
pentyl	C ₈	Poly(3-hydroxyoctanoate)
hexyl	C ₉	Poly(3-hydroxynonanoate)
heptyl	C ₁₀	Poly(3-hydroxydecanoate)
octyl	C ₁₁	Poly(3-hydroxyundecanoate)
nonyl	C ₁₂	Poly(3-hydroxydodecanoate)
decyl	C ₁₃	Poly(3-hydroxytridecanoate)
undecyl	C ₁₄	Poly(3-hydroxytetradecanoate)
dodecyl	C ₁₅	Poly(3-hydroxypentadecanoate)
tridecyl	C ₁₆	Poly(3-hydroxyhexadecanoate)

Figure 1-6. General structure of various PHAs, reproduced from [37]

The PHAs can be produced by either chemical synthesis, use of transgenic plant cells or by bacterial fermentation [41]. PHAs produced via bacterial

fermentation through MMC is preferred over pure cultures as it reduces the fermentation cost, because it is not required to pre-treat the substrate and sterilization is also not necessary. These benefits make MMC an attractive route for PHA production, extending the possibility of using inexpensive carbon sources such as municipal solid waste and industrial wastewater [42]. Synthesis through a MMC such as a wastewater treatment plant (WWTP) occurs in three stages as depicted in Figure 1-7. First, the primary sludge undergoes acidogenic fermentation to produce VFAs using either an anaerobic-aerobic process, an aerobic dynamic feeding or through fed batch systems [42,43]. Afterwards, the secondary sludge which acts as an incubator for microorganisms is enriched with these VFAs, followed by accumulated growth of PHAs in the secondary sludge and finally polymer recovery in the downstream process where it can then be used in different materials [39]. During the fermentation process, VFAs with an even number of carbons will produce more PHBs, whilst those with an odd number will produce a Poly(3-Hydroxybutyrate-co-3-Hydroxyvalerate) (PHBV) copolymer with varying HV ratios [44].

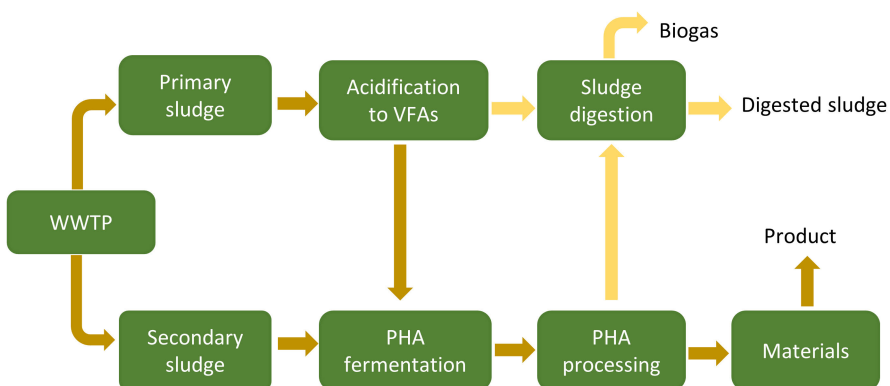


Figure 1-7. Production process of PHA via a wastewater treatment plant (WWTP) taken from [45]

During the synthesis by microorganisms, the PHAs bioaccumulate within the intracellular lipid as granules ranging between 0.2-0.5 μm [46]. The core of the granule predominately consists of PHAs (97.7%), with small amounts of proteins (1.8%) and phospholipids (0.5%).

Various separation techniques have been proposed to extract the PHA granules from the cells [47-50]. Among them, Solvent extraction is considered to be one of the most mature methods for the recovery of PHAs. It can involve a pre-treatment to rupture cells so the PHA is more easily accessible [51]. Previously, halogenated solvents such as 1,2-dichloroethane, chloroform, methylene chloride and 1,1,2-trichloroethane have been used to extract PHAs. However, as they are not environmentally friendly, other halogen-free solvents have been investigated as an alternative. Examples of such solvents include cyclic carbonic esters like 1,2-propylene carbonate and ethylene carbonate, esters like ethyl and butyl acetate, ketones like methyl isobutyl ketone and cyclohexanone or acids like acetic acids. Afterwards, the polymer can be precipitated out by various approaches such as cooling and adding an anti-solvent which would decrease its solubility in the solution. Such anti-solvents could be ethers, hexane and acetone which are best for precipitating SCL-PHAs, while most MCL-PHAs are soluble in these compounds. Solvent extraction results in a high purity of the polymer as well as its ability to remove endotoxins thereby enabling the polymer to be used in high grade medical applications [52]. Table 1-1 summarizes the performance of these solvents to extract PHAs from the biomass.

Ionic liquids were also investigated, these are salts which melt at or less than 100 °C, dissolving water insoluble substances [53,54]. They have been researched as an alternative for extraction as they can substitute the need

for volatile solvents. Proctor & Gamble own a patent where PHAs are extracted by a stripping process with ionic liquid in a water free environment. Recovery is followed by traditional separation methods including an anti-solvent and isolation method using centrifugation, sedimentation and etc. [55].

The recent focus of the research is on providing renewable and biobased solvents. Dimethyl carbonate (DMC) is a green and eco-friendly solvent produced by catalytic oxidative carbonylation of methanol via a green process established by Enichem (IT) and UBE Industries (JP) [49]. As shown in Table 1-1, DMC has shown great potential to be an appropriate green candidate to replace the halogenated solvents, because it yields relatively high and pure polymer under mild extraction conditions.

General Introduction and Literature Review

Table 1-1. Summary of the solvent extraction of PHAs using non-halogenated solvents

Culture	Solvent	Biomass/ solvent ratio [%g/mL]	Conditions	Yield [%]	Purity [%]	Ref.
<i>Ralstonia</i>	MIBK	2	50-100°C,	84	99	[56]
<i>Eutropha</i>	Ethyl acetate	-	4h	99	99	
<i>Burkholderia</i>	Anisole	1.5	120-130°C,	97	98	[57]
<i>Sacchari</i>	Cyclohexanone	-	0.5h	93	93	
<i>Cupriavidus</i> <i>Nectator</i>	1,3 Dioxolane	5	80°C, 6h	97.9	92.7	[58]
<i>Cupriavidus</i> <i>Nectator</i>	Propylene carbonate	7.6	130°C, 0.5h	95	84	[59]
<i>Cupriavidus</i> <i>Nectator</i>	Butyl acetate	1	103°C, 0.5h	96	98	[60] [61]
MMC	DMC	2.5	90°C, 1h	63	98	[62]
<i>R.Eutropha</i> And <i>Escherichia coli</i>	Methyl ethyl ketone	1	60°C, 1h	>90	>90	[50]
<i>Cupriavidus</i> <i>Nectator</i>	Water and Ethanol	2	30°C, 1h	96	81	[63]
<i>Cupriavidus</i> <i>Nectator</i>	Cyclohexanone	1	120°C, 3mins	95	95	[53]
<i>Cupriavidus</i> <i>Nectator</i>	DMC	2.5	90 C, 4h	>85	>95	[49]
<i>Modified</i> <i>Escherichia coli</i> <i>BL21 (DE3)</i>	DMC	2.5	90°C, 1.5h	>67	81	[64]

In this study, the application of two new bio-based solvents namely 2-methyltetrahydrofuran (2-MTHF) and dihydrolevoglucosenone (cyrene) to extract PHBV from MMC-based biomass was examined. To identify the limiting stages in the extraction procedure, the mass balance closure over

the polymer was studied. However, the source of the biomass and the characteristics of the polymer can have a great impact on the solubility of the polymer in a solvent and consequently on the extraction efficiency, meaning that a certain solvent can result in different extraction efficiency from various biomass types. This has not been focused on in previous works. For instance, Somori et al. [62] found that using DMC to extract PHBV from a MMC allows 49% recovery yield. Later, de Souza Reis et al. [47] reported 90% recovery under the same extraction conditions with DMC using MMC-based biomass. They concluded that the difference might be due to applying different wastewater as a feedstock for the microorganism and complex interactions between the PHBV and non-polymeric cell debris. Hence, in the current work, DMC and chloroform were used as reference solvents to compare the performance of the proposed solvents using the same batches of the biomass with different properties.

Using wastewater as a feedstock for the microorganisms enables producing inexpensive biopolymer. However, due to the daily variation in the composition of the waste/wastewater, the produced PHBV copolymer varies in its monomer composition which can influence the properties of the polymer such as melting point and crystallinity. Clearly, a polymer with variable properties per batch cannot find a broad application window in the polymer market. Instead, it can be depolymerized towards other value-added chemicals such as CA which is further discussed in the next section.

4. CA

CA is mainly used in the synthesis of copolymers. Among them, crotonic acid-vinyl acetate is the main copolymer, with trade names of Cevian, Gelva, Mowilith and Vinac [65]. They are commonly used in cosmetic and hair styling products. Apart from this, CA finds further applications in industries such as coatings, paint, textile, binders, adhesives, flocculants, ceramics and agrochemicals [66].

On industrial scale, CA is currently produced in a non-renewable pathway from fossil oil, requiring many synthesis steps which is a major drawback in the production process. It begins with the ethylene production by naphtha cracking, followed by the oxidation of ethylene into acetaldehyde, aldol condensation of acetaldehyde into acetaldol, dehydration of acetaldol into crotonaldehyde and lastly oxidation of crotonaldehyde into CA [65-67]. After all these steps, the current yield of CA is only 30%. Further purification involves fractional distillation and crystallization from water and causes product loss. Also highly contaminated effluent is formed during the crystallization step [67].

Other, not yet industrial scale production pathways of CA include isomerization of vinylacetic acid with sulfuric acid, photochemical oxidation or oxidative irradiation of crotonaldehyde with ultrasound, dehydration of 2-hydroxybutanoic acid, the condensation of acetaldehyde and malonic acid with pyridine as catalyst (85% yield), by the oxycarbonylation of propene with transition metal complex catalysts, the reaction of acetic anhydride with acetaldehyde with basic aluminum acetate as catalyst, the carbonylation of propylene oxide, the oxidation of butene with a heteropolymolybdic acid

containing catalyst system, and the carbonylation of allyl alcohol in a two-phase system with a nickel containing phase - transfer catalyst or a palladium catalyst [65]. All the aforementioned pathways are based on non-renewable sources.

Research has been done into bio-based CA. Several bacterial species (*Ralstonia Eutropha*, *Escherichia coli*, *Corynebacterium Glutamicum* and *Clostridium Acetobutanicum*) are capable of producing CA [66,68]. However, the quantitative yield and purity of CA were not reported, and a proper separation method is still needed to recover CA from the fermentation broth. Mamat et al.[66] proposed a different bio-based method, namely by direct pyrolysis of PHB, obtained from the fermentation broth of *Cupriavidus Necactor*. They found a yield of 63% CA which is about 30% higher than the conventional petrochemical route. In the next sub-section, the production of the bio-based CA through thermal decomposition of PHB/PHBV will be discussed in more detail.

5. PHB/PHBV pyrolysis

Depolymerization of PHA can be achieved by hydrolysis, alcoholysis and thermolysis, resulting in 2-hydroxyalkanoic acids, 2-hydroxyalkanoic esters and 2-alkenoic acids, respectively. So far, production of CA and cis-CA [66,69-74], methyl acrylate [75], methyl crotonate [75,76], propylene [77-79], 3-hydroxybutyric acid [66,70], methyl 3-hydroxybutanoate [80], cyclic and linear oligomers [69,81], and hydrocarbon oil [82] from PHB depolymerization have been reported. PHBV is the main bio-polymer which can be obtained by MMC. It consists of two monomers, HB and HV and both monomers are

converted during thermal breakdown of PHBV, producing CA and 2-PA, respectively [69].

Owing to the low cost, associated with the synthesis of PHB/PHBV by MMC using inexpensive feedstocks, the conversion of MMC-based PHB/PHBV into CA by pyrolysis seems to be a promising alternative for the complicated oil-based route. Pyrolysis is a thermal degradation process of organic materials in an inert (i.e. oxygen free) atmosphere [83]. An inert atmosphere is required to prevent thermo-oxidative reactions [84]. By subjecting organic material to high temperatures, the molecules are heavily stretched and shaken in such a way that the molecules are decomposed into smaller molecules [83]. The pyrolysis products can be categorized into three categories: char, non-condensable gasses and condensable gasses [83]. The yields of the products formed depend on many factors, such as the raw material used, temperature, reaction time, heating rate and cooling rate.

Several studies were performed on the thermal degradation mechanism of PHB/PHBV, in which different reaction paths were considered. Overall, it was concluded that a beta elimination, followed by an unzipping beta elimination at the crotonyl chain end is the dominant reaction path [85,86]. This path is schematically shown in Figure 1-8. The degradation rate of PHB/PHBV depends on the reactivity of the beta hydrogen. The relative acidity of the removed hydrogen atom determines the reactivity of the beta elimination. The carbonyl group which nucleophilically attacks the beta hydrogen can be interpreted as the Lewis base.

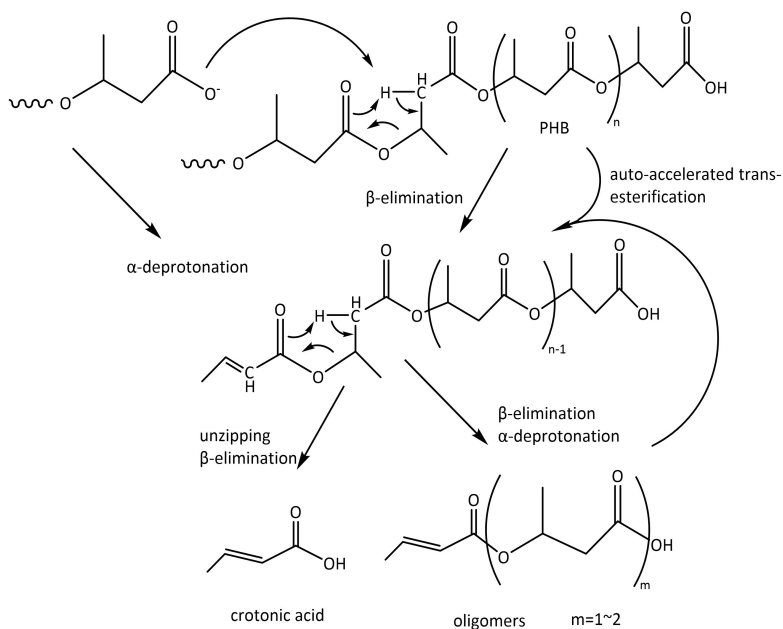


Figure 1-8. Thermal degradation of PHB towards CA, by H. Ariffin et al. reproduced with permission from [85]; published by Elsevier, 2008.

Several heterogeneous catalysts have been studied to enhance CA production through pyrolysis of PHB/PHBV such as $\text{Mg}(\text{OH})_2$, Ca^{2+} , Mg^{2+} and Na^+ [72,87-89]. It was found that some metal ions act as electrophiles, and thereby increase the reaction rate. The metal ions act as Lewis acids that interact with the carbonyl group, thereby enhancing the reactivity of the beta hydrogen towards the carbonyl group. Next to the heterogeneous catalysts, acetic acid was also investigated as a homogeneous catalyst [84]. Liquid catalysts with Lewis acidic behavior similar to the solid catalysts and their ability to dissolve the polymer or loosen up the structure, may catalyze the

thermal degradation of PHBV even better.

Table 1-2 summarizes PHB/PHBV pyrolysis experiments which are reported by now. As can be seen, CA production yield without using a catalyst varies from 57 to 65 wt%, whilst the catalyzed pyrolysis leads to 83 wt% CA yield with a purity of 97.7% [72]. The produced side-products are terminally unsaturated oligomers and iso-CA acid. 2-PA is also formed from the polymers that contain HV monomer. Secondary products can also be formed by further decomposition of the initial products, including: propylene, CO₂ and acetaldehyde [84]. The formation of CA is favored over the formation of iso-CA as the trans form is more stable, which is beneficial for synthesis of co-polymers with vinyl acetate which requires CA and not iso-CA. Aiming at production of CA by thermal treatment of PHB/PHBV, it should be considered that when temperatures exceed 100 °C largely, iso-CA can be formed through an isomerization reaction [90]. The use of catalysts such as MgO, Mg(OH)₂ [72] and Ca²⁺ [89] that lead to selective production of CA, is desired because various authors reported that uncatalyzed thermal degradation of PHB/PHBV occurs at a temperature range of 240 till 310 °C. With the use of catalysts, a significant reduction was observed in the degradation temperature of PHB/PHBV [72,89].

General Introduction and Literature Review

Table 1-2. An overview of pyrolysis PHB/PHBV towards CA

Ref.	HB [mol%]	Catalyst	Temp. [°C]	CA Yield [%]	Pyrolyzate composition [wt%]			
					CA	Iso-CA	2-PA	other
[85]	100	No	260	-	67.7	3.1	-	29.2
[66]	100	No	290	62.5	63.8	1	-	35.2
[87]	88	No	280	-	60.34	-	7.13	32.53
[87]	88	Mg(OH) ₂	260	-	85.31	-	10.9 2	3.77
[72]	100	No	280	57	57.1	3.6	-	39.3
[72]	100	Mg(OH) ₂	240	83	97.7	0.6	-	1.7
[86]	98.95	No	290	-	58.09	-	0.51	41.28
[67]	100	No	310	65	57.1	5	-	37.9
[67]	100	No, NaOH pretreatment	310	80	86.6	1.9	-	11.5
[91]	100	No	250	-	64.4	-	-	8.4
[74]	100	No	170 @ 150 mbar	58	92	0.1	-	0.5
[92]	100	Cyclohexane	210	89	91	-	-	-
[93]	100	IL, [EMIM][AcO]	140	97	>90	-	-	-

In the present study, to possibly ease the downstream purification of produced bio-based CA, direct depolymerization of PHBV towards CA and 2-

PA was investigated using a custom-built oven pyrolyzer set-up. The direct pyrolysis of the biomass was carried out either under vacuum condition or nitrogen stripping, allowing one to manipulate the mean residence time of the vapor phase in both oven and the condenser to obtain the highest acid production yield. Shorter residence times may not allow complete decomposition of the polymer and longer residence times may result in secondary cracking reactions. Therefore, various nitrogen gas flow rates were applied to vary the mean residence time of the vapor phase and study its effect on the acid production yield. Furthermore, the pyrolysis of the extracted polymer was performed using a vigreux distillation column, connected to the oven to examine the possibility of direct purification of CA in vapor phase.

Although the synthesis of CA via PHB/PHBV thermal decomposition has been examined over the last decades, its separation from the complex pyrolysis mixtures with relatively high purity has not been that well studied yet. Mullen et al.[71] have developed a fluidized bed set-up on pilot scale to pyrolyze a PHB/switchgrass blend and produce CA enriched bio-oil. They applied multistep condensation using water cooled (4 °C) condensers connected to an electrostatic precipitator for in-situ fractionation of the pyrolyzate mixture and production of bio-oil enriched with CA. The schematic view of this process is shown in Figure 1-9. The use of an electrostatic precipitator can be explained considering the melting point of CA, being 72 °C. Cooling of a vapor stream containing CA with cooling water of 4 °C will not only result in condensation, but also in partial precipitation. The presence of precipitated CA in aerosols that escaped the condensers through the vapor phase was confirmed experimentally [71]. The maximum CA yield of 45% was

obtained from a mixture of 10% PHB and 90% switchgrass using fine PHB particles at 375 °C. However, significant fractionation of CA from the total pyrolysis liquid was not achieved with this multistep separation procedure. The concentration of CA reduced from 11.2 to 8.7 wt% over the series of condensers, without following a pattern based on either water solubility or vapor temperature.

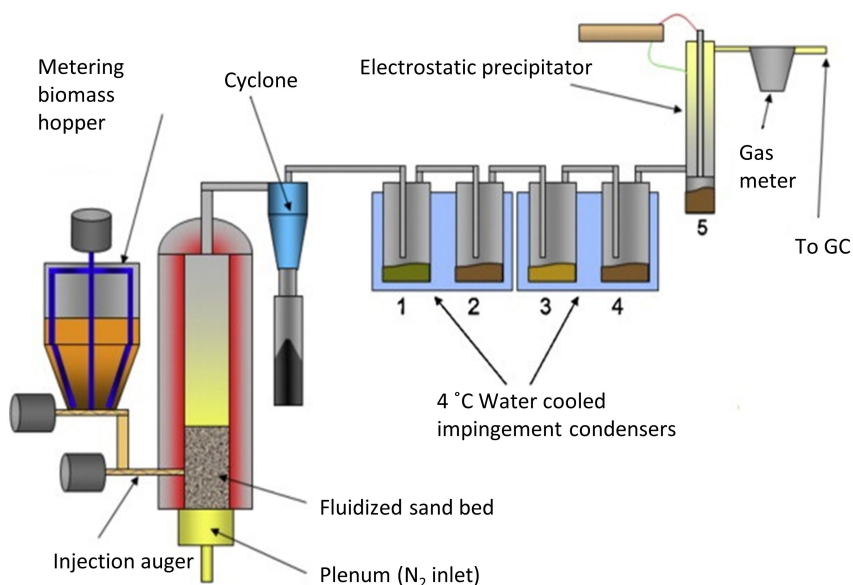


Figure 1-9. Schematic view of a fluidized bed PHB pyrolysis process. The Figure is reproduced with permission from [71], published by Elsevier, 2014.

Recently, Parodi et al.[74] developed a novel thermolytic distillation process, enabling pyrolysis of PHB and PHB-enriched biomass at 170 °C under reduced pressure of 150 mbar to yield CA. In thermolytic distillation under mild conditions (170 °C and 150 mbar), the pyrolysis of PHB occurs simultaneously

with the separation of volatile pyrolyzates such as CA. The integrated product removal at such mild conditions limits the isomerization of CA to iso-CA as the isomerization reaction happens mostly at elevated temperature. By means of this integrated technique, the authors could recover CA with a yield of 58% and purity of 92% from MMC-based biomass, containing 30 wt% PHB on dry basis. Indeed, pyrolysis of MMC-based PHB/PHBV enriched biomass using this novel method can increase both the yield and purity of CA. However, the vapor stream will still contain 2-PA as well as other side products, originated from HV monomer. Therefore, a next purification step is required to separate these carboxylic acids.

Table 1-3 presents the molecular properties of CA and 2-PA. The difference in their boiling and melting point is sufficient to consider distillation and crystallization as a separation approach, although a careful analysis of the vapor-liquid equilibria and solid-liquid equilibria should be performed. For affinity-based separation techniques (e.g., extractive distillation, liquid-liquid extraction and adsorption) to work, their similar molecular properties such as pK_a and both having a double C=C bond are expected to limit the operational window. For extractive distillation the difference in pK_a may either be too small or just enough [94]. The difference in hydrocarbon backbone length may result in a feasible difference in distribution over a polar phase and an apolar phase.

Table 1-3. Properties of CA and 2-PA

Property	CA	2-PA
Molecular weight [g.mol ⁻¹]	86.0892 [95]	100.117 [96]
Boiling point [°C @760mmHg]	184.7 [95]	200-203 [97]
Melting point [°C]	72 [95]	8-10 [97]
Water solubility [g.L ⁻¹ @25°C]	94 [95]	62.9 [96]
Density [g.ml ⁻¹ @ 25°C]	1.027 [98]	0.99 [99]
pK _a [@ 25°C]	4.817 [95]	5.02 [100]

In this work, the separation of a CA/2-PA mixture was examined by distillation. Initially, the vapor liquid equilibria (VLE) data of the mixture were obtained with a custom-designed VLE apparatus. Subsequently, a spinning band distillation column (SBC) was applied to further study this acid mixture separation.

6. Thesis outline

The following chapters describe the various project elements in this dissertation:

Chapter 1- This chapter includes an introduction and literature review for each step, including VFAs and their recovery, PHAs and their recovery, pyrolysis of PHA to produce CA and 2-PA, and the separation of CA and 2-PA mixtures.

Chapter 2- An adsorbent evaluation was performed using various polymeric resins with mild basic functionality, synthesized by Sylwia Ronka from Wrocław University of Technology. The experiments were carried out in batch using mimicked fermentation broth. From previous studies it was known that stronger basic resins adsorb mineral acids, limiting the capacity

for VFAs, and the goal was to identify whether these mildly basic resins have high affinity towards VFAs in highly diluted wastewater streams, while not adsorbing mineral acids.

Chapter 3- Separation of the VFAs by adsorption is studied in this chapter as well, intending to enhance the regeneration of the resin. It was aimed to develop an adsorbent which allows thermal desorption by magnetically heating. A superparamagnetic adsorbent is synthesized to recover the VFAs from a mimicked fermentation broth. Loading the superparamagnetic magnetite nanoparticles in the matrix of the resin allowed to perform the thermal desorption in two steps. First, water was removed using an alternating magnetic field (AMF), followed by acid recovery using hot nitrogen stripping.

Chapter 4- In this chapter, extraction of the PHBV from MMC-based biomass is investigated using bio-based solvents namely 2-MTHF and cyrene (dihydrolevoglucosenone). Various operation conditions have been optimized. Moreover, as the nature of the biomass and the average MW of the polymer have a great impact on the efficiency of the solvents in the extraction, diverse batches of the biomass possessing PHBV with different average MW have been used to examine the performance of the solvents.

Chapter 5- Thermal decomposition of the extracted PHBV from a MMC-based biomass towards CA and 2-PA production was investigated in this chapter. A custom-designed pyrolysis set-up was built, aiming to study the effect of the operation parameters on the polymer pyrolysis. The optimum mean residence time of the vapor phase in the hot oven was investigated to aid process design in the follow-up work.

Chapter 6- This chapter focuses on the final purification of the produced CA from pyrolysis of MMC-based PHBV. The main products in the thermal decomposition of PHBV are CA and 2-PA, origination from HB and HV monomers, respectively. Therefore, the goal was to investigate the feasibility of a distillation technique to separate these acids. First, the isobaric-VLE data of CA/2-PA mixture was collected using a custom-designed set-up. Afterwards, the separation of the acids was further studied using SBC. Moreover, the thermal stability of the acids was investigated under distillation conditions, because exposing the unsaturated acids at elevated temperatures at a certain contacting time results in isomerization or dimerization of the acids.

Chapter 7- The final conclusions and perspectives are presented in this chapter.

Nomenclature:

CA	Trans-Crotonic Acid
CAGR	Compound Annual Growth Rate
DMC	Dimethyl Carbonate
FW	Food Waste
HB	Hydroxy Butyrate
HV	Hydroxy Valerate
Iso-CA	Iso-Crotonic Acid
ILs	Ionic Liquid
LCL-PHA	Long carbon Chain Length Polyhydroxyalkanoates
MMC	Mixed Microbial Culture
MCCAs	Medium Carbon Chain carboxylic Acid
MIBK	Methyl Isobutyl Ketone
2-MTHF	2-Methyltetrahydrofuran
MCL-PHA	Medium carbon Chain Length Polyhydroxyalkanoates
OFMSW	Organic Fraction Of Municipal Solid Waste
PHAs	Polyhydroxyalkanoates
PHB	Poly(3hydroxybutyrate)
PHV	Poly(3-hydroxy Valerate)
PHBV	Poly(3-Hydroxybutyrate-co-3-Hydroxyvalerate)
2-PA	2-Pentenoic Acid
SS	Sewage Sludge
SBC	Spinning Band Column
SCL-PHA	Short carbon Chain Length Polyhydroxyalkanoates
VLE	Vapor Liquid Equilibria
VFAs	Volatile Fatty Acids
WWTP	Wastewater Treatment Plant

References

- [1] L.A. Hamilton; S. Feit; C. Muffett; M. Kelso; S.M. Rubright; C. Bernhardt; E. Schaeffer, Plastic & Climate The Hidden Costs of a Plastic Planet. *Center for International Environmental Law (CIEL)*. **2019**
- [2] E. Bugnicourt; P. Cinelli; V. Alvarez; A. Lazzeri, Polyhydroxyalkanoate (PHA): Review of synthesis, characteristics, processing and potential applications in packaging. *eXPRESS Polymer Letters*. **2014**, *8*, 791-808.

- [3] C. Kourmentza; J. Plácido; N. Venetsaneas; A. Burniol-Figols; C. Varrone; H.N. Gavala; M.A.M. Reis, Recent Advances and Challenges towards Sustainable Polyhydroxyalkanoate (PHA) Production. *Bioengineering*. **2017**, *4*, 55.
- [4] G.F.M.S.M. Saunders, Advances in biodegradable polymers. *iSmithers Rapra Publishing*. **1998**, *98*,
- [5] J. Blumenstein; J. Albert; R.P. Schulz; C. Kohlpaintner. Crotonaldehyde and Crotonic Acid. In *Ullmann's Encyclopedia of Industrial Chemistry*; pp. 1-20.
- [6] A. Patel; O. Sarkar; U. Rova; P. Christakopoulos; L. Matsakas, Valorization of volatile fatty acids derived from low-cost organic waste for lipogenesis in oleaginous microorganisms-A review. *Bioresource Technology*. **2021**, *321*, 124457.
- [7] J. Tamis; B. Joosse; M.v. Loosdrecht; R. Kleerebezem, High-rate volatile fatty acid (VFA) production by a granular sludge process at low pH. *Biotechnology and Bioengineering*. **2015**, *112*, 2248-2255.
- [8] M. Atasoy; I. Owusu-Agyeman; E. Plaza; Z. Cetecioglu, Bio-based volatile fatty acid production and recovery from waste streams: Current status and future challenges. *Bioresource Technology*. **2018**, *268*, 773-786.
- [9] S.K. Bhatia; Y.-H. Yang, Microbial production of volatile fatty acids: current status and future perspectives. *Reviews in Environmental Science and Bio/Technology*. **2017**, *16*, 327-345.
- [10] ACETIC ACID MARKET - GROWTH, TRENDS, COVID-19 IMPACT, AND FORECASTS (2021 - 2026). Available online: <https://www.mordorintelligence.com/industry-reports/acetic-acid-market> (accessed on
- [11] A.J.J. Straathof, Transformation of Biomass into Commodity Chemicals Using Enzymes or Cells. *Chemical Reviews*. **2014**, *114*, 1871-1908.
- [12] C. Bruni; A. Foglia; A.L. Eusebi; N. Frison; Ç. Akyol; F. Fatone, Targeted Bio-Based Volatile Fatty Acid Production from Waste Streams through Anaerobic Fermentation: Link between Process Parameters and Operating Scale. *ACS Sustainable Chemistry & Engineering*. **2021**, *9*, 9970-9987.
- [13] S. Bengtsson; J. Hallquist; A. Werker; T. Welander, Acidogenic fermentation of industrial wastewaters: Effects of chemostat retention time and pH on volatile fatty acids production. *Biochemical Engineering Journal*. **2008**, *40*, 492-499.
- [14] W. Fang; X. Zhang; P. Zhang; J. Wan; H. Guo; D.S.M. Ghasimi; X.C. Morera; T. Zhang, Overview of key operation factors and strategies for improving fermentative volatile fatty acid production and product regulation from sewage sludge. *Journal of Environmental Sciences*. **2020**, *87*, 93-111.
- [15] K. Dai; J.-L. Wen; F. Zhang; R.J. Zeng, Valuable biochemical production in mixed culture fermentation: fundamentals and process coupling. *Applied Microbiology and Biotechnology*. **2017**, *101*, 6575-6586.
- [16] W.S. Lee; A.S.M. Chua; H.K. Yeoh; G.C. Ngoh, A review of the production and applications of waste-derived volatile fatty acids. *Chemical Engineering Journal*. **2014**, *235*, 83-99.
- [17] F. Battista; N. Frison; P. Pavan; C. Cavinato; M. Gottardo; F. Fatone; A.L. Eusebi; M. Majone; M. Zeppilli; F. Valentino; et al., Food wastes and sewage sludge as feedstock for an urban biorefinery producing biofuels and added-value bioproducts. *Journal of Chemical Technology & Biotechnology*. **2020**, *95*, 328-338.
- [18] V. De Groof; M. Coma; T. Arnot; D.J. Leak; A.B. Lanham, Medium Chain Carboxylic Acids from Complex Organic Feedstocks by Mixed Culture Fermentation. *Molecules*. **2019**, *24*, 398.

- [19] E. Reyhanitash; S.R.A. Kersten; B. Schuur, Recovery of Volatile Fatty Acids from Fermented Wastewater by Adsorption. *ACS Sustainable Chemistry & Engineering*. **2017**, *5*, 9176-9184.
- [20] A. Gössi; F. Burgener; D. Kohler; A. Urso; B.A. Kolvenbach; W. Riedl; B. Schuur, In-situ recovery of carboxylic acids from fermentation broths through membrane supported reactive extraction using membrane modules with improved stability. *Separation and Purification Technology*. **2020**, *241*, 116694.
- [21] J. Marták; Š. Schlosser, Extraction of lactic acid by phosphonium ionic liquids. *Separation and Purification Technology*. **2007**, *57*, 483-494.
- [22] D. Rodríguez-Llorente; A. Bengoa; G. Pascual-Muñoz; P. Navarro; V.I. Águeda; J.A. Delgado; S. Álvarez-Torrellas; J. García; M. Larriba, Sustainable Recovery of Volatile Fatty Acids from Aqueous Solutions Using Terpenoids and Eutectic Solvents. *ACS Sustainable Chemistry & Engineering*. **2019**, *7*, 16786-16794.
- [23] L.M.J. Sprakel; B. Schuur, Solvent developments for liquid-liquid extraction of carboxylic acids in perspective. *Separation and Purification Technology*. **2019**, *211*, 935-957.
- [24] T. Eregowda; E.R. Rene; J. Rintala; P.N.L. Lens, Volatile fatty acid adsorption on anion exchange resins: kinetics and selective recovery of acetic acid. *Separation Science and Technology*. **2020**, *55*, 1449-1461.
- [25] A. Talebi; Y. Razali; N. Ismail; M. Rafatullah; H. Tajarudin, Selective Adsorption and Recovery of Volatile Fatty Acids from Fermented Landfill Leachate by Activated Carbon Process. *Science of the Total Environment*. **2019**, *707*, 134533.
- [26] X.-R. Pan; W.-W. Li; L. Huang; H.-Q. Liu; Y.-K. Wang; Y.-K. Geng; P. Kwan-Sing Lam; H.-Q. Yu, Recovery of high-concentration volatile fatty acids from wastewater using an acidogenesis-electrodialysis integrated system. *Bioresource Technology*. **2018**, *260*, 61-67.
- [27] H. Ravishankar; P. Dessi; S. Trudu; F. Asunis; P.N.L. Lens, Silicone membrane contactor for selective volatile fatty acid and alcohol separation. *Process Safety and Environmental Protection*. **2021**, *148*, 125-136.
- [28] Á. Bóna; P. Bakonyi; I. Galambos; K. Bélafi-Bakó; N. Nemestóthy, Separation of Volatile Fatty Acids from Model Anaerobic Effluents Using Various Membrane Technologies. *Membranes*. **2020**, *10*.
- [29] T. Brouwer; B.C. Dielis; J.M. Bock; B. Schuur, Hydrophobic Deep Eutectic Solvents for the Recovery of Bio-Based Chemicals: Solid-Liquid Equilibria and Liquid-Liquid Extraction. *Processes*. **2021**, *9*, 796.
- [30] E. Reyhanitash; E. Fufachev; K.D. van Munster; M.B.M. van Beek; L.M.J. Sprakel; C.N. Edelijn; B.M. Weckhuysen; S.R.A. Kersten; P.C.A. Buijninx; B. Schuur, Recovery and conversion of acetic acid from a phosphonium phosphinate ionic liquid to enable valorization of fermented wastewater. *Green Chemistry*. **2019**, *21*, 2023-2034.
- [31] U. Jomnonkhaow; C. Uwineza; A. Mahboubi; S. Wainaina; A. Reungsang; M.J. Taherzadeh, Membrane bioreactor-assisted volatile fatty acids production and in situ recovery from cow manure. *Bioresource Technology*. **2021**, *321*, 124456.
- [32] P. Sukphun; S. Sittijunda; A. Reungsang, Volatile Fatty Acid Production from Organic Waste with the Emphasis on Membrane-Based Recovery. *Fermentation*. **2021**, *7*, 159.

- [33] F. Rizzioli; F. Battista; D. Bolzonella; N. Frison, Volatile Fatty Acid Recovery from Anaerobic Fermentate: Focusing on Adsorption and Desorption Performances. *Industrial & Engineering Chemistry Research*. **2021**, *60*, 13701-13709.
- [34] E.V. Fufachev; B.M. Weckhuysen; P.C.A. Bruijninx, Toward Catalytic Ketonization of Volatile Fatty Acids Extracted from Fermented Wastewater by Adsorption. *ACS Sustainable Chemistry & Engineering*. **2020**, *8*, 11292-11298.
- [35] M. Koller; H. Niebelschütz; G. Braunegg, Strategies for recovery and purification of poly[(R)-3-hydroxyalkanoates] (PHA) biopolyesters from surrounding biomass. *Engineering in Life Sciences*. **2013**, *13*, 549-562.
- [36] K. Sudesh; H. Abe; Y. Doi, Synthesis, structure and properties of polyhydroxyalkanoates: biological polyesters. *Progress in Polymer Science*. **2000**, *25*, 1503-1555.
- [37] G.-Y.A. Tan; C.-L. Chen; L. Li; L. Ge; L. Wang; I.M. Razaad; Y. Li; L. Zhao; Y. Mo; J.-Y. Wang, Start a Research on Biopolymer Polyhydroxyalkanoate (PHA): A Review. *Polymers*. **2014**, *6*,
- [38] B. Kunasundari; K. Sudesh, Isolation and recovery of microbial polyhydroxyalkanoates. *Express Polymer Letters*. **2011**, *5*, 620-634.
- [39] R. Khajuria, Polyhydroxyalkanoates: Biosynthesis to commercial production- A review. *Journal of microbiology, biotechnology and food sciences*. **2017**, *6*, 1098-1106.
- [40] J.Y. Chee; S. Yoga; N.-S. Lau; S. Ling; R. Abed; K. Sudesh. Bacterially produced polyhydroxyalkanoate (PHA): Converting renewable resources into bioplastic. 2010; Volume 2, pp. 1395-1404.
- [41] N. Jacquél; C.-W. Lo; Y.-H. Wei; H.-S. Wu; S.S. Wang; S.S. Wang, Isolation and purification of bacterial poly(3-hydroxyalkanoates). *Biochemical Engineering Journal*. **2008**, *39*, 15-27.
- [42] C. Nielsen; A. Rahman; A.U. Rehman; M.K. Walsh; C.D. Miller, Food waste conversion to microbial polyhydroxyalkanoates. *Microbial biotechnology*. **2017**, *10*, 1338-1352.
- [43] E.R. Coats; B.S. Watson; C.K. Brinkman, Polyhydroxyalkanoate synthesis by mixed microbial consortia cultured on fermented dairy manure: Effect of aeration on process rates/yields and the associated microbial ecology. *Water Research*. **2016**, *106*, 26-40.
- [44] C. Kourmentza; J. Plácido; N. Venetsaneas; A. Burniol-Figols; C. Varrone; H.N. Gavala; M.A.M. Reis, Recent Advances and Challenges towards Sustainable Polyhydroxyalkanoate (PHA) Production. *Bioengineering (Basel)*. **2017**, *4*,
- [45] E.D. Bluemink; A.F. van Nieuwenhuijzen; E. Wypkema; C.A. Uijterlinde, Bio-plastic (polyhydroxy-alkanoate) production from municipal sewage sludge in the Netherlands: a technology push or a demand driven process? *Water Science and Technology*. **2016**, *74*, 353-358.
- [46] K. Balakrishnan, Isolation and recovery of microbial polyhydroxyalkanoates. *Express Polymer Letters*. **2011**, *5*, 620-634.
- [47] G.A. de Souza Reis; M.H.A. Michels; G.L. Fajardo; I. Lamot; J.H. de Best, Optimization of Green Extraction and Purification of PHA Produced by Mixed Microbial Cultures from Sludge. *Water*. **2020**, *12*, 1185.
- [48] M. Koller, Established and advanced approaches for recovery of microbial polyhydroxyalkanoate (PHA) biopolyesters from surrounding microbial biomass. *The EuroBiotech Journal*. **2020**, *4*, 113-126.

- [49] C. Samori; M. Basaglia; S. Casella; L. Favaro; P. Galletti; L. Giorgini; D. Marchi; L. Mazzocchetti; C. Torri; E. Tagliavini, Dimethyl carbonate and switchable anionic surfactants: two effective tools for the extraction of polyhydroxyalkanoates from microbial biomass. *Green Chemistry*. **2015**, *17*, 1047-1056.
- [50] Y.-H. Yang; J. Jong-Min; D. Yi; J.-H. Kim; H.-M. Seo; C. Rha; A. Sinskey; C. Brigham, Application of a non-halogenated solvent, methyl ethyl ketone (MEK) for recovery of poly(3-hydroxybutyrate-co-3-hydroxyvalerate) [P(HB-co-HV)] from bacterial cells. *Biotechnology and Bioprocess Engineering*. **2015**, *20*, 291-297.
- [51] Z. Raza; S. Abid; I. Banat, Polyhydroxyalkanoates: Characteristics, production, recent developments and applications. *International Biodeterioration & Biodegradation*. **2018**, *126*, 45-56.
- [52] M. Koller; H. Niebelschütz; G. Braunegg, Strategies for Recovery and Purification of Poly[(R)-3-hydroxyalkanoates] (PHA) Biopolyesters from Surrounding Biomass. *Engineering in Life Sciences*. **2013**, *13*, 549-562.
- [53] G. Jiang; B. Johnston; D. E. Townrow; I. Radecka; M. Koller; P. Chaber; G. Adamus; M. Kowalczyk. *Biomass Extraction Using Non-Chlorinated Solvents for Biocompatibility Improvement of Polyhydroxyalkanoates*; Polymers: 2018; Volume 10, p. 731.
- [54] C. Pérez-Rivero; J.P. López-Gómez; I. Roy, A sustainable approach for the downstream processing of bacterial polyhydroxyalkanoates: state-of-the-art and latest developments. *Biochemical Engineering Journal*. **2019**, *150*, 107283.
- [55] S.E. Hecht; R.L. Niehoff; K. Narasimhan; C.W. Neal; P.A. Forshey; D. Van Phan; A.D.M. Brooker; K.H. Combs. Extracting biopolymers from a biomass using ionic liquids. 2010.
- [56] S.L. Riedel; C.J. Brigham; C.F. Budde; J. Bader; C. Rha; U. Stahl; A.J. Sinskey, Recovery of poly (3-hydroxybutyrate-co-3-hydroxyhexanoate) from *Ralstonia eutropha* cultures with non-halogenated solvents. *Biotechnology and Bioengineering*. **2013**, *110*, 461-470.
- [57] A. Rosengart; M.T. Cesário; M.C.M. de Almeida; R.S. Raposo; A. Espert; E.D. de Apodaca; M.M.R. da Fonseca, Efficient P (3HB) extraction from *Burkholderia sacchari* cells using non-chlorinated solvents. *Biochemical Engineering Journal*. **2015**, *103*, 39-46.
- [58] N. Yabueng; S.C. Napathorn, Toward non-toxic and simple recovery process of poly (3-hydroxybutyrate) using the green solvent 1, 3-dioxolane. *Process Biochemistry*. **2018**, *69*, 197-207.
- [59] M.L. Fiorese; F. Freitas; J. Pais; A.M. Ramos; G.M. de Aragão; M.A. Reis, Recovery of polyhydroxybutyrate (PHB) from *Cupriavidus necator* biomass by solvent extraction with 1, 2-propylene carbonate. *Engineering in Life Sciences*. **2009**, *9*, 454-461.
- [60] A. Aramvash; N. Banadkuki; F. Moazzeni-Zavareh; S. Hajizadeh-Turchi, An environment-friendly and efficient method for extraction of PHB biopolymer by non-halogenated solvents. *Journal of Microbiology and Biotechnology*. **2015**, *25*,
- [61] A. Aramvash; F. Moazzeni Zavareh; N. Gholami Banadkuki, Comparison of different solvents for extraction of polyhydroxybutyrate from *Cupriavidus necator*. *Engineering in Life Sciences*. **2018**, *18*, 20-28.
- [62] C. Samori; F. Abbondanzi; P. Galletti; L. Giorgini; L. Mazzocchetti; C. Torri; E. Tagliavini, Extraction of polyhydroxyalkanoates from mixed microbial cultures: Impact on polymer quality and recovery. *Bioresource Technology*. **2015**, *189*, 195-202.

- [63] M. Mohammadi; M.A. Hassan; L.-Y. Phang; H. Ariffin; Y. Shirai; Y. Ando, Recovery and purification of intracellular polyhydroxyalkanoates from recombinant *Cupriavidus necator* using water and ethanol. *Biotechnology Letters*. **2012**, *34*, 253-259.
- [64] B. Mongili; A. Abdel Azim; S. Fraterrigo Garofalo; E. Batuecas; A. Re; S. Bocchini; D. Fino, Novel insights in dimethyl carbonate-based extraction of polyhydroxybutyrate (PHB). *Biotechnology for Biofuels*. **2021**, *14*, 13.
- [65] R.P. Schulz; J. Blumenstein; C. Kohlpaintner. Crotonaldehyde and crotonic acid. Ullmann's Encyclopedia of Industrial Chemistry: 2002; pp. 463-469.
- [66] M.R.Z. Mamat; H. Ariffin; M.A. Hassan; M.A.K. Mohd Zahari, Bio-based production of crotonic acid by pyrolysis of poly(3-hydroxybutyrate) inclusions. *Journal of Cleaner Production*. **2014**, *83*, 463-472.
- [67] N.F.S.M. Farid; H. Ariffin; M.R.Z. Mamat; M.A.K. Mohd Zahari; M.A. Hassan, Non-solvent-based pretreatment of poly(3-hydroxybutyrate) for improved bio-based crotonic acid production. *RSC Advances*. **2015**, *5*, 33546-33553.
- [68] D. Koch; G. Meurer, Means and methods for producing crotonic acid. *EP Pat*. **2012**, *2*,
- [69] H. Morikawa; R. Marchessault, Pyrolysis of bacterial polyalkanoates. *Canadian Journal of Chemistry*. **2011**, *59*, 2306-2313.
- [70] X. Yang; K. Odelius; M. Hakkarainen, Microwave-Assisted Reaction in Green Solvents Recycles PHB to Functional Chemicals. *ACS Sustainable Chemistry & Engineering*. **2014**, *2*, 2198-2203.
- [71] C.A. Mullen; A.A. Boateng; D. Schweitzer; K. Sparks; K.D. Snell, Mild pyrolysis of P3HB/switchgrass blends for the production of bio-oil enriched with crotonic acid. *Journal of Analytical and Applied Pyrolysis*. **2014**, *107*, 40-45.
- [72] H. Ariffin; H. Nishida; Y. Shirai; M.A. Hassan, Highly selective transformation of poly[(R)-3-hydroxybutyric acid] into trans-crotonic acid by catalytic thermal degradation. *Polymer Degradation and Stability*. **2010**, *95*, 1375-1381.
- [73] C. Samorì; A. Kiwan; C. Torri; R. Conti; P. Galletti; E. Tagliavini, Polyhydroxyalkanoates and Crotonic Acid from Anaerobically Digested Sewage Sludge. *ACS Sustainable Chemistry & Engineering*. **2019**, *7*, 10266-10273.
- [74] A. Parodi; A. Jorea; M. Fagnoni; D. Ravelli; C. Samorì; C. Torri; P. Galletti, Bio-based crotonic acid from polyhydroxybutyrate: synthesis and photocatalyzed hydroacylation. *Green Chemistry*. **2021**, *23*, 3420-3427.
- [75] C. Fernández-Dacosta; J.A. Posada; A. Ramirez, Techno-economic and carbon footprint assessment of methyl crotonate and methyl acrylate production from wastewater-based polyhydroxybutyrate (PHB). *Journal of Cleaner Production*. **2016**, *137*, 942-952.
- [76] J. Spekreijse; J. Le Nôtre; J.P.M. Sanders; E.L. Scott, Conversion of polyhydroxybutyrate (PHB) to methyl crotonate for the production of biobased monomers. *Journal of Applied Polymer Science*. **2015**, *132*,
- [77] Y. Li; T.J. Strathmann, Kinetics and mechanism for hydrothermal conversion of polyhydroxybutyrate (PHB) for wastewater valorization. *Green Chemistry*. **2019**, *21*, 5586-5597.
- [78] C. Torri; T.D.O. Weme; C. Samorì; A. Kiwan; D.W.F. Brillman, Renewable Alkenes from the Hydrothermal Treatment of Polyhydroxyalkanoates-Containing Sludge. *Environmental Science & Technology*. **2017**, *51*, 12683-12691.
- [79] S. Kang; H. Chen; Y. Zheng; Y. Xiao; Y. Xu; Z. Wang, One-Pot Catalytic Conversion of Poly(3-hydroxybutyrate) to Propylene at 240 °C. *ChemistrySelect*. **2019**, *4*, 403-406.

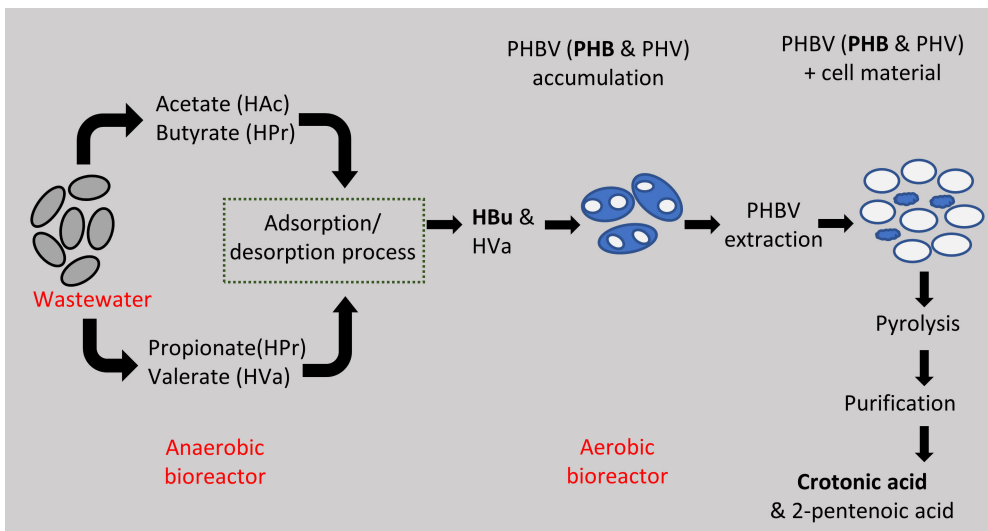
- [80] X. Song; F. Liu; H. Wang; C. Wang; S. Yu; S. Liu, Methanolysis of microbial polyester poly(3-hydroxybutyrate) catalyzed by Brønsted-Lewis acidic ionic liquids as a new method towards sustainable development. *Polymer Degradation and Stability*. **2018**, *147*, 215-221.
- [81] H. Nishida; H. Ariffin; Y. Shirai; M.A. Hassan, Precise depolymerization of poly(3-hydroxybutyrate) by pyrolysis. *Biopolymers*. **2010**, *19*, 370-386.
- [82] S. Kang; J. Yu, One-pot production of hydrocarbon oil from poly(3-hydroxybutyrate). *RSC Advances*. **2014**, *4*, 14320-14327.
- [83] H. Al-Haj Ibrahim. Introductory Chapter: Pyrolysis. 2020.
- [84] A. Fraga; R.A. Ruseckaite; A. Jiménez, Thermal degradation and pyrolysis of mixtures based on poly(3-hydroxybutyrate-8%-3-hydroxyvalerate) and cellulose derivatives. *Polymer Testing*. **2005**, *24*, 526-534.
- [85] H. Ariffin; H. Nishida; Y. Shirai; M.A. Hassan, Determination of multiple thermal degradation mechanisms of poly(3-hydroxybutyrate). *Polymer Degradation and Stability*. **2008**, *93*, 1433-1439.
- [86] H. Xiang; X. Wen; X. Miu; Y. Li; Z. Zhou; M. Zhu, Thermal depolymerization mechanisms of poly(3-hydroxybutyrate-co-3-hydroxyvalerate). *Progress in Natural Science: Materials International*. **2016**, *26*, 58-64.
- [87] H. Ariffin; H. Nishida; M.A. Hassan; Y. Shirai, Chemical recycling of polyhydroxyalkanoates as a method towards sustainable development. *Biotechnology Journal*. **2010**, *5*, 484-492.
- [88] K.J. Kim; Y. Doi; H. Abe, Effects of residual metal compounds and chain-end structure on thermal degradation of poly(3-hydroxybutyric acid). *Polymer Degradation and Stability*. **2006**, *91*, 769-777.
- [89] K.J. Kim; Y. Doi; H. Abe, Effect of metal compounds on thermal degradation behavior of aliphatic poly(hydroxyalkanoic acid)s. *Polymer Degradation and Stability*. **2008**, *93*, 776-785.
- [90] M.B. Hocking, The Effect of Heat on cis- and trans-Crotonic Acids: Alternatives to Direct cis-trans Isomerism. *Canadian Journal of Chemistry*. **1972**, *50*, 1224-1232.
- [91] H. Morikawa; R.H. Marchessault, Pyrolysis of bacterial polyalkanoates. *Canadian Journal of Chemistry*. **1981**, *59*, 2306-2313.
- [92] S. Kang; R. Chen; J. Fu; J. Liang; S. Chen; L. Lu; R. Miao, Catalyst-free valorization of poly-3-hydroxybutyrate to crotonic acid. *Reaction Chemistry & Engineering*. **2021**, *6*, 1791-1795.
- [93] P. Jablonski; D. Nikjoo; J. Warna; K. Irgum; J.-P. Mikkola; S.G. Khokarale, Sustainable, highly selective, and metal-free thermal depolymerization of poly-(3-hydroxybutyrate) to crotonic acid in recoverable ionic liquids. *Green Chemistry*. **2022**, *24*, 4130-4139.
- [94] T. Brouwer; R. van Lin; A.J.B. ten Kate; B. Schuur; G. Bargeman, Influence of Solvent and Acid Properties on the Relative Volatility and Separation Selectivity for Extractive Distillation of Close-Boiling Acids. *Industrial & Engineering Chemistry Research*. **2021**, *60*, 7406-7416.
- [95] PubChem Available online: https://pubchem.ncbi.nlm.nih.gov/compound/crotonic_acid (accessed on 08-12-2021).
- [96] PubChem. Available online: <https://pubchem.ncbi.nlm.nih.gov/compound/2-Pentenoic-acid#section=Computed-Properties> (accessed on 8-12-2021).
- [97] Chemspider. Available online: <http://www.chemspider.com/Chemical-Structure.553682.html> (accessed on 08-12-2021).

General Introduction and Literature Review

- [98] Sigma -Aldrich Available online:
<https://www.sigmaaldrich.com/NL/en/product/aldrich/113018> (accessed on 08-12-2021).
- [99] Sigma -Aldrich. Available online:
<https://www.sigmaaldrich.com/NL/en/product/aldrich/259276> (accessed on 08-12-2021).
- [100] Y. Zeng; H. Qian; X. Chen; Z. Li; S. Yu; X. Xiao, Thermodynamic Estimate of pKa Values of the Carboxylic Acids in Aqueous Solution with the Density Functional Theory. *Chinese Journal of Chemistry*. **2010**, *28*, 727-733.

Chapter 2

Methacrylonitrile-based Adsorbents for Recovery of VFAs from Fermentation Broth



This chapter is adapted from:

Elhami, V.; Ronka, S.; Schuur, B.; “Methacrylonitrile-based Adsorbents for Recovery of VFAs from Fermentation Broth”, 2023, (under preparation).

Abstract

Adsorption is a promising affinity separation technique to target a sorbate in extremely dilute solutions. In this chapter, methacrylonitrile (MAN)-functionalized resins were investigated to recover volatile fatty acids (VFAs) from a mimicked fermentation broth as an alternative for the already known amine-based resins and non-functionalized crosslinked polystyrene-divinyl benzene (PS-DVB) based resins, aiming for high VFA capacity and selectivity. Next to comparison with commercial PS-DVB resin, also several PS-DVB resins were synthesized as non-functionalized analogues for the new MAN-functionalized resins. For MAN-functionalized resins, a maximum equilibrium VFA loading of about 153 was found, which is higher than the 125 [g Acid/kg Adsorbent] for the PS-DVB non-functionalized resins. Overall, the MAN-functionalized adsorbents retained higher loading capacity for corresponding acids, compared to the PS-DVB resins. It is due to the hydrogen bonding between the nitrile groups of the resins with the carboxyl group of the acids. Moreover, none of the adsorbents displayed an affinity towards the salts, presented in the fermentation broth.

1. Introduction

Valorizing waste/wastewater is an interesting approach to the circular economy model, allowing to recover valuable chemicals from waste [1-7]. Over the last decades, researchers have been focused on converting waste/wastewater to value-added chemicals by fermentation. Various organic-enriched wastes have potential to be anaerobically fermented into Volatile fatty acids (VFAs) which are short carboxylic acids with a wide range

of applications in industry [4,8-12]. Every year, 50.3 M tons of waste are produced at the urban level in EU-27 with the organic fractions of municipal solid (OFMSW) and sewage sludge (SS) being the predominant wastes [8]. Anaerobic digestion of this carbon-rich waste/wastewater towards VFAs have been well studied [8,11,13-15]. Indeed, the bio-based pathways through fermentation of inexpensive feedstocks appears to be a feasible approach to produce such essential platform chemicals [16]. However, a robust recovery technique is still necessary to recover the produced VFAs from the fermentation broth. This is because, anaerobic fermentation of waste/wastewater results in extremely dilute aqueous solutions of VFAs (~1 wt%) due to their low carbon content [17]. Thus, affinity separation techniques such as liquid-liquid extraction (LLE) and adsorption, targeting the VFAs rather than water can be economic routes to recover the VFAs [17-21]. LLE using Ionic liquids (ILs) has also been investigated to recover the carboxylic acids [22-24]. From the extraction point of view, ILs appear to be an interesting solvent class to recover the acids from the broths with limited acid content [23-25]. However, the regeneration of ILs remains still challenging [25].

Adsorption has displayed a promising potential to separate VFAs from extremely dilute solutions [17,26,27]. Various adsorbents have been employed to recover the VFAs from the fermentation broth [19,28]. Ahasa Yousef et al. [28] reported 42.68 mg/g adsorption capacity with activated carbon to separate butyric acid from a broth obtained by dark fermentation of food waste, containing 6.6 g/L butyric acid. A total VFA capacity of 76 g/kg is reported for non-functionalized styrene-divinylbenzene based adsorbent with the commercial name of Lewatit VP OC 1064 MD PH (called "Lewatit" in

this work) [17]. Lewatit is a microporous hydrophobic resin with high surface area and large pore volume. Its high thermal stability and remarkable capacity towards VFAs made it as a promising adsorbent to separate VFAs from the aqueous solutions, followed by thermal regeneration of the resin and recovering the acids in highly concentrated solution [17]. The hydrophobic interaction between the carbon chain of the acids and the aromatic ring of the resin is the main affinity responsible for separation of VFAs from water using Lewatit while water physically fills the pores. Therefore, it is worthwhile to investigate hydrophobic resins with small pore volumes and high surface area to limit the water up-take during adsorption and consequently obtain acids in concentrated solution in a final thermal regeneration step.

Furthermore, various amine functionalized ion exchange resins have also been proposed to extract carboxylic acids from the fermentation broth [26,29-31]. Quaternary ammonium based adsorbent attracts the carboxylates via anion exchange. Whilst the primary, secondary and tertiary amines can form either hydrogen bonding with the acids or transfer protons with the carboxylates to maintain the charge neutrality of the resin [32]. These ion exchangers are interesting adsorbents, since the pH of the fermentation broth is usually between 5-7 and consequently the VFAs are in their dissociated form [30]. However, the regeneration of the ion exchangers requires another ion exchange reaction using an extra agent (e.g. mineral acids) to protonate them and recover the VFAs which produces a stoichiometric amount of salts [31]. Moreover, these resins can attract not only the acids, but also the minerals (salts) present in the fermentation broth via ion exchange reactions [17]. Therefore, we aimed to apply resins

functionalized with nitrile instead of amine groups, where it is aimed to prevent ion exchange reactions while introducing another interaction mechanism between the acids and the adsorbent to enhance the recovery yield and the acid selectivity. The nitrile based active sites can form hydrogen bonding with the carboxyl group of the acids, but proton transfer is not expected.

In this chapter, the main goal is to explore whether the possible adsorbents based on nitrile functionality can perform similar to amine functionalized Lewatit in terms of adsorption capacity, but without co-adsorption of mineral acids. Different adsorbents with either methacrylonitrile (MAN) or styrene (ST) crosslinked with divinyl benzene (DVB) were provided by Wrocław University of Science and Technology. The MAN-functionalized adsorbents were aimed to enhance VFA recovery by hydrogen bonding between the carboxyl group of the acids and nitrile group of the resins. The PS-DVB resins were synthesized, aiming to control the morphology and possibly reduce the water up-take with introducing small pore volumes, while maintaining a reasonable internal surface area. The performance of MAN-functionalized resins was compared to the PS-DVB adsorbent by conducting batch adsorption experiments using a mimicked fermentation broth.

2. Materials and methods

2.1. Chemicals

Butyric acid (HBu, >99%), Acetic acid (HAc, >99.7%), propionic acid (HPr, >99.5%), anhydrous sodium phosphate dibasic (>99%), anhydrous sodium

sulfate (>99%), potassium chloride (>99%), were purchased from Sigma-Aldrich. Crystalline lactic acid (HLa, >98%) was provided by Corbion. Potassium hydroxide (1 M) was supplied by Merck. The water used was ultrapure (Milli-Q, with a resistance of 18.2 $\mu\Omega$ cm at 25 °C). Lewatit VP OC 1064 MD PH adsorbent was purchased from Lenntech. The resins have been synthesized by Sylwia Ronka from Wrocław University of Science and Technology.

2.2. Adsorbent screening to recover VFAs from fermentation broth

Following the method described by Reyhanitash et al. [17], the batch adsorption experiments were performed for each resin to determine their equilibrium loading using a model solution as a feed. The composition of the feed is given in Table 2-1. 0.5 g Of each adsorbent was contacted with 11 g feed for 1 h at >500 rpm. Afterwards, a sample was taken from the eluent and analysed by high pressure liquid chromatography (HPLC) and ion chromatography (IC) to determine the concentration of the acids and salts, respectively.

Table 2-1. The composition of the concentrated mimicked fermentation broth

solution	Concentration [wt%]				Concentration [mol/L]			pH
	HAc	HPr	HBu	HLa	KCl	Na ₂ SO ₄	Na ₂ HPO ₄	
Feed	1.25	1.25	1.25	1.25	0.25	0.25	0.5	4.98

The capacity of the adsorbent was calculated using Eq. (2-1):

$$q = \frac{(C_0 - C_e) \times F}{m} \quad (2-1)$$

Where q is the amount of adsorbate adsorbed by the adsorbent [g of Acid/kg of adsorbent], F is the mass of feed [g], m is the mass of resin [kg] used for batch adsorption, C_0 [wt%] is the initial concentration of each acid in the feed and C_e [wt%] is the equilibrium concentration of corresponding acid in the eluent.

2.3. Analysis

The Brunauer-Emmett-Teller (BET). Specific surface area of commercial Lewatit was obtained using N_2 adsorption isotherms determined at 77K using a Micromeritics Gemini VII 2390a. First, the commercial resins were washed with water and dried using N_2 at 100 °C and 0.2 L/min. Afterwards, the sample was degassed at 180 °C for 15 h and analyzed by BET equipment.

High Performance Liquid Chromatography (HPLC). The concentrations of HPr, HBU, HAc and HLa were measured with an inaccuracy of < 0.5% using a HPLC [Agilent Hi-Plex H column (300 × 7.7 mm) using a refractive index detector on an Agilent 1200 series HPLC system; mobile phase, 5 mM H_2SO_4 solution; column temperature of 65 °C at a flow rate of 0.6 mL/min].

Ion chromatography (IC). Cl^- , PO_4^{3-} and SO_4^{2-} concentrations were quantified with IC (Metrosep A Supp 16-150/4.0 column on a Metrohm 850 Professional IC; mobile phase, 7.5 mM Na_2CO_3 + 0.75 mM KOH solution; column temperature, 45 °C; flow rate, 0.8 mL/min). Na^+ and K^+ concentrations were measured with IC as well (Metrosep C6-150/ 4.0 column on a Metrohm 850

Professional IC; mobile phase, 1.7 mM HNO₃ + 1.7 mM dipicolinic acid solution; column temperature, 20 ±1 °C; flow rate, 1.0 mL/min).

pH values were measured with a Metrohm pH probe (6.0234.100) connected to a Metrohm 780 pH-meter.

3. Results and discussion

3.1. Characterization of the adsorbents

The separation efficiency of an adsorption process depends on the physicochemical properties of both the adsorbate and the adsorbent, as well as on the fluid phase properties. Surface chemistry, pore size and internal surface area are the relevant characteristics of an adsorbent which directly influence its capacity. These properties have been determined, and are summarized in Table 2-2. In total, 8 resins have been synthesized, of which five MAN-functionalized and three PS-DVB-based resins. The PS crosslinked with DVB resins have been synthesized using various porogens to vary the porosity in the particles. Toluene ($\delta=18.3 \text{ MPa}^{1/2}$), octanol ($\delta=20.9 \text{ MPa}^{1/2}$), and solutions of poly(ethylene glycol) (PEG, oligomer; $\delta=20.8 \text{ MPa}^{1/2}$) and polystyrene (PS, polymer; $\delta=18.3 \text{ MPa}^{1/2}$) have been applied to produce the resins which are examined in the present work.

As shown in Table 2-2, using PEG dissolved in toluene as a porogen resulted in the highest BET surface area for both MAN and PS-DVB-based resins, whilst PS solution in THF yields resins with remarkably low surface area and small mesopores. The function of each diluent depends mainly on their solubility parameters. The Hildebrand solubility parameters (δ) for MAN, ST and DVB are $21.9 \text{ MPa}^{1/2}$, $19.0 \text{ MPa}^{1/2}$ and $18.2 \text{ MPa}^{1/2}$, respectively. Solvents having a

solubility parameter (δ) similar to the δ of the monomer (good solvents) yield small pores (inducing micropores) and a high surface area. The non-solvating diluents result in worse solvation of monomer and consequently, the average pore size becomes large (inducing macropores or mesopores), and the surface area decreases [33]. Usually, the pore sizes are designed using different types of solvent mixtures [34-36]. Another possibility is to use porogens, containing large size molecules, such as oligomers [37]. Using an oligomer as co-porogen with a good solvent can induce phase separation in two stages: an early event in which the oligomer phase separates to produce macropores and a late event in which the solvent phase separates to produce micropores. Optimally a bimodal pore size distribution might be achieved. This increase in surface area by increasing the population of mesopores in these polymers, which probably makes previously inaccessible or closed micropores accessible, while also contributing directly to the surface area [37]. Polymer solutions, such as a toluene solution of polystyrene, can generate pores in polymers with diameters usually greater than 50 nm (i.e., macropores) [33,38].

Overall, the average pore size and pore volume of the synthesized particles are smaller than the ones for the commercial resin Lewatit. Unfortunately, there is no information available about the polymerization mechanism and the type of the diluent used in the synthesis of Lewatit.

Methacrylonitrile-based Adsorbents for Recovery of VFAs

Table 2-2. Summary of the characterization of the various adsorbents.

Resins	Water up-take [g/g]	N content [mmol/g]	BET Surface area [m ² /g]	Mesopores		Micropores		Porogen
				Pore volume [cm ³ /g]	Pore size [nm]	Pore volume [cm ³ /g]	Pore size [nm]	
MAN-DVB 1	1.38	5.14	550	0.88	6.41	0.08	0.69	PEG in toluene
MAN-DVB 2	1.17	4.83	412	0.29	2.78	0.07	0.69	PS in toluene
MAN-DVB 3	0.99	4.68	2	0.004	7.10	-	-	PS in THF
MAN-DVB 4	1.19	5.19	526	0.87	6.64	0.08	0.69	Toluene
MAN-DVB 5	1.85	4.93	327	0.54	6.63	-	-	Octanol
PS-DVB 1	0.60	-	502	0.55	4.39	0.07	0.72	PEG in toluene
PS-DVB 2	0.87	-	429	0.31	2.93	0.07	0.69	PS in toluene
PS-DVB 3	0.53	-	6	0.009	6.00	-	-	PS in THF
Lewatit	1.00	-	931	-	-	1.50	8.74	N/A

The water up-take of the investigated co-polymers is due to the retention of water in the pores of the polymer. As shown in Table 2-2, MAN-based co-polymers have relatively high water up-take (0.99-1.85 g/g) which is almost twice greater water up-take than PS-DVB resins. This is because of the more polar nature of MAN compared to ST. Moreover, the water up-take of the synthesized PS-DVB is lower than commercial Lewatit due to their small pores volumes. The determination of nitrogen content by the Kjeldahl method enables to determine the content of nitrile groups, present in the MAN-based co-polymers structure. They can play a key role in sorption intensification due to the possibility of forming hydrogen bonds. The nitrogen present in this group as a strongly electronegative atom is a proton acceptor. The number of nitrile groups in synthesized MAN-based particles are also presented in Table 2-2. They contain 4.68 - 5.19 mmol/g nitrogen, which indicates a satisfactory amount of the nitrile groups in the adsorbents structure. These groups can increase the adsorption capacity by creating specific interactions between the sorbent and sorbate.

3.2. VFAs recovery using the synthesized resins

Figure 2-1 represents the capacity of each resin to recover VFAs from a mimicked fermentation broth. The maximum loading capacity is observed for HBU in all the resins applied in batch adsorption. It indicates the hydrophobic interaction between the carbon chain of the acids and aromatic rings of the resins. The longer the carbon chain, the higher the capacity of the resins [17,39]. Lewatit has the highest equilibrium loadings of 115 ± 9 and 44 ± 3 [g Acid/kg Adsorbent] for HBU and HPr, respectively. The equilibrium capacity of Lewatit has previously been reported to be 65.2 [g Acid/kg Adsorbent] and 26.5 for HBU and HPr, respectively [17]. The difference might be because of using different batches of Lewatit which possibly differ in the surface area. The maximum loadings of 106 ± 3 , 98 ± 7 and 104 ± 3 [g Acid/kg Adsorbent] were achieved for MAN-DVB 1, MAN-DVB 2 and MAN-DVB 4, respectively. Considering the difference in the BET surface area of Lewatit and these MAN-based resins, their capacity for HBU and HPr is significant, indicating extra affinity between the acids and the adsorbents. The nitrile groups in the structure of MAN-based resins enable the formation of hydrogen bonds with the acids. In comparison, the capacity of the PS-based resins is relatively low with PS-DVB 3 having the lowest loading of 25 [g Acid/kg Adsorbent] as well as the lowest surface area. In terms of HPr and HAc adsorption capacity, it is approximately in the same order of magnitude for all MAN-based resins and Lewatit. Generally, MAN-based adsorbents have higher loading values than non-functionalized PS-DVB-based resins for the corresponding acid.

Methacrylonitrile-based Adsorbents for Recovery of VFAs

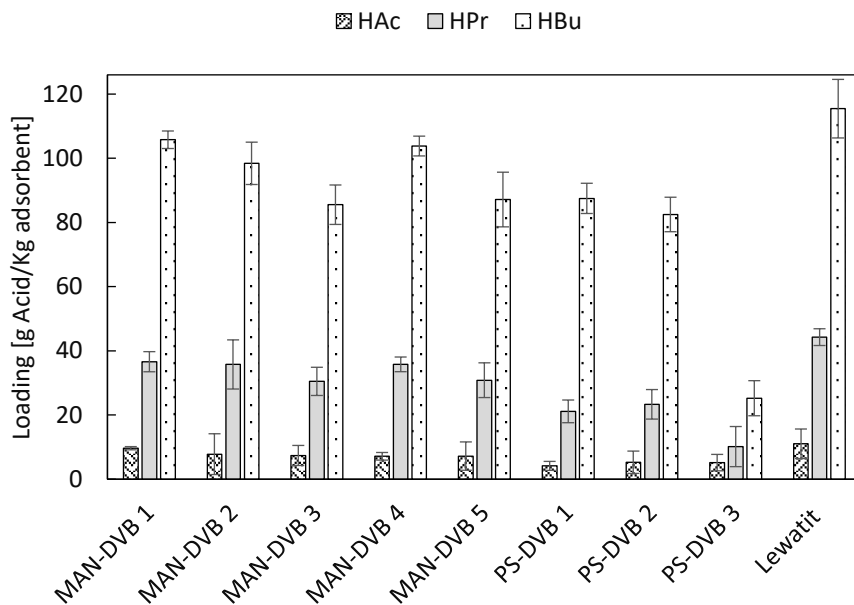


Figure 2-1. Measured capacity of various hydrophobic resins to recover the VFAs from a concentrated mimicked fermentation broth, the concentration of each acid in the feed is 1.25 wt%, batch adsorption is performed with resin to feed mass ratio of 0.5:11 at room temperature, contact time of 1 h and >500 rpm.

Methacrylonitrile-based Adsorbents for Recovery of VFAs

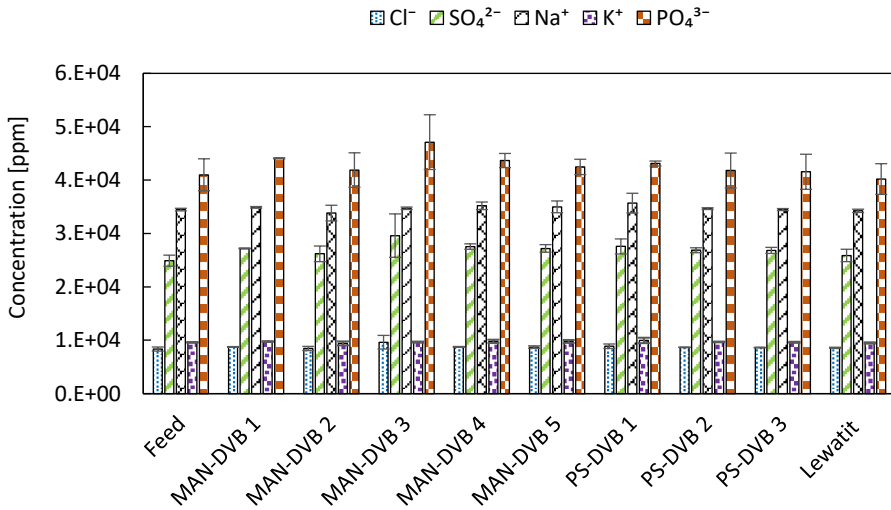


Figure 2-2. Determination of the capacity of various hydrophobic resins to adsorb salts from the concentrated mimicked fermentation broth during VFA recovery, batch adsorption is performed with resin to feed mass ratio of 0.5:11 at room temperature, contact time of 1 h and >500 rpm.

Next to the acid loading, it is also relevant to study the impact of the salts on the capacity of the resins, as these salts are usually present in wastewaters. The ions Cl^- , SO_4^{2-} , Na^+ , K^+ and $\text{H}_2\text{PO}_4^-/\text{HPO}_4^{2-}/\text{PO}_4^{3-}$ are representing the salts as they are the dissociated form of their corresponding salts in the aqueous solution. Therefore, comparing their concentration before and after adsorption can provide more information on whether or not there is a competitive adsorption between the VFAs and the salts. Figure 2-2 shows the concentration of the ions, determined by IC. The concentration of the ions in the “Feed” represents their concentration before starting batch adsorption. As can be clearly seen from the graph, the concentration of all the ions remains constant before and after adsorption for each adsorbent. It illustrates that there is no interaction between the resins and the salts which

is a benefit to have high capacity for the VFAs. This observation is highly interesting, since it was previously reported that amine-based adsorbents have high affinity towards the mineral acids, originating from the salts [17]. In fact, the amine-based ion exchange resins attract the salts via ion exchange reaction with their corresponding mineral acid form to comply to the charge neutrality constraint [17]. For example, the competitive adsorption capacity of amine-functionalized resins for H_3PO_4 is reported to be about 200 [g Acid/kg Adsorbent], reducing the VFAs loading capacity significantly [17]. In the present work, the nitrile-based particles did not attract the mineral acids which can be explained by the lower basicity of the nitrile groups than the amine groups [40,41]. It implies a higher selectivity of the nitrile-based adsorbents towards VFAs rather than minerals (salts). Since also a higher adsorption was measured for the VFAs than with non-functionalized PS-DVB, the use of nitrile functionality for VFA adsorption appears to represent a new direction for future research and application of adsorption technology in VFA recovery from diluted broths.

4. Conclusion

In this chapter, the recovery of the VFAs from a mimicked fermentation broth is studied by an adsorption technique. The loading capacity of various adsorbents was examined by performing batch experiments. The maximum equilibrium VFA loading of about 153 [g Acid/kg Adsorbent] was obtained using MAN-based resins. While having a comparable surface area to MAN-based resins, the non-functionalized PS-DVB-based adsorbents exhibited lower adsorption capacity. This observation is tentatively explained by

assuming that hydrogen bonding interactions are operational between the acid constituents and the MAN-based particles, involving nitrile groups of the adsorbents.

In this study, low water up-take was the great feature of the synthesized PS-DVB due to their high hydrophobicity and small pore volume. They displayed 3-4 times lower water-up take, compared to MAN-functionalized resins. Moreover, their water up-take was less than commercial Lewatit. The low water loading implies PS-DVB resins with small pore volume and high surface area can also be an appropriate candidate to selectively separate the acids from a dilute aqueous solution, followed by thermal regeneration to effectively recover the VFAs at high concentration.

Nomenclature:

BET	Brunauer-Emmett-Teller
DVB	Divinylbenzene
HBu	Butyric acid
HPr	Propionic acid
HAc	Acetic acid
HLa	Lactic acid
HPLC	High Pressure Liquid Chromatography
IC	Ion Chromatography
MAN	Methacrylonitrile
OFMSW	Organic Fraction of Municipal Solid Waste
PS	Polystyrene
PEG	Polyethylene Glycol
SS	Sewage Sludge
ST	Styrene
THF	Tetrahydrofuran
VFAs	Volatile Fatty Acids
δ	Solubility Parameter

References

- [1] J. Tamis; B.M. Joosse; M.C.M.v. Loosdrecht; R. Kleerebezem, High-rate volatile fatty acid (VFA) production by a granular sludge process at low pH. *Biotechnology and Bioengineering*. **2015**, *112*, 2248-2255.
- [2] R. Kleerebezem; B. Joosse; R. Rozendal; M.C.M. Van Loosdrecht, Anaerobic digestion without biogas? *Reviews in Environmental Science and Bio/Technology*. **2015**, *14*, 787-801.
- [3] K. Johnson; Y. Jiang; R. Kleerebezem; G. Muyzer; M.C.M. van Loosdrecht, Enrichment of a Mixed Bacterial Culture with a High Polyhydroxyalkanoate Storage Capacity. *Biomacromolecules*. **2009**, *10*, 670-676.
- [4] P. Sukphun; S. Sittijunda; A. Reungsang, Volatile Fatty Acid Production from Organic Waste with the Emphasis on Membrane-Based Recovery. *Fermentation*. **2021**, *7*, 159.
- [5] Y. Razali; H. Tajarudin; Z. Daud, Extraction of Volatile Fatty Acids from Leachate via Liquidliquid Extraction and Adsorption Method. *International Journal of Integrated Engineering*. **2018**, *10*, 79-84.
- [6] A. Patel; O. Sarkar; U. Rova; P. Christakopoulos; L. Matsakas, Valorization of volatile fatty acids derived from low-cost organic waste for lipogenesis in oleaginous microorganisms-A review. *Bioresource Technology*. **2021**, *321*, 124457.

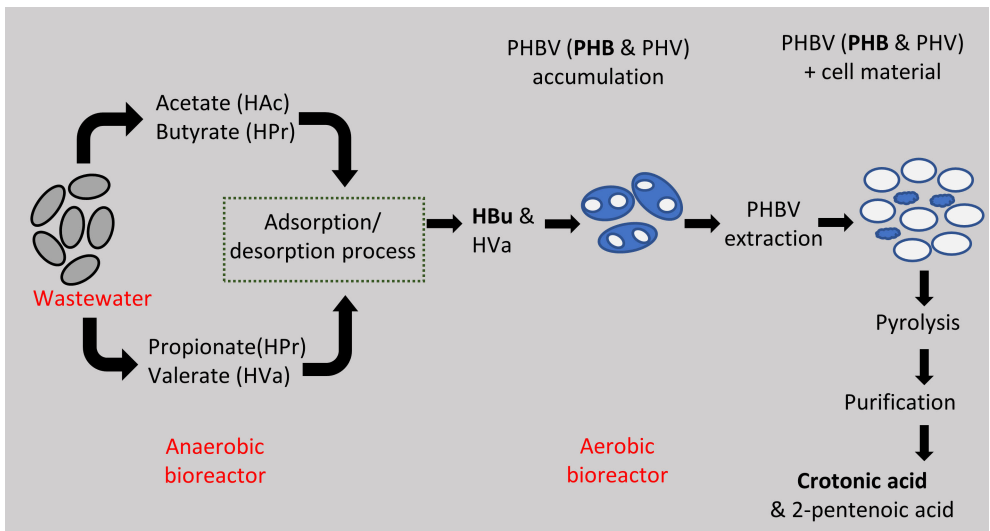
- [7] S. Greses; E. Tomás-Pejó; C. González-Fernández, Agroindustrial waste as a resource for volatile fatty acids production via anaerobic fermentation. *Bioresource Technology*. **2020**, *297*, 122486.
- [8] F. Battista; G. Strazzera; F. Valentino; M. Gottardo; M. Villano; M. Matos; F. Silva; M.A. M. Reis; J. Mata-Alvarez; S. Astals; et al., New insights in food waste, sewage sludge and green waste anaerobic fermentation for short-chain volatile fatty acids production: A review. *Journal of Environmental Chemical Engineering*. **2022**, *10*, 108319.
- [9] M. Atasoy; I. Owusu-Agyeman; E. Plaza; Z. Cetecioglu, Bio-based volatile fatty acid production and recovery from waste streams: Current status and future challenges. *Bioresource Technology*. **2018**, *268*, 773-786.
- [10] S. Bengtsson; J. Hallquist; A. Werker; T. Welander, Acidogenic fermentation of industrial wastewaters: Effects of chemostat retention time and pH on volatile fatty acids production. *Biochemical Engineering Journal*. **2008**, *40*, 492-499.
- [11] C. Bruni; A. Foglia; A.L. Eusebi; N. Frison; Ç. Akyol; F. Fatone, Targeted Bio-Based Volatile Fatty Acid Production from Waste Streams through Anaerobic Fermentation: Link between Process Parameters and Operating Scale. *ACS Sustainable Chemistry & Engineering*. **2021**, *9*, 9970-9987.
- [12] J. Tamis; B. Joosse; M.v. Loosdrecht; R. Kleerebezem, High-rate volatile fatty acid (VFA) production by a granular sludge process at low pH. *Biotechnology and Bioengineering*. **2015**, *112*, 2248-2255.
- [13] W.S. Lee; A.S.M. Chua; H.K. Yeoh; G.C. Ngoh, A review of the production and applications of waste-derived volatile fatty acids. *Chemical Engineering Journal*. **2014**, *235*, 83-99.
- [14] H. Chen; F. Liu; Q. Wang; X. Zhen; B. Wang; S. Wang; J. Zhang; L. Su; Z. Wang; S. Zhu, Production of volatile fatty acids concomitant with phosphorus removal and lignin recovery by co-fermentation of waste activated sludge and black liquor. *Journal of Cleaner Production*. **2022**, *355*, 131806.
- [15] Z.W.W.L.P.L.Y.W.J.C.P.o.V.F.A.f.S.M.D.o.P.C.V.C.D. Wang; A. Fermentation Broth Availability. *Water* **2022**, *14*.
- [16] M.R.Z. Mamat; H. Ariffin; M.A. Hassan; M.A.K. Mohd Zahari, Bio-based production of crotonic acid by pyrolysis of poly(3-hydroxybutyrate) inclusions. *Journal of Cleaner Production*. **2014**, *83*, 463-472.
- [17] E. Reyhanitash; S.R.A. Kersten; B. Schuur, Recovery of Volatile Fatty Acids from Fermented Wastewater by Adsorption. *ACS Sustainable Chemistry & Engineering*. **2017**, *5*, 9176-9184.
- [18] T. Brouwer; B.C. Dielis; J.M. Bock; B. Schuur, Hydrophobic Deep Eutectic Solvents for the Recovery of Bio-Based Chemicals: Solid-Liquid Equilibria and Liquid-Liquid Extraction. *Processes*. **2021**, *9*, 796.
- [19] F. Rizzioli; F. Battista; D. Bolzonella; N. Frison, Volatile Fatty Acid Recovery from Anaerobic Fermentate: Focusing on Adsorption and Desorption Performances. *Industrial & Engineering Chemistry Research*. **2021**, *60*, 13701-13709.
- [20] D. Rodríguez-Llorente; A. Bengoa; G. Pascual-Muñoz; P. Navarro; V.I. Águeda; J.A. Delgado; S. Álvarez-Torrellas; J. García; M. Larriba, Sustainable Recovery of Volatile Fatty Acids from Aqueous Solutions Using Terpenoids and Eutectic Solvents. *ACS Sustainable Chemistry & Engineering*. **2019**, *7*, 16786-16794.
- [21] L.M.J. Sprakel; B. Schuur, Solvent developments for liquid-liquid extraction of carboxylic acids in perspective. *Separation and Purification Technology*. **2019**, *211*, 935-957.

- [22] Š. Schlosser; J. Marták; M. Blahušiak, Specific phenomena in carboxylic acids extraction by selected types of hydrophobic ionic liquids. *Chemical Papers*. **2018**, *72*, 567-584.
- [23] F.S. Oliveira; J.M.M. Araújo; R. Ferreira; L.P.N. Rebelo; I.M. Marrucho, Extraction of l-lactic, l-malic, and succinic acids using phosphonium-based ionic liquids. *Separation and Purification Technology*. **2012**, *85*, 137-146.
- [24] M. Blahušiak; Š. Schlosser; J. Marták, Extraction of butyric acid with a solvent containing ammonium ionic liquid. *Separation and Purification Technology*. **2013**, *119*, 102-111.
- [25] E. Reyhanitash; E. Fufachev; K.D. van Munster; M.B.M. van Beek; L.M.J. Sprakel; C.N. Edelijn; B.M. Weckhuysen; S.R.A. Kersten; P.C.A. Bruijninx; B. Schuur, Recovery and conversion of acetic acid from a phosphonium phosphinate ionic liquid to enable valorization of fermented wastewater. *Green Chemistry*. **2019**, *21*, 2023-2034.
- [26] T. Eregowda; E.R. Rene; J. Rintala; P.N.L. Lens, Volatile fatty acid adsorption on anion exchange resins: kinetics and selective recovery of acetic acid. *Separation Science and Technology*. **2020**, *55*, 1449-1461.
- [27] A. Talebi; Y. Razali; N. Ismail; M. Rafatullah; H. Tajarudin, Selective Adsorption and Recovery of Volatile Fatty Acids from Fermented Landfill Leachate by Activated Carbon Process. *Science of the Total Environment*. **2019**, *707*, 134533.
- [28] A. Yousuf; F. Bonk; J.R. Bastidas-Oyanedel; J.E. Schmidt, Recovery of carboxylic acids produced during dark fermentation of food waste by adsorption on Amberlite IRA-67 and activated carbon. *Bioresource Technology*. **2016**, *217*, 137-140.
- [29] S. Rebecchi; D. Pinelli; L. Bertin; F. Zama; F. Fava; D. Frascari, Volatile fatty acids recovery from the effluent of an acidogenic digestion process fed with grape pomace by adsorption on ion exchange resins. *Chemical Engineering Journal*. **2016**, *306*, 629-639.
- [30] C. Fernando-Foncillas; C.I. Cabrera-Rodríguez; F. Caparrós-Salvador; C. Varrone; A.J.J. Straathof, Highly selective recovery of medium chain carboxylates from co-fermented organic wastes using anion exchange with carbon dioxide expanded methanol desorption. *Bioresource Technology*. **2021**, *319*, 124178.
- [31] C.I. Cabrera-Rodríguez; L. Paltrinieri; L.C.P.M. de Smet; L.A.M. van der Wielen; A.J.J. Straathof, Recovery and esterification of aqueous carboxylates by using CO₂-expanded alcohols with anion exchange. *Green Chemistry*. **2017**, *19*, 729-738.
- [32] C.S. López-Garzón; A.J.J. Straathof, Recovery of carboxylic acids produced by fermentation. *Biotechnology Advances*. **2014**, *32*, 873-904.
- [33] M.T. Gokmen; F.E. Du Prez, Porous polymer particles—A comprehensive guide to synthesis, characterization, functionalization and applications. *Progress in Polymer Science*. **2012**, *37*, 365-405.
- [34] D.J. Malik; A.W. Trochimczuk; S. Ronka, Nanostructured Synthetic Carbons Obtained by Pyrolysis of Spherical Acrylonitrile/Divinylbenzene Copolymers. *PLOS ONE*. **2012**, *7*, e43354.
- [35] S. Ronka, New sulfur-containing polymeric sorbents based on 2,2'-thiobisethanol dimethacrylate. *Pure and Applied Chemistry*. **2019**, *91*, 409-420.
- [36] M. Wawrzkiwicz; B. Podkościelna, Innovative Polymer Microspheres with Chloride Groups Synthesis, Characterization and Application for Dye Removal. *Processes*. **2022**, *10*, 1568.

- [37] F.S. Macintyre; D.C. Sherrington, Control of Porous Morphology in Suspension Polymerized Poly(divinylbenzene) Resins Using Oligomeric Porogens. *Macromolecules*. **2004**, *37*, 7628-7636.
- [38] O. Okay, Macroporous copolymer networks. *Progress in Polymer Science*. **2000**, *25*, 711-779.
- [39] E.V. Fufachev; B.M. Weckhuysen; P.C.A. Bruijninx, Toward Catalytic Ketonization of Volatile Fatty Acids Extracted from Fermented Wastewater by Adsorption. *ACS Sustainable Chemistry & Engineering*. **2020**, *8*, 11292-11298.
- [40] E.D. Raczyńska; J.-F. Gal; P.-C. Maria, Enhanced Basicity of Push–Pull Nitrogen Bases in the Gas Phase. *Chemical Reviews*. **2016**, *116*, 13454-13511.
- [41] M.A. Smith, Organic chemistry, 3rd edition. *Journal of Chemical Education*. **1974**, *51*, A181.

Chapter 3

Recovery of Dilute (Bio-Based) Volatile Fatty Acids by Adsorption with Magnetic Hyperthermal Swing Desorption



This chapter is adapted from:

Elhami V., Hempenius M.A., Vancso G.J., Krooshoop E.J.G., Alic L., Qian X., Jebur M., Wickramasinghe R., Schuur B., *“Recovery of Dilute (Bio-Based) Volatile Fatty Acids by Adsorption with Magnetic Hyperthermal Swing Desorption”*, **2023**, (under preparation).

Abstract

In this study, we describe the preparation of superparamagnetic porous adsorbent beads to recover volatile fatty acids (VFAs) in concentrated form from dilute aqueous streams. Our system is based on poly(divinylbenzene) (PDVB) impregnated with superparamagnetic magnetite nanoparticles (MNPs). The MNPs were synthesized by the coprecipitation method and functionalized with oleic acid (OA). Following this step, the OA-MNPs (OA grafted MNPs) were embedded in the matrix of the polymer during suspension polymerization. The porous particles had an average size of $222\pm 40\ \mu\text{m}$ with a surface area of $496\pm 10\ \text{m}^2/\text{g}$. Furthermore, they contained $11\pm 1\ \text{wt}\%$ MNPs with an average core size of 10 nm. VFAs were adsorbed from a dilute aqueous solution (containing 0.25 wt% of each acid). A corresponding total saturation capacity of 43 g carboxylic acid per kg adsorbent was found, with the highest capacities for butyric acid at 30 [g acid/kg adsorbent]. Desorption was performed in two steps, starting with alternating magnetic field (AMF) heating at 25 mT and 52 kHz, followed by a hot N_2 stripping stage. During AMF heating, it was found that $90\pm 9\%$ of the water in the pores was removed which physically filled the pores during adsorption of VFAs, while only $11\pm 2\%$ of total loaded VFAs were removed by AMF heating. Subsequently, the remaining VFAs were completely recovered in concentrated form using hot N_2 stripping.

1. Introduction

VFAs are short chain carboxylic acids consisting of less than six carbon atoms and have a wide range of applications in the food, pharmaceutical and chemical industries. For instance, they may be used in the production of biodiesel, biogas, bioplastics, biohydrogen and electricity [1-4]. VFAs are one of the main intermediates during anaerobic sludge fermentation [3,5-7]. However, producing VFAs via fermented wastewater streams yields a broth with low VFA contents [8]. Therefore, there is a great need for a robust recovery and concentration technique to produce VFAs in a profitable biological process, promoting circular chemistry. Implementing green chemistry is identified as one of the most important demands for the chemical manufacturers [9].

Affinity separation techniques enable to recover the target chemicals from dilute and relatively complex streams [10,11]. Adsorption is one of the affinity separation methods, which demonstrated a great potential to effectively recover VFAs from dilute solutions [12-14]. Various adsorbents were reported for adsorption of carboxylic acids from a fermentation broth [12,15,16]. For example, anion exchange resins can separate dissociated acids in carboxylate form, which is interesting as the pH of the mixed microbial culture is usually higher than the pK_a of the VFAs [17,18]. However, the recovery of the carboxylates in acid form from anion exchange resins is challenging, because they must be protonated by adding extra chemicals (e.g. H_2SO_4) which produce a stoichiometric amount of salt waste [17]. Cabrera-Rodríguez et al. proposed a regeneration method for anion exchange resins loaded with acetate which prevents salt waste production [17]. The authors applied CO_2 -expanded methanol to recover acetic acid in a

solution of methanol and CO₂, followed by direct esterification of the acid to produce methyl acetate. Although it simplified the effective regeneration of the resin, the acids were obtained as ester, and not as pure and protonated acid. For certain applications this route is a good solution. In cases when the acids in pure form are required, recovery through the vapor phase enables a simpler downstream fractionation which was observed using a non-functionalized polystyrene divinyl benzene resin [13].

Non-functionalized polystyrene divinylbenzene based polymers with the commercial name Lewatit VP OC 1064 MD PH displayed high selectivity towards carboxylic acids in a mineral rich aqueous stream [13]. It was found that it is possible to recover the acids through the vapor phase by thermal desorption. During adsorption with this hydrophobic polymer, the pores become filled with the dilute solution of VFAs. The VFAs then bind to the surface of the particle through hydrophobic interactions and hydrogen bond- π interactions, but the pores of the particle remain filled with water. When these particles are directly regenerated using an efficient recovery technique such as hot N₂ stripping, both the water and the VFAs evaporate from the particle, resulting in a product stream with 10 wt% VFAs. This indicates that the VFAs are already significantly (ten times) more concentrated than the fermentation broth, while for propionic acid and butyric acid the concentration factor was even higher [13]. However, further reducing the amount of water and obtaining an even stronger concentration factor would be desired. In order to achieve even higher concentration factors, it would be beneficial to remove the water in the pores of the particle prior to recovering the VFAs that bind to the

surface of the particles. A product obtained this way with a lower water content reduces the energy use in further processing.

Reyhanitash et al. investigated the possibility of varying the temperature of the hot nitrogen stripping, similar to the temperature profile used in gas chromatography, to directly fractionate the loaded acids during regeneration of the adsorbent [13]. The authors found that indeed it is possible to recover the acids in high purity by applying a proper temperature profile based on the boiling point of the loaded components. The highest boiling of the VFAs in the mixture, butyric acid, was obtained in concentrations up to 90 wt% while its initial concentration in the feed was 0.25 wt%. However, this high acid concentration is only achieved for a fraction of the total loaded acid. During the desorption stages in the process, the acid concentration in the condensed vapor recovered from the desorption continuously increases, meaning that they evaporate already partially in earlier stages. As a result, a large fraction of the acids has been co-desorbed during removal of water from the pores and the quantity of the recovered acids in the most concentrated samples was not so high. Therefore, further improvement of the adsorption-desorption technique is desired, especially aiming at developing an improved desorption approach to effectively recover larger fractions of the adsorbed VFAs at high concentration.

The current study aimed at substantially enhancing the fractionation efficiency during desorption to obtain larger amounts of acids with high concentrations. One hypothesis is that the heat-insulating character of polystyrene-based resins limits heating up the interior of the resin

particles by hot N₂ stripping, resulting in a temperature gradient inside the particles that hinders sharper fractionation. Because the temperature profile shows the lowest temperature in the center of the resins and the highest temperature at the outer surface, a gradient is formed that is opposite to the concentration gradient which is directed from higher concentration in the center towards lower concentration on the outside of the particles. At the increasing temperature towards the outer radius of the particles, the carboxylic acids exhibit higher volatility, and for that reason the selectivity of water removal is reduced.

Ideally, the thermal and concentration gradients should be aligned in the same direction. In the present work, we achieve this alignment by synthesis and application of a novel adsorbent that may heat particles from inside to facilitate separation of water and the acids during thermal desorption. A superparamagnetic adsorbent was synthesized by impregnating poly(divinylbenzene) (PDVB) polymer with oleic acid coated magnetic nanoparticles (OA-MNPs). Loading the adsorbent with MNPs that are coated with a bio-based shell provides an opportunity to generate heat inside the particles by applying an alternating magnetic field (AMF) [19], while part of the actual mass of fossil-based polymers in the resins is replaced by molecules of bio-based nature and MNP that are so safe that they are also applied in medicine [20-22].

Heat generation via an AMF was previously used to locally produce heat for hyperthermia treatment whereby cancer cells are disrupted by injecting MNPs in the tumor and exposing the patient to an oscillating magnetic field [20-22]. Magnetite particles contain Weiss domains in

which magnetic spins are aligned [23]. After temporal magnetic actuation, upon relaxation the MNPs can release heat. Theoretically, the single domain MNPs can produce heat in the presence of an oscillating magnetic field via two relaxation mechanisms, i.e. Brownian and Neel relaxations [21,24]. In Brownian relaxation, the heat is generated due to the energy loss produced by the rotation of the whole MNPs to align along the external magnetic field direction. Neel relaxation involves the internal rotation of the magnetic moments of the MNPs [25]. By immobilizing the MNPs in the polymer matrix, they are no longer free to rotate. Therefore, the relaxation mechanism is dominated by Neel relaxation [26,27].

The possibility to generate bubbles inside the porous resin by evaporation of water upon inducing the magnetic hyperthermia was also considered as an opportunity to mechanically remove water from the pores of the polymer. Bubble formation due to evaporation of part of the water will then drive liquid water mechanically from the pores, without having to evaporate the corresponding fraction of the water. The focus of the present work is to explore temperature swing-based desorption where heating is generated inside the resin matrix. We achieve this by synthesis and characterization of the superparamagnetic resin. Using model fermentation broths, we determine adsorption capacity and investigate desorption due to magnetically induced heating followed by hot N₂ stripping as shown in Figure 3-1.

VFA Adsorption with Magnetic Hyperthermal Swing Desorption

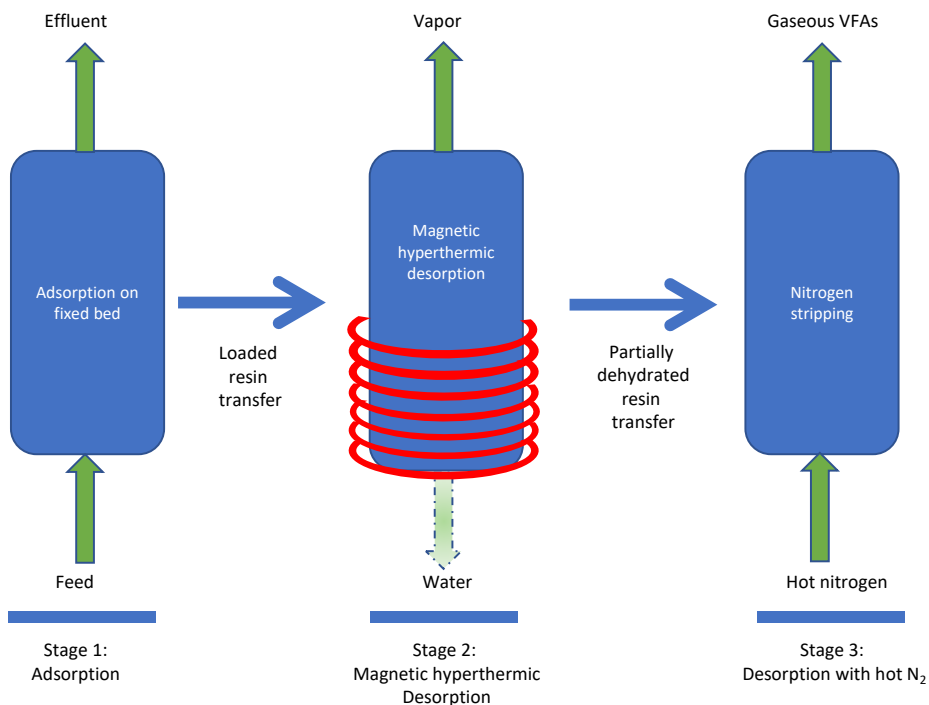


Figure 3-1. Schematic overview of adsorption and thermal desorption of VFAs from superparamagnetic polymer

During the first desorption stage, the resins were visually inspected to detect whether liquid water was expelled from the resin particles, and overall mass balances over the acids were calculated to conclude on the applicability of this new magnetically actuated approach in desorption.

2. Material and Methods

2.1. Chemicals

Hydrochloric acid (37%) was purchased from Honeywell Fluka. Ammonium hydroxide solution (28.0-30.0% NH₃ basis), methanol (MeOH, >99%), diethyl ether (>99%), anhydrous iron(III) chloride (97%), butyric acid (Hbu, >99%), Acetic acid (HAc, >99.7%), propionic acid (HPr, >99.5%), anhydrous sodium phosphate dibasic (>99%), anhydrous sodium sulphate (>99%), potassium chloride (>99%), poly(vinyl alcohol) (PVA; 88% hydrolyzed, Mn~125000 (Mowiol 18-88)), sodium chloride (>99%), Polydimethylsiloxane (PDMS) (viscosity 200/100 cSt), azobis(isobutyronitrile) (AIBN), and Divinylbenzene 80% (DVB) were purchased from Sigma-Aldrich. Crystalline lactic acid (HLA, >98%) was provided by Corbion. Potassium hydroxide (1 M) and toluene (≥99.9%) were supplied by Merck, iron(II) chloride tetrahydrate (99>%) by Acros Organics and Oleic acid (70%) by Fisher Scientific. The water used was ultrapure (Milli-Q, with a resistance of 18.2 μΩ cm at 25 °C).

2.2. Synthesis of OA-MNPs

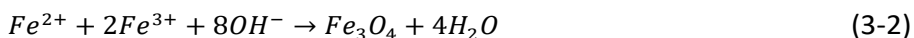
MNPs were synthesized by a coprecipitation method [28]. Briefly, the pH of 50 mL Milli-Q water was adjusted to pH = 2 by adding a few drops of hydrochloric acid solution. Afterwards, 1.6326 g of iron(III) chloride and 1.0241 g iron(II) chloride tetrahydrate with a molar ratio of 2:1 were dissolved in the prepared solution at room temperature and sonicated under nitrogen gas for 1 h. Subsequently, 20 mL of

ammonium hydroxide solution was rapidly added to the mixture and sonicated for another 1 h.

To functionalize the nanoparticles, the mixture was heated to 80 °C and 0.5989 g OA was added to the solution [29]. After 1 h, the OA-MNPs were collected from the solution using a static magnet, washed several times with Milli-Q water and ethanol, and dried in a vacuum oven for 12 h at 50 °C. The yield of synthesized MNPs was calculated using Eq. (3-1):

$$Yield [\%] = \frac{(m_{OA-Fe_3O_4} \times w_{Fe_3O_4}) \times 100}{m_{Fe_3O_4}^t} \quad (3-1)$$

Where $m_{OA-Fe_3O_4}$ is the mass of collected OA-MNPs after drying, $w_{Fe_3O_4}$ is the MNPs weight fraction of the OA-MNPs as determined by analysis and $m_{Fe_3O_4}^t$ is the theoretical mass of MNPs at 100% conversion of all ferric and ferrous ions in the following coprecipitation reaction:



2.3. Polymerization of magnetic PDVB resins

Magnetic PDVB resins were prepared via suspension polymerization as reported by Macintyre and Sherrington [30] with a modification in terms of adding hydrophobic OA-MNPs. The aqueous phase was prepared by dissolving 0.52 g PVA and 2.31 g sodium chloride in 70 mL Milli-Q water in the reactor. The organic phase containing 1.75 mL DVB, 0.14 mL PDMS, 1.61 mL toluene, 0.0175 g AIBN and 0.175 g OA-MNPs

was sonicated for 15 minutes, and then added to the continuous aqueous phase dropwise while vigorously stirring with a mechanical stirrer at 350 rpm. The polymerization was performed at 80 °C for 6 h under nitrogen atmosphere. The resulting beads were separated from the solution using a static magnet. Subsequently, they were washed with water and methanol, and then extracted overnight in a Soxhlet apparatus using toluene to remove any unreacted monomers and the porogens. Afterwards, the polymer beads were washed with methanol and diethyl ether and dried in a vacuum oven at 50 °C. Eq.(3-3) was used to calculate the yield of suspension polymerization:

$$Yield [\%] = \frac{m_{Polymer} \times (1 - w_{Fe_3O_4})}{m_{Monomer}} \times 100 \quad (3-3)$$

Where $m_{Polymer}$ is the mass of the collected dry polymer, $w_{Fe_3O_4}$ is the weight fraction magnetite content of the polymer based on AAS analysis and $m_{Monomer}$ is the mass of DVB used for the polymerization.

2.4. Adsorption in a packed bed column

Figure 3-2 represents the schematic of the setup used for adsorption and hot N₂ stripping. While in a previous study only hot N₂ stripping was applied [13], in the current work, we included a magnetic hyperthermal desorption phase by AMF between the adsorption and the desorption by hot N₂ stripping. The setup for AMF desorption is displayed in Figure 3-3. The capacity of the adsorbent to adsorb VFAs was determined in a packed bed column using a model fermentation broth with the composition as shown in Table 3-1, which is referred to as the feed. The

VFA Adsorption with Magnetic Hyperthermal Swing Desorption

adsorbent (0.5 g) was loaded into the column (d=1 cm, l=3 cm, $\frac{3}{4}$ filling allowing for some swelling), and the feed was pumped through it at a flow rate of 0.2 mL/min at room temperature for >200 minutes. Sampling was done from the outlet of the column over time and analysed to measure the concentration of the acids.

Table 3-1. Composition of the mimicked fermentation broth.

solution	Concentration [wt%]				Concentration [mol/L]			pH
	HAc	HPr	HBu	HLa	KCl	Na ₂ SO ₄	Na ₂ HPO ₄	
Feed	0.25	0.25	0.25	0.25	0.05	0.05	0.1	4.98

After a complete breakthrough, and stopping of the pump, the major fraction of the remaining feed was removed from the dead volume of the column by flushing with nitrogen at room temperature. Afterwards, a sample of the particles was washed with 1M KOH to measure the total mass of the loaded acids. The ratio of the base solution to the adsorbent was 15 mL to 1 g based on a previously published method [13]. The capacity of the adsorbent was calculated using Eq. (3-4):

$$q = \frac{(C_e \times m_s) \times M}{m_p} \quad (3-4)$$

Where q is the amount of adsorbate in the adsorbent [g of Acid/Kg of adsorbent], m_s is the total mass of liquid after base washing of the particles, m_p is the mass of loaded adsorbent used for KOH washing, C_e is the final concentration for the VFAs expressed in weight percent of the corresponding compound in the base solution, W [kg] is the total

VFA Adsorption with Magnetic Hyperthermal Swing Desorption

mass of the resins used for adsorption and M is the total mass of loaded adsorbents after adsorption.

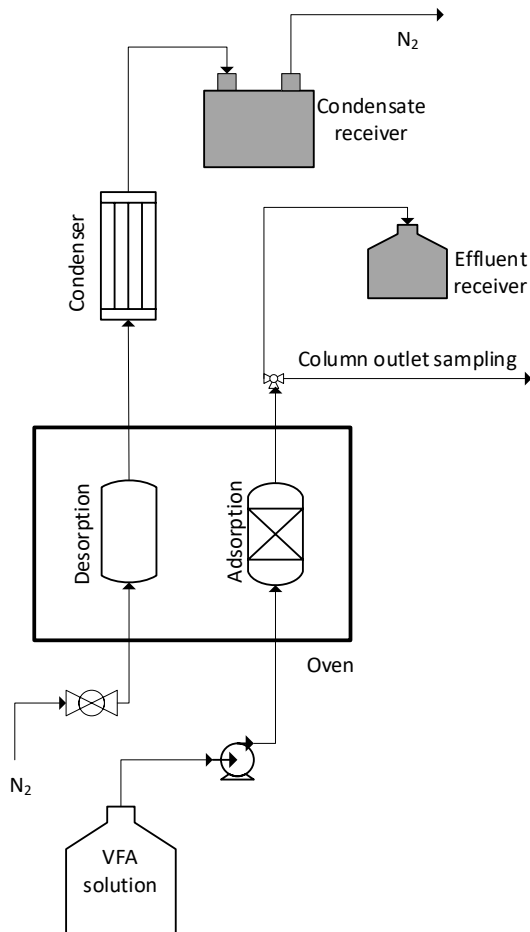


Figure 3-2. Schematic view of the setup used for adsorption and hot N₂ desorption

2.5. Thermal desorption experiments

Thermal desorption was performed using magnetic heating followed by hot N₂ stripping. An AMF was applied to generate the heat inside the particles. Subsequently, hot-nitrogen stripping was used to recover the adsorbed acids. A custom-designed set-up was built to generate an AMF illustrated in Figure 3-3. A hollow copper coil (6 mm outer diameter, and 4 mm inner diameter) was used to allow circulating chilled water to pass through to keep the temperature of the coil at an acceptable level. The copper coil with 30 mm diameter contained 7 turns with a distance of 2 mm between the turns. It was attached to a heat station which was connected to a 320 W power supply (Bench, EA Electro-Automatik, EA-PS 2000 B series). The voltage and current were set at 25 V and 13 A, respectively. The actual values fluctuated between $24.5 < V < 25.3$ and $11.8 < I < 12.9$. Thus, a magnetic field with 25 mT and 52 kHz was produced. The loaded particles from the adsorption step were transferred to the column which featured an adiabatic shield (double walled, vacuum shielded), which was placed inside the copper coil. The adiabatic shield around the column prevented heat loss between the column and the coil. Subsequently, the magnetic field was employed to remove most of the water present in the pores of the resin.

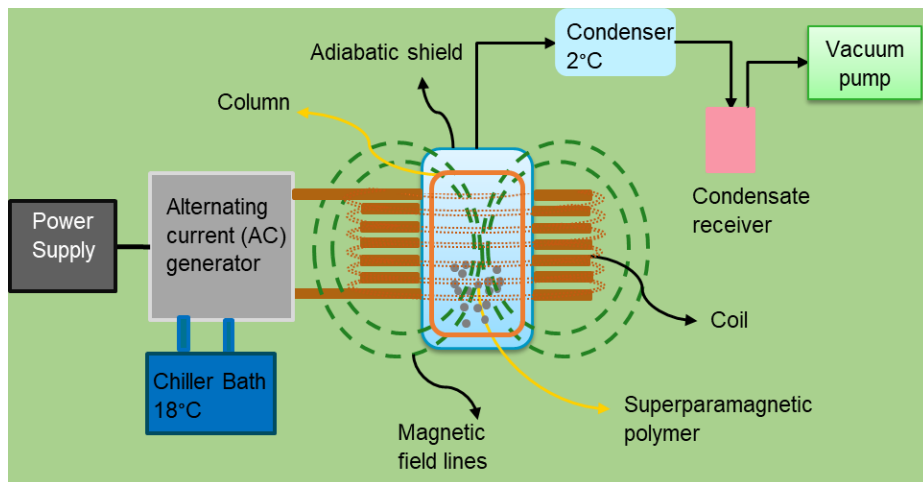


Figure 3-3. Schematic view of the alternating magnetic field setup used for magnetic desorption step

After magnetic hyperthermic desorption, the particles were transferred to another column and placed in the desorption section of the setup as shown in Figure 3-2. Afterwards, hot nitrogen gas was flushed at 0.1 L/min to desorb the VFAs from the adsorbent and collect them by condensation at 2 °C. In essence, this is the same procedure as published earlier [13]. Of course, in future applications, the magnetic coil should be integrated in a column that can also facilitate the adsorption step and the nitrogen stripping step. However, here we applied the adiabatic shield and cooled the coil to demonstrate the concept of magnetically induced heating without affecting the measurements by significant heat losses from the column and the generated heat by the coil. Table 3-2 represents the temperature profile which was employed for hot N₂ stripping. After completing the thermal desorption step, KOH washing was performed on the regenerated particles to determine the mass of remaining acids.

VFA Adsorption with Magnetic Hyperthermal Swing Desorption

Table 3-2. Temperature profile used for thermal desorption by stripping with 0.1 L/min hot N₂.

Temperature [°C]	Duration [h]
50	1
120	1
180	1

The desorption efficiency of both regeneration steps for each of the acids was calculated by Eq.(3-5):

$$\eta_{desorption} [\%] = \frac{m_{recovered\ acid}}{m_{loaded\ acid}} \times 100 \quad (3-5)$$

where the mass of the loaded acid [g] was calculated from the capacity determination experiment in section 2.4 and the mass of recovered acid [g] was measured by analysis of collected condensate after each desorption step.

2.6. Analysis

Atomic absorption spectroscopy (AAS). The iron content of the synthesized particles was determined using a Varian SpectrAA 220. The preparation of the sample was performed based on a previously reported method [31]. Briefly, a mixture of HCl and HNO₃ was applied to completely digest the particles. A strong acidic medium was required for the reduction of the magnetite nanoparticles to ferrous ions. A ferrous chloride standard was used for the calibration curve.

The Brunauer-Emmett-Teller (BET). Specific surface areas of the synthesized adsorbents were obtained using N₂ adsorption isotherms determined at 77K using a Micromeritics Gemini VII 2390a.

Scanning electron microscope (SEM). The morphologies of the magnetic polymers were examined by SEM using a Jeol JSM-6010LA analytical electron microscope at a magnification of 45 and 11000, respectively.

Transmission electron microscope (TEM). The core size of magnetite nanoparticles was assessed by TEM. The particles were first dispersed in toluene and then TEM images were taken using a Philips CM300ST-FEG Transmission Electron Microscope 300 kV. The obtained images were analyzed by ImageJ software to calculate the size of the MNPs.

Vibrating-sample magnetometer (VSM). The magnetic susceptibility of the nanoparticles was measured with a Physical Properties Measurement system magnetometer (Quantum Design) at 300 K. The measurement range was -2 T to 2 T. The magnetization was assessed using small vials with weighed amounts of particles added.

High Performance Liquid Chromatography (HPLC). The concentrations of HPr, HBU, HAc, HLa, and H₃PO₄/H₂PO₄⁻/HPO₄²⁻/PO₄³⁻ were measured to an inaccuracy of < 0.5% using a HPLC [Agilent Hi-Plex H column (300 × 7.7 mm) using a refractive index detector on an Agilent 1200 series HPLC system; mobile phase, 5 mM H₂SO₄ solution; column temperature of 65 °C at a flow rate of 0.6 mL/min].

Karl- Fischer Titration (KFT). The water content of the condensate was determined by Karl- Fischer Titration using a Metrohm 787 KFTitrino. Hydranal composite 5 was titrated from a 20 mL burette filled with a mixture of methanol and dichloromethane in volume ratio of 3 to 1. The sample was analyzed in triplicate with a relative error less than 1%.

pH values were measured with a Metrohm pH probe (6.0234.100) connected to a Metrohm 780 pH-meter.

3. Results and discussion

3.1. Characterization of the adsorbent







The synthesized OA-MNPs were characterized by TEM before using them in polymerizations. The MNPs are classified as superparamagnetic when their size is less than approximately 15 nm, being single Weiss domain particles [32]. The core size of the OA-MNPs as measured by TEM was 10 nm demonstrating that superparamagnetic magnetite nanoparticles had been formed.

A series of polymers with various loadings of MNPs was synthesized by varying the mass of OA-MNPs in the polymerization. Table 3-3 is a summary of the synthesized and characterized superparamagnetic polymers. The polymerization yield calculated by Eq. (3-3) was >95% for all batches. The loading of OA-MNPs in the polymer matrix was determined by AAS. It varied from 0 to 15 wt%, resulting in polymer beads with average BET surface areas between 581.98 and 476.34 m²/g. The BET N₂ adsorption- desorption isotherm is included in the

supporting information in the appendix Figure S-3 . Despite the sufficient surface area of the superparamagnetic polymer containing high content of MNPs, it was experimentally observed that by increasing the loading of MNPs above 11 wt%, the resulting beads were not completely spherical and uniform. Therefore, the superparamagnetic polymer with 11 wt% MNPs and $496\pm 10\text{ m}^2/\text{g}$ was selected as an optimum adsorbent for further study. The average pore diameter of the optimum particles was calculated using the BJH (Barrett, Joyner and Halenda) method, and was found to be 8.3 nm, indicating a mesoporous polymer [33]. To control the porosity of the particles, it is possible to adjust the ratio of the porogens in the polymerization method [34,35]. There are three types of porogens, consisting of solvating porogens, non-solvating porogens and linear polymer [36]. The solvating porogens which are a good solvent for the corresponding polymer, result in high porosity with a small pore diameter and a relatively low pore volume [34]. Using a linear polymeric porogen results in a low internal surface area, low pore volume and a large pore diameter [36]. In this work, a mixture of toluene as a solvating diluent and PDMS as a linear polymer was applied, aiming at high internal surface area with a limited pore volume and a large average pore diameter.

VFA Adsorption with Magnetic Hyperthermal Swing Desorption

Table 3-3. Summary of the Characterization of the particles obtained in this study. ^a

Component	Batch No.	Component picture	Yield [%]	Fe ₃ O ₄ [wt%] by AAS	N ₂ BET surface area [m ² /g]	N ₂ BJH average pore diameter [nm]	N ₂ BJH average pore Volume [cm ³ /g]
OA-Fe ₃ O ₄	1		97	75	-	-	-
PDVB	2		97	0	582	8.3	0.41
PDVB+2 wt% OA-Fe ₃ O ₄	3		95	2	578	8.5	0.53
PDVB+5 wt% OA-Fe ₃ O ₄	4		96	5	540	8.4	0.51
PDVB+11 wt% OA-Fe ₃ O ₄	5, 7, 8 ^b		95±3	11±1	496±10	8.3±0.005	0.4±0.002
PDVB+15 wt% OA-Fe ₃ O ₄	6		95	15	476	8.7	0.63

^aAll polymers synthesized once, except for PDVB+11 wt% OA-Fe₃O₄. The photos were taken by a Digital Microscope camera 2.0 Scale with 200x magnification.

^bAs the polymer PDVB+11 wt% OA-Fe₃O₄ visually represented the polymer with high Fe content and uniform particle shape and size distribution, this batch was reproduced.

The morphology of the magnetic polymer was analyzed by SEM. The images are presented in Figure 3-4 which shows that the microspheres are spherical with a smooth surface and with an average particle size of 222 ± 40 μm . Figure 3-4.b shows that there are many pores on the surface of the magnetic polymer beads.

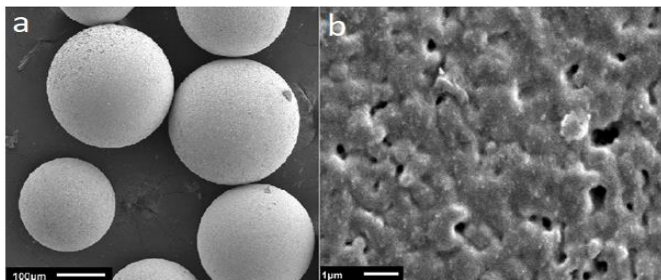


Figure 3-4. Scanning electron microscopy images of (a) magnetic polymer microspheres and (b) surface detail.

The magnetic hysteresis loops of the synthesized Fe_3O_4 and the superparamagnetic polymer microspheres were recorded by VSM and are shown in Figure 3-5. As can be clearly seen from the graph, no hysteresis is visible for both Fe_3O_4 and superparamagnetic polymer which confirms the production of superparamagnetic particles [37,38]. The saturation magnetization of the OA-MNPs was 69 emu/g while it was 17 emu/g for the fixed OA-MNPs in the matrix of the polymer. The lower saturation magnetization of the fixed OA-MNPs might be due to reduced contribution of Brownian relaxation in the overall relaxation after magnetization of the fixed MNPs and oxidation of the surface of the nanoparticles, which leads to a non-magnetic outer layer on the MNPs [39].

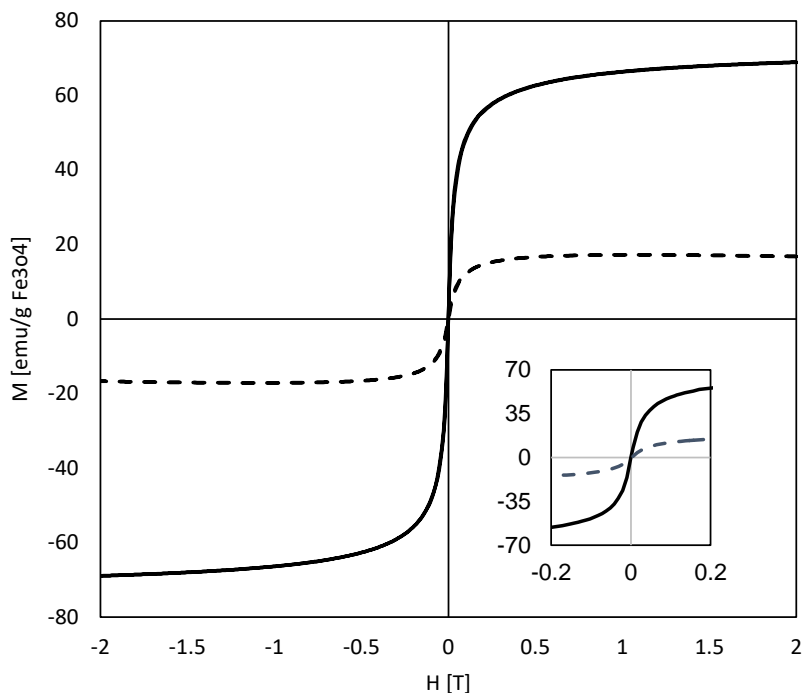


Figure 3-5. Magnetization curve for OA-MNPs (solid line) and OA-MNPs immobilized in the polymer matrix (dashed line). The magnetization was measured in the range of $-2T$ to $2T$ at 300 k .

3.2. Capacity determination in column

The adsorption capacity of the superparamagnetic polymer beads was examined in the packed bed column configuration using approximately 0.5 g magnetic adsorbent. The feed was continuously pumped to the column at a flow rate of 0.2 mL/min at room temperature. By determining the concentration of the eluent over time, breakthrough curves of the acids were obtained which are shown in Figure 3-6. The slowest breakthrough curve was observed for HBU, representing the highest adsorbent capacity towards this acid.

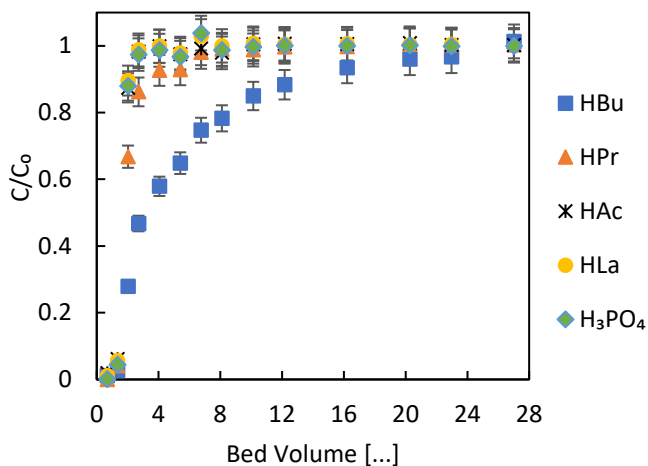


Figure 3-6. Breakthrough curves for the acids in a packed bed column using 0.5 g adsorbent, feed flow rate 0.2 mL/min at room temperature with initial concentration of 0.25 wt% for each carboxylic acid.

The highest capacity for HBu, the acid with the longest carbon chain, supports the assumption that the hydrophobic interaction between the aromatic rings of the adsorbent and carbon chains of the acids are dominant.

The capacity of the adsorbent for each acid after a complete breakthrough is displayed in Table 3-4. Generally, the particles are saturated with all the adsorbates after 27 bed volumes with a total saturation capacity of 43 g carboxylic acid per kg adsorbent using a model fermentation broth containing 1wt% carboxylic acids. Although the commercial non-functionalized polystyrene divinyl benzene polymer had shown a capacity of 76 [g carboxylic Acids/kg adsorbent] due to its higher surface area than the synthesized polymer, the same

trend was observed for adsorption of the VFAs, with the highest capacity for HBU, followed by HPr, and lower capacities for HAc and HLa [13]. Competitive adsorption of the VFAs resulted in the highest loading for HBU and limited capacity for HAc. Due to partial dissociation of H_3PO_4 , there was an interaction between the adsorbent and H_3PO_4 , yielding a capacity of 10 [g Acid/Kg adsorbent]. It can be explained by hydrogen bond- π interactions between undissociated acids and the aromatic rings of the adsorbent which illustrates the potential of the synthesized adsorbent to remove phosphorous from wastewater as well. In this type of hydrogen bonding, the hydrogen attached to the oxygen in the acid structure is attracted by π -electron density which is a poor acceptor [40].

Table 3-4. Capacities determined after a complete breakthrough at room temperature

Adsorbate	Loading [gAcid/Kg adsorbent]
HBU	30
HPr	8
HAc	3
HLa	2
H_3PO_4	10

3.3. Regeneration of the adsorbent

Thermal regeneration of the adsorbent was done in two steps, as indicated in the general outline of the procedure in Figure 3-1. Figure 3-7 displays desorption efficiency for the acids for the two sequential steps. The error bars in Figure 3-7 represent the standard deviation of

duplicate experiments. First, internal heating was conducted using AMF. The loaded particles were subjected to the magnetic field with 25 mT field intensity and 52 kHz frequency under vacuum condition for 1 h, during which from time to time, the column was visually inspected (see also the photographs, Figure S-4 in the appendix). Almost immediately after switching on the magnet, vapor condenses on the walls of the column. We had anticipated that bubbles might be formed inside the particles, so that a significant amount of water could be mechanically pushed out of the particles, without having to evaporate it. This would be manifested by “sweating” of the particles. Due to the condensate on the walls of the column, this hypothesis could unfortunately not be verified by direct visual inspection. On the other hand, the quick condensate formation was an excellent proof that significant amounts of heat were generated by the MNPs inside the polymer matrix, resulting in evaporation of water from the pores of the resin. Following these experiments, the condensate was analyzed by KFT and HPLC to determine water and acids content, respectively. The results indicate that the condensate consists of 1 wt% VFAs and 98 wt% water.

Over the period of magnetic heating, about $90\pm 9\%$ of the total water on the adsorbent was removed, while only $11\pm 2\%$ of total loaded VFAs were co-removed. When N_2 -stripping at $70^\circ C$ was applied instead of AMF, only 68% of the water was removed, while also 28% of the loaded VFAs were co-evaporated (see Table 3-5 for the comparison). These results are comparable with results of Fufachev et al. [41] who regenerated a very similar PS-DVB resin by direct thermal regeneration

with N₂ stripping. This very clearly illustrates the advantage of the magnetic heating, offering a much stronger concentration of VFAs during the regeneration, which will positively enhance downstream fractionations, requiring much less energy due to the significantly reduced amount of water in the stream. Furthermore, conversions can benefit, as follows from the work of Fufachev et al. [41] who applied non-functionalized PS-DVB resin to recover the volatile acids from the fermentation broth and convert them to ketones. The excess amount of water in the condensate deactivated the catalyst and decreased the efficiency of the ketonization reaction. Thus, to reduce the water content in the final condensate, these authors subjected the particles to a drying step at 70 °C prior to thermal desorption. Although it facilitated the removal of 80% of total water, up to 40% of the loaded acids were removed as well [41]. Magnetic actuation of the MNPs thus results in a water removal with much higher selectivity.

Table 3-5. Comparison of the water removal step before acid recovery in two stage approaches. For the water removal AMF-based regeneration is compared with N₂-stripping at 70 °C similar to Fufachev et al.'s procedure [41].

Approach	Water removal [%]	VFAs removal [%]
N ₂ -stripping at 70 °C	68	28
AMF heating	90±9	11±2

In order to gain insight in the origins of this difference, the theoretical impact of physical removal of water without evaporation needs to be considered. As a starting point, it was determined what would be the theoretical loss of HBU in the condensate when both water and HBU

were just physically present in the pores of the resin and not adsorbed on the polymer surface in the pores (HBu was taken as it is the highest boiling of the VFAs). Since the evaporation process took place over multiple hours, it is safe to assume that at the boiling surface the liquid composition is at equilibrium, and concentration gradients in the liquid phase are absent. Then, using the non-random two-liquids (NRTL) activity coefficient model, the evaporation of water and HBu was simulated by stepwise evaporation of 1% of the total loaded liquid per step. Assuming a 10 wt% HBu mixture, the mol fraction of water in the mixture is 0.98, and using these starting conditions, the residual concentration profiles were plotted in Figure S-6 in the appendix, while in the Tables S-3 and S-4 supporting data is presented.

The results confirm that due to an evaporation selectivity for water that is below 1, it is impossible to selectively remove water just by evaporation from extremely dilute aqueous solutions of HBu. In fact, about 82% of HBu co-evaporates during the process, assuming that the mixture is just present in the pores and no molecules are adsorbed on the resin. The co-evaporation of HBu being much more severe than experimentally observed in previous studies [13,41] is a proof of the hypothesis that HBu is adsorbed on the surface of the resin, while water is essentially physically present in the pores. Due to the adsorption on the resin, the activity of HBu inside the resin pore is much lower than calculated for the vapor liquid equilibrium, which allows one to selectively remove water during N₂ stripping.

In the present work, the magnetic heating step enables the removal of about $90\pm 9\%$ of the total water while only $11\pm 2\%$ of total loaded volatile acids are discharged. The high standard deviation in the quantity of desorbed water is due to the small scale of the experiments. The quantity of the loaded water was determined by measuring the difference in the mass of adsorbent before and after adsorption and taking into account the mass of the adsorbed acids while neglecting the amount of the salts present in the pores. Still, if the regeneration would proceed purely through evaporation, then the balance between adsorption energy and the activity coefficient of H₂O in the liquid phase should result in the same selectivity for both experimental methods. This indicates that there must actually be a difference in the regeneration mechanisms, and the most logical assumption is that the efficient separation of water by AMF might be explained with a significant fraction of water being physically pushed out of the pores by the bubbles formed in the vicinity of the hot nanoparticles. Therefore, it can be assumed that first relatively pure water moves in the liquid state from the pores to the surface of the particles and then evaporates under the applied conditions. As shown in Figure 3-7, the desorption efficiency for HAc, the most volatile acid in the solution, was less than 40% illustrating that an excellent balance was found between removing as much water as possible, without desorbing the acids. This is attributed to the fact that small superparamagnetic nanoparticles were not able to generate very high quantities of heat under the applied mild magnetic field conditions [42]. Thus, the acids remain largely adsorbed during the AMF treatment, while nearly all water was removed.

VFA Adsorption with Magnetic Hyperthermal Swing Desorption

Recovering the acids subsequently by more harsh heating with an alternating magnetic field can result in a high local temperature in the polymer matrix. The adsorbent might melt from the inside. Therefore, a hot nitrogen stripping step was added after the magnetic heating to apply sufficient energy for recovering the volatile acids without damaging the resins.

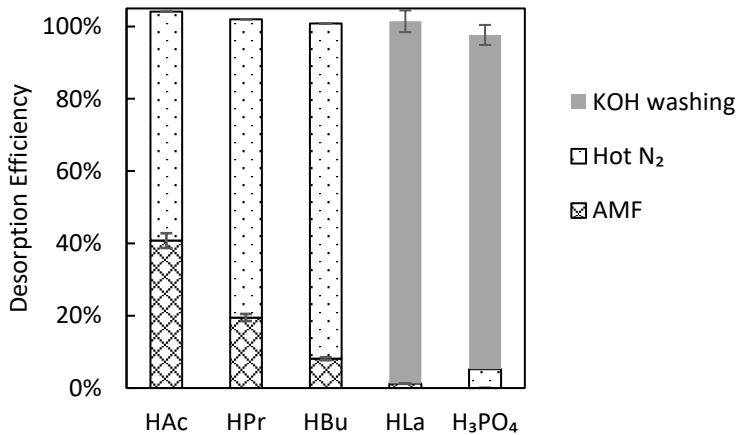


Figure 3-7. Desorption efficiency of the acids determined for the subsequent regeneration steps. First AMF was applied, then hot N₂-stripping. KOH washing is not an envisioned process step, but just applied to analyze how much acid is remaining after stripping.

Table 3-2 presents the temperature profile applied for desorption by N₂ stripping. This temperature profile was chosen to fractionate the acids during regeneration of the adsorbent. However, there was an insufficient amount of the acids to individually collect the different fractions at each temperature ramp due to the small scale of the experiment. As the majority of the water was already removed by AMF heating, the remaining VFAs are highly concentrated. It was

experimentally challenging to collect concentrated acids in a condensate receiver as they left the receiver with nitrogen gas at the end of desorption due to their high volatility. This means that the receiver container should also be cooled to extremely low temperature to completely prevent evaporation of the acids. Due to the configuration of the set-up, it was not possible to place the condensate container in a very low temperature cooled bath such as liquid nitrogen.

Here, a strong base was placed in the condensate receiver to accurately quantify the acids. After a complete thermal desorption, KOH washing was performed on regenerated particles to determine the remaining acids in the adsorbent and the desorption efficiency was calculated using Eq. (3-5). The overall results can be found in Figure 3-7. As can be seen from the histograms, no volatile fatty acid was detected in the solution from the alkaline washing of the regenerated particles which implies that the combination of magnetic heating and hot nitrogen stripping is a robust method to completely recover the volatile acids. The removal of the majority of the loaded water by AMF enabled us to obtain as much as 89% of the H_{Bu}, 81% H_{Pr} and 68% H_{Ac} essentially water-free during the N₂ stripping phase. With a larger setup a stronger variation in temperature steps during nitrogen stripping will be possible, but this is outside the scope of this work. In terms of H_{La} and H_{3PO₄}, as expected, these compounds did not completely desorb by thermal desorption and were quantified by final KOH washing.

3.3. Reusability of the adsorbent

The stability of the adsorbent was examined by reusing it for four adsorption- desorption cycles. After each cycle, the regenerated particles were washed with milliQ water using the adsorption section of the set-up depicted in Figure 3-2 and the pH of the eluent was measured over time. To ensure complete removal of the loaded acids, the washing was continued until the pH of the eluent reached approximately 7. Afterwards, the particles were first dried using the desorption section of the set-up at 90 °C with a N₂ flow rate of 0.2 L/min and then applied in the next cycle.

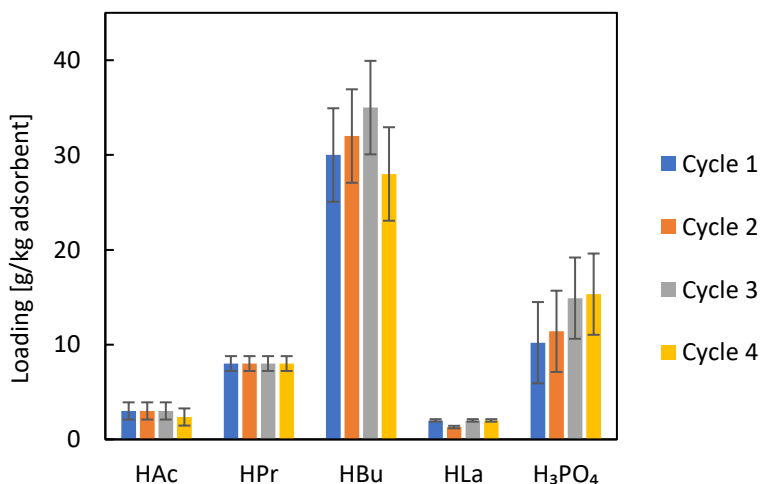


Figure 3-8. Reusability of the magnetic adsorbent over four successful adsorption-desorption cycles. Adsorption was performed in a packed bed column using 0.5 g adsorbent, feed flow rate 0.2 mL/min at room temperature with initial concentration of 0.25 wt% for each carboxylic acid, followed by desorption in two steps using AMF heating and hot N₂ stripping.

VFA Adsorption with Magnetic Hyperthermal Swing Desorption

Figure 3-8 presents the results including the error bars which show the standard deviation of duplicated experiments. It can be clearly seen from the histogram that the capacity of the adsorbent remains constant for four cycles. The capacity of the adsorbent for HBu and H₃PO₄ slightly increased in the first three cycles which might be either due to gradually releasing the nanoparticles from the polymer matrix or due to removal of the remaining porogens from the pores. To verify these hypotheses, the particles were analysed by AAS and BET after each cycle to determine the content of the remaining nanoparticles and surface area, respectively.

The results shown in Table 3-6 confirm an increase in surface area after each cycle. According to an AAS analysis taken from a small sample of the resins, the content of magnetite nanoparticles is constant during all four cycles indicating stable immobilization of the nanoparticles in the matrix of the polymer. Therefore, the minor increase in surface area can be attributed to washing out the remaining PDMS porogen from the pores during adsorption. Overall, it can be concluded that the novel magnetic adsorbent can be used for at least four adsorption-desorption cycles.

Table 3-6. Characterizations of the adsorbent after each adsorption-desorption cycle determined by BET and AAS techniques.

cycle	NP content of polymer [wt%]	N ₂ BET surface area [m ² /g]	N ₂ BJH average pore diameter [nm]	N ₂ BJH average pore Volume [cm ³ /g]
1	11±1	496± 10	8.3±0.005	0.4±0.002
2	11±0.5	503±7	8.3±0.005	0.45±0.002
3	11±1	514±4	8.2±0.08	0.45±0.002
4	10±1	517±2	8±0.08	0.44±0.0004

4. Conclusion

Circular chemistry is one of the main focuses of the researchers to achieve green chemistry goals. This study explored a novel magnetic adsorbent to separate volatile fatty acids (VFAs) from dilute waste/wastewater-based solutions. The PDVB adsorbent incorporating bio-based oleic acid functionalized magnetite nanoparticles was obtained by suspension polymerization using toluene and PDMS as porogens. The fabricated adsorbent showed high selectivity and capacity towards VFAs in dilute aqueous solution. A two-step regeneration procedure was utilized to remove the water that physically filled the pores prior to recovering the VFAs. By magnetic actuation of the magnetite nanoparticles at 25 mT field intensity and 52 kHz frequency, it was possible to generate enough heat inside the resins to remove 90±9% of the water from the pores, while 89% of the adsorbed VFAs remained in the particles. In contrast, only 80% water removal with 60% retention of the adsorbed acids is achieved for traditional stripping. Afterwards, hot N₂ stripping was employed to recover the VFAs at high concentration. Overall, a desorption efficiency of 100% was achieved for all the VFAs by combining hot N₂ stripping with an AMF heating step, and a much larger fraction of the VFAs could be obtained at high concentration, than when only hot N₂ stripping was used. This adsorbent enabled us to remove a large fraction of water from the pores by physically pushing it out the pores without having to evaporate the water. At the optimized process, physical water removal can save a significant amount of energy for thermal regeneration.

Nomenclature:

AIBN	Azobisisobutyronitrile
AAS	Atomic Absorption Spectroscopy
AMF	Alternating Magnetic Field
BET	Brunauer-Emmett-Teller
HBu	Butyric acid
HPr	Propionic acid
HAc	Acetic acid
HLa	Lactic acid
HPLC	High Pressure Liquid Chromatography
KFT	Karl-Fischer Titration
MNPs	Superparamagnetic Magnetite Nanoparticles
NRTL	Non-Random Two-Liquids
OA	Oleic Acid
OA-MNPs	OA grafted MNPs
PDMS	Polydimethylsiloxane
PDVB	Poly(divinylbenzene)
PVA	Poly Vinyl Alcohol
TEM	Transmission Electron Microscopy
VFAs	Volatile Fatty Acids
VSM	Vibrating Sample Magnetometer

References

- [1] M. Atasoy; I. Owusu-Agyeman; E. Plaza; Z. Cetecioglu, Bio-based volatile fatty acid production and recovery from waste streams: Current status and future challenges. *Bioresource Technology*. **2018**, *268*, 773-786.
- [2] S.D.M. Hasan; C. Giongo; M.L. Fiorese; S.D. Gomes; T.C. Ferrari; T.E. Savoldi, Volatile fatty acids production from anaerobic treatment of cassava waste water: effect of temperature and alkalinity. *Environmental Technology*. **2015**, *36*, 2637-2646.
- [3] H. Ma; X. Chen; H. Liu; H. Liu; B. Fu, Improved volatile fatty acids anaerobic production from waste activated sludge by pH regulation: Alkaline or neutral pH? *Waste Management*. **2016**, *48*, 397-403.
- [4] E.B. Sydney; A.C. Novak; D. Rosa; A.B. Pedroni Medeiros; S.K. Brar; C. Larroche; C.R. Soccol, Screening and bioprospecting of anaerobic consortia for biohydrogen and volatile fatty acid production in a vinasse based medium through dark fermentation. *Process Biochemistry*. **2018**, *67*, 1-7.

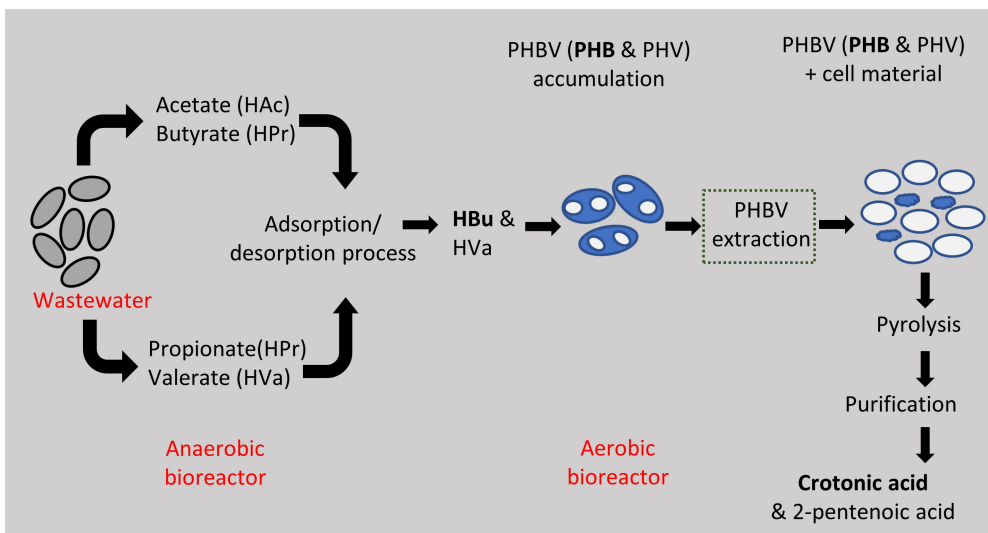
- [5] Y. Chen; R. Ruhyadi; J. Huang; W. Yan; G. Wang; N. Shen; W. Hanggoro, A novel strategy for improving volatile fatty acid purity, phosphorus removal efficiency, and fermented sludge dewaterability during waste activated sludge fermentation. *Waste Management*. **2021**, *119*, 195-201.
- [6] R.J. Jones; R. Fernández-Feito; J. Massanet-Nicolau; R. Dinsdale; A. Guwy, Continuous recovery and enhanced yields of volatile fatty acids from a continually-fed 100 L food waste bioreactor by filtration and electrodialysis. *Waste Management*. **2021**, *122*, 81-88.
- [7] L. Zhang; K.-C. Loh; Y. Dai; Y.W. Tong, Acidogenic fermentation of food waste for production of volatile fatty acids: Bacterial community analysis and semi-continuous operation. *Waste Management*. **2020**, *109*, 75-84.
- [8] M.-P. Zacharof; R.W. Lovitt, Recovery of volatile fatty acids (VFA) from complex waste effluents using membranes. *Water Science and Technology*. **2013**, *69*, 495-503.
- [9] R.J. Giraud; P.A. Williams; A. Sehgal; E. Ponnusamy; A.K. Phillips; J.B. Manley, Implementing Green Chemistry in Chemical Manufacturing: A Survey Report. *ACS Sustainable Chemistry & Engineering*. **2014**, *2*, 2237-2242.
- [10] D. Tharani; M. Ananthasubramanian, Process intensification in separation and recovery of biogenic volatile fatty acid obtained through acidogenic fermentation of organics-rich substrates. *Chemical Engineering and Processing - Process Intensification*. **2021**, *169*, 108592.
- [11] S. Ronka; M. Kucharski, Application of novel polymeric, highly specific adsorbent for the removal of terbuthylazine from complex environmental samples. *International Journal of Environmental Analytical Chemistry*. **2020**, 1-14.
- [12] T. Eregowda; E.R. Rene; J. Rintala; P.N.L. Lens, Volatile fatty acid adsorption on anion exchange resins: kinetics and selective recovery of acetic acid. *Separation Science and Technology*. **2020**, *55*, 1449-1461.
- [13] E. Reyhanitash; S.R.A. Kersten; B. Schuur, Recovery of Volatile Fatty Acids from Fermented Wastewater by Adsorption. *ACS Sustainable Chemistry & Engineering*. **2017**, *5*, 9176-9184.
- [14] A. Talebi; Y. Razali; N. Ismail; M. Rafatullah; H. Tajarudin, Selective Adsorption and Recovery of Volatile Fatty Acids from Fermented Landfill Leachate by Activated Carbon Process. *Science of the Total Environment*. **2019**, *707*, 134533.
- [15] Y. Ahn; S.-Y. Kwak, Functional mesoporous silica with controlled pore size for selective adsorption of free fatty acid and chlorophyll. *Microporous and Mesoporous Materials*. **2020**, *306*, 110410.
- [16] D.L. Uribe Santos; J.A. Delgado Dobladez; V.I. Águeda Maté; S. Álvarez Torrellas; M. Larriba Martínez, Recovery and purification of acetic acid from aqueous mixtures by simulated moving bed adsorption with methanol and water as desorbents. *Separation and Purification Technology*. **2020**, *237*, 116368.
- [17] C.I. Cabrera-Rodríguez; L. Paltrinieri; L.C.P.M. de Smet; L.A.M. van der Wielen; A.J.J. Straathof, Recovery and esterification of aqueous carboxylates by using CO₂-expanded alcohols with anion exchange. *Green Chemistry*. **2017**, *19*, 729-738.
- [18] C. Fernando-Foncillas; C.I. Cabrera-Rodríguez; F. Caparrós-Salvador; C. Varrone; A.J.J. Straathof, Highly selective recovery of medium chain carboxylates from co-fermented organic wastes using anion exchange with carbon dioxide expanded methanol desorption. *Bioresource Technology*. **2021**, *319*, 124178.

- [19] C. Caizer, Optimization Study on Specific Loss Power in Superparamagnetic Hyperthermia with Magnetite Nanoparticles for High Efficiency in Alternative Cancer Therapy. *Nanomaterials*. **2021**, *11*, 40.
- [20] J. Jose; R. Kumar; S. Harilal; G.E. Mathew; D.G.T. Parambi; A. Prabhu; M.S. Uddin; L. Aleya; H. Kim; B. Mathew, Magnetic nanoparticles for hyperthermia in cancer treatment: an emerging tool. *Environmental Science and Pollution Research*. **2020**, *16*, 19214-19225.
- [21] Z. Surowiec; A. Miaskowski; M. Budzyński, Investigation of magnetite Fe₃O₄ nanoparticles for magnetic hyperthermia. *Nukleonika*. **2017**, *62*, 183-186.
- [22] F. Reyes-Ortega; Á.V. Delgado; G.R. Iglesias, Modulation of the Magnetic Hyperthermia Response Using Different Superparamagnetic Iron Oxide Nanoparticle Morphologies. *Nanomaterials*. **2021**, *11*, 627.
- [23] L. Wu; A. Mendoza-Garcia; Q. Li; S. Sun, Organic Phase Syntheses of Magnetic Nanoparticles and Their Applications. *Chemical Reviews*. **2016**, *116*, 10473-10512.
- [24] Suriyanto; E. Ng; D.K. Srinivasan, Physical mechanism and modeling of heat generation and transfer in magnetic fluid hyperthermia through Néelian and Brownian relaxation: a review. *BioMedical Engineering OnLine*. **2017**, *16*,
- [25] I. Obaidat; Narayanaswamy; S. Alaabed; S. Sangaraju; C. Gopi, Principles of Magnetic Hyperthermia: A Focus on Using Multifunctional Hybrid Magnetic Nanoparticles. *Magnetochemistry*. **2019**, *5*, 67.
- [26] E.A. Elfimova; A.O. Ivanov; P.J. Camp, Static magnetization of immobilized, weakly interacting, superparamagnetic nanoparticles. *Nanoscale*. **2019**, *11*, 21834-21846.
- [27] J.-H. Park; A.M. Derfus; E. Segal; K.S. Vecchio; S.N. Bhatia; M.J. Sailor, Local Heating of Discrete Droplets Using Magnetic Porous Silicon-Based Photonic Crystals. *Journal of the American Chemical Society*. **2006**, *128*, 7938-7946.
- [28] P. Zolfaghari; M. Aghbolaghy; A. Karimi; A. Khataee, Continuous degradation of an organic pollutant using heterogeneous magnetic biocatalyst and CFD analysis of the process. *Process Safety and Environmental Protection*. **2019**, *121*, 338-348.
- [29] M. Mahdavi; M.B. Ahmad; M.J. Haron; F. Namvar; B. Nadi; M.Z. Rahman; J. Amin, Synthesis, surface modification and characterisation of biocompatible magnetic iron oxide nanoparticles for biomedical applications. *Molecules*. **2013**, *18*, 7533-7548.
- [30] F.S. Macintyre; D.C. Sherrington, Control of Porous Morphology in Suspension Polymerized Poly(divinylbenzene) Resins Using Oligomeric Porogens. *Macromolecules*. **2004**, *37*, 7628-7636.
- [31] M. Song; W.K. Moon; Y. Kim; D. Lim; I.-C. Song; B.-W. Yoon, Labeling Efficacy of Superparamagnetic Iron Oxide Nanoparticles to Human Neural Stem Cells: Comparison of Ferumoxides, Monocrystalline Iron Oxide, Cross-linked Iron Oxide (CLIO)-NH₂ and tat-CLIO. *Korean journal of radiology : official journal of the Korean Radiological Society*. **2007**, *8*, 365-371.
- [32] W. Wu; Q. He; C. Jiang, Magnetic iron oxide nanoparticles: synthesis and surface functionalization strategies. *Nanoscale research letters*. **2008**, *3*, 397-415.
- [33] J. Chen; W. Han; J. Chen; W. Zong; W. Wang; Y. Wang; G. Cheng; C. Li; L. Ou; Y. Yu, High performance of a unique mesoporous polystyrene-based adsorbent for blood purification. *Regenerative Biomaterials*. **2017**, *4*, 31-37.

- [34] M.T. Gokmen; F.E. Du Prez, Porous polymer particles—A comprehensive guide to synthesis, characterization, functionalization and applications. *Progress in Polymer Science*. **2012**, *37*, 365-405.
- [35] F.R. Mansour; S. Waheed; B. Paull; F. Maya, Porogens and porogen selection in the preparation of porous polymer monoliths. *Journal of Separation Science*. **2020**, *43*, 56-69.
- [36] W.L. Sederel; G.J. De Jong, Styrene–divinylbenzene copolymers. Construction of porosity in styrene divinylbenzene matrices. *Journal of Applied Polymer Science*. **1973**, *17*, 2835-2846.
- [37] F. Wang; C. Yin; X. Wei; Q. Wang; L. Cui; Y. Wang; T. Li; J. Li, Synthesis and Characterization of Superparamagnetic Fe₃O₄ Nanoparticles Modified with Oleic Acid. *Integrated Ferroelectrics*. **2014**, *153*, 92-101.
- [38] H. Xu; L. Cui; N. Tong; H. Gu, Development of High Magnetization Fe₃O₄/Polystyrene/Silica Nanospheres via Combined Miniemulsion/Emulsion Polymerization. *Journal of the American Chemical Society*. **2006**, *128*, 15582-15583.
- [39] M. Yamaura; D.A. Fungaro, Synthesis and characterization of magnetic adsorbent prepared by magnetite nanoparticles and zeolite from coal fly ash. *Journal of Materials Science*. **2013**, *48*, 5093-5101.
- [40] J.W. Steed; J.L. Atwood. *Supramolecular chemistry*, 2nd ed. ed.; Wiley: Chichester, UK, 2009.
- [41] E.V. Fufachev; B.M. Weckhuysen; P.C.A. Buijninx, Toward Catalytic Ketonization of Volatile Fatty Acids Extracted from Fermented Wastewater by Adsorption. *ACS Sustainable Chemistry & Engineering*. **2020**, *8*, 11292-11298.
- [42] S. Tong; C.A. Quinto; L. Zhang; P. Mohindra; G. Bao, Size-Dependent Heating of Magnetic Iron Oxide Nanoparticles. *ACS Nano*. **2017**, *11*, 6808-6816.

Chapter 4

Extraction of Low Molecular Weight Polyhydroxyalkanoates from Mixed Microbial Cultures using Bio-based Solvents



This chapter is adapted from:

Elhami, V.; van de Beek, N.; Wang, L.; Picken, S.J.; Tamis, J.; Sousa, J.A.B.; Hempenius, M.A.; Schuur, B., "Extraction of low molecular weight polyhydroxyalkanoates from mixed microbial cultures using bio-based solvents" *Separation and Purification Technology*, 2022, 299, 121773.

Abstract

Poly(3-hydroxybutyrate-co-3-hydroxyvalerate) (PHBV) was obtained in a mixed microbial culture (MMC) using food waste as a feedstock. The average molecular weight (MW) of PHBV was purposely reduced from about 1 MDa to about 200 kDa by drying the PHBV-rich biomass at elevated temperature of 120 °C for 18 h to ease extraction and handling. The bio-based solvents 2-methyltetrahydrofuran (2-MTHF) and dihydrolevoglucosenone (cyrene) were used to extract PHBV from MMC-based biomass. The maximum extraction yield of 62±3% with a purity of >99% was achieved with 2-MTHF at 80 °C for an hour with a high biomass to solvent ratio of 5% [g/mL]. Cyrene-based extractions resulted in the highest yield of 57±2% with a purity of >99% at 120 °C in 2h with 5% [g/mL] biomass to solvent ratio. The mass balance closure over the extraction process indicated that about 15% and 10% of polymer remained in the residual biomass after extraction by 2-MTHF and cyrene, respectively. The performance of these new solvents to extract polymers with various average MW was compared to the benchmark extractions using chloroform and dimethyl carbonate (DMC). It was found that for the polymers with low average MW the extraction efficiency of the proposed solvents exceeds the benchmark solvents.

1. Introduction

Polyhydroxyalkanoates (PHAs) are a class of thermoplastics derived from renewable biomass sources [1]. The variability in the applications of PHA's is diverse, ranging from biodegradable packaging to medical products [2]. PHAs are considered as an attractive alternative to conventional fossil fuel derived polymers due to their biodegradability and biocompatibility, as well as their

renewable character, thereby reducing fossil feedstock dependency and its associated environmental impact [3]. Two routes exist for PHAs produced via bacterial fermentation, being either through pure cultures, or via mixed cultures. Sterile conditions are used to grow monocultures in the pure culture-route, which contains a single species of microorganism. The monocultures are fed with substrates like glucose, starch, or vegetable oil to produce PHA rich biomass. Whereas via a mixed culture, more than one type of microorganisms is grown on the same substrate, using volatile fatty acids (VFAs) as ideal precursors for PHA synthesis. This approach is characterized by reduced fermentation costs as it is not required to pre-treat the substrate and sterilization is not necessary. These benefits make mixed cultures an attractive route for PHA production, extending the possibility to use cheaper carbon sources such as municipal solid waste and industrial wastewater [4]. Food waste is currently a global concern due to the rapid growth of urban population and economic development [5]. Although the number of food waste treatment plants has also increased, traditional treatment techniques come with several limitations. Greenhouse gases emission, odor production and leaching are the main issues driven from conventional food waste treatment techniques such as incineration, composting and landfilling [6]. Therefore, valorizing these waste streams by fermentation to produce high-value bio-based platform chemicals increasingly gains interest [7,8]. For instance, food waste is a potential feedstock for microorganisms due to the large quantity of VFAs production during its anaerobic digestion process [9-11]. In 2012, Paques Biomaterials B.V. established a pilot plant to produce PHA from different waste streams, such as industrial wastewater and food waste. From 2015 to 2021, the pilot plant operated continuously using

source separated organics, which are dominated by food and garden waste. This process on source separated organics, including food waste, has the potential to produce a biomass with high PHBV content e.g. up to 77 ± 18 gPHA.gVSS⁻¹ (n=3) in pilot-scale trials [12].

During the fermentation process in the MMC, the ratio between VFAs with an even number of carbons and with an odd number of carbons, will impact the ratio of HB (hydroxybutyrate) and HV (hydroxyvalerate) monomers in the final PHBV copolymer [13]. When a waste stream is used as feedstock, it is challenging to produce PHBV copolymer with a constant quality in large scale due to the daily variation in the composition of the waste stream. Alternatively, it is possible to obtain highly valuable chemicals by pyrolysis of PHBV copolymers[14]. CA and 2-PA are the main pyrolysates in thermal decomposition of PHBV. CA and its esters have a wide range of applications in textile, paint, coating and as a building block in synthesis of co-polymers with vinyl acetate [14,15]. The esters of 2-pentenoic acid can be used in flavoring essences. However, its function is currently limited to use as a raw chemical in biomedical and pharmaceutical research purposes [16,17]. Despite their great potential to be employed in various applications, the current market of these unsaturated carboxylic acids is limited as a result of their complex production routes. Thus, providing a relatively straightforward and bio-based pathway is expected to enhance their market. In the current chapter, we focused on the solvent extraction of MMC-based PHBV with various average MW. The thermal decomposition of the polymer towards 2-alkenoic acids will be studied in the next chapter.

The average MW of PHBV copolymers is one of the crucial characteristics determining their solubility. The higher the MW, the lower the solubility of

polymer, which leads to lower extraction yields in the solvent extraction method for polymer recovery. Solvent extraction of PHA from biomass has been widely studied [18,19]. It involves dissolution of the polymer in a solvent followed by an appropriate recovery technique, for which mostly precipitation techniques are used to retrieve the polymer in the solid form. Various types of solvents have been reported to extract PHA from a MMC [20]. Among them, DMC is gaining more interest as a green solvent [20-23]. Samori et al. [24] reported an extraction yield of 49% with a purity of 94% for PHB recovery from a MMC using DMC. Although applying a good solvent such as DMC enhances the extraction yield of the polymer, next to the extraction also the recovery from the solvent should be considered. To retrieve the polymer from the solvent in high purity, an antisolvent must be applied. For solvents such as DMC and chloroform (not green, but often reported as a reference solvent [22,25,26]), it can be challenging to precipitate out the polymers when they have a lower MW due to their high solubility. Overall, the performance of a solvent- antisolvent couple can be affected by the nature of the biomass as well as the characteristics of the polymer.

In this study, three batches of biomass containing PHBV with different MW were produced. The recovery of low molecular weight polymer has been investigated using two biobased solvents, 2-MTHF and cyrene. Cyrene is a new bio-based solvent produced by reduction of levoglucosenone which is a pyrolyzate from the fast pyrolysis of cellulose [27]. The application of this new solvent is dramatically growing over the time. It is used in lipase-catalyzed bio-transformations [28], polymerization of the methacrylic derivative of cyrene [29] and as a solvent for polyethersulfone and poly(vinylidene fluoride) membrane preparation via phase inversion [30]. Cyrene has also

been used as a diluent in extractive distillation to purify bio-based levulinic acid [31]. Moreover, it was found that cyrene can be a promising candidate in separation of aromatic/aliphatic systems [32]. To the best of our knowledge, these solvents have never been employed to extract PHA from MMC. Thus, the effect of several operational conditions on PHA recovery from MMC using cyrene and 2-MTHF were investigated. Furthermore, chloroform and DMC based extractions were performed as benchmark extractions for the comparative assessment of the biobased solvents in terms of extraction yield, polymer purity and characterizations of the extracted polymers. Lastly, the performance of all four solvents was assessed for extraction of PHBV with various average MWs from a MMC.

2. Material and methods

2.1. Chemicals

2-Methyltetrahydrofuran (2-MTHF, ($\geq 99\%$)), chloroform (CHCl_3 , ($\geq 99.8\%$)), dimethyl carbonate (DMC, ($\geq 99\%$)), n-heptane ($\geq 99\%$), n-hexane ($\geq 95\%$), benzoic acid ($\geq 99.5\%$), sulfuric acid (95-98%), poly(3-hydroxybutyrate) (PHB (99%)), methyl(R)-3-hydroxyvalerate ($\geq 98\%$), chloroform-D ($\geq 99.8\%$), methanol (MeOH, ($\geq 99.9\%$)), ethanol (EtOH, ($\geq 99.9\%$)), trans-crotonic acid ($\geq 98\%$), trans-2-pentenoic acid ($\geq 98\%$), acetone, 1,2,4,5-tetrachloro-3-nitrobenzene and tetrahydrofuran were purchased from Sigma-Aldrich. Cyrene ($\geq 98.5\%$) was kindly provided by the CIRCA Group. The water used was ultrapure (Milli-Q, with a resistance of $18.2 \mu\Omega \text{ cm}$ at $25 \text{ }^\circ\text{C}$). The chemicals and nutrient composition used for PHA production are described in the latest publication of the Paques Biomaterials pilot plant [12].

2.2. PHBV production using mixed microbial culture

Three separate batches of dry biomass were used in this work. Batch 1 and 2 contained PHBV-rich biomass that was produced in a pilot bioreactor system with a liquid volume of ca. 200 L (Biocel Orgawold, Lelystad, The Netherlands) from leachate from organic waste [12]. They were obtained by mechanical dewatering with a centrifuge at 3000 g and dried in a tray oven for 18 h at 120 °C. Batch 3 was produced in a different 4 m³ bioreactor system from Paques Biomaterials according to the procedure described by Werker et al. [33] and the PHBV biomass was stabilized with acid [34] and dried with a contact type dryer at around 100 °C for 1 min.

2.3. Recovery of PHBV from biomass

A schematic view on the recovery process is shown in Figure 4-1. In all experiments, first the polymer was extracted from the biomass by solvent extraction. After extraction, the solution was separated from the residual biomass by either centrifugation or filtration. Next, an antisolvent was added to the solution to precipitate the PHBV. The precipitated polymer was separated from the supernatant (the remaining solution) using a centrifuge at 7000 rpm for 10 minutes.

Extraction of low molecular weight PHA from a mixed microbial culture

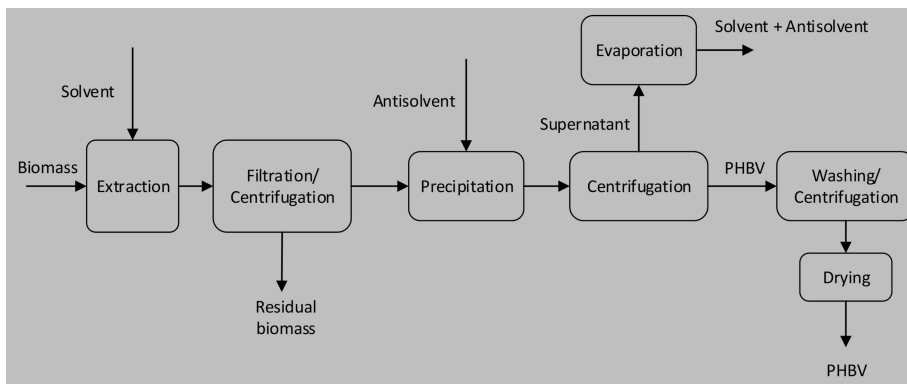


Figure 4-1. The schematic view of the extraction process to recover PHBV from the biomass.

For selection of solvent extraction conditions to obtain PHBV from biomass, an important consideration is that there is not one generalized method that can be applied for all solvents to compare the performance of these solvents with each other. The optimum conditions vary from solvent to solvent. Therefore, for the biobased solvents investigated in this study, a range of conditions was applied, and for the reference solvents chloroform and DMC, the methods reported by Mongili et al.[22] were used.

Investigations on the extraction conditions with the biobased solvents 2-MTHF and cyrene were executed using biomass from batch 1. The optimization was carried out in two steps. First, the precipitation step was enhanced by varying solvent to antisolvent volume ratio (1 to 5), time (24 to 48 h) and temperature (20 to 4 °C). To consider the possible impact of the impurities associated to the soluble non-polymeric part of biomass on precipitation efficiency, a preliminary extraction was carried out at a certain condition for all the experiments, followed by precipitation at various conditions. Second, the operation parameters of extraction (time,

temperature, and biomass to solvent ratio) were optimized. The temperature was kept constant at 80 °C for 2-MTHF and differed from 80 to 140 °C for cyrene based extraction experiments.

In the solvent extraction experiments, a quantity of 1 to 6% [g/mL] of dry biomass was suspended in 5 mL of the selected solvent in a borosilicate glass screw cap tube lined with a polytetrafluoroethylene (PTFE) rubber cap. The solution was heated using a block heater and agitation was carried out with a magnetic stirrer at 800 rpm. After the chosen extraction time (0.5 – 3 h), the solution was hot filtered through a pre-damped Whatman filter paper (8-12 µm retention) to remove the cell debris. Afterwards, the polymer was precipitated by adding a desired amount of an antisolvent to the filtered solution. Finally, the polymer was separated by centrifuge at 7000 rpm for 10 minutes followed by washing with ethanol and dried in a vacuum oven at 50 °C for 24 h.

The mass balance over the extraction process was investigated to discover the limiting stages during the extraction. The initial PHBV content of the biomass and remaining quantity of the PHBV in residual biomass and supernatant was determined by gas chromatography (GC). The fraction of the polymer that was lost during the handling was calculated based on mass balance closure over the PHBV for the entire process.

2.4. PHBV quantification

GC and thermal gravimetric analysis (TGA) were applied to quantify PHBV. Following the method of Brauneegg et al [35], about 10 mg of a sample was

Extraction of low molecular weight PHA from a mixed microbial culture

treated with 2 mL of acidified methanol with H₂SO₄ (3%[v/v]), 2 mL of chloroform and an internal standard of 50 µL benzoic acid (2 g benzoic acid in 50 mL methanol). The samples were placed in screw cap borosilicate glass tubes and heated to 100 °C for 4 h. The tubes were vortexed every 30 minutes for roughly 15 seconds. After the solution had cooled down, it was transferred to a falcon centrifuge tube followed by adding 2 mL of milli-Q water to remove non-reacted acid. Then, the solution was centrifuged for 5 minutes at 8000 rpm. Afterwards, the bottom layer of the solution was transferred to a GC vial using a syringe. An amount of 1 µL of the sample was injected in a Thermo Scientific Trace 1300 gas chromatograph equipped with a Flame ionization detector (FID) and an Agilent DB-Wax column (60 m, 0.25 mm, 0.25 µm). The carrier gas was helium at a flow rate of 35 mL/min. The temperature gradient started at 30 °C with a constant heating rate of 5 °C/min until it reached 120 °C and then at a rate of 25 °C/min till it reached 250 °C. The samples were analyzed in triplicate. A calibration curve for PHB and PHBV was produced using pure PHB and methyl(R)-3-hydroxyvalerate, respectively.

The fraction of PHB and PHBV in the sample were defined by:

$$x_{PHB} = \frac{m_{PHB,GC}}{m_{Sample}} \quad (4-1)$$

$$x_{PHV} = 1 - x_{PHB} \quad (4-2)$$

$$Purity \% = (x_{PHB} + x_{PHBV}) \times 100 \quad (4-3)$$

Where $m_{PHB,GC}$ is the amount of PHB calculated from the GC, m_{Sample} is the amount of extracted material applied for analysis. Eq.(4-4) was used to determine the recovery yield of the polymer:

$$\text{Extraction yield \%} = \frac{m_{\text{PHBV,E}} \times \text{Purity}}{m_{\text{DB}} \times x_{\text{PHBV,DB}}} \times 100 \quad (4-4)$$

Where $m_{\text{PHBV,E}}$ is the total amount of the collected polymer after extraction, m_{DB} is the mass of dry biomass used for extraction and $x_{\text{PHBV,DB}}$ is the polymer fraction in the biomass.

2.5. PHBV qualification

Thermal Gravimetric Analysis (TGA) The degradation temperature of the extracted polymers was measured using a TGA-550 instrument operated under nitrogen flow and heating samples from room temperature to 400 °C at a rate of 10 °C/min.

Gel Permeation Chromatography (GPC) The sample was dissolved in tetrahydrofuran (THF) with 6 mg/mL concentration and filtered through 0.2 µm disc filters into a vial. In the case of high molecular weight polymers, the samples were prepared in the screw cap vials and heated at 55 °C until about 90% of the polymer is dissolved. GPC analysis was done at room temperature by injecting 20 µL of the dissolved polymer in an Agilent 1200 series GPC using THF as the eluent at a flowrate of 0.35 mL/min. Well-defined polystyrenes were used as calibration standards. The analysis was done in triplicate to determine the analysis error which was less than 0.5%.

3. Results and discussion

3.1. Optimization of the extraction with 2-MTHF and cyrene

To the best of our knowledge, 2-MTHF and cyrene have not been used before to recover PHA from biomass. In this study, the capability of these new bio-based solvents to extract PHBV was examined, and the extraction conditions were optimized to achieve the highest yield.

3.1.1. 2-MTHF

Initially, the precipitation step was optimized. By performing an extraction experiment using 2-MTHF at 80 °C, 1 h, and biomass to solvent ratio of 5% [g/mL], followed by precipitation of the polymer at various conditions. Due to the insolubility of the polymer in alkanes and full miscibility of 2-MTHF and alkanes, *n*-pentane and *n*-heptane were selected as antisolvent. Moreover, the solubility of the polymer in the solvent reduces by decreasing the temperature. Therefore, the precipitation was examined at room temperature (20 °C) and in the refrigerator (4 °C). Finally, the ratio of the antisolvent to solvent was varied from 1 to 4. The contact time for all the samples were kept constant at 24 h. As can be seen from Figure 4-2, *n*-heptane performs better than *n*-pentane in precipitating the PHBV dissolved in 2-MTHF. Moreover, the precipitation efficiency increases about 10% by decreasing the temperature from ambient condition to 4 °C. Regarding the required amount of the antisolvent, the volume ratio of the antisolvent to solvent varied from 1 to 4. As shown in Figure 4-2.C, the yield gradually rises by increasing the antisolvent to solvent ratio from 1 to 3. However, further increasing the amount of the antisolvent does not result in higher yields. Overall, it was found that *n*-heptane results in a high precipitation efficiency at an antisolvent to solvent ratio of 3, and a temperature of 4 °C within 24 h.

Extraction of low molecular weight PHA from a mixed microbial culture

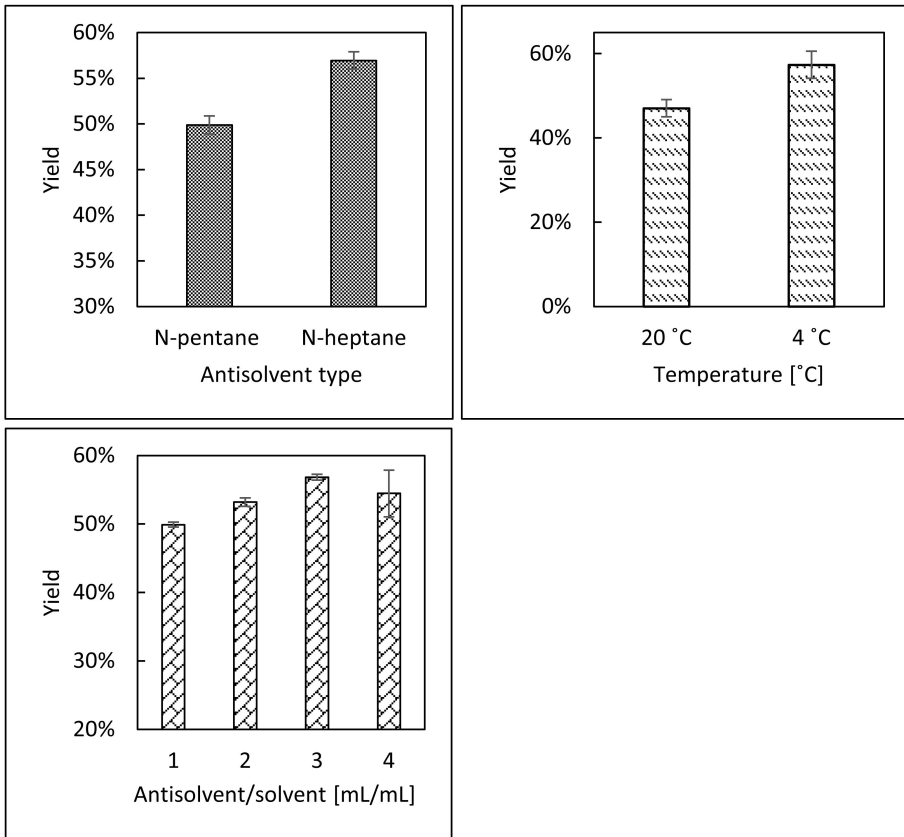


Figure 4-2. optimization of the precipitation step for the extraction using 2-MTHF at 80 °C, 1 h, and biomass to solvent ratio of 5% g/mL).

After obtaining the optimum precipitation conditions, the extraction parameters were optimized. One of the critical operation parameters is extraction temperature. The higher the temperature, the higher dissolution capacity of the polymer in the solvent and consequently the higher the extraction yield. However, PHBV is a polyester which is not a thermally stable

Extraction of low molecular weight PHA from a mixed microbial culture

polymer, meaning that at too high temperature, the polymer will thermally degrade and there is an optimum extraction temperature to achieve the highest recovery yield without degrading the polymer. The boiling point of 2-MTHF is 87 °C. In order to operate it at atmospheric pressure, 80 °C was selected for extraction. The thermal stability of the polymer was examined by a preliminary extraction experiment and sampling over the course of time. The samples were analyzed by GPC to measure the average MW and PDI of the extracted polymer. As shown in Figure 4-3, the average MW and PDI of the polymer are approximately constant within the extraction. This indicates that the PHBV is stable under these extraction conditions and 2-MTHF is capable to dissolve PHBV with average MW of 80 kDa at 80 °C.

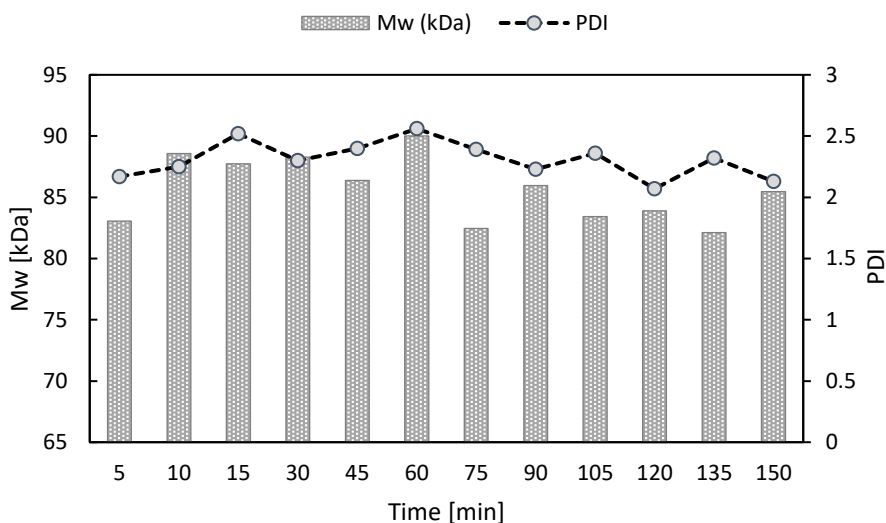


Figure 4-3. Extraction of PHBV from the biomass (batch 1) using 2-MTHF at 80 °C with a biomass to solvent ratio of 5% [g/mL] and n-heptane as an antisolvent with a volume ratio of 1:3 at 4 °C for 24h.

Extraction of low molecular weight PHA from a mixed microbial culture

Figure 4-3 displays the molar weight and PDI, while the extraction yield as function of time is presented in Figure 4-4. As can be clearly seen from Figure 4-4, the extraction yield reaches a steady value within the first hour, and while the extraction yield increases from 54 to 62% during the first hour, it does not increase further beyond 1 hour extraction time. The stabilized yield around 60% is likely due to saturation of the solvent. Therefore, 1 h was considered as an optimum extraction time. In a next series of experiments, the minimum required amount of the solvent was investigated by varying the ratio of biomass to solvent from 1 to 6% [g/mL]. The results are shown in Figure 4-5, the yield is improved by about 3% by decreasing the ratio from 5 to 2%. However, from an economic point of view, gaining only 3% more polymer by increasing the volume of the solvent with a factor 2.5 is not efficient. In the next experiment, the ratio of the biomass to solvent was increased to 6% [g/mL]. As shown in Figure 4-5, the recovery yield is slightly decreasing from about 62 to 55% by increasing the ratio from 5 to 6% [g/mL]. Although the reduction in the yield might not be statistically significant, performing the experiments at a ratio higher than 5% [g/mL] was challenging, because of the formation of a sludge when a limited volume of the solvent was applied. Thus, the optimum biomass to solvent ratio with regards to experimental handling was set at 5% [g/mL]. Overall, the maximum yield of $62\pm 3\%$ was obtained at optimum operation conditions (including both extraction and antisolvent precipitation). Since this yield is far from the theoretical maximum yield of 100%, the polymer should remain either in the biomass or in the solvent. To gain more information, the mass balance over the complete recovery process was studied to identify the limiting stages during the recovery.

Extraction of low molecular weight PHA from a mixed microbial culture

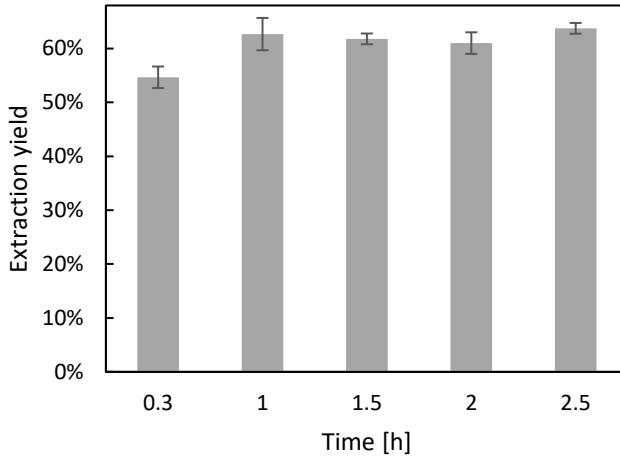


Figure 4-4. Optimization of the extraction time to recover PHBV from the biomass using 2-MTHF at 80 °C with a biomass to solvent ratio of 5% [g/mL] and n-heptane as an antisolvent with a volume ratio of 1:3 at 4 °C for 24h.

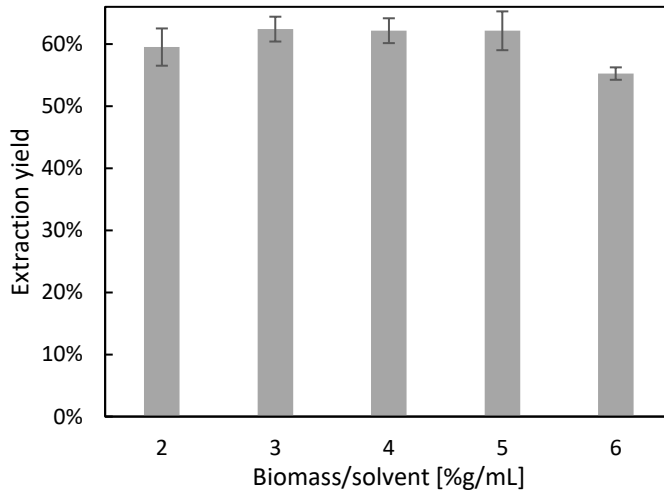


Figure 4-5. Optimization of the biomass to solvent ratio to recover PHBV from the biomass using 2-MTHF at 80 °C for 1 h with and n-heptane as an antisolvent with a volume ratio of 1:3 at 4 °C for 24h.

Extraction of low molecular weight PHA from a mixed microbial culture

A schematic view of the process is shown in Figure 4-1. The polymer content of each step was measured as explained in section 2.4. After each extraction experiment, the polymer content of the residual biomass and supernatant were determined by GC. Regarding the extraction process using the biomass from batch 1 with 2-MTHF, it was found that about 15% of the polymer was left in the supernatant after the precipitation by antisolvent. The large fraction of polymer not precipitating upon addition of the antisolvent can be explained through the relatively low average MW and resulting high solubility of the polymer. For this PHBV it can be concluded that the main limiting stage in the overall process is likely the precipitation. Moreover, about 15% of the polymer remains in the residual biomass after extraction at optimum operation conditions. This content did not reduce significantly even by applying a second extraction with 2-MTHF. The cross flow multistage extraction with 2-MTHF on the residual biomass increased the yield only by about 3%. It confirms that a strong and complex cellular matrix is formed that results in an impenetrable barrier around the polymer in MMC. This formation of the complex cellular matrix was first suggested by Patel et al. [36] and later confirmed by Samori et al [24]. Mass balance closure over the polymer in a single stage extraction indicates that less than 10% of polymer was lost during the handling. To confirm the mass balance closure of the PHBV, the extraction was repeated without the antisolvent precipitation. The polymer was retrieved by evaporating the solvent leading to $85\pm 7\%$ recovery yield with a purity of $79\pm 5\%$ which is in line with the previous method.

3.1.2. Cyrene

For optimization of the precipitation, a preliminary extraction was performed at 180 °C, 15 minutes, and solvent to antisolvent ratio of 5% [g/mL] for all the experiments, followed by precipitating the polymer at various conditions. Due to insolubility of the PHBV in water and ethanol, and full miscibility of cyrene with water and ethanol, they were chosen as an antisolvents. The performance of each antisolvent alone and as a mixture was examined. As can be seen from Figure 4-6, ethanol is not able to precipitate the majority of the dissolved polymer. On the other hand, water retrieves not only the polymer but also biomass residuals resulting in non-pure brown polymer. However, a mixture of these two antisolvents in the ratio of 1:1 delivers the highest yield. Due to the low average MW of the polymer, it was not possible to completely precipitate the polymer. Moreover, reducing the temperature resulted in the precipitation of dissolved residuals of the biomass as well. Therefore, all the precipitation experiments were done at room temperature for 24 h. In general, the highest precipitation efficiency was achieved an equal volume ratio of solvent (cyrene) to antisolvent (water: ethanol (1:1 [v:v])) at 20 °C within 24 h.

Extraction of low molecular weight PHA from a mixed microbial culture

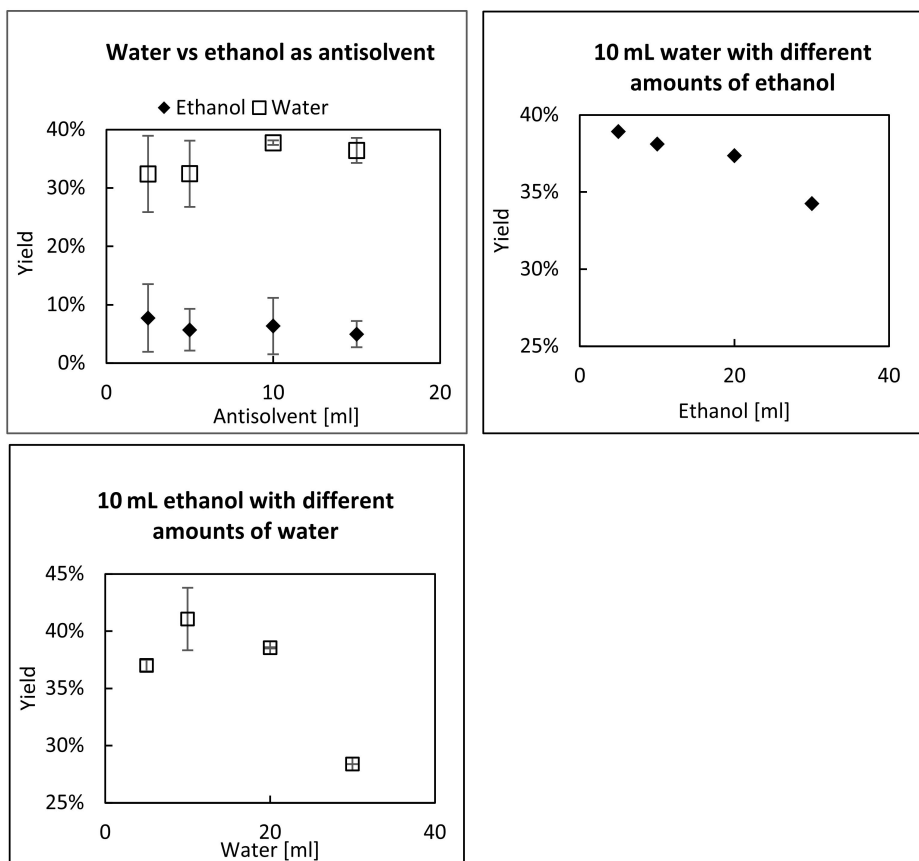


Figure 4-6. Optimization of the precipitation for cyrene based extraction at 180 °C and 15 min using ethanol and water as an antisolvent at 20 °C.

Extraction of low molecular weight PHA from a mixed microbial culture

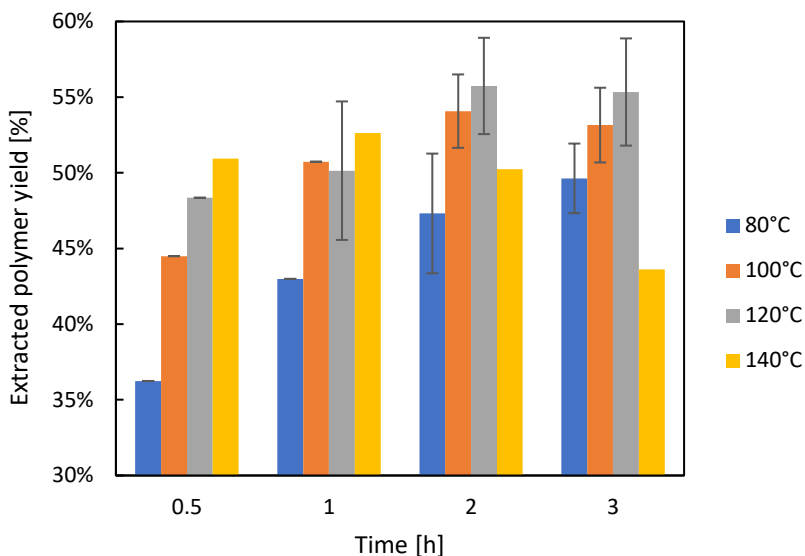


Figure 4-7. Extraction yield as function of extraction time and temperature. Displayed is the amount of PHBV recovered from the biomass using cyrene with a biomass to solvent ratio of 5% [g/mL] and in the antisolvent precipitation stage a water: ethanol (1:1 [v: v]) mixture as an antisolvent with a volume ratio of 1:1 at 20 °C for 24 h.

After optimizing the precipitation step, the extraction parameters were further investigated to obtain the highest extraction yield using cyrene. Figure 4-7 represents the extraction yield at different temperatures over the course of time. As can be seen from the graph, there is a clear increase in the extraction yield over time at 80 °C (the lowest temperature), while the initially much higher yield at 140 °C (the highest temperature applied) clearly drops after more than 1h. The time-dependent yield profiles are much less pronounced for the intermediate temperatures of 100 and 120 °C. Overall, the highest yield seems to be obtained at 120 °C. The opposite trends at lowest and highest operational temperatures are the result of two opposing effects that occur simultaneously. An improved solubility of the polymer in

Extraction of low molecular weight PHA from a mixed microbial culture

cyrene is observed at increasing temperature, while at the higher temperatures the limited thermal stability of the polymer reduces the yield after prolonged exposure to such high temperatures. When 120 °C was set as an extraction temperature, the recovery yield reached a plateau after 2 h which might be because of the saturation of the solvent. Thereupon, the proper mass ratio of the biomass to solvent was further examined by keeping the mass of the biomass constant at 0.5 g while the solvent amounts were adjusted to achieve a ratio of 4 to 8% [g/mL]. As can be seen from Figure 4-8, there is not a remarkable reduction in the yield by increasing the ratio from 3 to 5% [g/mL]. However, a further increase in the ratio led to both reduction in yield and to processing problems due to the high concentration of the mixture. It leads to the conclusion that the minimum required amount of solvent is 10 mL which is equal to 5% [g/mL] of biomass to solvent ratio. Overall, the highest yield of $57\pm 2\%$ was obtained at 120 °C and 2 h.

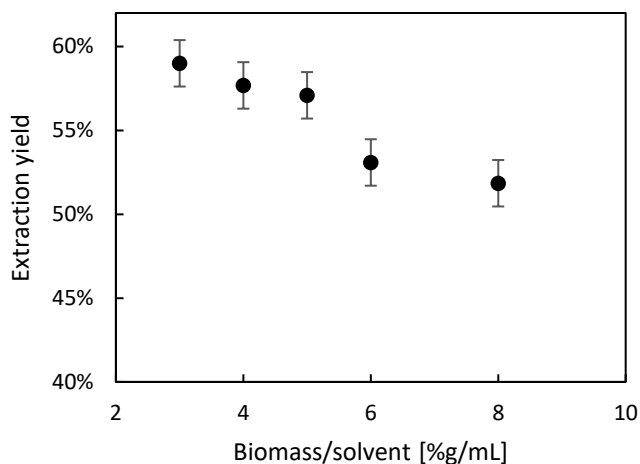


Figure 4-8. Optimization of biomass to solvent ratio to recover PHBV from the biomass using cyrene at 120 °C for 2 h with water: ethanol (1:1[v: v]) as an antisolvent with a volume ratio of 1:1 at 20 °C for 24 h.

The analysis of the residual biomass illustrated that about 10% of the polymer was left in the residual biomass at optimized extraction conditions. The quantification of the polymer by GC requires a transesterification reaction in the presence of a strong mineral acid. Due to the instability of cyrene under acidic conditions, the remaining polymer in the supernatant was not measured by GC. However, it is reasonable to assume that a quantity of polymer was lost during handling. The lost polymer is expected to be of similar amount as observed during handling after extraction with 2-MTHF (which was about 7% loss). Based on this assumption, it is calculated that about 26% of the polymer did not precipitate from the supernatant.

3.2. Comparative assessment of the solvents for extraction of PHBV from mixed microbial culture

The average MW of a polymer has a great impact on its solubility in corresponding solvent and consequently on the maximum capacity of the solvent to extract it. In this study, the average MW of the PHBV is much lower than what has been reported in the literature. Therefore, it was not possible to fairly compare the performance of these new solvents with previously discovered solvents. Furthermore, the capacity of the solvent can be affected by the nature of the biomass as well. For instance, Somori et al. [24] found that using DMC to extract PHBV from a MMC allows 49% recovery yield. Later, de Souza Reis et al. [23] reported 90% recovery at the same extraction condition with DMC. They concluded that the difference might be due to applying different wastewater as a feedstock for the microorganism and complex interaction between the PHBV and non-polymeric cell debris. To

allow for direct comparison of the yields with the solvents DMC and chloroform and to eliminate the impact of unknown parameters associated to biomass-specific effects on extraction efficiency of each solvent, also extractions with DMC and chloroform were performed. The extraction condition for chloroform and DMC were based on the latest work by Mongili [22]. The results are shown in Table 4-1. The biomass named batch 1 and batch 2 were both produced via fermentation of food wastes. They differ only in average MW which is higher for batch 2. On the other hand, batch 3 was prepared by fermentation of a secondary sludge of a municipal wastewater treatment plant which possessed the highest average MW. It became clear that by decreasing the average MW of the polymer, the extraction yield with chloroform and DMC decreased because of the difficulties encountered in the precipitation of highly soluble molecules. An inverse trend was observed for 2-MTHF and cyrene, showing the highest yield for lowest MW PHBV of 62 and 57%, respectively. However, the solubility of the polymers with high average MW is limited for these solvents. It leads to the conclusion that there is an optimum average MW for every solvent-antisolvent pair to achieve the highest recovery yield. Up to that point the yield is limited by the precipitation using an antisolvent and above that MW, the solubility of the polymer in the solvent is limiting the extraction.

For batch 3 with the highest average MW, the maximum quantity of the polymer was harvested using chloroform with a yield of 74% and purity of 96%. Similar results were obtained with DMC, illustrating that indeed DMC has a high potential to replace chlorinated solvents [20,23]. Also, the effect of the extraction procedure on monomer composition of the polymer and its

Extraction of low molecular weight PHA from a mixed microbial culture

thermal degradation temperature were investigated by GC and TGA, respectively. According to the GC results for the biomass, the mass ratio of HB to HV monomer before the extraction is 2, 3 and 3 for batch 1, batch 2 and batch 3, respectively. The mass ratio of the monomers for the polymer after extraction by various solvents is presented in Table 4-1. There is an increase in the monomer ratio for some polymer meaning that the corresponding solvent has possibly dissolved more HB units. Regarding the thermal analysis of the polymer, the degradation temperature (T_{deg}) of polymers was determined by TGA in which the inflection point of the curve was considered as T_{deg} . As can be seen from Table 4-1, the T_{deg} of the polymer with low average MW does not vary for various solvent-antisolvent couples. However, the T_{deg} for the polymer extracted from batch 3 by 2-MTHF is about 35 °C lower than the polymer extracted by other solvents using the same batch of biomass. It might be due to the relatively low average MW of the polymer obtained by 2-MTHF.

Extraction of low molecular weight PHA from a mixed microbial culture

Table 4-1. Solvent extraction of PHBV from mixed microbial culture with chloroform, DMC, 2-MTHF and cyrene at their optimum operation conditions using three biomass batches with different average MW.

Biomass	solvent	Extraction condition	Precipitation condition	Yield [%]	Purity [%]	HB/HV [g/g]	Mw [kDa]	Mn [kDa]	PDI	T _{deg.}
Batch 1	Chloroform	2h, 60°C, 5% [g/mL]	n-Hexane,1:3 [v: v], 24h, 4°C	32	>99	4	100	40	2.5	240
	DMC	1.5h, 90°C, 2.5% [g/mL]	EtOH,1:3 [v: v], 24h, 4°C	20	>99	4	148	78	1.9	240
	2-MTHF	1h, 80°C, 5% [g/mL]	n-Heptane,1:3 [v: v], 24h, 4°C	63	>99	3	74	19	3.9	235
	Cyrene	2h, 120°C, 5% [g/mL]	Water: EtOH 1:1:1 [v: v], 24h, 20°C	57	>99	3	79	25	3.16	240
Batch 2	Chloroform	2h, 60°C, 5% [g/mL]	n-Hexane,1:3 [v: v], 24h, 4°C	44	>99	4	146	41	3.5	245
	DMC	1.5h, 90°C, 2.5% [g/mL]	EtOH,1:3 [v: v], 24h, 4°C	39	>99	4	178	81	2.2	245
	2-MTHF	1h, 80°C, 5% [g/mL]	n-Heptane,1:3 [v: v], 24h, 4°C	64	>99	4	122	25	4.9	240
	Cyrene	2h, 120°C, 5% [g/mL]	Water: EtOH 1:1:1 [v: v], 24h, 20°C	65	>99	3	120	28	4.29	243
Batch 3	Chloroform	2h, 60°C, 5% [g/mL]	n-Hexane,1:3 [v: v], 24h, 4°C	74	96	5	581	298	2	265
	DMC	1.5h, 90°C, 2.5% [g/mL]	EtOH,1:3 [v: v], 24h, 4°C	71	96	4	526	260	2	260
	2-MTHF	1h, 80°C, 5% [g/mL]	n-Heptane,1:3 [v: v], 24h, 4°C	11	99	3	475	208	2.3	230
	Cyrene	2h, 120°C, 5% [g/mL]	Water: EtOH 1:1:1 [v: v], 24h, 20°C	40	98	4	525	238	2.2	265

3.3. Mass balance over the benchmark extraction process

The mass balance closure over the PHBV was applied for the extraction process with reference solvents using the biomass from batch 1. The overall results are displayed in Table 4-2. Based on the highest fraction of the polymer remaining in the supernatant, the main limiting stage in extraction with the benchmark solvents is the precipitation. Because of the high solubility of the polymer with low average MW, the applied antisolvents are not capable of completely retrieving the polymer. It may be possible to improve the recovery of the polymer from the solvent by applying another antisolvent such as an alkane. The optimization of the precipitation step for the reference solvents was out of this work's scope. The focus of the present work is to investigate the impact of average MW of PHBV on the extraction yield for the investigated solvents and to select a proper solvent-antisolvent couple and extraction process.

The amount of remaining polymer in the residual biomass is much lower for DMC and chloroform than reported by Samori et al. [24]. They achieved an extraction yield of 49% with DMC followed by solvent evaporation. The second extraction from residual biomass with DMC improved the yield up to 61%. The third extraction did not increase the yield any further, meaning that about 39% of the polymer remained in the residual biomass and is not extractable. Such a large amount of polymer not being extractable is most likely due to the complex interaction between polymeric and non-polymeric parts of the microbial cells in MMC. It is noteworthy that the source of biomass and particularly the average MW of the polymer are very different in our study. As already mentioned, a similar behavior for DMC was also found by Souza Reis et al. [23].

Extraction of low molecular weight PHA from a mixed microbial culture

Table 4-2. The summary of the mass balance closure over PHBV during extraction from batch 1 with chloroform, DMC, 2-MTHF and cyrene at corresponding optimum extraction conditions.

Extraction solvent	Yield [%]	PHBV in residual biomass [%]	PHBV in supernatant [%]	PHBV lost during handling [%]
2-MTHF	63	15	15	7
Cyrene	57	10	33	
Chloroform	32	6	58	4
DMC	20	6	69	5

3.4. Investigation the combined solvent evaporation-antisolvent as precipitation method

2-MTHF showed a great potential to recover PHBV with low average MW. However, obtaining pure polymer requires using n-heptane as an antisolvent with a volume ratio of 3. From an economic point of view, a lower antisolvent usage is preferred. Therefore, we investigated further how to reduce the required amount of antisolvent while still obtaining relatively pure polymer. Combing two precipitation methods, namely solvent evaporation and applying an antisolvent is the approach that was taken to lower the antisolvent consumption for retrieving pure polymer. At the optimized condition, 2-MTHF and DMC based extraction experiments were carried out, followed by evaporating a fraction of the solvent using a vacuum oven at 30 °C. Afterwards, 3 volumes of antisolvent to remaining solvent were added to retrieve the polymer. As shown in Table 4-3, regarding 2-MTHF based extractions, the yield slightly increased from 63 to 67% by evaporating the majority of the solvent prior to adding antisolvent. Also, the purity dropped from >99 to 94% by removing 91% of the solvent meaning that it is possible to obtain relatively pure polymer with less antisolvent consumption by

Extraction of low molecular weight PHA from a mixed microbial culture

removing a large fraction of the solvent beforehand. Recovering the polymer with complete solvent evaporation resulted in $85\pm 7\%$ extraction yield with a purity of $79\pm 5\%$. A picture of the polymer obtained by solvent evaporation and antisolvent precipitation is shown in Figure 4-9. Precipitating the polymer with an antisolvent yields white granules while the one obtained by solvent evaporation has a yellowish cake-like appearance. Similarly, for DMC based extractions, removing 91% of the solvent before adding the antisolvent increases the yield from 20 to 80% with a relatively high purity of 98%. It is in line with the previous conclusion that the precipitation is the main limiting stage to recover low average MW polymer by DMC. Moreover, the precipitation of the polymer by complete evaporation of DMC results in $94\pm 5\%$ extraction yield and $98\pm 1\%$ purity.

Table 4-3. Extraction with 2-MTHF (1 h, 80 °C and 5% [g/mL]) and DMC (1.5 h, 90 °C, 2.5% [g/mL]) retrieving the polymer by evaporation of a fraction of the solvent, followed by precipitation using the antisolvent.

Solvent	Evaporated fraction of the solvent [%]	Yield [%]	Purity [%]
2-MTHF	0	63	>99
2-MTHF	75	67	96
2-MTHF	91	67	94
2-MTHF	100	85 ± 7	79 ± 5
DMC	0	20	>99
DMC	80	32	98
DMC	91	80	98
DMC	100	94 ± 5	98 ± 1

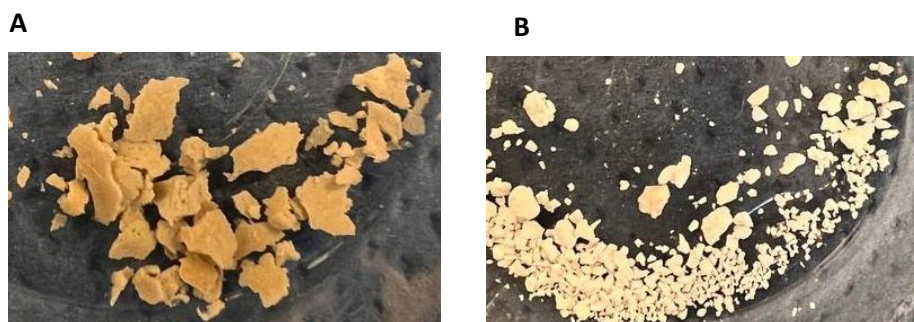


Figure 4-9. A picture of the polymer extracted by 2-MTHF at 80 °C for 1 h, A) retrieving the polymer by solvent evaporation and B) with *n*-heptane as an antisolvent with a volume ratio of 1:3 at 4 °C for 24 h.

3.5. PHBV extraction from wet biomass

Extraction of PHBV directly from a wet biomass is preferred to reduce the cost associated with the drying of the biomass. Cyrene is fully miscible in water and therefore it is not recommended to apply cyrene for polymer extraction from a wet biomass. However, the solubility of 2-MTHF in water is limited. Therefore, the performance of 2-MTHF (at 80 °C, 1 h, 2.5 %[g/mL]) to recover the polymer from a wet biomass was compared to DMC (at 90 °C, 1.5 h, 2.5 %[g/mL]). The wet biomass contained 90 wt% water and 43% PHBV on dry basis. It was found that 2-MTHF is capable to extract PHBV with 73±1% yield and a purity of >99% which is a similar performance compared to DMC, since DMC based extraction resulted in 66±8% yield and >99% purity. The polymer obtained by 2-MTHF and DMC have an average MW of 535 and 555 kDa, respectively.

3.6. Solvent and antisolvent recovery consideration

The recovery and reusability of the solvent and antisolvent is crucial for an economic extraction process. 2-MTHF is a volatile solvent with a boiling point of 87 °C. The extraction was performed at 80 °C in a closed vial with a sufficient volume to prevent the evaporation of the solvent. After the extraction, the remaining 2-MTHF in the biomass residual can be easily recovered by drying the residuals and condensing the vapor phase. The separation of 2-MTHF and n-heptane can be also done by distillation. Regarding cyrene, it is not volatile and has a high boiling point of 227 °C. The remaining solvent in the residual biomass can be obtained by rinsing the residuals with ethanol, followed by ethanol/cyrene separation with distillation. Similarly, the mixture of the antisolvent (ethanol/water) can be also separated from cyrene by distillation, where it is noted that a small part of the cyrene will be in the geminal diol state [37].

4. Conclusion

In this study, bio-based PHBV-enriched biomass was prepared using organic waste leachate as a feedstock. The wet produced biomass was subjected to an elevated temperature of 120 °C for 18 h to simultaneously dry the biomass and reduce the average MW of the polymer, as the reduction of the average MW can enhance the solubility of the polymer and increase the extraction efficiency by solvent extraction. The extraction of the polymer with low average MW was optimized using 2-MTHF and cyrene as a solvent. The maximum extraction yield of 62±3% with a purity of >99% was achieved with 2-MTHF at 80 °C for an hour with a high biomass to solvent ratio of 5 %[g/mL].

Extraction of low molecular weight PHA from a mixed microbial culture

Cyrene-based extractions resulted in the highest yield of $57\pm 2\%$ with a purity of $>99\%$ at $120\text{ }^{\circ}\text{C}$ in 2h with 5 %[g/mL] biomass to solvent ratio. The mass balance closure over the extraction process indicated that about 15% and 10% of polymer remained in the residual biomass after extraction by 2-MTHF and cyrene, respectively.

Moreover, the performance of these proposed bio-based solvents was compared with chloroform and DMC as benchmark solvents using different batches of the PHBV-enriched biomass with various average MW. The results indicate that the proposed new solvents are preferred over the benchmarks when the average MW of polymer is low. For example, 2-MTHF resulted in $62\pm 3\%$ extraction efficiency for PHBV with MW of about 100 kDa while it was only 32 and 20% for chloroform and DMC, respectively. It can be explained with the difficulties in precipitating out the small polymer molecules from the good solvents due to their high solubility. In fact, the mass balance closure over the extraction process confirmed that the precipitation step is the main limiting stage when a good solvent is used to recover a polymer with relatively low average MW. About 58 and 69% of the polymer remained in the supernatant using respectively chloroform and DMC to extract PHBV with the average MW of 100 kDa while it was only 15% for 2-MTHF based extraction for the same batch of the biomass. This leads to the conclusion that selecting a proper solvent-antisolvent couple to recover pure polymer strongly depends on the average MW of the polymer.

To reduce the antisolvent usage, the solvent evaporation and adding an antisolvent were combined for 2-MTHF based extraction experiments. It was found that by evaporating 91% of the solvent prior to adding the antisolvent,

Extraction of low molecular weight PHA from a mixed microbial culture

it is still possible to recover the PHBV with a relatively high purity of 94%. Moreover, applying 2-MTHF for the PHBV extraction from wet biomass resulted in $73\pm 1\%$ yield and a purity of $>99\%$ which is a performance comparable to results obtained by DMC based wet extraction.

Nomenclature:

CA	Trans-Crotonic Acid
DMC	Dimethyl Carbonate
FID	Flame ionization detector
GC	Gas Chromatography
GPC	Gel Permeation Chromatography
HB	Hydroxy Butyrate
HV	Hydroxy Valerate
MW	Molecular Weight
MMC	Mixed Microbial Culture
Mn	Number of average MW
2-MTHF	2-Methyltetrahydrofuran
PTFE	Polytetrafluoroethylene
PHB	Poly(3-hydroxybutyrate)
PHV	Poly(3-hydroxyvalerate)
PHBV	Poly(3-Hydroxybutyrate-co-3-Hydroxyvalerate)
2-PA	2-Pentenoic Acid
PHAs	Polyhydroxyalkanoates
PDI	Polydispersity Index
TGA	Thermal Gravimetric Analysis
THF	Tetrahydrofuran
VFAs	Volatile Fatty Acids

References

- [1] E. Bugnicourt; P. Cinelli; V. Alvarez; A. Lazzeri, Polyhydroxyalkanoate (PHA): Review of synthesis, characteristics, processing and potential applications in packaging. *eXPRESS Polymer Letters*. **2014**, *8*, 791-808.
- [2] B. Kunasundari; K. Sudesh, Isolation and recovery of microbial polyhydroxyalkanoates. *Express Polymer Letters*. **2011**, *5*, 620-634.
- [3] A. Aramvash; N. Gholami-Banadkuki; F. Moazzeni-Zavareh; S. Hajizadeh-Turchi, An Environmentally Friendly and Efficient Method for Extraction of PHB Biopolymer with Non-Halogenated Solvents. *Journal of Microbiology and Biotechnology*. **2015**, *25*, 1936-1943.
- [4] C. Nielsen; A. Rahman; A.U. Rehman; M.K. Walsh; C.D. Miller, Food waste conversion to microbial polyhydroxyalkanoates. *Microb Biotechnol*. **2017**, *10*, 1338-1352.

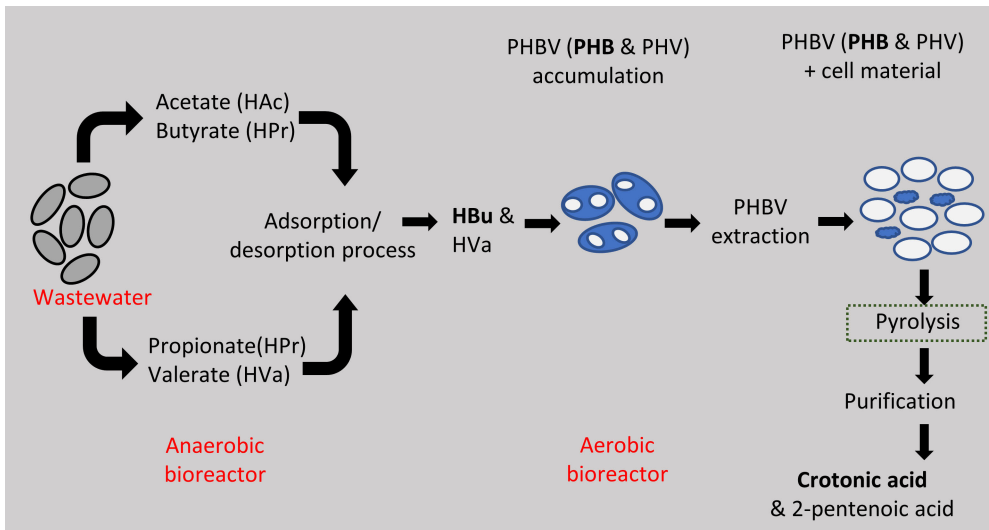
- [5] L. Zhang; K.-C. Loh; Y. Dai; Y.W. Tong, Acidogenic fermentation of food waste for production of volatile fatty acids: Bacterial community analysis and semi-continuous operation. *Waste Management*. **2020**, *109*, 75-84.
- [6] G. Capson-Tojo; E. Trably; M. Rouez; M. Crest; N. Bernet; J.-P. Steyer; J.-P. Delgenès; R. Escudié, Cardboard proportions and total solids contents as driving factors in dry co-fermentation of food waste. *Bioresource Technology*. **2018**, *248*, 229-237.
- [7] C. Da Ros; V. Conca; A.L. Eusebi; N. Frison; F. Fatone, Sieving of municipal wastewater and recovery of bio-based volatile fatty acids at pilot scale. *Water Research*. **2020**, *174*, 115633.
- [8] M. Ramos-Suarez; Y. Zhang; V. Outram, Current perspectives on acidogenic fermentation to produce volatile fatty acids from waste. *Reviews in Environmental Science and Bio/Technology*. **2021**, *20*, 439-478.
- [9] H. Ma; X. Chen; H. Liu; H. Liu; B. Fu, Improved volatile fatty acids anaerobic production from waste activated sludge by pH regulation: Alkaline or neutral pH? *Waste Management*. **2016**, *48*, 397-403.
- [10] R.J. Jones; R. Fernández-Feito; J. Massanet-Nicolau; R. Dinsdale; A. Guwy, Continuous recovery and enhanced yields of volatile fatty acids from a continually-fed 100 L food waste bioreactor by filtration and electrodialysis. *Waste Management*. **2021**, *122*, 81-88.
- [11] Y. Chen; R. Ruhyadi; J. Huang; W. Yan; G. Wang; N. Shen; W. Hanggoro, A novel strategy for improving volatile fatty acid purity, phosphorus removal efficiency, and fermented sludge dewaterability during waste activated sludge fermentation. *Waste Management*. **2021**, *119*, 195-201.
- [12] M. Mulders; J. Tamis; B. Abbas; J. Sousa; H. Dijkman; R. Rozendal; R. Kleerebezem, Pilot-Scale Polyhydroxyalkanoate Production from Organic Waste: Process Characteristics at High pH and High Ammonium Concentration. *Journal of Environmental Engineering*. **2020**, *146*, 04020049.
- [13] X. Wang; G. Carvalho; M.A.M. Reis; A. Oehmen, Metabolic modeling of the substrate competition among multiple VFAs for PHA production by mixed microbial cultures. *Journal of Biotechnology*. **2018**, *280*, 62-69.
- [14] A. Parodi; A. Jorea; M. Fagnoni; D. Ravelli; C. Samorì; C. Torri; P. Galletti, Bio-based crotonic acid from polyhydroxybutyrate: synthesis and photocatalyzed hydroacylation. *Green Chemistry*. **2021**, *23*, 3420-3427.
- [15] J. Blumenstein; J. Albert; R.P. Schulz; C. Kohlpaintner. Crotonaldehyde and Crotonic Acid. In *Ullmann's Encyclopedia of Industrial Chemistry*; pp. 1-20.
- [16] G.J. Raugi; T.C. Liang; J.J. Blum, Effects of pentanoic acid and 4-pentenoic acid on the intracellular fluxes of acetyl coenzyme A in Tetrahymena. *Journal of Biological Chemistry*. **1975**, *250*, 4067-4072.
- [17] N. Ahmad; B. Colak; M.J. Gibbs; D.-W. Zhang; J.E. Gautrot; M. Watkinson; C.R. Becer; S. Krause, Peptide Cross-Linked Poly(2-oxazoline) as a Sensor Material for the Detection of Proteases with a Quartz Crystal Microbalance. *Biomacromolecules*. **2019**, *20*, 2506-2514.
- [18] G. Pagliano; P. Galletti; C. Samorì; A. Zaghini; C. Torri, Recovery of Polyhydroxyalkanoates From Single and Mixed Microbial Cultures: A Review. *Frontiers in Bioengineering and Biotechnology*. **2021**, *9*,
- [19] M. Koller, Established and advanced approaches for recovery of microbial polyhydroxyalkanoate (PHA) biopolyesters from surrounding microbial biomass. *The EuroBiotech Journal*. **2020**, *4*, 113-126.

- [20] C. Samori; M. Basaglia; S. Casella; L. Favaro; P. Galletti; L. Giorgini; D. Marchi; L. Mazzocchetti; C. Torri; E. Tagliavini, Dimethyl carbonate and switchable anionic surfactants: two effective tools for the extraction of polyhydroxyalkanoates from microbial biomass. *Green Chemistry*. **2015**, *17*, 1047-1056.
- [21] S. Righi; F. Baioli; C. Samori; P. Galletti; E. Tagliavini; C. Stramigioli; A. Tugnoli; P. Fantke, A life cycle assessment of poly-hydroxybutyrate extraction from microbial biomass using dimethyl carbonate. *Journal of Cleaner Production*. **2017**, *168*, 692-707.
- [22] B. Mongili; A. Abdel Azim; S. Fraterrigo Garofalo; E. Batuecas; A. Re; S. Bocchini; D. Fino, Novel insights in dimethyl carbonate-based extraction of polyhydroxybutyrate (PHB). *Biotechnology for Biofuels*. **2021**, *14*, 13.
- [23] G.A. de Souza Reis; M.H.A. Michels; G.L. Fajardo; I. Lamot; J.H. de Best, Optimization of Green Extraction and Purification of PHA Produced by Mixed Microbial Cultures from Sludge. *Water*. **2020**, *12*, 1185.
- [24] C. Samori; F. Abbondanzi; P. Galletti; L. Giorgini; L. Mazzocchetti; C. Torri; E. Tagliavini, Extraction of polyhydroxyalkanoates from mixed microbial cultures: Impact on polymer quality and recovery. *Bioresource Technology*. **2015**, *189*, 195-202.
- [25] A. Aramvash; F. Moazzeni Zavareh; N. Gholami Banadkuki, Comparison of different solvents for extraction of polyhydroxybutyrate from *Cupriavidus necator*. *Engineering in Life Sciences*. **2018**, *18*, 20-28.
- [26] P. Murugan; L. Han; C.Y. Gan; F.H. Maurer; K. Sudesh, A new biological recovery approach for PHA using mealworm, *Tenebrio molitor*. *Journal of Biotechnology*. **2016**, *239*, 98-105.
- [27] T. Brouwer; B. Schuur, Bio-based solvents as entrainers for extractive distillation in aromatic/aliphatic and olefin/paraffin separation. *Green Chemistry*. **2020**, *22*, 5369-5375.
- [28] N. Guajardo; P. María, Assessing biocatalysis using dihydrolevoglucosenone (Cyrene™) as versatile bio-based (co)solvent. *Molecular Catalysis*. **2020**, *485*,
- [29] P. Ray; T. Hughes; C. Smith; M. Hibbert; K. Saito; G.P. Simon, Development of bio-acrylic polymers from Cyrene™: transforming a green solvent to a green polymer. *Polymer Chemistry*. **2019**, *10*, 3334-3341.
- [30] T. Marino; F. Galiano; A. Molino; A. Figoli, New frontiers in sustainable membrane preparation: Cyrene™ as green bioderived solvent. *Journal of Membrane Science*. **2019**, *580*,
- [31] T. Brouwer; M. Blahusiak; K. Babic; B. Schuur, Reactive extraction and recovery of levulinic acid, formic acid and furfural from aqueous solutions containing sulphuric acid. *Separation and Purification Technology*. **2017**, *185*, 186-195.
- [32] T. Brouwer; B. Schuur, Dihydrolevoglucosenone (Cyrene), a Biobased Solvent for Liquid-Liquid Extraction Applications. *ACS Sustainable Chemistry & Engineering*. **2020**, *8*, 14807-14817.
- [33] A. Werker; S. Bengtsson; L. Korving; M. Hjort; S. Anterrieu; T. Alexandersson; P. Johansson; A. Karlsson; L. Karabegovic; P. Magnusson; et al., Consistent production of high quality PHA using activated sludge harvested from full scale municipal wastewater treatment - PHARIO. *Water Science and Technology*. **2018**, *78*, 2256-2269.
- [34] A. Werker; F. Maurer; P. Jannasch; P. Magnusson; P. Johansson. Method for the recovery of stabilized polyhydroxyalkanoates from biomass that has been used to treat organic waste. EP2606080 (A1) 2016.

- [35] G. Braunegg; B. Sonnleitner; R.M. Lafferty, A rapid gas chromatographic method for the determination of poly- β -hydroxybutyric acid in microbial biomass. *European journal of applied microbiology and biotechnology*. **1978**, *6*, 29-37.
- [36] M. Patel; D.J. Gapes; R.H. Newman; P.H. Dare, Physico-chemical properties of polyhydroxyalkanoate produced by mixed-culture nitrogen-fixing bacteria. *Applied Microbiology and Biotechnology*. **2009**, *82*, 545-555.
- [37] M. De bruyn; V.L. Budarin; A. Misefari; S. Shimizu; H. Fish; M. Cockett; A.J. Hunt; H. Hofstetter; B.M. Weckhuysen; J.H. Clark; et al., Geminal Diol of Dihydrolevoglucosenone as a Switchable Hydrotrope: A Continuum of Green Nanostructured Solvents. *ACS Sustainable Chemistry & Engineering*. **2019**, *7*, 7878-7883.

Chapter 5

Crotonic acid production by pyrolysis and vapor fractionation of mixed microbial culture-based Poly(3-hydroxybutyrate-co-3-hydroxyvalerate)



This chapter is adapted from:

Elhami, V.; Hempenius, M.A.; Schuur, B., "Crotonic acid production by pyrolysis and vapor fractionation of mixed microbial culture-based Poly(3-hydroxybutyrate-co-3-hydroxyvalerate)", **Industrial & Engineering Chemistry research**, 2023, 62, 916-923.

Abstract

Due to sustainability issues regarding petroleum-based materials, providing renewable alternatives to produce platform chemicals is essential. Crotonic acid (CA) and trans-2-pentenoic acid (2-PA) are examples of such renewables, and can be obtained by pyrolysis of the bio-based poly(3-hydroxybutyrate-co-3-hydroxyvalerate) (PHBV) copolymer. In this study, aiming at obtaining high yields of both CA and 2-PA from mixed microbial cultures (MMC), direct pyrolysis of the PHBV-enriched biomass into CA and 2-PA was studied either under an inert atmosphere using N₂ carrier gas flow or under reduced pressure. The average residence time of the hot vapor phase was manipulated by changing the nitrogen flow rate. The highest yields of 80±2% for CA and 67±1% for 2-PA were obtained at 0.15 L/min nitrogen flow rate corresponding to a mean residence time of 20 s, 240 °C for 1 hour. A similar acid yield was achieved when the pyrolysis was performed under reduced pressure (150 mbar) instead of using nitrogen gas. The combined pyrolysis of extracted PHBV at 220 °C and 90 minutes with vapor fractionation by distillation resulted in yields of 81% and 92% for CA and 2-PA, respectively. The top product of the distillation column was enriched with CA (76%) and the bottom product with 2-PA (51%), meaning that it is possible to separate these acids by distillation and produce them with relatively high purity by this bio-based approach. A detailed distillation study will be available in follow-up work.

1. Introduction

Polyhydroxyalkanoates (PHAs) are a class of biodegradable and renewable polymers which can be produced by various bacteria as an energy reserve, ensuring the long-term survival of the bacteria during nutrient-scarce conditions [1,2]. These bio-based polymers are considered as green polymers of the future due to their potential to replace conventional polymers [3]. It has been shown that the bacteria can yield high quality PHAs using pure substrates and sterile conditions, but under these expensive growth conditions the polymers are not economically competitive with the conventional polymers [4]. Alternatively, it is possible to apply an open mixed microbial culture (MMC) to produce low cost PHAs. MMC enables the use of inexpensive feedstocks such as waste/wastewater under non-sterile conditions [5-10]. This approach involves anaerobic fermentation of waste/wastewater to produce volatile fatty acids (VFAs), followed by aerobic conversion of the VFAs into the PHAs. During the fermentation process in the MMC, VFAs with an odd number will produce poly(3-hydroxybutyrate-co-3-hydroxyvalerate) (PHBV) copolymer with varying hydroxyvalerate (HV) ratios, and those with an even number of carbons will yield poly(3-hydroxybutyrate)(PHB) [3]. Polymers with a low HV content (< 10% HV) are hard and brittle, resembling unplasticized polyvinyl chloride (PVC), mid-range HV content (between 10-25%) polymers maintain a good balance of toughness and resemble polypropylene (PP), whilst high HV content (25-40%) polymers are soft and tough having a polyethylene (PE) like feel [11].

In most cases, PHBV is the main bio-polymer spontaneously produced by fermentation of VFA enriched waste/wastewater. Naturally, the composition of waste/wastewater varies from day to day which can affect the quality of

the polymer. For instance, the monomer composition of the co-polymer might vary per batch and consequently the thermal and physical properties of the polymer differ, which can limit the application window of the bio-based polymer. Alternatively, it is still possible to valorize the biopolymers of low quality by depolymerizing them to produce other value-added chemicals such as 2-alkenoic acids. 2-Butenic acid/ crotonic acid (CA) is the main product of PHB decomposition [12]. CA is used in textile, cosmetic, painting, and coating applications and as building block in the synthesis of co-polymers, for example by copolymerization with vinyl acetate [13]. Regardless of its wide range of application, the current production pathway of CA through a petrochemical route is neither renewable nor straightforward. The 2021 selling price in Europe was about USD 15.4 per kg, while the selling price of CA produced via thermal degradation of the bio-based PHB obtained from a pure culture was estimated to be USD 7.80-11.05 per kg in 2014 [12]. With such high market prices, it is worthwhile to further investigate the efficient production of CA from bio-based PHB/PHBV. For example, by replacing a pure culture with an open MMC and applying waste/wastewater as feedstock, the production cost of CA can be reduced, and sustainable valorization of waste may be realized [14]. Over the last decades, the thermal degradation mechanism of PHBV/PHB has been investigated in several studies using thermogravimetric analyses (TGA) and a pyrolysis gas chromatography-mass spectroscopy (Py GC-MS) apparatus, in which different reaction paths were considered [15-17]. Generally, it is concluded that a random beta elimination, followed by an unzipping beta elimination at the crotonyl chain end is the dominant reaction path [15-18]. First, a random beta elimination occurs in which the PHB/PHBV undergoes

chain scission. With the beta elimination, the beta hydrogen linked to the ester oxygen is nucleophilically attacked by the ester carbonyl group. In this way, two new chain-ends are formed, one having a carboxyl chain end and the other a crotonyl chain-end. Finally, if the molecule with the crotonyl chain-end undergoes a beta elimination at the ester group neighboring the crotonyl chain-end, CA or 2-pentenoic acid (2-PA) is formed depending on which monomer (hydroxybutyrate (HB) or HV) is present at the chain-end. The CA production yield through pyrolysis of PHB/PHB-enriched biomass at 310 °C is reported to be about 63% which is 30% higher than the yield obtained by the conventional petroleum based route [12,19,20]. Moreover, the biobased CA yield can be increased to about 80% using a catalyst [19] or a pretreatment technique [20]. Solvent based pyrolysis of the commercial PHB can increase the CA yield even further [21,22]. Thermal decomposition of the PHB in cyclohexane solvent at 210 °C and 5h, followed by solvent separation by distillation, resulted in 89% CA yield with a purity of 91% [22]. Ionic liquid based media were also examined as green solvent and catalyst to obtain CA from PHB [21]. About 97% yield of CA was obtained by applying an ionic liquid named [EMIM][AcO] as a solvent and catalyst at 140 °C and 90 min. Based on these PHB-pyrolysis results, showing promising potential to obtain CA on scales beyond analytical, we decided to study PHBV pyrolysis from MMC-based PHBV to obtain a mixture of CA and 2-PA, originating from PHB and poly(3-hydroxyvalerate) (PHV) repeating units, respectively. Recently, Parodi et al. [23] developed a thermolysis method to directly pyrolyze PHB/PHB-enriched biomass and obtain relatively pure CA. By means of this approach, it was possible to produce CA with a purity of 92% from pyrolysis of a PHB-enriched biomass containing 30 wt% PHB on dry basis.

Crotonic acid production through PHBV pyrolysis

Since both catalytic and non-catalyzed thermal approaches have shown highly interesting results for either pure PHB, or for PHBV on an analytical scale, it was decided to study direct pyrolysis for PHBV co-polymers and examine the impact of process conditions to aid further process design. Moreover, PHBV is the main co-polymer usually obtained from a waste digestion in MMC. Thus, it is worth to investigate the possibility of producing relatively pure CA from MMC-PHBV which might provide an economic approach due to the low cost of polymer synthesis. Figure 5-1 shows the schematic overview of the process to produce CA through MMC-based PHBV depolymerization. To the best of our knowledge, the production of CA from MMC-based PHBV using a lab scale pyrolysis set-up has not been studied yet, and such a study can aid process design because aspects like thermal degradation, as well as optimum mean residence time of the hot vapor phase in the oven need to be understood on lab scale aiming at before further development. As PHBV is the main polymer which can be naturally produced by fermentation of VFA enriched waste/wastewater, it is worthwhile to investigate the possibility of obtaining relatively pure CA from PHBV depolymerization.

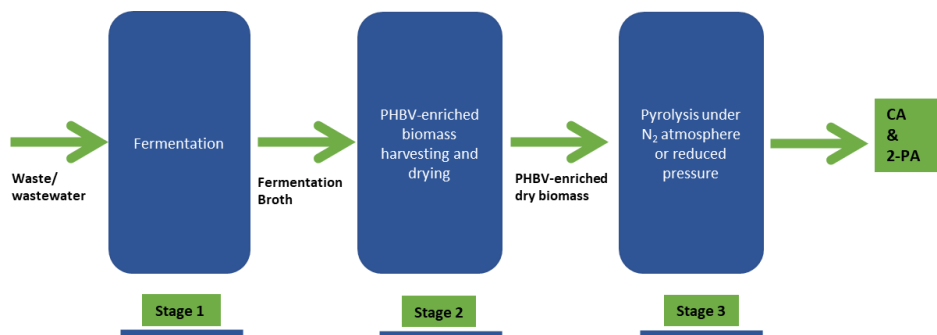


Figure 5-1. Schematic overview of the CA/2-PA production from MMC-based PHBV.

In the present study, we developed a lab scale pyrolysis set-up to study CA production from decomposition of MMC-based PHBV/PHBV-enriched biomass. The thermal degradation experiments were performed under an inert atmosphere using either N₂ gas or vacuum. The effect of the vapor phase residence time on the acid production yield was studied by varying the flow rate of the N₂ gas. As 2-PA is the main byproduct in the PHBV pyrolysis, a Vigreux was applied to upgrade the purity of the CA by distillation and to study the possibility of in-situ separation of CA and 2-PA from the vapor phase.

2. Material and methods

2.1. Chemicals

Crotonic acid ($\geq 98\%$) and *trans*-2-pentenoic acid ($\geq 98\%$) were purchased from Sigma Aldrich. Acetone ($>99\%$, extra pure) was supplied by Thermo Fischer Scientific. Chemical were used as received.

2.2. MMC-based PHBV/PHBV-enriched biomass preparation

The dry PHBV-enriched biomass containing 30 wt% PHBV (35 wt% HV) on dry basis was obtained from Paques Biomaterials, which was produced from municipal food waste [24]. For the experiments in which pure PHBV was used, the polymer was extracted using 2-methyltetrahydrofuran (2-MTHF) and characterized according to the procedure described in chapter 4 [25]. Briefly, a certain quantity of the biomass was added to 2-MTHF solvent to reach a concentration of 5% (g/mL), followed by heating the mixture at 80 °C for 1h.

Afterwards, *n*-heptane was used as an antisolvent to precipitate the polymer. Finally, the collected polymer was dried in a vacuum oven at 50 °C for 24 h.

The water content of the biomass was measured by drying it in an oven at 105 °C for an hour. The difference in the mass of the biomass before and after drying was used to calculate the water content.

2.3. Pyrolysis of PHBV and PHBV-enriched biomass

A custom-built oven pyrolyzer set-up was applied to pyrolyze the MMC based PHBV/PHBV enriched biomass. As depicted in Figure 5-2, the oven pyrolyzer set-up consisted of a temperature-controlled oven, a round bottom flask loaded with the PHBV/PHBV-enriched biomass and placed inside the oven, and a thermocouple to monitor the round bottom flask temperature with an accuracy of ± 1 °C, a condenser at -5 °C to condense the vapor phase and a receiving flask to collect the products. The set-up was connected to either a vacuum pump or N₂ supply, depending on the experimental procedure.

First the PHBV and PHBV-enriched biomass were analyzed by thermal gravimetric analysis (TGA) to determine the degradation temperature of the polymer and to set the oven at the required decomposition temperature. Then, the pyrolysis experiment was started by heating the PHBV/PHBV-enriched biomass to the set temperature for 1 h. Various nitrogen gas flows (0.05 to 0.2 L/min) were applied, or reduced pressure (either 50 or 150 mbar). After 1 h of pyrolysis, the condenser was flushed with acetone to collect the pyrolyzates that had crystallized there. Pyrolyzates refers to all the materials which condensed in the condenser and were collected there. It includes CA, 2-Pa and other side products. Acetone was removed from the

samples by overnight atmospheric evaporation, followed by final evaporation in a vacuum oven at maximum vacuum for 2 hours at room temperature. Subsequently, the pyrolyzates were analyzed by various analysis techniques to determine the yield and purity of the produced acids. Each experiment was duplicated.

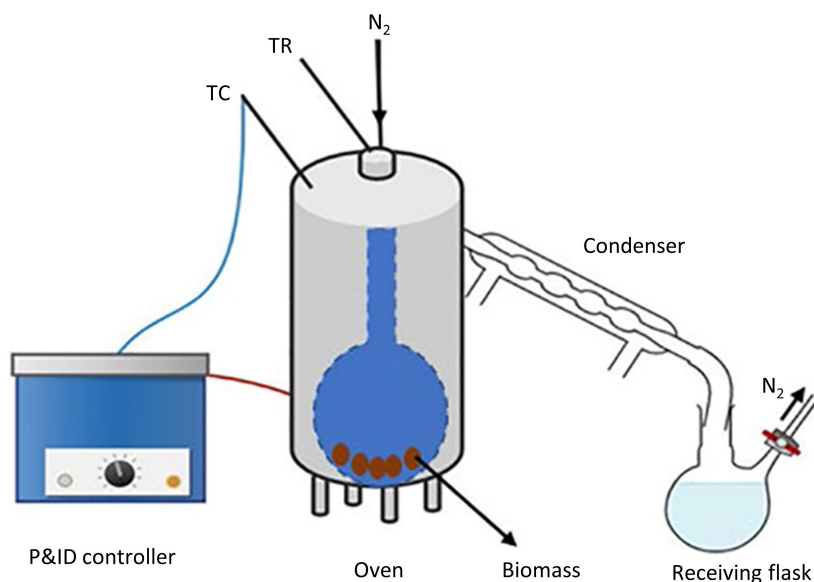


Figure 5-2. A schematic view of the custom-built oven pyrolyzer set-up to produce CA from MMC based PHBV / PHBV-enriched biomass.

2.4. Integrated pyrolysis-distillation approach for PHBV decomposition

In the next step, the goal was to not only obtain relatively pure CA from MMC-based PHBV, but also to retrieve 2-PA as a side product. Thus, a vacuum-insulated Vigreux distillation column was placed between the oven pyrolyzer and the condenser. To limit the byproduct formation due to

reactivity between the formed CA and 2-PA, The experiments were performed at a reduced pressure of 50 mbar and the main fraction of CA was collected after it passed the condenser, while the majority of 2-PA remained at the bottom of the heated flask.

2.5. Analysis

High Performance Liquid Chromatography (HPLC). The concentrations of CA and 2- PA were measured using a HPLC [Agilent Hi-Plex H column (300 × 7.7 mm) with a refractive index detector on an Agilent 1200 series HPLC system; mobile phase, 5 mM H₂SO₄ solution; column temperature of 65 °C at a flow rate of 0.6 mL/min].

Due to overlapping of the peaks of the acids with side products, symmetrical peaks were fitted with a Gaussian function using OriginPro 2019b software (see Figure S-13 in the appendix for more details). Afterwards, the fitted peaks were integrated to quantify the acids. The acid yield was defined as Eq.(5-1):

$$Acid\ yield(wt\%) = \frac{Amount\ of\ collected\ acid(g)}{Theoretical\ amount\ of\ the\ acid(g)} \times 100 \quad (5-1)$$

Where the amount of the collected acid was determined by HPLC and the theoretical amount of the acid was defined based on the HB content in the PHBV for CA and the amount of HV repeat units for 2-PA. Thus, a 100% CA yield means that the total quantity of HB units present in the PHBV is completely converted into CA.

Gas chromatography-Mass Spectroscopy (GC-MS) analyses were performed to determine the main side products from the PHBV/PHBV-enriched biomass pyrolysis. The pyrolyzate samples were dissolved in acetone with concentrations of less than 500 ppm and analyzed using a GC-FID/MS (GC – 7890A, MS – 5975C Agilent Technologies system) equipped with an Agilent HP-5MS HP19091S-433 capillary column (60 m, ID 0.25 mm, Film thickness: 0.25 μm). The column was packed with (5%-phenyl)-methylpolysiloxane. Helium was used as carrier gas with a constant flow rate of 1.95 mL/min. The oven temperature was programmed from 45 °C (4 min) to 280 °C at a heating rate of 3 °C/min and was held at 280 °C for 20 min. The injector and the column to the MS interface were maintained at a constant temperature of 250 °C and 280 °C, respectively. A sample of 1 μL was injected into the GC. The MS was operated in electron ionization mode, and ions were scanned in a m/z range from 15 to 500.

Refinery GC was used to identify the non-condensed gases. A sample was taken from a N_2 stream in the outlet of the condenser and injected in a Varian 450-RGA. Details of the instrument were previously provided elsewhere [26].

Thermal Gravimetric Analysis (TGA) was employed to measure the degradation temperature of the polymers using a TGA-550 instrument operated under nitrogen flow. The samples were heated from room temperature to 400 °C at a rate of 10 °C/min under nitrogen atmosphere

Karl-Fischer titration (KFT) was used to analyze the water content of the pyrolyzate mixture using a Metrohm 787 KFTitrino. Hydranal composite 5 was titrated from a 20 mL burette filled with a mixture of methanol and dichloromethane in a volume ratio of 3 to 1. The samples were analyzed in triplicate with a relative error less than 1%.

3. Results and discussion

3.1. Pyrolysis of the PHBV-enriched biomass

The characteristics of the PHBV and PHBV-enriched biomass are given in Table 5-1. The polymer content of the biomass, the composition (repeat unit ratio) of the polymer, average molecular weight (MW) and polydispersity index (PDI) are taken from our previous work as the same batch of the biomass was used for pyrolysis experiments [25]. The composition, polymer content of the biomass and water content of the polymer and biomass were taken into account in the calculation of the yield in each experiment. The PHBV and PHBV enriched biomass are known to be hygroscopic. Therefore, their water content was measured beforehand, resulting in about $4\pm 1\%$ and $<1\%$ for the biomass and extracted PHBV, respectively. To apply a proper temperature range for the pyrolysis of the polymer, the degradation temperature (T_{deg}) of the biomass and the extracted PHBV was determined by TGA in which the inflection point of the curve was considered as T_{deg} . As shown in Table 5-1, the T_{deg} of the polymer in PHBV-enriched biomass is $240\text{ }^{\circ}\text{C}$, thus, the experiments of direct pyrolysis of the biomass were performed at $240\text{ }^{\circ}\text{C}$. The T_{deg} of extracted PHBV increased by $5\text{ }^{\circ}\text{C}$, possibly due to the purification of the polymer during the extraction, as it is known that metal ions present in the biomass can accelerate thermal degradation of the polymer [17] and perhaps other molecules in the biomass.

Crotonic acid production through PHBV pyrolysis

Table 5-1. The characteristics of the PHBV-enriched biomass and the extracted PHBV used in the pyrolysis experiments.

Material	PHBV [wt%]	T _{deg.} [°C]	HB/HV [mol]	MW [kDa]	PDI	Water [%]
PHBV-enriched biomass	30	240	65/35	146	3.5	4±1
Extracted PHBV	>99	245	65/35	122	4.9	<1

The heating time of the polymer in the set-up and the residence time of the produced, thermally sensitive monomers in the vapor phase in the hot set-up are crucial parameters to be controlled in order to achieve a complete degradation of the polymer and maximize monomer yields. To establish an estimate for the heating time for the polymer pyrolysis, a preliminary experiment was carried out using about 5 g biomass at 240 °C and 1 h of heating. Afterwards, the residual biomass was analyzed by TGA to determine whether or not a significant fraction of the polymer remained in the biomass after pyrolysis. In Figure 5-3, two TGA experiments are shown, one of biomass before pyrolysis, and one of the residue remaining after pyrolysis. In the temperature range of 180 to 280 °C the line for the biomass before pyrolysis shows a distinct reduction in weight, occurring in the temperature range where PHBV degrades. The mass reduction of the residue of biomass after pyrolysis is not as pronounced as that of the biomass before pyrolysis. Most likely, this indicates that the polymer content of the residual biomass is not significant anymore and from that, it can be concluded that 1h of pyrolysis at 240 °C sufficed to pyrolyze the vast majority of the polymers in the biomass. Thus, the contact time and temperature for pyrolysis were kept constant at 1 h and 240 °C in all experiments.

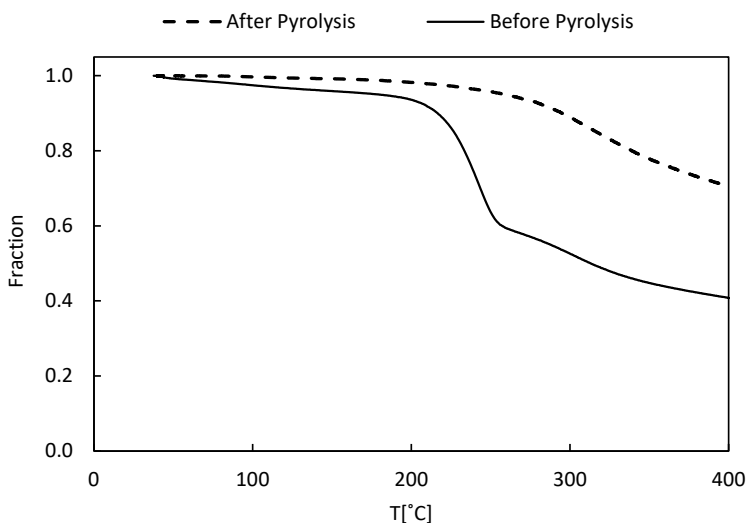


Figure 5-3. TGA graph of the biomass before and after pyrolysis at 240 °C for 1 h under a nitrogen flow rate of 0.1 L/min.

To study the influence of the residence time of the vapor phase in the hot zone on the acids yield, pyrolysis of the PHBV-enriched biomass and extracted PHBV was carried out under either a N₂ stream or under vacuum, and the obtained results were compared. Applying nitrogen as a carrier gas allows varying the residence time of the vapor phase both in the hot pyrolyzer and in the condenser. CA and 2-PA are unsaturated acids which are not thermally stable. At long residence times in the hot zone these monomers can undergo decomposition, isomerization and polymerization [27]. On the other hand, short residence times might result in only partial decomposition of the polymers, yielding oligomers as the main side product instead of the desired monomers. Therefore, the influence of the hot vapor residence time was experimentally examined by varying the flow rate of the nitrogen carrier gas and assuming that the produced vapor phase has the

same flow rate. Figure 5-4 represents the yield obtained under various pyrolysis conditions. As can be clearly seen from the graph, the acid yield is lowest when there is neither carrier gas (e.g. nitrogen) nor reduced pressure to pull out the vapor phase. The yield increased about 15% at a N₂ flow rate of 0.05 L/min as compared to the experiment where no carrier gas was used. Increasing the flow to 0.15 L/min resulted in 80±2% and 67±1% yield of CA and 2-PA, respectively. A further increase of the nitrogen flow rate did not significantly enhance the pyrolysis yield. Following the method of Parodi et al.[23], a few pyrolysis experiments were also performed under reduced pressures of 150 mbar and 50 mbar. As shown in Figure 5-4, at 150 mbar similar yields were obtained in comparison with applying nitrogen gas at flow rates of 0.15 and 0.2 L/min. However, the acid yields were low at 50 mbar, which may be, because they are not condensing in the condenser, for which two explanations may be given. First, it might be due to the short residence time of the vapor phase in both the hot zone and the condenser. Second, due to the pumping out of vapor molecules by the pump as it maintains the setpoint pressure of 50 mbar, or by adding N₂ flow, in both cases, the system may not reach the dewpoint [28]. For situations where the rate of pyrolysis is relatively low compared to the flow of N₂, the mol fraction of the acids also becomes low, which may result in portions of the acids that do not condense due to thermodynamic equilibrium (Eq. (5-2)), not reaching the dewpoint [28].

$$y_i P = \gamma_i x_i P^{sat,i} \quad (5-2)$$

Crotonic acid production through PHBV pyrolysis

When the kinetic effect is the major cause, this could be countered by adding a longer condenser, but when nitrogen flows are applied, some of the vapors do not condense due to the dewpoint not being reached. In that case longer condensers do not help. As a check to calculate whether this would be a significant amount of CA not condensing, the dewpoint was calculated as function of the vapor fraction CA in N₂ (see section 17 in the appendices). It was determined that at -5 °C the dewpoint corresponds to a mol fraction CA of 5.2×10^{-5} and at 0.2 L/min N₂ flow, this corresponds to a loss of only 0.085% of the CA. this calculation shows that any significant effect must be due to kinetics, as the equilibrium would dictate that most CA would condense and crystallize.

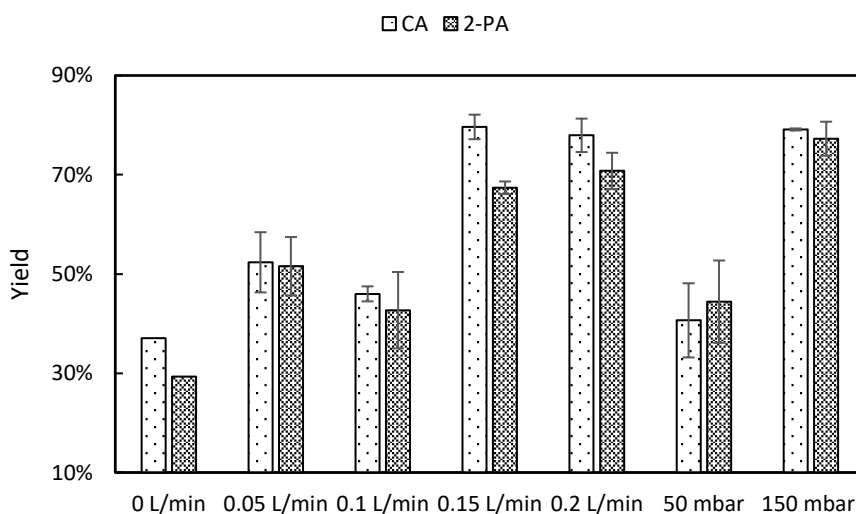


Figure 5-4. CA and 2-PA yield obtained by direct pyrolysis of the PHBV-enriched biomass at various operation conditions.

The highest CA yield achieved in this work is higher than what has been published for direct pyrolysis of PHB-enriched biomass (about 60%) [12,23]

and comparable to the yield obtained by either catalytic thermal degradation (83%) [19] or by thermal decomposition of pretreated PHB (80%) [20]. Although differences in yield may be explained by different characteristics of the polymer and biomass used in this work, the distinct pyrolysis set-up and experimental procedure used here also contribute to the high monomer yields. Especially considering the significant impact that process conditions have on the yields, as can be seen in Figure 5-4, optimization of the procedure is essential. As a further example, Mamat et al. [12] performed pyrolysis experiments at a high temperature of 310 °C which can accelerate the isomerization and polymerization of CA, resulting in low CA production yields. As the reported CA yields from direct pyrolysis of the biomass [12,23] are similar to the ones we obtained under less favorable conditions (hot vapor residence time of 61 s corresponding to N₂ flow rate of 0.05 L/min), the configuration of the pyrolysis set-up and the residence time of the vapor phase in the hot oven are indeed major parameters determining the differences in yield obtained in the literature and in this work.

When comparing the polymer used in this study with other studies, the most distinctive properties of the polymer in this study are its high HV content and low average MW, obtained by MMC, using food waste as a feedstock. It has been found that the HV content in PHBV polymers does not affect the T_{deg} of the polymer [29]. The glass transition temperature [30], crystallinity and melting point [29] of the polymer, however, are lowered by increasing the HV content, and these thermal characteristics may have an impact on the pyrolysis process. Therefore, a generalized conclusion on the impact of the HV content on the thermal decomposition of PHBV polymers can not be presented yet.

To gain more information regarding the possible reasons for different yields obtained from various experiments, the composition of the pyrolyzates was investigated, followed by a mass balance closure over the biomass during pyrolysis. Pyrolyzates refers to all the materials which condensed in the condenser and were collected there. It includes CA, 2-PA and other side products. Table 5-2 represents the composition of the pyrolyzate mixture obtained at various pyrolysis conditions, which illustrates that the pyrolysis at different nitrogen flow rates results in mixtures with a similar acid content. The mixture from the experiment at 50 mbar has the lowest acids content and the largest amount of condensed side products which might be due to the short residence time in the condenser, leading to partial condensation of the vapor phase. To verify this hypothesis, the samples were analyzed by GC-MS to identify the side products present in the pyrolyzate mixture. According to GC-MS, isocrotonic acid, 3-butenic acid, 3-pentenoic acid, 4-pentenoic acid, crotonamide and 2,2,6,6-tetramethyl-4-piperidone are the main side products in all the experiments, regardless of the pyrolysis conditions. To compare the quantity of the aforementioned side products in each experiment, their corresponding peak areas were normalized to the area of the 2-PA peak in each sample. It was found that the operation conditions do not have a significant impact on the pyrolyzate composition in terms of the dominant side products masses. Regarding water content in the pyrolyzate mixture which originated from the moisture content of the biomass, it is <1% based on Karl-Fischer analysis which is lower than the water content of the starting biomass ($4\pm 1\%$). It can be explained by the evaporation of water while removing acetone from the pyrolyzate mixture using a vacuum oven at room temperature. Furthermore, it is also expected that a fraction of the

Crotonic acid production through PHBV pyrolysis

water in vapor phase leaves the condenser without condensing during pyrolysis (same reasoning as for the acid yields being limited by a fraction of the acids not condensing).

Table 5-2. Summary of the composition of the pyrolyzate mixtures obtained by direct pyrolysis of the PHBV-enriched biomass at various operation conditions.

Exp.	RT ^a [s]	Composition [wt%]			
		CA	2-PA	water	condensed by-products
N ₂ -0 L/min	-	50	21	<1	28
N ₂ -0.05 L/min	61	53±1	27±1	<1	19±0.3
N ₂ -0.1 L/min	30	52±8	25±2	<1	22±6
N ₂ -0.15 L/min	20	52±1	24±1	<1	24±1
N ₂ -0.2 L/min	15	54±5	26±2	<1	19±8
Vacuum-50 mbar	-	36±1	21±0.3	<1	41±1
Vacuum-150 mbar	-	45±2	24±0.1	<1	31±2

^aRT is the mean residence time of the vapor phase in the hot zone of the oven pyrolyzer.

The mass balance closure over the biomass pyrolysis was performed to compare the performance of the various pyrolysis conditions in terms of the overall conversion. As can be seen from Figure 5-5, the char formation is high (~62%) at low nitrogen flow rates due to the long residence of the vapor in the hot zone. The vapor phase contains mainly CA and 2-PA which are not thermally stable and can undergo isomerization and polymerization at elevated temperatures during prolonged residence times [27]. Moreover, it was observed that a brown layer forms on the walls of the glassware at low nitrogen flow rates which can be explained by possible dimerization of the acids. The char formation is around 53% in the experiments under reduced pressures of 50 and 150 mbar, and nitrogen flow rates of 0.15 and 0.2 L/min which is about 10% less than other experiments. The largest quantity of

Crotonic acid production through PHBV pyrolysis

pyrolyzate mixture collected under N₂ flow was around 28% on the basis of the starting biomass amount, using flow rates of 0.15 and 0.2 L/min, while the highest pyrolyzate mass obtained under vacuum (150 mbar) was around 33%. Considering that the amount of polymer in the biomass was estimated at approximately 30 wt% (discussion on results in Figure 5-3), this yield is excellent. In all experiments with various pyrolysis conditions, a fraction of the small molecules derived from the PHBV-enriched biomass did not condense in the condenser at -5 °C. Therefore, a gas sample was taken to be analyzed with Micro-GC to identify the non-condensed gases. Since the set-up was an open system with a continuous flow of nitrogen, it was not possible to precisely quantify the non-condensed gas phase. According to Micro-GC, the vapor phase at a nitrogen flow rate of 0.1 L/min contained ethylene, methane, propylene, 1-butene, 1,3-butadiene and 1-butyne.

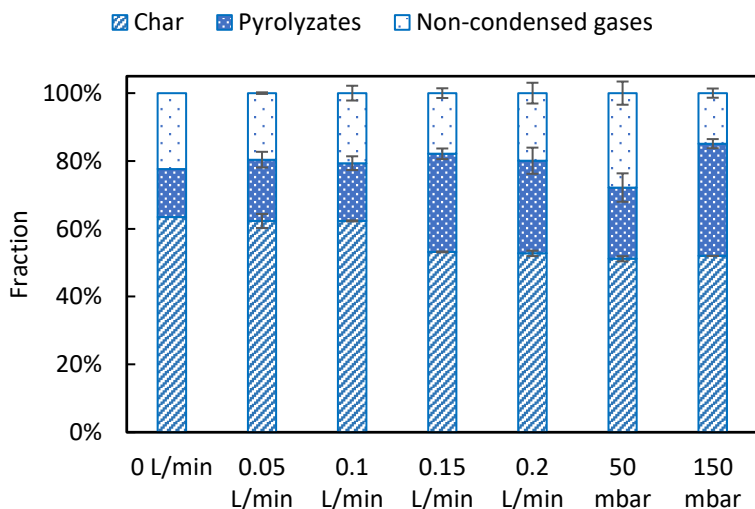


Figure 5-5. Mass balance closure over the PHBV-enriched biomass pyrolyzed at various operation conditions.

3.2. Integrated pyrolysis of PHBV and distillation of pyrolyzates under vacuum conditions

To directly produce the acids with high purity from pyrolysis of the PHBV, a vacuum-isolated Vigreux column was placed in the outlet of the oven pyrolyzer to in-situ separate CA and 2-PA in vapor phase by distillation. A vacuum-isolated Vigreux column prevents crystallization of CA within the column because it loses much less heat to the surroundings compared to unisolated Vigreux columns. This approach was already mentioned by Parodi et al. [23]. However, these authors used PHB/PHB-enriched biomass to obtain CA, and not the copolymer PHBV. We aimed to produce CA and 2-PA with the highest possible purity from a MMC-PHBV, as the PHBV is the dominant polymer usually produced in MMC, using VFA-rich waste streams as feedstock. Therefore, preliminary integrated pyrolysis of PHBV and distillation experiments were performed to examine the fractionation of the vapor phase containing mainly CA and 2-PA. The experiments were carried out at 50 mbar (instead of using a nitrogen flow). In the first experiment, the temperature was set at 170 °C following the method of Parodi et al. [23]. However, there was no vapor flow entering the column after an 1 hour. Thus, the temperature was gradually increased until a vapor flow was observed which occurred at 220 °C. The experiment was repeated in which the temperature was set at 220 °C from the starting point.

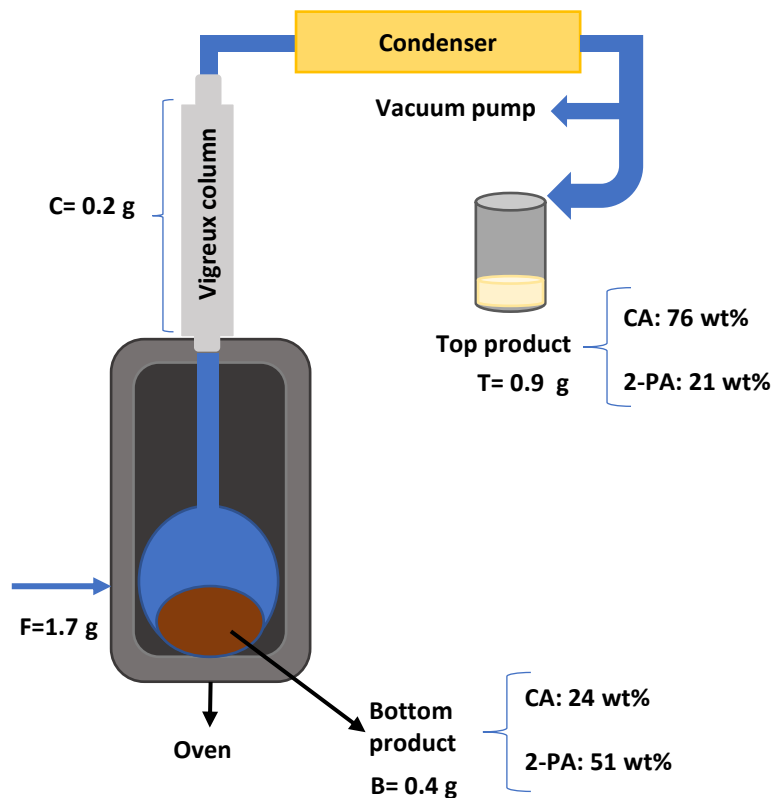


Figure 5-6. Pyrolysis of PHBV at 220 °C, 50 mbar and 90 minutes with in-situ fractionation of the vapor phase by distillation. F, C, T and B represent the mass of PHBV used for pyrolysis, mass of the acids remained in the column, total mass of the top and bottom products, respectively.

After 90 minutes at 220 °C, the flow of vapor was diminished. Thus, the experiment was stopped and samples were taken to be analyzed by HPLC. The yields of 2-CA and 2-PA were 81 and 92%, respectively. The Overall mass balance closure indicated that 85% of the PHBV was converted into the CA and 2-PA, including both top and bottom products. About 6% can be accounted for the side products in the bottom stream and 6% is converted into a non-condensed gas products. 3% was remained as a char in the round

bottom flask. Moreover, a small fraction can be also considered to be lost during handling and collecting the products. As shown in Figure 5-6, the top product is rich in CA (76 wt%) while the bottom product contained 2-PA in 51 wt%, meaning that it is possible to separate these acids by distillation and produce them with relatively high purity from MMC-based PHBV. In the current setup, only a limited number of distillation stages are available, and further distillation studies are recommended for follow-up work to reach higher purities.

4. Conclusion

In this work, the direct pyrolysis of the PHBV-enriched biomass produced by an open MMC, using food waste as feedstock, was studied in a custom-made oven pyrolyzer, operated either under reduced pressure conditions or a nitrogen atmosphere. Applying nitrogen as a carrier gas enabled the manipulation of the mean residence time of the hot vapor phase and the experimental optimization of the thermal depolymerization of the PHBV towards CA and 2-PA. At low nitrogen flow rates <0.1 L/min, the acid yield is lower and the char formation is higher than with experiments performed at N_2 flow rates of 0.15 and 0.2 L/min. According to the mass balance closure over the pyrolysis system, the non-condensed vapor phase is almost constant in all the experiments performed under nitrogen gas. It indicates that regardless of the operation conditions, a part of the biomass forms non-condensable gases at 240°C . The GC analysis of the gas phase in the outlet of the condenser indeed confirmed the formation of non-condensable gases such as ethylene, methane, propylene, 1-butene, 1,3-butadiene and 1-butyne. The maximum acid yields of $80\pm 2\%$ and $67\pm 1\%$ for CA and 2-PA were

achieved at a nitrogen flow rate of 0.15 L/min, 240 °C and 1 h. By replacing the nitrogen gas with a vacuum of 150 mbar, similar acid yields were obtained. The highest obtained CA yield is comparable with the results achieved by catalyzed prolysis, and by pyrolysis of pretreated PHB/PHB-enriched biomass. However, due to the nature of the PHBV, 2-PA is also formed, requiring an appropriate downstream separation technique to yield pure CA. Therefore, the suitability of distillation was investigated by integrated pyrolysis-distillation experiments. The integrated pyrolysis-distillation approach indeed allowed to directly fractionate the vapor phase, originating from pyrolysis of the extracted PHBV. The product at the top of the column was mainly CA (76%), indicating that distillation is a viable technique for separating CA and 2-PA and thereby producing relatively pure CA and 2-PA from MMC based PHBV. It is expected that the purity of CA can be increased even further by using a proper distillation column with more equilibrium stages.

Nomenclature:

CA	Trans-Crotonic Acid
GC-MS	Gas Chromatography
GPC	Gel Permeation Chromatography
HB	Hydroxy Butyrate
HV	Hydroxy Valerate
HPLC	High Pressure Liquid Chromatography
KFT	Karl-Fischer Titration
MW	Molecular Weight
MMC	Mixed Microbial Culture
2-MTHF	2-Methyltetrahydrofuran
PHAs	Polyhydroxyalkanoates
PHB	Poly(3-hydroxybutyrate)
PHV	Poly(3-hydroxyvalerate)
PHBV	Poly(3-Hydroxybutyrate-co-3-Hydroxyvalerate)
Py GC-MS	Pyrolysis Gas Chromatography-Mass Spectroscopy
2-PA	2-Pentenoic Acid
PDI	Polydispersity Index
PP	Polypropylene
PVC	Polyvinyl chloride
PE	Polyethylene
TGA	Thermal Gravimetric Analysis
THF	Tetrahydrofuran
VFAs	Volatile Fatty Acids

References

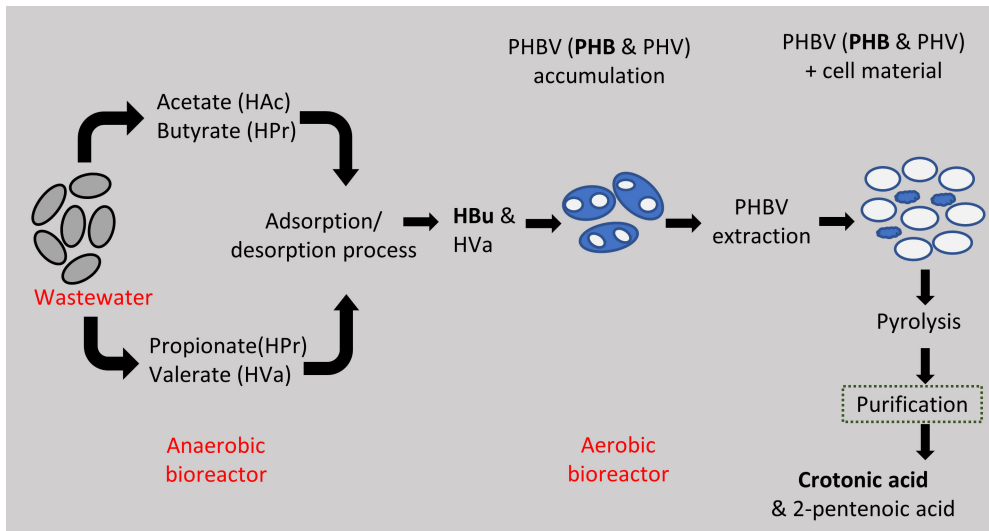
- [1] M. Koller; H. Niebelschütz; G. Brauneegg, Strategies for recovery and purification of poly[(R)-3-hydroxyalkanoates] (PHA) biopolyesters from surrounding biomass. *Engineering in Life Sciences*. **2013**, *13*, 549-562.
- [2] K. Sudesh; H. Abe; Y. Doi, Synthesis, structure and properties of polyhydroxyalkanoates: biological polyesters. *Progress in Polymer Science*. **2000**, *25*, 1503-1555.
- [3] C. Kourmentza; J. Plácido; N. Venetsaneas; A. Burniol-Figols; C. Varrone; H.N. Gavala; M.A.M. Reis, Recent Advances and Challenges towards Sustainable Polyhydroxyalkanoate (PHA) Production. *Bioengineering*. **2017**, *4*, 55.
- [4] K. Adrah; D. Ananey-Obiri; R. Tahergorabi. Development of Bio-based and Biodegradable Plastics. In *Handbook of Nanomaterials and Nanocomposites for Energy and*

- Environmental Applications*, Kharissova, O.V., Torres-Martínez, L.M., Kharisov, B.I., Eds.; Springer International Publishing: Cham, 2021; pp. 3663-3687.
- [5] C. Nielsen; A. Rahman; A.U. Rehman; M.K. Walsh; C.D. Miller, Food waste conversion to microbial polyhydroxyalkanoates. *Microb Biotechnol.* **2017**, *10*, 1338-1352.
- [6] E.D. Bluemink; A.F. van Nieuwenhuijzen; E. Wypkema; C.A. Uijterlinde, Bio-plastic (polyhydroxy-alkanoate) production from municipal sewage sludge in the Netherlands: a technology push or a demand driven process? *Water Science and Technology.* **2016**, *74*, 353-358.
- [7] E.R. Coats; B.S. Watson; C.K. Brinkman, Polyhydroxyalkanoate synthesis by mixed microbial consortia cultured on fermented dairy manure: Effect of aeration on process rates/yields and the associated microbial ecology. *Water Research.* **2016**, *106*, 26-40.
- [8] S. Guleria; H. Singh; V. Sharma; N. Bhardwaj; S.K. Arya; S. Puri; M. Khatri, Polyhydroxyalkanoates production from domestic waste feedstock: A sustainable approach towards bio-economy. *Journal of Cleaner Production.* **2022**, *340*, 130661.
- [9] Z. Raza; S. Abid; I. Banat, Polyhydroxyalkanoates: Characteristics, production, recent developments and applications. *International Biodeterioration & Biodegradation.* **2018**, *126*, 45-56.
- [10] K. Khatami; M. Perez-Zabaleta; Z. Cetecioglu, Pure cultures for synthetic culture development: Next level municipal waste treatment for polyhydroxyalkanoates production. *Journal of Environmental Management.* **2022**, *305*, 114337.
- [11] G. Moore; S. Saunders. *Advances in biodegradable polymers*; iSmithers Rapra Publishing: 1998; Volume 98.
- [12] M.R.Z. Mamat; H. Ariffin; M.A. Hassan; M.A.K. Mohd Zahari, Bio-based production of crotonic acid by pyrolysis of poly(3-hydroxybutyrate) inclusions. *Journal of Cleaner Production.* **2014**, *83*, 463-472.
- [13] J. Blumenstein; J. Albert; R.P. Schulz; C. Kohlpaintner. Crotonaldehyde and Crotonic Acid. In *Ullmann's Encyclopedia of Industrial Chemistry*; pp. 1-20.
- [14] V. Elhami; E.C. Antunes; H. Temmink; B. Schuur, Recovery Techniques Enabling Circular Chemistry from Wastewater. *Molecules.* **2022**, *27*, 1389.
- [15] H. Ariffin; H. Nishida; Y. Shirai; M.A. Hassan, Determination of multiple thermal degradation mechanisms of poly(3-hydroxybutyrate). *Polymer Degradation and Stability.* **2008**, *93*, 1433-1439.
- [16] N. Grassie; E.J. Murray; P.A. Holmes, The thermal degradation of poly(-(d)- β -hydroxybutyric acid): Part 3-The reaction mechanism. *Polymer Degradation and Stability.* **1984**, *6*, 127-134.
- [17] H. Xiang; X. Wen; X. Miu; Y. Li; Z. Zhou; M. Zhu, Thermal depolymerization mechanisms of poly(3-hydroxybutyrate-co-3-hydroxyvalerate). *Progress in Natural Science: Materials International.* **2016**, *26*, 58-64.
- [18] F.-D. Kopinke; M. Remmler; K. Mackenzie, Thermal decomposition of biodegradable polyesters—I: Poly (β -hydroxybutyric acid). *Polymer Degradation and Stability.* **1996**, *52*, 25-38.
- [19] H. Ariffin; H. Nishida; Y. Shirai; M.A. Hassan, Highly selective transformation of poly[(R)-3-hydroxybutyric acid] into trans-crotonic acid by catalytic thermal degradation. *Polymer Degradation and Stability.* **2010**, *95*, 1375-1381.

- [20] N.F.S.M. Farid; H. Ariffin; M.R.Z. Mamat; M.A.K. Mohd Zahari; M.A. Hassan, Non-solvent-based pretreatment of poly(3-hydroxybutyrate) for improved bio-based crotonic acid production. *RSC Advances*. **2015**, *5*, 33546-33553.
- [21] P. Jablonski; D. Nikjoo; J. Warna; K. Irgum; J.-P. Mikkola; S.G. Khokarale, Sustainable, highly selective, and metal-free thermal depolymerization of poly-(3-hydroxybutyrate) to crotonic acid in recoverable ionic liquids. *Green Chemistry*. **2022**, *24*, 4130-4139.
- [22] S. Kang; R. Chen; J. Fu; J. Liang; S. Chen; L. Lu; R. Miao, Catalyst-free valorization of poly-3-hydroxybutyrate to crotonic acid. *Reaction Chemistry & Engineering*. **2021**, *6*, 1791-1795.
- [23] A. Parodi; A. Jorea; M. Fagnoni; D. Ravelli; C. Samorì; C. Torri; P. Galletti, Bio-based crotonic acid from polyhydroxybutyrate: synthesis and photocatalyzed hydroacylation. *Green Chemistry*. **2021**, *23*, 3420-3427.
- [24] M. Mulders; J. Tamis; B. Abbas; J. Sousa; H. Dijkman; R. Rozendal; R. Kleerebezem, Pilot-Scale Polyhydroxyalkanoate Production from Organic Waste: Process Characteristics at High pH and High Ammonium Concentration. *Journal of Environmental Engineering*. **2020**, *146*, 04020049.
- [25] V. Elhami; N. van de Beek; L. Wang; S.J. Picken; J. Tamis; J.A.B. Sousa; M.A. Hempenius; B. Schuur, Extraction of low molecular weight polyhydroxyalkanoates from mixed microbial cultures using bio-based solvents. *Separation and Purification Technology*. **2022**, *299*, 121773.
- [26] V.R. Paidá; D.W.F. Brillman; S.R.A. Kersten, Hydrothermal gasification of sorbitol: H₂ optimisation at high carbon gasification efficiencies. *Chemical Engineering Journal*. **2019**, *358*, 351-361.
- [27] M.B. Hocking, The Effect of Heat on cis- and trans-Crotonic Acids: Alternatives to Direct cis–trans Isomerism. *Canadian Journal of Chemistry*. **1972**, *50*, 1224-1232.
- [28] A.B.d. Haan; H.B. Eral; B. Schuur. *Industrial Separation Processes: Fundamentals*; De Gruyter: Berlin, Boston, 2020.
- [29] Y. Wang; R. Chen; J. Cai; Z. Liu; Y. Zheng; H. Wang; Q. Li; N. He, Biosynthesis and Thermal Properties of PHBV Produced from Levulinic Acid by *Ralstonia eutropha*. *PLOS ONE*. **2013**, *8*, e60318.
- [30] L. Wei; N.M. Guho; E.R. Coats; A.G. McDonald, Characterization of poly(3-hydroxybutyrate-co-3-hydroxyvalerate) biosynthesized by mixed microbial consortia fed fermented dairy manure. *Journal of Applied Polymer Science*. **2014**, *131*, 40333.

Chapter 6

Separation of Crotonic Acid and 2-Pentenoic Acid Obtained by Pyrolysis of Bio-based Polyhydroxyalkanoates using a Spinning Band Distillation Column



This chapter is adapted from:

Elhami, V.; Neuendorf, L.M.; Kock, T.; Kockmann, N.; Schuur, B., "Separation of crotonic acid and 2-pentenoic acid obtained by pyrolysis of bio-based polyhydroxyalkanoates using a spinning band distillation column", **Sustainable Chemistry and Engineering**, **2023**, (the manuscript is submitted).

Abstract

In the search for renewable alternatives to produce platform chemicals, various types of biomass have shown great potential to be used as feedstock for value-added chemicals. For instance, aerobic digestion of aqueous volatile fatty acid-enriched waste yields a biomass, that under appropriate growth conditions can be rich in the co-polymer poly(3-hydroxybutyrate-co-3-hydroxyvalerate) (PHBV). Pyrolysis of PHBV yields a mixture of crotonic acid (CA) and 2-pentenoic acid (2-PA). Aiming to apply CA and 2-PA as bio-based monomers, requires a purification step to obtain the pure acids. Vapor-liquid equilibria (VLE) of CA and 2-PA have not been published in the open literature. Furthermore, the high melting point of CA (72 °C) in combination with the high polymerization potential limits the operation window for distillation severely. In this study, we have experimentally explored the use of a spinning band distillation column (SBC) under vacuum operation to separate these acids. The thermodynamic feasibility for the distillation was first studied by measuring VLE-data of the mixture at process-relevant pressures of 50 and 100 mbar using a custom-designed VLE set-up. The separation in SBC was accomplished at 50 mbar and 40-110 °C for about 5h. A successful recovery of CA with high purity of >98% was achieved using a synthetic mixture of acids with a mass ratio of 80/20 (CA/2-PA). Furthermore, applying the actual pyrolyzate mixtures obtained by pyrolysis of the biomass and extracted pure PHBV as a feed for the distillation column resulted in separation of CA with relatively high purity of 96% and 93%, respectively.

1. Introduction

There is a pronounced growth in industrial interest for renewable and environmentally sustainable pathways to produce chemicals. Driven by the desire to move away from linear economic models based on the supply of fossil fuel-based materials, renewable sources for chemicals are being explored. Major classes of bio-based chemicals include bio-based solvents [1,2], bio-based platform chemicals [3], and bio-based carboxylic acids,[4-6] and bio-based polymers [7-9]. In most cases, poly(3-hydroxybutyrate-co-3-hydroxyvalerate) (PHBV) co-polymer is the main bio-based co-polymer that can be obtained during fermentation of volatile fatty acids (VFAs)-enriched wastewater. Starting from wastewater as an inexpensive feedstock for the microorganisms can result in a low-cost bio-based pathway to produce PHBV. However, the drawback of wastewater as feedstock for PHBV-production is a varying product composition and quality, which are important characteristics of the produced PHBV. It is because during the fermentation process in the mixed microbial cultures (MMCs), VFAs with an even number of carbons will be converted to poly(3-hydroxybutyrate) (PHB). The ones with an odd number will be converted into a PHBV copolymer with varying hydroxyvalerate (HV) contents [10]. It is possible to adjust the composition of the wastewater prior to the fermentation to produce polymers with certain properties. However, controlling the feed would increase the cost of the bio-based production pathway. For a process based on fermenting a mixture of odd and even VFAs, PHBV with varied properties are the main bio-polymers produced in the MMCs without controlling the feed composition.

An alternative to direct use, the PHBV grown without well-controlled conditions in MMCs can be pyrolyzed to produce their corresponding 2-

Separation of CA/ 2-PA mixture using spinning band distillation column

alkenoic acids. Crotonic acid (CA) and 2-pentenoic acid (2-PA) are the main pyrolyzates during pyrolysis of the PHBV, originating from hydroxybutyrate (HB) and HV monomers, respectively.

CA, or trans-2-butenoic acid, is mainly used in the synthesis of co-polymers. Among the known co-polymers based on CA, crotonic acid-vinyl acetate is the main copolymer, with the trade names of Cevian, Gelva, Mowilith, and Vinac [11], which are used in cosmetic and hair styling products. Apart from this, CA finds further applications in industries such as coatings, paint, textile, binders, adhesives, flocculants, ceramics, and agrochemicals [12]. The esters of 2-PA can be used in flavoring essences and its current application is mainly in medicine studies [13,14]. The ongoing market of these unsaturated carboxylic acids is limited due to their complex production routes. Therefore, providing a relatively straightforward and bio-based pathway is expected to enhance their market.

Although the synthesis of CA via PHB/PHBV thermal decomposition has been examined over the last decades [12,15-20], its separation from the complex pyrolysis mixtures has not been that well studied. A fluidized bed set-up was developed by Mullen et al. [21] to pyrolyze a PHB/switchgrass blend and yield CA-enriched bio-oil on a pilot scale. In-situ fractionation of the pyrolyzate mixture was achieved by multistep condensation using water-cooled (4 °C) condensers connected to an electrostatic precipitator. Considering the melting point of CA (72 °C), cooling a vapor stream containing CA to 4 °C will result in condensation as well as partial precipitation. An optimum CA yield of 45% was achieved from a mixture of 10% PHB and 90% switchgrass with fine PHB particles at 375 °C. However, recovery of CA from the total pyrolysis liquid was not significant with this multistep separation procedure.

Recently, Parodi et al. [22] developed a thermolytic distillation process to pyrolyze PHB and PHB-enriched biomass at 170 °C under vacuum conditions at 150 mbar to produce CA. The pyrolysis of PHB occurs simultaneously with the separation of volatile pyrolyzates such as CA during thermolytic distillation. The researchers recovered CA with a yield of 58% and a purity of 92% using this integrated method from MMC-based biomass containing 30 wt% PHB on a dry basis. Indeed, pyrolysis of MMC-based PHB/PHB-enriched biomass with this method can increase both the yield and purity of CA. However, in the case of MMC-based PHBV/PHBV-enriched biomass, the vapor stream will also contain 2-PA, originating from the HV monomers. Therefore, an additional purification is required to separate these carboxylic acids. Considering various separation techniques for the desired fractionation, membranes might work, and low temperature membrane solutions are available for bio-based saturated volatile fatty acids [23-25]. However, because the vapor stream is prone to polymerization due to the unsaturation in the fatty acids CA and 2-PA, and the solidification of CA at 72°C is a factor to be considered as well, operating a membrane separation for the vapor fractionation appears difficult. Given the high temperature from the pyrolysis, distillation appears as most attractive primary separation, since high temperature liquid-liquid extraction with these reactive monomers would impose a risk of unwanted chemical reactions. While crystallization appears strong given the large difference in the melting points, it only applies at lower temperatures, and therefore may be the secondary separation technique.

Therefore, in this work, we studied the possibility to do the separation of a CA/2-PA mixture by distillation based on differences in the relative volatility.

Separation of CA/ 2-PA mixture using spinning band distillation column

The natural boiling points of CA and 2-PA are 184.7 °C [26] and 200–203 °C [27], respectively. The described study is comprised of an equilibrium study to determine the thermodynamic feasibility of the distillation, and a multistage distillation study in a novel spinning band distillation column (SBC) [28,29]. The core idea of a SBC is the use of rotating internals as opposed to using packed or tray columns. The advantages of SBCs over the other two mentioned columns are their low holdup, very low pressure drop, and still high separation efficiency. Usually, this type of fractionating columns are used for analytical purposes with small amounts particularly. Since with the CA and 2-PA from PHBV, we face a separation system with a very limited amount of available chemicals, and the low holdup is ideal. The acids are not only polar, but also organic molecules with a small hydrocarbon chain. The polytetrafluoroethylene (PTFE) spinning band, that is known to improve the separation efficiency for several organic systems [30,31]. Thus, it is also expected that PTFE band is suitable for this system. Spinning bands which stir only the vapor phase and also hinder the vapor flow directly to the top are suited for operation under vacuum conditions [29]. By using vacuum conditions it is possible to shift the mixture to temperatures where a separation becomes possible (at too high temperatures, the acids are not stable).

In the current study, the used SBC was operated batch-wise, where the feed mixture was placed in the reboiler, and boiled up. CA was collected in the distillate outlet, while 2-PA remained in the final bottom product. The use of the SBC in vacuum operation was first explored for the distillation of a model mixture prepared with a commercial CA and 2-PA system. Afterwards, the purification of the acids from an actual pyrolyzate mixture obtained by

pyrolysis of PHBV-enriched biomass and extracted pure PHBV were investigated using the same distillation column to demonstrate the proof of concept for distillative purification of CA.

2. Material and methods

2.1. Chemicals

Crotonic acid ($\geq 98\%$), trans-2-pentenoic acid ($\geq 98\%$), acetone (99.5%), 1,2,4,5-Tetrachloro-3-nitrobenzene and chloroform-D were purchased from Sigma Aldrich. The water used was ultrapure (Milli-Q, with a resistance of $18.2 \mu\Omega \text{ cm}$ at 25°C).

2.2. VLE measurement for CA/2-PA mixture

Initially the VLE measurement of a CA and 2-PA mixture was performed in a Fischer Labodest VLE 602 ebulliometer. Due to the high melting point of CA (72°C), crystallization occurred in the cold spots of the ebulliometer resulting in inaccurate VLE data for the samples with a high concentration of CA. Therefore, an equilibrium cell was developed to perform the isobaric-VLE study, which is depicted in Figure 6-1. First about 15 mL of a mixture of the acids was prepared with a desired ratio of the acids ($0 < x < 1$) and placed in the heating mantle. The mixture was heated and stirred using a magnetic stirrer. The temperature of the gas and liquid phases were measured using Pt-100 sensors with an accuracy of $\pm 0.5^\circ \text{C}$. The pressure was set at either 100 mbar or 50 mbar using a the vacuum pump PC 3001 VARIO select (Vacuubrand GmbH, Wertheim, Germany). For each mixture at the set pressure, the power of the heater was increased until there was no change in the temperature of the acid mixture upon further increasing the heater set

Separation of CA/ 2-PA mixture using spinning band distillation column

point. Afterwards, the mixture was kept at that temperature for about 40 min to ensure equilibrium conditions (this was experimentally validated). Subsequently, a small glass tube was cooled by liquid nitrogen. By opening the valve, the glass vial was carefully moved into the vapor phase through a mounted septum. As the valve was opened only after placing the glass tube, the reduced pressure in the system could be maintained. Then, samples were taken from the vapor and liquid phases. The vapor phase sample was collected by freezing the vapor phase on the cooled vial. The samples were dissolved in milliQ water to be analyzed by high performance liquid chromatography (HPLC).

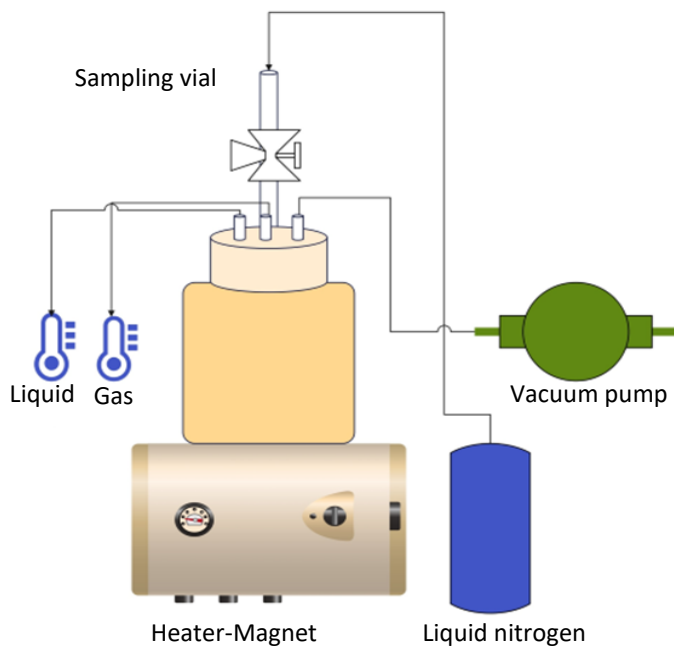


Figure 6-1. Schematic view of the custom-designed VLE measurement set-up.

The experimental isobaric-VLE data was fitted using the Aspen Plus V12.1 regression tool to predict the parameters of the non-random two-liquid (NRTL) model.

2.3. Thermal stability study

The thermal stability of the acids during the distillation process was examined. About 5 g of CA/2-PA mixture was prepared in a vial with a mass ratio of 80 to 20, respectively. Afterwards, the vial was subjected to 110 °C and 145 °C for a certain contact time in the range of 0-10 h. The samples were taken before and after heating and analyzed by Proton Nuclear Magnetic Resonance (¹H-NMR) to investigate the isomerization and polymerization of the acids. 1,2,4,5-Tetrachloro-3-nitrobenzene was added as an internal standard. The peaks were identified using ChemDraw 20.0 software.

2.4. Distillation of the CA/2-PA mixture using the spinning band column

The distillation in the SBC from NORMAG (now Pfaunder Group, Ilmenau, Germany) was performed in a batch-wise operation mode inside of a mobile fume-hood. The PTFE spinning band consists of seven segments of each 95.8 mm height, screwed together thus adding up to a length of 670.6 mm as an active separation length. The whole band was mounted to a bearing with a downside direction and driven by a stirrer motor (IKA Eurostar 200, Staufen, Germany) connected by a shaft at the top side. Rotation speed of the spinning band is set to 50 rpm for the whole time. The column's heating

Separation of CA/ 2-PA mixture using spinning band distillation column

jacket is located over the whole column, except for the sump. It was preheated to 110 °C by a glass heat exchanger connected with a thermostat (Ministat 125 cc, Huber, Offenburg, Germany).

The most crucial part was to ensure that the column was operated under a high vacuum condition of 50 mbar. Therefore, the vacuum pump PC 3001 VARIO select (Vacuubrand GmbH, Wertheim, Germany) was connected to the reflux condenser via a cold trap. To begin the distillation process, at first the column's heating jacket was filled with silicone oil (Lauda Ultra 350) to preheat the distillation column to 110 °C. Moreover, deionized water was fed into the column to heat up the column from the inside, and evaporated and then removed from the system at the top outlet.

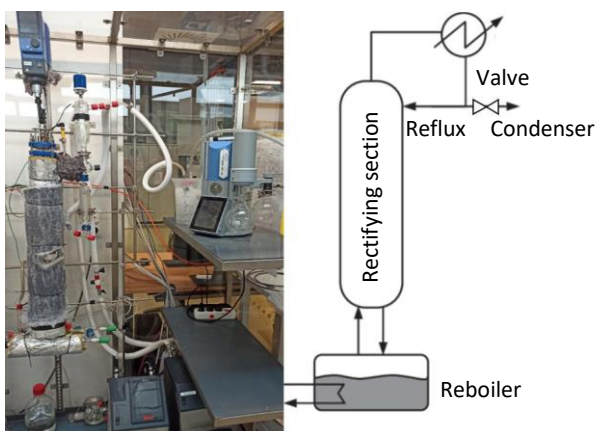


Figure 6-2. Experimental set-up of the insulated vacuum distillation plant in batch operation mode, right side scheme of a batch distillation column adapted after [32].

The feed mixture runs down the column in the gap between the glass wall of the column and the spinning band, guided by the helical band. By rotation of the band, a thin liquid film is formed on the glass wall and continuously refreshed by the rotation. The vapor streaming upwards follows along the

path of the spinning band and continuously contacts the liquid film. This effect is similar to an Archimedean screw, where the rotation induces upward force to the liquid. Flooding is always caused because of an excessive accumulation of liquid at a specific location that negatively affects the desired separation process. It occurs due to the liquid level being too high, either due to high rotation speed or the evaporation rate. At this point, the vapor cannot pass through the gap and a high pressure drop and flooding along the column occurs, similar to conventional industrial scale columns [30,31] Since mass transfer in the column takes place primarily in the falling film on the glass wall, it is particularly important to minimize the heating loss as much as possible. Due to this, the DN25 glass column was insulated with a DN50 vacuum double jacket over the whole active separation area. Moreover, aluminum cladding and a combination of 10 mm Spaceloft and 30 mm rockwool insulation surrounded the whole column during operation, as seen in Figure 6-2.

The vapor leaves the column at its top, enters the reflux condenser and condenses there. Depending on the valve's position (see Figure 6-2) the condensate flows back into the column (when the reflux value is larger than zero) or is led to the distillate condenser and leaves the column as the top product.

2.5. Analysis

High Performance Liquid Chromatography (HPLC), The concentrations of CA and 2- PA were measured using a HPLC [Agilent Hi-Plex H column (300 × 7.7 mm) with a refractive index detector on an Agilent 1200 series HPLC system;

Separation of CA/ 2-PA mixture using spinning band distillation column

mobile phase, 5 mM H₂SO₄ solution; column temperature of 65 °C at a flow rate of 0.6 mL/min].

Gas Chromatography – Mass Spectroscopy (GC-FID/MS), The acid mixture samples were dissolved in acetone and analyzed by using GC-MS (GC – 7890A, MS – 5975C Agilent Technologies system) equipped with an Agilent HP-5MS HP19091S-433 capillary column (60 m, ID 0.25 mm, Film thickness: 0.25 μm). The column was packed with (5%-Phenyl)-methylpolysiloxane. Helium was used as carrier gas with a constant flow of 1.95 mL.min⁻¹. The oven temperature was programmed from 45 °C (4 min) to 280 °C at a heating rate of 3 °C.min⁻¹ and was held at 280 °C for 20 min. The injector and the column to the MS interface were maintained at a constant temperature of 250 °C and 280 °C, respectively. A sample of 1 μL was injected into the GC. The MS was operated in electron ionization mode, and ions were scanned in an m/z range from 15 to 500.

Proton Nuclear Magnetic Resonance (¹H-NMR), The final purity of CA collected as a top product was further evaluated by ¹H-NMR. Moreover, to study whether or not the polymerization and the isomerization occur during distillation of this unsaturated acids mixture, thermal stability experiments were performed in which the samples were analyzed by ¹H-NMR as well. All the samples were dissolved in deuterated chloroform and analyzed by ¹H-NMR, using a Bruker Ascend 400 (400.1316 MHz).

Karl- Fischer Titration (KFT), The water content of the condensate was determined by Karl- Fischer Titration using a Metrohm 787 KFTitrino. Hydranal composite 5 was titrated from a 20 mL burette filled with a mixture

of methanol and dichloromethane in volume ratio of 3 to 1. The sample was analyzed in triplicate with a relative error less than 1%.

3. Results and discussion

3.1. VLE study for CA/2-PA mixture

The isobaric-VLE behavior of the acids mixture was investigated under reduced pressures of 50 and 100 mbar. To test the performance of the newly developed VLE set-up, the isobaric-VLE data for the CA/2-PA mixture with mass ratio of 10 to 90, was first measured using a Fischer Labodest VLE 602 ebulliometer. At this composition, also the ebulliometer could be applied, while at high CA compositions the crystallization in the cold zones of the ebulliometer caused operational problems. Then, VLE data of the same mixture was obtained with the custom-designed set-up. As shown in Table 6-1, the difference in mass fraction of CA in the vapor phase (y) obtained by both apparatuses for the same mixture was only 0.0125. Therefore, it can be concluded that the newly designed set-up provides comparable isobaric-VLE data to the Fischer Labodest VLE 602 ebulliometer. Thus, the isobaric-VLE data was collected for CA/2-PA mixtures at various compositions ranging up to pure CA using the custom-designed VLE equilibrium cell.

Table 6-1. Comparison of the performance of Fischer Labodest VLE 602 ebulliometer and custom-designed equilibrium cell, using CA and 2-PA mixture with mass ratio of 10:90, at 50 mbar and 110 °C.

X	$Y_{\text{Ebulliometer}}$	Y_{Cell}
0.10	0.203±0.012	0.216±0.020

Separation of CA/ 2-PA mixture using spinning band distillation column

The x-y and T-xy diagrams of the mixture are shown in Figure 6-3 and 6-4, respectively. Based on the VLE-results, it can be concluded that ordinary distillation appears to be a feasible method to separate CA and 2-PA mixture, as no azeotrope is observed, and appropriate relative volatility is shown without severe pinch-point(s).

A data regression of the experimental VLE data was made using the Aspen Plus V12.1 regression tool to predict the binary interaction parameters of the NRTL model. The parameter C_{ij} was fixed at 0.3 which found to be a suitable value for the carboxylic acid mixture [33]. The other parameters were modeled using the default equations in the simulator and the convergence algorithm of Britt-Leucke with a tolerance of 0.0001. The estimated NRTL binary parameters are given in Table 6-2. These parameters can be used to design a distillation process for separation of the CA/2-PA mixture.

Separation of CA/ 2-PA mixture using spinning band distillation column

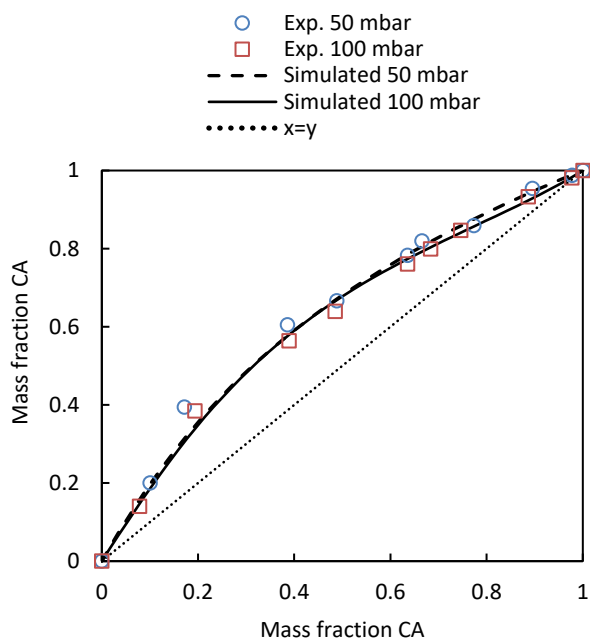


Figure 6-3. y - x diagram for CA/2-PA mixture at 50 and 100 mbar.

Table 6-2. Estimated NRTL parameters for CA/2-PA mixture over the temperature range is between 101 to 127 °C.^a

Parameter	Value
A _{ij}	19.499
A _{ji}	-6.369
B _{ij}	-7036.650
B _{ji}	2147.260
C _{ij}	0.3 (fixed)

^aBy regression of experimental isobaric-VLE data at 50 and 100 mbar using the Aspen Plus V12.1 regression tool. The standard deviation of VLE data obtained by equilibrium cell are about 0.0006 and 0.005 for x and y , respectively

Separation of CA/ 2-PA mixture using spinning band distillation column

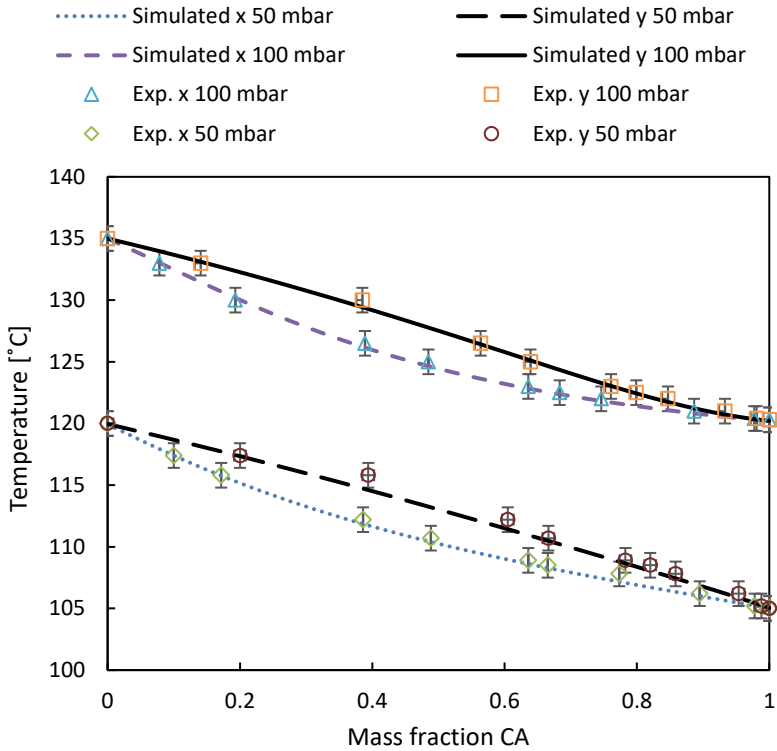


Figure 6-4. T-xy diagram for CA/2-PA mixture at 50 and 100 mbar.

As shown in Figure 6-3 and 6-4, there is a very good agreement between the experimental data and the model predictions based on the NRTL-model that was fitted on the data obtained at 50 and 100 mbar. The relative volatility of CA over 2-PA is similar at both experimental pressures, and no significant improvement was achieved at lower CA compositions with reducing the pressure by a factor of two. However, as can be clearly seen from the graph, the increase in vapor phase mass fraction (y) at highly concentrated CA mixtures ($x > 0.6$) is considerable when the pressure is reduced from 100 mbar to 50 mbar. It seems there is a pinch point at $x > 0.9$ at a pressure of 100 mbar,

while being much less pronounced or even absent at 50 mbar. Since the lower pressure is also beneficial in terms of product stability (the acids tend to polymerize at higher temperatures), a minimum achievable vacuum was applied in the subsequent SBC studies, allowing us to obtain the highest purity of CA in the top product and limiting polymerization as much as possible.

3.2. Theoretical stages for full separation

Using the McCabe-Thiele method and NRTL-based fitted y - x diagram of 50 mbar, the total number of stages was calculated at reflux ratio of 2. The results are shown in Figure 6-5. Accordingly, the total number of equilibrium stages is almost 9, including the partial condenser. Based on this analysis, and the results obtained in a previous study where the SBC was developed [28,29], performing a distillation in the SBC set-up to obtain CA with high purity appears to be well-feasible. However, this stage construction should be taken as a first orientation for process design, but has to be validated for scale-up purposes.

Separation of CA/ 2-PA mixture using spinning band distillation column

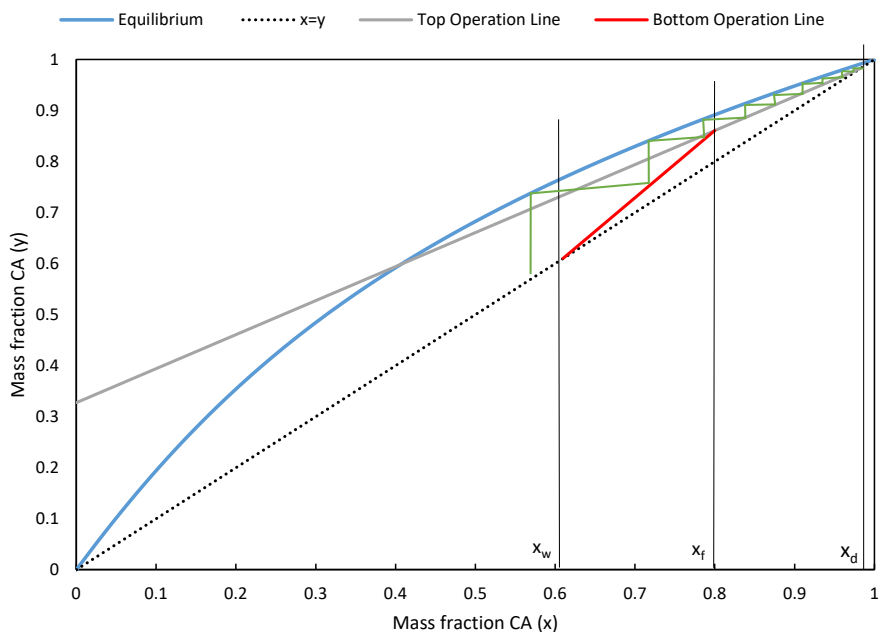


Figure 6-5. y - x diagram for CA/2-PA mixture (mass ratio: 80/20) at 50 mbar, fitted by the NRTL model. The stages are calculated by the McCabe-Thiele method with reflux ratio of 2.

3.3. Investigation of thermal stability of CA/2-PA mixture

CA and 2-PA are unsaturated carboxylic acids which can undergo dimerization (eventually polymerization) and isomerization at elevated temperature [34]. Thus, the thermal stability of the CA/2-PA mixture was investigated under applied distillation conditions. A mixture of CA/2-PA (mass ratio of 20:80) was exposed to elevated temperatures of 110 and 145 °C for contact times up to 10 h. The $^1\text{H-NMR}$ spectrum of the samples before and after heating are shown in Figure 6-6. In the first trial, the actual distillation process was simulated in which the acid mixture was subjected to 110 °C and 50 mbar for 5 h. As can be seen from the graphs, a peak appears

at around 1.3 ppm which corresponds to CA dimers, according to the ChemDraw $^1\text{H-NMR}$ spectrum prediction tool. By performing the experiments at ambient pressure, similar results are found. By increasing the temperature to 145 °C, the isomerization and polymerization can be accelerated as these reactions mainly happen at elevated temperatures[34]. For the samples which were subjected to high temperature for 10 h, a few more peaks are visible at 0.89, 2.5, 5.3 and 6.9 ppm. Based on ChemDraw prediction, the peak at 0.89 ppm is related to methyl group of the dimers of 2-PA, while the peaks at 2.5, 5.3 and 6.9 ppm can be assigned to the dimers of both acids. In terms of the isomer of both acids, their methine group shift should occur one at around 5.9 ppm and another one at about 6.5 ppm [12]. The peak at 5.9 ppm is overlapped for all the isomers. There is no distinguishable peak at around 6.5 ppm. However, it is only an estimation and the peak might be shifted in the real mixture. It could be that the peak at 6.9 ppm is the overlapped methine group of the acids, isomers and dimers. Overall, it can be concluded that during distillation of a CA/2-PA mixture at 110 °C and 50 mbar for about 5h, 2-pentenoic acid is thermally stable, while for CA a small quantity of the acid undergoes a dimerization reaction. Due to the complexity of the simulated mixture after heating, containing the acids, their corresponding isomers and dimers, and overlapping their $^1\text{H-NMR}$ peaks, the quantification of the isomers and dimers was not possible.

Separation of CA/ 2-PA mixture using spinning band distillation column

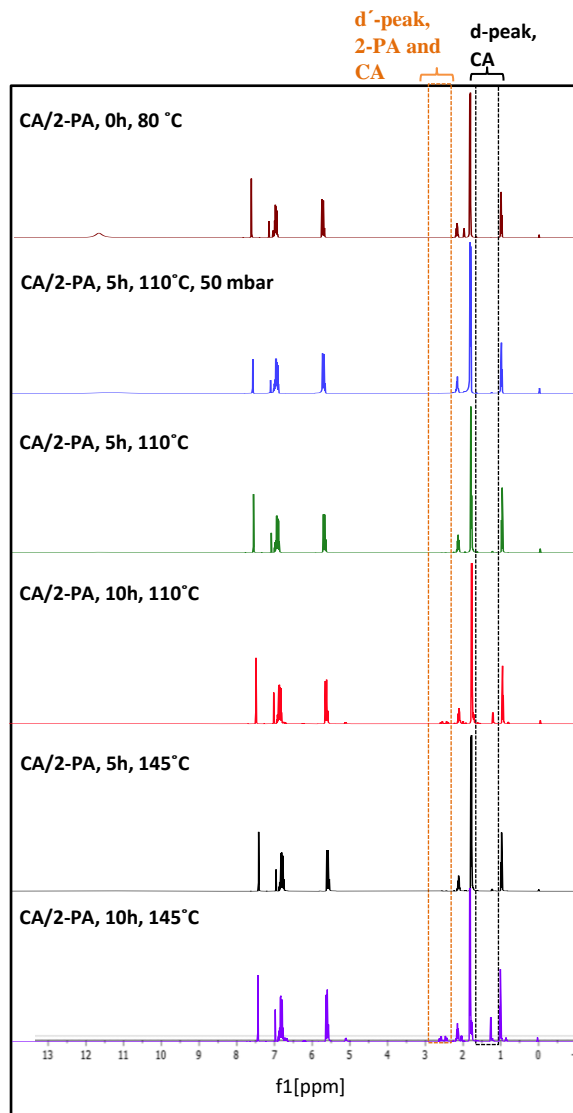


Figure 6-6. $^1\text{H-NMR}$ spectra of CA/2-PA mixture at 110 and 145 °C, *d*-peak corresponds to $-\text{CH}_3$ group of CA dimer and *d'*-peak corresponds to $-\text{CH}_2$ group of the dimers of both CA and 2-PA.

3.4. Separation of CA/2-PA by distillation

The distillation column is operated under a reduced pressure of about 50-60 mbar. When the column's bottom temperature reaches a stable 100 °C, a mixture of CA/2-PA was prepared at the mass ratio of 80 to 20, and filled into the bottom of the column.

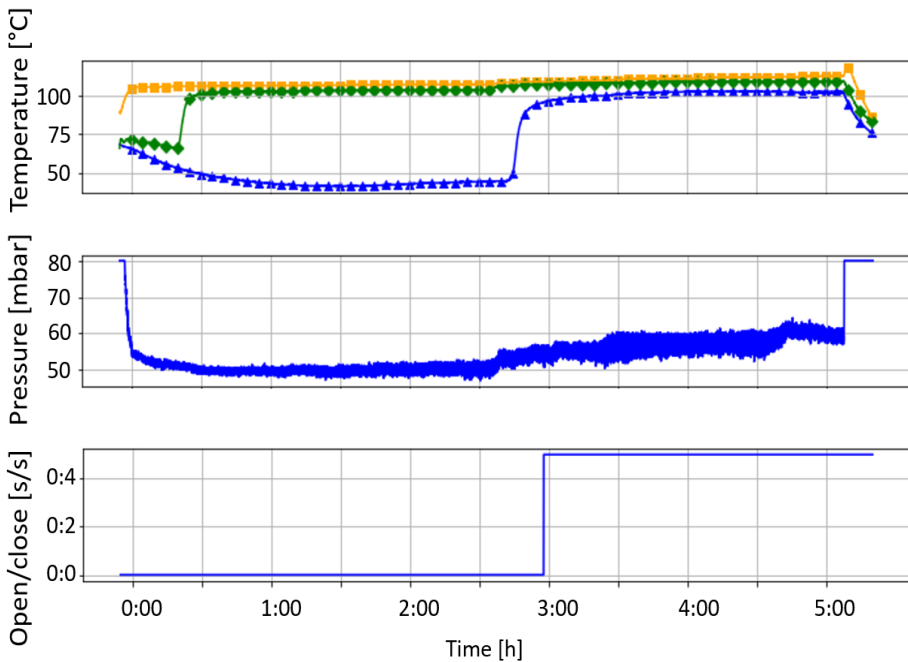


Figure 6-7. Temporal course of the distillation process, showing (top figure): temperatures in the bottom temperature in yellow, mid-section temperature in green, top temperature indicated in blue; (middle figure): bottom pressure in the distillation column; (bottom figure): The reflux ratio, depicted as the ratio of valve open time divided by valve closed time. The valve opens the distillate exit.

The process was run for about 5 h and during this time, the temperature was monitored in the top, the middle, and the bottom of the column. The pressure in the bottom was monitored, and the reflux was controlled by

Separation of CA/ 2-PA mixture using spinning band distillation column

alternating the opening and closing of the valve towards the distillate exit. From the profiles shown in Figure 6-7, it can be concluded that the temperature at the bottom was stable at around 108-110 °C. The temperature in the middle of the column started significantly lower at about 75 °C, and after about 20 min the temperature rose to about 102 °C, just under the bottom temperature, and stayed there during the next hours. The temperature is well in agreement with the VLE behavior reported in Figure 6-4.

While initially the temperature in the top of the column was also 75 °C, like in the middle section of the column, during the first hour of operation the temperature dropped to 40 °C at an infinite reflux operation. It takes a long time for the vapor from the bottom to the top because on its way upwards the spinning band there is a small front of crystals forming that needs to be brought upward. The temperature rise marks the point at the experiment where the vapor gradually arrives at the top section. After the vapor has arrived, the reflux ratio is increased from 0 to 0.5 s⁻¹, which occurred approximately after three hours. Then, the middle sections temperature increased slightly to 106 °C.

The increase of the reflux means that the cooler now divides one part of the liquid back into the column and the other to the distillate cooler. Then the top temperature almost immediately increased to 100 °C. This occurs because the temperature sensor only measures the liquid phase temperature and with zero reflux there was no liquid phase present. During process operation the bottom pressure remained relatively constant at around 50-60 mbar. For the first three hours of operation of this batch-wise distillation,

Separation of CA/ 2-PA mixture using spinning band distillation column

no distillate product was obtained since the vapor phase had not yet arrived at the column top.

Furthermore, the overall mass balance of the process is not closed. Of 146.8 g feed in the beginning of the process, afterwards 78.26 g at the bottom and 40.94 g top product was obtained, resulting in an average mass loss of 27.6 g (18.80 % of the feed mixture). We found the pH of the washing water to be around 3-4. Hence, a sample of washing water was analyzed by HPLC which established that indeed a fraction of CA left the condenser in vapor phase. However, its quantity is <1g which is not that significant. We assume the main fraction of the lost mass remained in the middle section of the column in form of crystals remaining on the spinning band and column wall. Moreover, some amount might be still attached to the gaskets as well as maybe in the tubes behind the condensers. Furthermore, a part should be accounted for the lost during handling such as in collecting the top products from the condensers.

Table 6-3. Separation of the CA/2-PA mixture with a mass ratio of 80/20 at 5h by distillation using a SBC.

P[mbar] T[°C]	Top/ Bottom	Composition [wt%]		
		CA	2-PA	water
50	Top	98.2	<0.5	<1
110	Bottom	61	30	<1

Regarding the separation efficiency, as depicted in Table 6-3, GC-MS analysis of the top and bottom product confirms the successful separation of the acid mixture, as the top product is mainly CA with a purity of >98%. To ensure about the 2-PA content in the top product, ¹H-NMR analysis was also

conducted to calculate the purity. According to ¹H-NMR and GC-MS, 2-PA content in the top product is less than 0.5 wt%. The water content is <1 wt% based on KFT analysis. Thus, it can be concluded that distillation is definitely an appropriate technology to recover CA with high purity from CA and 2-PA mixture.

3.5. Purification of CA obtained by pyrolysis of PHBV/PHBV-enriched biomass by distillation

Even though the separation of CA and 2-PA was successfully done using the commercial acids in SBC, the actual mixture obtained by pyrolysis of either the extracted PHBV or the PHBV-enriched biomass contains not only these acids, but also other side products. Therefore, it is worthwhile to investigate the purification of CA using the actual mixture. The pyrolysis was performed following the procedure reported in chapter 5. Briefly, a certain quantity of the PHBV-enriched biomass was separately loaded in the oven and pyrolyzed at around 240 °C under a nitrogen flow rate of 0.15 L/min. In the case of using the extracted PHBV, pyrolysis was conducted under reduced pressure of 50 mbar at 220 °C. Finally, the pyrolyzate (the vapor phase) was condensed and collected to be applied in the distillation process. Due to the scale of the pyrolysis set-up and limited amount of the bio-based materials, it was not possible to produce a high quantity of pyrolyzate which can be applicable in SBC. Therefore, a certain quantity of CA/2-PA mixture were added to the pyrolyzate mixtures, allowing a proper amount of feed to be used in SBC. Table 6-4 represents the distillation results for these mixtures. The purity of CA gained using the pyrolyzate mixture of PHBV and PHBV-enriched biomass

Separation of CA/ 2-PA mixture using spinning band distillation column

are 96 and 93%, respectively. Compared to CA achieved by distillation of the commercial chemicals, there is a slight reduction in the purity of CA obtained from the pyrolyzate mixture distillation. This can be explained by other possible volatile side-products, originating from the pyrolysis step. According to GC-MS, isocrotonic acid, 4-pentenoic acid and 3-butenoic acid are the main volatile by-products that can end up in the top product and consequently decrease the purity of CA. Furthermore, the 2-PA purity that was obtained was much lower than the CA purity, which is due to the drying up of the vapor stream, which prohibited continued distillation. Future work on a continuous distillation process would allow us to also obtain 2-PA in high purity. Overall, the achieved purity is similar to the results obtained by Parodi et al. [22] using MMC-based PHB in thermolytic distillation, meaning that a relatively pure CA production is also feasible using MMC-based PHBV which can be an excellent candidate to reduce acid production cost through the bio-based pathway.

Table 6-4. Recovery of CA from the pyrolyzate mixtures obtained by pyrolysis of pure MMC-based PHBV and PHBV-enriched biomass using SBC at 50 mbar, 110 °C and 5h.

Feed (CA/2-PA) [wt%]	Material used for pyrolysis	Top/Bottom	Composition [wt%]		
			CA	2-PA	water
80/20 + 2% Py _{PHBV}	PHBV	Top	96	0.06	<1
		Bottom	65	22	<1
80/20 + 6% Py _{Biomass-PHBV}	PHBV-enriched biomass	Top	93	16.5	<1
		Bottom	60	25	<1

4. Conclusion

The production of pure CA through thermal depolymerization of bio-based PHBV co-polymer requires downstream purification steps because of the various side-products, originating from each monomer. 2-PA is the main by-product, arising from thermal decomposition of the HV monomer. Therefore, separation of CA/2-PA mixtures via distillation was investigated in this study. To assure thermal stability of these unsaturated acids, distillation must be performed under reduced pressure conditions. The results indicate that indeed distillation appears to be a feasible technique to recover CA with a purity of >98% from CA/2-PA mixture using the SBC at 50 mbar. Moreover, the purification of CA obtained by pyrolysis of either PHBV-enriched biomass or extracted PHBV itself was also studied under the same applied conditions. It was found that CA can be recovered from pyrolysis oil with a purity of 96 and 93% using the pyrolyzate mixture, obtained from pyrolysis of the PHBV-enriched biomass and extracted pure PHBV from the same biomass batch, respectively. Regarding the operation condition of the SBC for this mixture at semi-batch mode, overall, the distillation process under vacuum is controllable. A stable operation can be achieved during distillation for several hours. Although the entire column was insulated, crystallization of CA still was observed at the top section of the column, which may be prevented by further improvement of the insulation. The observed product purity was very high. Further optimization potential could be offered by further increasing the temperature of the silicone oil at the bottom of the column. To minimize the mass loss in the process, potentially renewed gaskets might help to a small extent. Due to the vibrations of the rotation of the spinning band it is assumed though that it can never be perfectly sealed. Maybe it would

Separation of CA/ 2-PA mixture using spinning band distillation column

possible to use vacuum distillation but no spinning band distillation to minimize vibrations. On the other hand, it could be investigated further whether after the process the column can be washed with acetone and the product can be obtained out of the acetone as well and if that is feasible to do.

Considering all technical results on the CA and 2-PA separation, we conclude that it is certainly possible to separate these two acids by distillation after pyrolysis of PHBV. The future availability of much more starting materials from pilot scale PHBV production and extraction studies at Paques Biomaterials BV will also enable studies on fully continuous distillation, which is expected to be easier to control. The distillation may be combined with crystallization of CA for the final purification. Further studies towards bio-based polymer production from these bio-based monomers could include a more general sustainability analysis.

Nomenclature:

CA	Trans-Crotonic Acid
GC-MS	Gas Chromatography-Mass Spectroscopy
GC- FID/MS	Gas Chromatography-Flame IR Detector/Mass Spectroscopy
HV	Hydroxy Valerate
HB	Hydroxy Butyrate
HPLC	High Performance Liquid Chromatography
¹ H-NMR	Proton Nuclear Magnetic Resonance
KFT	Karl- Fischer Titration
MMC	Mixed Microbial Culture
NRTL	Non-Random Two-Liquid model
PHB	Poly(3-hydroxy butyrate)
PHBV	Poly(3-Hydroxybutyrate-co-3-Hydroxyvalerate)
2-PA	2-Pentenoic Acid
PTFE	Polytetrafluoroethylene
Py _{PHBV}	Pyrolyzate mixture of PHBV
Py _{Biomass-PHBV}	Pyrolyzate mixture of PHBV-enriched Biomass
SBC	Spinning Band Column
VLE	Vapor Liquid Equilibrium
VFA	Volatile Fatty Acid

References

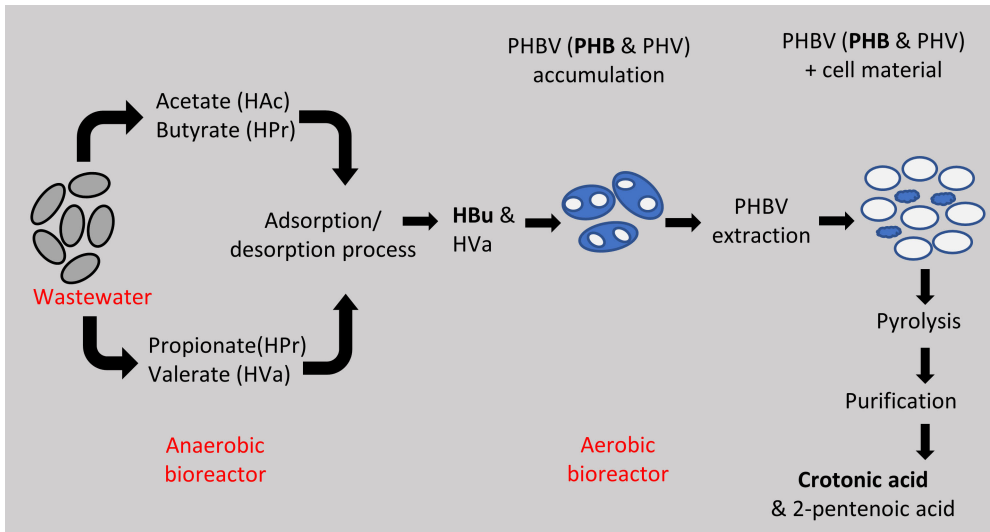
- [1] A. Leal-Duaso; P. Pérez; J.A. Mayoral; E. Pires; J.I. García, Glycerol as a source of designer solvents: physicochemical properties of low melting mixtures containing glycerol ethers and ammonium salts. *Physical Chemistry Chemical Physics*. **2017**, *19*, 28302-28312.
- [2] T. Brouwer; B. Schuur, Bio-based solvents as entrainers for extractive distillation in aromatic/aliphatic and olefin/paraffin separation. *Green Chemistry*. **2020**, *22*, 5369-5375.

- [3] R.-J. van Putten; J.C. van der Waal; E. de Jong; C.B. Rasrendra; H.J. Heeres; J.G. de Vries, Hydroxymethylfurfural, A Versatile Platform Chemical Made from Renewable Resources. *Chemical Reviews*. **2013**, *113*, 1499-1597.
- [4] T. Eregowda; E.R. Rene; J. Rintala; P.N.L. Lens, Volatile fatty acid adsorption on anion exchange resins: kinetics and selective recovery of acetic acid. *Separation Science and Technology*. **2020**, *55*, 1449-1461.
- [5] E.V. Fufachev; B.M. Weckhuysen; P.C.A. Bruijninx, Toward Catalytic Ketonization of Volatile Fatty Acids Extracted from Fermented Wastewater by Adsorption. *ACS Sustainable Chemistry & Engineering*. **2020**, *8*, 11292-11298.
- [6] E. Reyhanitash; S.R.A. Kersten; B. Schuur, Recovery of Volatile Fatty Acids from Fermented Wastewater by Adsorption. *ACS Sustainable Chemistry & Engineering*. **2017**, *5*, 9176-9184.
- [7] V. Elhami; N. van de Beek; L. Wang; S.J. Picken; J. Tamis; J.A.B. Sousa; M.A. Hempenius; B. Schuur, Extraction of low molecular weight polyhydroxyalkanoates from mixed microbial cultures using bio-based solvents. *Separation and Purification Technology*. **2022**, *299*, 121773.
- [8] S.L. Riedel; C.J. Brigham; C.F. Budde; J. Bader; C. Rha; U. Stahl; A.J. Sinskey, Recovery of poly(3-hydroxybutyrate-co-3-hydroxyhexanoate) from *Ralstonia eutropha* cultures with non-halogenated solvents. *Biotechnology and Bioengineering*. **2013**, *110*, 461-470.
- [9] M. Mulders; J. Tamis; B. Abbas; J. Sousa; H. Dijkman; R. Rozendal; R. Kleerebezem, Pilot-Scale Polyhydroxyalkanoate Production from Organic Waste: Process Characteristics at High pH and High Ammonium Concentration. *Journal of Environmental Engineering*. **2020**, *146*, 04020049.
- [10] C. Kourmentza; J. Plácido; N. Venetsaneas; A. Burniol-Figols; C. Varrone; H.N. Gavala; M.A.M. Reis, Recent Advances and Challenges towards Sustainable Polyhydroxyalkanoate (PHA) Production. *Bioengineering*. **2017**, *4*, 55.
- [11] R.P. Schulz; J. Blumenstein; C. Kohlpaintner. Crotonaldehyde and crotonic acid. *Ullmann's Encyclopedia of Industrial Chemistry*: 2002; pp. 463-469.
- [12] M.R.Z. Mamat; H. Ariffin; M.A. Hassan; M.A.K. Mohd Zahari, Bio-based production of crotonic acid by pyrolysis of poly(3-hydroxybutyrate) inclusions. *Journal of Cleaner Production*. **2014**, *83*, 463-472.
- [13] G.J. Raugi; T.C. Liang; J.J. Blum, Effects of pentanoic acid and 4-pentenoic acid on the intracellular fluxes of acetyl coenzyme A in *Tetrahymena*. *Journal of Biological Chemistry*. **1975**, *250*, 4067-4072.
- [14] N. Ahmad; B. Colak; M.J. Gibbs; D.-W. Zhang; J.E. Gautrot; M. Watkinson; C.R. Becer; S. Krause, Peptide Cross-Linked Poly(2-oxazoline) as a Sensor Material for the Detection of Proteases with a Quartz Crystal Microbalance. *Biomacromolecules*. **2019**, *20*, 2506-2514.
- [15] A. Fraga; R.A. Ruseckaite; A. Jiménez, Thermal degradation and pyrolysis of mixtures based on poly(3-hydroxybutyrate-8%-3-hydroxyvalerate) and cellulose derivatives. *Polymer Testing*. **2005**, *24*, 526-534.
- [16] H. Morikawa; R. Marchessault, Pyrolysis of bacterial polyalkanoates. *Canadian Journal of Chemistry*. **2011**, *59*, 2306-2313.
- [17] H. Ariffin; H. Nishida; Y. Shirai; M.A. Hassan, Highly selective transformation of poly[(R)-3-hydroxybutyric acid] into trans-crotonic acid by catalytic thermal degradation. *Polymer Degradation and Stability*. **2010**, *95*, 1375-1381.

- [18] Y. Li; T.J. Strathmann, Kinetics and mechanism for hydrothermal conversion of polyhydroxybutyrate (PHB) for wastewater valorization. *Green Chemistry*. **2019**, *21*, 5586-5597.
- [19] C. Torri; T.D.O. Weme; C. Samori; A. Kiwan; D.W.F. Brillman, Renewable Alkenes from the Hydrothermal Treatment of Polyhydroxyalkanoates-Containing Sludge. *Environmental Science & Technology*. **2017**, *51*, 12683-12691.
- [20] H. Xiang; X. Wen; X. Miu; Y. Li; Z. Zhou; M. Zhu, Thermal depolymerization mechanisms of poly(3-hydroxybutyrate-co-3-hydroxyvalerate). *Progress in Natural Science: Materials International*. **2016**, *26*, 58-64.
- [21] C.A. Mullen; A.A. Boateng; D. Schweitzer; K. Sparks; K.D. Snell, Mild pyrolysis of P3HB/switchgrass blends for the production of bio-oil enriched with crotonic acid. *Journal of Analytical and Applied Pyrolysis*. **2014**, *107*, 40-45.
- [22] A. Parodi; A. Jorea; M. Fagnoni; D. Ravelli; C. Samori; C. Torri; P. Galletti, Bio-based crotonic acid from polyhydroxybutyrate: synthesis and photocatalyzed hydroacylation. *Green Chemistry*. **2021**, *23*, 3420-3427.
- [23] V. Elhami; E.C. Antunes; H. Temmink; B. Schuur, Recovery Techniques Enabling Circular Chemistry from Wastewater. *Molecules*. **2022**, *27*, 1389.
- [24] Á. Bóna; P. Bakonyi; I. Galambos; K. Bélafi-Bakó; N. Nemestóthy, Separation of Volatile Fatty Acids from Model Anaerobic Effluents Using Various Membrane Technologies. *Membranes*. **2020**, *10*.
- [25] P. Sukphun; S. Sittijunda; A. Reungsang, Volatile Fatty Acid Production from Organic Waste with the Emphasis on Membrane-Based Recovery. *Fermentation*. **2021**, *7*, 159.
- [26] PubChem Available online: https://pubchem.ncbi.nlm.nih.gov/compound/crotonic_acid (accessed on 08-12-2021).
- [27] Chemspider. Available online: <http://www.chemspider.com/Chemical-Structure.553682.html> (accessed on 08-12-2021).
- [28] L. Bittorf; K. Pathak; N. Kockmann, Spinning Band Distillation Column–Rotating Element Design and Vacuum Operation. *Industrial & Engineering Chemistry Research*. **2021**, *60*, 10854-10862.
- [29] L. Bittorf; N. Böttger; D. Neumann; A. Winter; N. Kockmann, Characterization of an Automated Spinning-Band Column as a Module for Laboratory Distillation. *Chemical Engineering & Technology*. **2021**, *44*, 1660-1667.
- [30] W.L. Luyben. Chapter 1 - Distillation Control. In *Distillation*, Górák, A., Schoenmakers, H., Eds.; Academic Press: Boston, 2014; pp. 1-35.
- [31] A. Gorak; H. Schoenmakers. *Distillation: Operation and applications*; Academic Press: 2014.
- [32] K.-J. Kim; U. Diwekar, 5 Batch Distillation. **2005**,
- [33] A. Londoño; M.T.G. Jongmans; B. Schuur; A.B. de Haan, Isobaric low pressure vapor–liquid equilibrium data for the binary system monochloroacetic acid+dichloroacetic acid. *Fluid Phase Equilibria*. **2012**, *313*, 97-101.
- [34] M. Hocking, Structure of crotonic acid dimers and higher polymers with partial stereochemistry of the dimers. *Canadian Journal of Chemistry*. **1969**, *47*, 821-830.

Chapter 7

Conclusions and Perspective



1. Conclusions and outlook

The aim of this thesis was to provide a bio-based pathway to produce crotonic acid (CA) from a waste/wastewater. Anaerobic digestion of a carbon-rich waste results in production of volatile fatty acids (VFAs) [1]. These VFAs can be used as feedstock for bacteria operating in an aerobic digestion. Under manipulated fluctuating stressful conditions (feast and famine), where in periods bacteria are given a limited amount of nutrients, alternated with periods of abundance, during the abundance periods some of these bacteria convert VFAs into polymers of the family Polyhydroxyalkanoates (PHAs) as a storage of carbon and/or energy source [2,3]. Such PHAs are bio-based and green polymers which can be appropriate replacement for conventional polymers such as polyethylene (PE) and polypropylene (PP) [4]. Nonetheless, the price of PHA bio-polymer from sugar solutions in single sterile cultures is still about three to four times higher than the aforementioned fossil-based polymers [5]. An alternative to dedicated sugar solutions in single sterile cultures to reduce the total price of PHA is to use a carbon-enriched waste/wastewater (e.g. food waste) as a feedstock for the microorganisms in an open mixed microbial culture (MMC) [6]. However, the main drawback of this approach is daily variation in the composition of the waste which results in production of PHAs with variation in properties. If the produced polymer does not meet the polymer market requirement, it can be alternatively further valorized by depolymerizing it towards its corresponding monomers [7]. In most cases, Poly(3-hydroxybutyrate-co-3-hydroxyvalerate) (PHBV) co-polymer is the type of PHA which is produced in MMC using a waste as a feedstock. Since it consists of two monomeric units, the thermal depolymerization of PHBV yields into the two monomeric

products CA and 2-pentenoic acid (2-PA), which have a wide range of applications in various industries. In this study, these monomers have been produced by a multistep process. The main conclusions and prospective for each step are given in the following sub-sections.

1.1. Recovery of the VFAs from a fermentation broth by adsorption

Adsorption is an affinity separation technique, enabling to separate a target molecule from highly dilute solutions [8-10]. Therefore, it was selected to recover the VFAs from a fermentation broth as the VFA content of these broths are usually less than 1%. In the previous work in SPT group, the separation of VFAs from a mimicked fermentation broth was studied using poly(styrene divinylbenzene) (PS-DVB) based adsorbents (referred as Lewatit) [11]. It was found that the amine functionalized resins attracted not only the VFAs but also the mineral acids (the salts) which are typically present in the fermentation broth. Thus, their capacity towards VFAs was limited. A different trend was observed for the non-functionalized adsorbent, where no affinity towards minerals was found and a high loading capacity for the VFAs. The physical interaction between the VFAs and the Lewatit (and not ion exchange) enabled regenerating the resins by thermal desorption and recovering the loaded acids through the vapor phase. In the previous work, the findings of the author displayed that it is possible to fractionate the loaded acids during thermal regeneration to obtain them in concentrated form by applying a proper temperature profile based on the boiling points of the loaded components. Although there is no interaction between the water

Conclusions and Perspective

and hydrophobic Lewatit, water physically filled the pores during adsorption. Hence, the fractionation of the water and VFAs was challenging in thermal desorption. Because a large fraction of the loaded VFAs were desorbed during water removal, meaning that a limited amount of VFAs were obtained in highly concentrated form. Therefore, in the current study, the goal was to enhance the concentration factor during adsorption-desorption of VFAs by improving the balance between the acids and water either in adsorption step or during desorption.

To enhance the adsorption stage, there were two directions; either increasing the affinity between the adsorbent and VFAs to increase the capacity, or limiting the water uptake by the adsorbent to increase the selectivity. In this thesis, the methacrylonitrile (MAN) and styrene (ST), crosslinked with DVB were investigated which were provided by Wrocław University of Science and Technology in a collaborative study. The MAN-DVB was applied aiming to enhance adsorption stage by increasing the VFAs loading via hydrogen bonding between the nitrile groups of the MAN-DVB and the acids. While ST-DVB with small pore volume was applied aiming to reduce water uptake during adsorption. A maximum VFAs loading capacity of about 153 [gAcid/kgAdsorbent] was found for the MAN-DVB resins which is comparable to the ones obtained by Lewatit. Whilst the maximum surface area of MAN-DVB particles was about twice lower than Lewatit. It indicates that hydrophobic interaction is not the only separation mechanism for MAN-DVB resins. The nitrile groups of the adsorbent also enabled hydrogen bonding between the resin and the carboxyl group of the acids. Moreover, the MAN-DVB resins showed no affinity towards the mineral acids (salts) which is an excellent finding as there is no competitive adsorption between

Conclusions and Perspectives

the VFAs and the salts. However, the nitrile groups increase the polarity of the adsorbent, resulting in high water uptake for MAN-DVB resins.

The second hypothesis to enhance the adsorption step was to limit the water uptake of ST-DVB while maintaining the VFAs loading constant. Thus, ST-DVB with small pores were employed to adsorb the VFAs from a mimicked broth. The results illustrated that indeed the water uptake of ST-DVB resin reduces significantly by reducing the average pore size and pore volume of the particles. ST-DVB resin with limited water uptake can also be a proper candidate to separate the acids from a dilute aqueous solution, followed by effective thermal desorption to recover the VFAs at high concentration due to their limited water uptake. Overall, at similar surface area, the MAN-DVB adsorbents retained a higher loading capacity for corresponding acid, compared to the ST-DVB resins, due to the hydrogen bonding between the adsorbent and the acids. It can be concluded that selecting MAN-DVB or ST-DVB with small pores depends on the required final concentration of the recovered VFAs. If recovering highly concentrated acids is the goal, it is recommended to use ST-DVB with limited pore volume and reasonable surface area to reduce water uptake and enhance thermal regeneration stage. If high VFAs adsorption capacity is the main focus, it is better to apply MAN-DVB resins due to their high selectivity towards the VFAs.

In the next step, a superparamagnetic polymer was synthesized, aiming at enhancing the fractionation of water and acids during the thermal regeneration of the adsorbent and recovering the loaded VFAs in highly concentrated solution. Previously, the thermal desorption of the non-functionalized PS-DVB adsorbent was performed by hot N₂ gas stripping [11]. The heat-insulating character of PS-DVB resins limits heating up the interior

Conclusions and Perspective

of the resin particles by hot N₂ stripping, resulting in a temperature gradient inside the particles that hinders sharper fractionation. Loading the adsorbent with superparamagnetic nanoparticles provided an opportunity to generate heat inside the particles by applying an alternating magnetic field (AMF). Moreover, by heating the particles from inside, it was possible to generate water bubbles in the pores which can physically push out a fraction of water without evaporating. The main goal of this thesis was to recover water as much as possible without remarkably removing the loaded VFAs using AMF heating. Hence, recovering a significant quantity of the acids in concentrated form by hot N₂ stripping in the next stage. Therefore, a superparamagnetic resin was synthesized, and an AMF set-up was designed.

The basis of the superparamagnetic beads was poly(divinylbenzene) (PDVB) incorporated with oleic acid (OA) grafted superparamagnetic magnetite nanoparticles (OA-MNPs). The MNPs were synthesized by the coprecipitation method and functionalized with oleic acid. Following this step, the OA-MNPs were embedded in the matrix of the polymer during suspension polymerization. Adsorption was conducted using the synthesized beads in a packed bed column. Desorption was performed in two steps, starting with AMF heating at 25 mT and 52 kHz to remove a large fraction of the loaded water, followed by a hot N₂ stripping stage to recover the adsorbed VFAs. It was found that 90±9% of the water in the pores was recovered while only 11±2% of total loaded VFAs were removed by AMF heating. Although this preliminary study confirmed a successful fractionation of water and VFAs by AMF heating prior to hot N₂ stripping, it is required to further optimize this approach. Due to the limited time and broadness of the thesis, optimization of the AMF powered fractionated regeneration could not

be realized. Therefore, the recommendations for possible future work on this approach are given in the following sub-sections:

There are three different mechanisms for an MNP to generate heat during AMF, Brownian relaxation, Neel relaxation and Weiss domain relaxation. Brownian relaxation refers to the rotation of an MNP to align in the same direction of the applied external magnetic field. Neel relaxation is the rotation of the magnetic moments of a single MNP according to the external magnetic field lines. Domain rotation is only possible for the MNPs with larger diameters in which each single MNP can contain multiple Weiss domains where the magnetic moments are randomly aligned. Therefore, a fixed superparamagnetic particle subjected to an AMF can dissipate heat only by Neel relaxation mechanism. In the current study, the OA-MNPs are small superparamagnetic particles, fixed in the matrix of the polymer. It means the heat generation by these OA-MNPs was not optimal. Moreover, the function of the preliminary custom-built AMF set-up in this work was limited to a certain frequency (52 kHz) and magnetic field intensity (25 mT) using a small column. While the higher the frequency and magnetic field, the higher heat generation by MNPs. Therefore, the heat dissipation in AMF can be enhanced even further by following alternatives:

1. Increasing the size of the OA-MNPs. The core size of OA-MNPs used in this study was about 10 nm. Tong et al. [12] explored that the magnetic nanoparticles with size greater than 20 nm have significantly high heat dissipation. By optimizing the synthesis of the MNPs to limit the size distribution and achieve the average size between 20-40 nm, the heat generation could most likely be remarkably enhanced. The particles with core size above 20 nm are

most likely not single domain superparamagnetic nanoparticle. They are ferromagnetic nanoparticles with multiple Weiss domains. Although the saturation magnetization of the particles with larger core diameters is lower than superparamagnetic particles, the total heat produced may be larger due to the rotation of the Weiss domains with respect to the applied magnetic field in AMF that can contribute to the heat production. It is worth mentioning that increasing the size of nanoparticles beyond 40 nm is not beneficial for this application. Because they require significantly high applied power to generate strong AMF and consequently dissipate heat.

2. Physically incorporating the OA-MNPs in the pores, without encapsulating them in the polymeric matrix, and thus allowing them to rotate in the AMF. By physically entrapping the MNPs in the pores of already synthesized resin, it may be possible to prepare a superparamagnetic polymer in which the MNPs are able to rotate and increase heat generation by Brownian relaxation. This method is feasible using a porous resin with pore size greater than the size of the MNPs and by dispersing the MNPs in a solvent which can easily penetrate into the pores of the resins. Finally, by evaporating the solvent, the MNPs can be impregnated in the pores.
3. Enhancing the AMF set-up to reach high frequency and magnetic field intensity. The higher the frequency and magnetic field intensity the higher produced heat by MNPs. The impact of the frequency is greater than the magnetic field intensity. According to linear response theory (LRT), the maximum heating efficiency of MNPs can be achieved when their relaxation time approaches the period of

AMF. This theory can be used to predict the required frequency for MNPs with certain core size to generate heat with optimal efficiency. For example, it is predicted by LRT that the highest heat dissipation by MNPs with 40 nm can be obtained at 300 kHz [12]. Moreover, the AMF set-up can be modified to monitor the temperature of the particles loaded in column by an infrared camera thermocouple during AMF. It can aid the calculation of the produced heat by measuring the increase in the temperature of the solution that the particles are dispersed. In the current set-up, the diameter of the outlet of the column is small (<1 cm). The system was working under reduced pressure, meaning that the outlet was well insulated. Thus, it was challenging to properly place an infrared camera to directly monitor the temperature change in the column during AMF.

Another possible optimization of the total VFA recovery through the proposed method can be obtained by heat integration. In the current set-up, the cold water pumped through the hollow coil to cool it down during AMF. In the optimized process, it is recommended to integrate the induced heat in the coil in the process. For example, it can be used to heat up the N₂ gas for the hot nitrogen stripping phase, allowing further optimization towards less power consumption in the overall process.

1.2. Recovery of MMC-based PHBV using solvent extraction

PHBV was obtained from a waste/ wastewater using a mixed microbial culture (MMC). In the current study, the average molecular weight (MW) of PHBV was purposely reduced from about 1 MDa to about 200 kDa by drying

Conclusions and Perspective

the PHBV-rich biomass at elevated temperature of 120 °C for 18 h to ease extraction and handling. At the company Paques Biomaterials, drying time can be varied to manipulate the molar weight of the PHBV. As the final application of these PHBV co-polymer was to be pyrolyzed towards CA and 2-PA, having high average MW was not essential. However, lowering the average MW can extremely affect the solubility of the polymer and consequently the extraction yield using a solvent. Because solvent extraction of PHBV requires a next step to retrieve the polymer in solid form which can be done by either evaporating the solvent or adding an antisolvent, depending on the nature of the solvent and required purity of polymer. If a solvent has low boiling point, the polymer can be retrieved by solvent evaporation. However, its purity would be much lower than polymer obtained by using an antisolvent. For the polymers with low average MW, it can be challenging to fully recover them from good solvents using an antisolvent due to their high solubility.

In this thesis, the bio-based solvents 2-methyltetrahydrofuran (2-MTHF) and dihydrolevoglucosenone (cyrene) were used to extract PHBV with low average MW. Moreover, the performance of these proposed bio-based solvents was compared with chloroform and dimethyl carbonate (DMC) as benchmark solvents using different batches of the PHBV-enriched biomass with various average MW. The results indicated that the proposed new solvents are preferred over the benchmarks for the extraction of PHBV with low average MW. For example, 2-MTHF resulted in 62±3% extraction efficiency for PHBV with MW of about 100 kDa while it was only 32 and 20% for chloroform and DMC, respectively. Based on the mass balance closure over the extraction process, the precipitation step is the major limiting stage

when a good solvent is employed to extract a polymer with relatively low average MW.

In this study, the extraction with 2-MTHF and cyrene was optimized to recover the PHBV with the lowest average MW out of the samples available. However, due to the limited amount of the available PHBV-enriched biomass, the solvent extraction experiments were performed in small scales using 10 mL solvent and about 0.5 g biomass. Therefore, it is recommended to scale up the extraction procedure at optimized conditions for both solvents to experimentally determine the maximum reusability of the solvent and its loss per cycle. These are also the required parameters for final process design and scale-up. Obviously, a fraction of solvent remains in the residual biomass after the extraction. For 2-MTHF based extractions, the remaining solvent in the biomass residue can be easily recovered by drying the residues and condensing the vapor phase. Regarding cyrene, it is not volatile and has a high boiling point of 227 °C. The remaining solvent in the residual biomass can be obtained by rinsing the residues with ethanol, followed by ethanol/cyrene separation with distillation. In terms of recovering solvent from the supernatant, the separation of 2-MTHF and n-heptane can be also done by distillation. Similarly, the mixture of the antisolvent (ethanol/water) can be also separated from cyrene by distillation, where it is noted that a small part of the cyrene will be converted in the geminal diol [13].

1.3. Pyrolysis of MMC-based PHBV towards CA and 2-PA

Depolymerization of PHBV yields into CA and 2-PA, originating from hydroxy butyrate (HB) and hydroxy valerate (HV) repeating units, respectively. In this

thesis, aiming at obtaining high yields of both CA and 2-PA from MMC, direct pyrolysis of the PHBV-enriched biomass into CA and 2-PA was studied either under an inert atmosphere using N₂ carrier gas flow or under reduced pressure using a custom-designed oven pyrolyzer. Applying nitrogen as a carrier gas enabled to experimentally optimize thermal depolymerization of the PHBV towards CA and 2-PA by manipulating the mean residence time of the hot vapor phase. The highest yields of 80±2% for CA and 67±1% for 2-PA were obtained at 0.15 L/min nitrogen flow rate corresponding to a mean residence time of 20 s, 240 °C for 1 hour. When the pyrolysis was conducted at a reduced pressure of 150 mbar instead of using nitrogen gas, a comparable acid yield was obtained. In this thesis, the highest yield of CA that was attained is comparable to those obtained by pyrolysis of pretreated PHB/PHB-enriched biomass and catalyzed pyrolysis. Overall, the custom-built pyrolysis set-up displayed an excellent operation performance using both N₂ flow and reduced pressure.

1.4. Separation of CA and 2-PA mixture by distillation

According to the results obtained in chapter 5, pyrolysis of PHBV yields a mixture containing CA, 2-PA, isocrotonic acid, 3-butenic acid, 4-pentenoic acid, 3-pentenoic acid and oligomers with CA and 2-PA being the predominant products. Aiming to use CA and 2-PA as bio-based monomers, requires a purification step to obtain the pure acids. In this thesis, we have experimentally explored the use of a spinning band distillation column (SBC) under vacuum operation to separate these acids. First, the thermodynamic feasibility for the distillation was studied by measuring VLE-data of the

Conclusions and Perspectives

mixture at process-relevant pressures of 50 and 100 mbar using a custom-designed VLE set-up. Due to the high melting point of CA, Fischer Labodest VLE 602 ebulliometer was not applicable for the mixtures with high CA concentration. Thus, a custom-designed VLE set-up was fabricated which is a small equilibrium cell. The performance of the custom-built VLE cell was compared with Fischer ebulliometer using a CA/2-PA (mass ratio: 10/90) mixture in both apparatuses at 50 mbar. A similar equilibrium mass fraction was obtained using both set-ups which confirmed the custom-designed VLE cell is relatively accurate and can be used to obtain the equilibrium data for a mixture. However, the temperature of the gas and liquid phase in this set-up were measured using Pt-100 sensors, connected to a reader. The corresponding measurement error was about ± 1 °C which can be reduced by replacing the sensors with a thermometer with high accuracy (e.g., RS PRO RS1710 Wired Digital thermometer) in the follow-up studies. The VLE data obtained by this equilibrium cell showed that there was a reasonable relative volatility over the entire composition range and no severe pinch points for the CA/2-PA mixture, which indicated that separation is achievable by distillation. Thus, SBC was employed to further examine the separation of CA/2-PA by distillation. A successful separation of CA with extremely high purity was achieved using SBC at 50 mbar and 110 °C.

Regarding the operation condition of SBC for this mixture at semi-batch mode, several hours of distillation can be completed with a stable operation. Although, the entire column was insulated, crystallization of CA still was observed at the top section of the column, which may be prevented by further improvement of the insulation. Moreover, implementing two condensers in series with different operation temperature might increase

Conclusions and Perspective

the recovery yield. Because in this thesis, the temperature of the condenser was kept at 75-80 °C to collect CA in liquid form and provide reflux in the column. Therefore, a fraction of CA left the condenser without being condensed due to its high melting point (72 °C). Installing a second condenser with lower temperature can improve the total recovery yield. According to the results obtained from batch-wise distillation with SBC, for the final process design, it is recommended to experimentally study the continuous distillation process using either SBC or a conventional distillation column with at least 10 stages, which is well insulated to prevent CA crystallization in the relatively cold spots (<72 °C).

Nomenclature:

AMF	Alternating magnetic field
CA	trans-Crotonic Acid
DMC	Dimethyl Carbonate
DVB	Divinylbenzene
GC	Gas-Chromatography
HB	Hydroxy Butyrate
HV	Hydroxy Valerate
MAN	Methacrylonitrile
2-MTHF	2-Methyltetrahydrofuran
MMC	Mixed Microbial Culture
MNP	Magnetite nanoparticles
MW	Molecular weight
OA	Oleic Acid
PHAs	Polyhydroxyalkanoates
PHB	Poly(3hydroxybutyrate)
PHV	Poly(3-hydroxy Valerate)
PHBV	Poly(3-Hydroxybutyrate-co-3-Hydroxyvalerate)
2-PA	2-Pentenoic Acid
PP	Polypropylene
PE	Polyethylene
PDVB	Poly(divinylbenzene)
PS-DVB	Poly(styrene divinylbenzene)
SBC	Spinning Band Column
ST	Polystyrene
VFAs	Volatile Fatty Acids
VLE	Vapor Liquid Equilibria

References

- [1] O. García-Depraect; R. Lebrero; S. Rodríguez-Vega; R.A. Börner; T. Börner; R. Muñoz, Production of volatile fatty acids (VFAs) from five commercial bioplastics via acidogenic fermentation. *Bioresource Technology*. **2022**, *360*, 127655.
- [2] K. Johnson; Y. Jiang; R. Kleerebezem; G. Muyzer; M.C.M. van Loosdrecht, Enrichment of a Mixed Bacterial Culture with a High Polyhydroxyalkanoate Storage Capacity. *Biomacromolecules*. **2009**, *10*, 670-676.

Conclusions and Perspective

- [3] V.C. Kalia; S.K. Singh Patel; R. Shanmugam; J.-K. Lee, Polyhydroxyalkanoates: Trends and advances toward biotechnological applications. *Bioresource Technology*. **2021**, *326*, 124737.
- [4] G. Moore; S. Saunders. *Advances in biodegradable polymers*; iSmithers Rapra Publishing: 1998; Volume 98.
- [5] C. Kourmentza; J. Plácido; N. Venetsaneas; A. Burniol-Figols; C. Varrone; H.N. Gavala; M.A.M. Reis, Recent Advances and Challenges towards Sustainable Polyhydroxyalkanoate (PHA) Production. *Bioengineering*. **2017**, *4*, 55.
- [6] S. Guleria; H. Singh; V. Sharma; N. Bhardwaj; S.K. Arya; S. Puri; M. Khatri, Polyhydroxyalkanoates production from domestic waste feedstock: A sustainable approach towards bio-economy. *Journal of Cleaner Production*. **2022**, *340*, 130661.
- [7] A. Parodi; A. Jorea; M. Fagnoni; D. Ravelli; C. Samori; C. Torri; P. Galletti, Bio-based crotonic acid from polyhydroxybutyrate: synthesis and photocatalyzed hydroacylation. *Green Chemistry*. **2021**, *23*, 3420-3427.
- [8] T. Eregowda; E.R. Rene; J. Rintala; P.N.L. Lens, Volatile fatty acid adsorption on anion exchange resins: kinetics and selective recovery of acetic acid. *Separation Science and Technology*. **2020**, *55*, 1449-1461.
- [9] F. Rizzioli; F. Battista; D. Bolzonella; N. Frison, Volatile Fatty Acid Recovery from Anaerobic Fermentate: Focusing on Adsorption and Desorption Performances. *Industrial & Engineering Chemistry Research*. **2021**, *60*, 13701-13709.
- [10] P.O. Saboe; L.P. Manker; H.R. Monroe; W.E. Michener; S. Haugen; E.C.D. Tan; R.L. Prestangen; G.T. Beckham; E.M. Karp, Energy and techno-economic analysis of bio-based carboxylic acid recovery by adsorption. *Green Chemistry*. **2021**, *23*, 4386-4402.
- [11] E. Reyhanitash; S.R.A. Kersten; B. Schuur, Recovery of Volatile Fatty Acids from Fermented Wastewater by Adsorption. *ACS Sustainable Chemistry & Engineering*. **2017**, *5*, 9176-9184.
- [12] S. Tong; C.A. Quinto; L. Zhang; P. Mohindra; G. Bao, Size-Dependent Heating of Magnetic Iron Oxide Nanoparticles. *ACS Nano*. **2017**, *11*, 6808-6816.
- [13] M. De bruyn; V.L. Budarin; A. Misefari; S. Shimizu; H. Fish; M. Cockett; A.J. Hunt; H. Hofstetter; B.M. Weckhuysen; J.H. Clark; et al., Geminal Diol of Green Nanostructured Solvents. *ACS Sustainable Chemistry & Engineering*. **2019**, *7*, 7878-7883.

Appendices

1. BET N₂ adsorption-desorption isotherm for Fe₃O₄

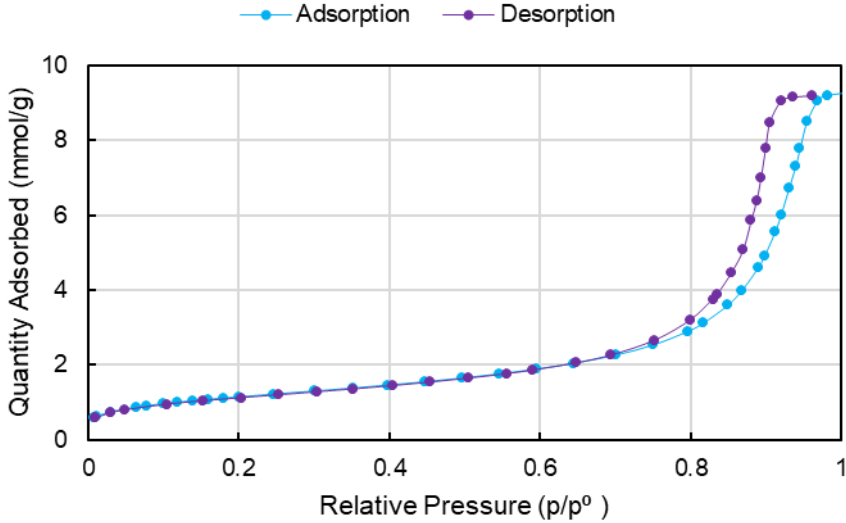


Figure S-1. Nitrogen adsorption-desorption isotherm for the synthesized magnetite nanoparticles. The particles were degassed at 280 °C for 150 h in a nitrogen environment prior to analysis.

2. Calculation of the monolayer coverage for oleic acid grafted magnetite nanoparticles

The following equation was used to calculate the minimum required quantity of oleic acid for a full monolayer coverage around the nanoparticles.

$$m_{OA} = \frac{M_{OA} * S_{BET} * 10^{20} * m_{NPS}}{S_P * N_A} \quad (S-1)$$

Where M_{OA} is the molecular weight of oleic acid in [g/mol], S_{BET} is the BET surface area of the nanoparticles [$m^2/g_{Fe_3O_4}$], m_{NPS} is the mass of the nanoparticles used for the functionalization in [g], S_P is the grafted area for a

single oleic acid molecule in [\AA] and N_A is Avogadro's number. To ensure a complete coverage on the surface of the nanoparticles, about 1.5 fold of the calculated quantity of oleic acid was used in the experiments.

3. TEM image of the oleic acid grafted magnetite nanoparticles

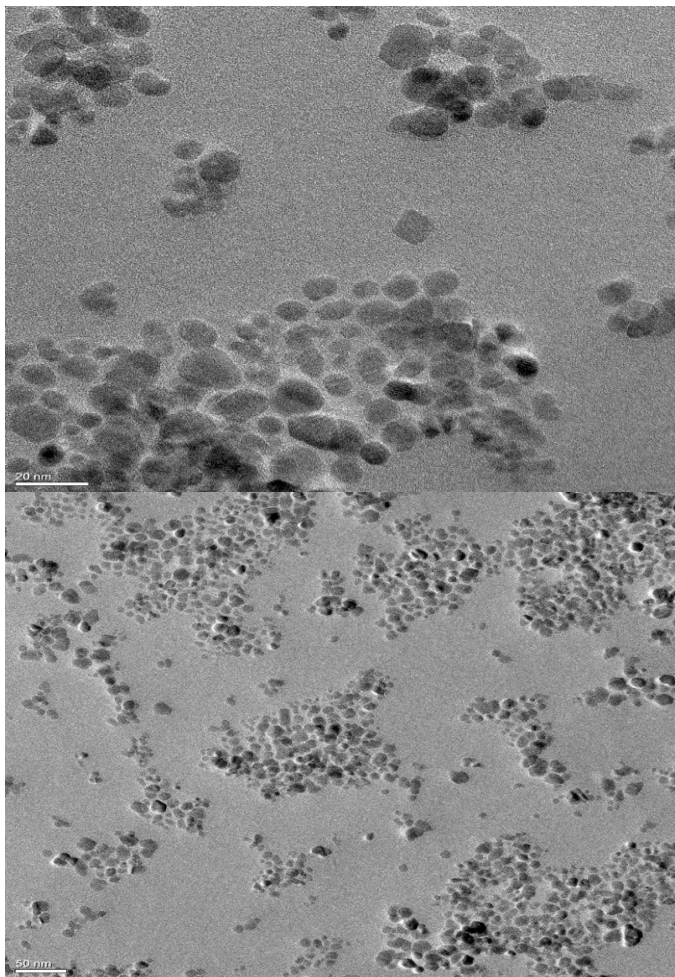


Figure S-2. TEM images of the synthesized oleic acid grafted magnetite nanoparticles. The particles were dispersed in toluene.

4. Calculation of the nanoparticle content in superparamagnetic polymer

Atomic absorption spectroscopy (AAS) was applied to determine the magnetite content of the synthesized superparamagnetic polymers. The nanoparticle content of the superparamagnetic polymer was calculated based on the method described by Kokate et al. [1] There are 8 Fe₃O₄ per unit cell. Total Fe and O atoms per unit cell is 24 and 32, respectively. The weight of one unit cell can be calculated using the atomic mass of individual Fe atoms ($55.84/6.02 \times 10^{23} = 9.275 \times 10^{-23}$ g) and O atoms ($16/6.02 \times 10^{23} = 2.3657 \times 10^{-23}$ g). Thus, the weight of one unit cell is equal to 307.6×10^{-23} g. An overview of the numbers involved in the calculation is given in Table S-1.

Table S-1. Calculation of the magnetite content in the synthesized superparamagnetic polymer using AAS.

The mass of magnetic polymer used for AAS [g]	Mass of Fe based on calibration curve [g]	No. of Fe atoms in	No. of unit cells	No. of Fe ₃ O ₄	Moles of Fe ₃ O ₄	Mass of Fe ₃ O ₄ [g]	Fe ₃ O ₄ in sample [wt%]
0.0123	0.0010	1.1e19	4.6e17	3.7×10^8	6.1e-6	0.0014	11

5. BET N₂ adsorption-desorption isotherm for superparamagnetic polymer

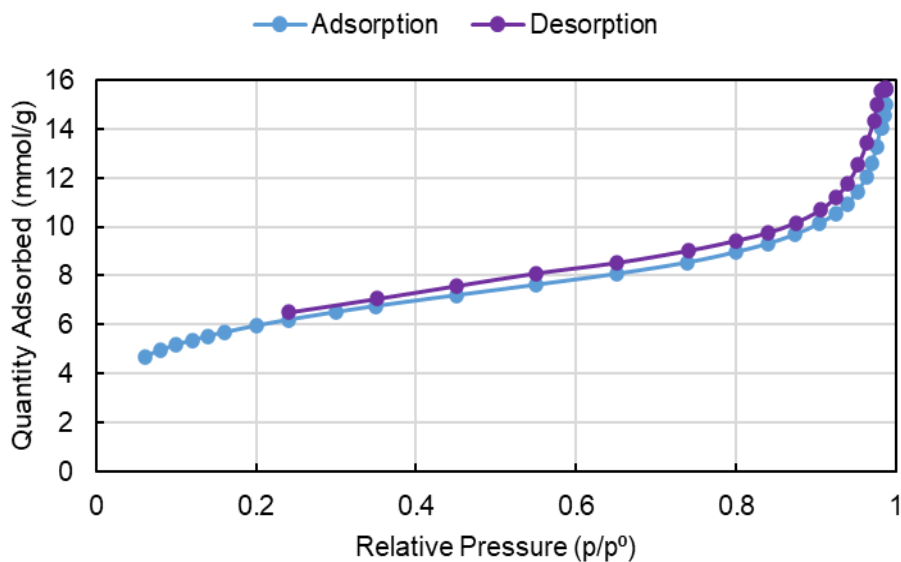


Figure S-3. Nitrogen adsorption-desorption isotherm for the synthesized superparamagnetic polymer. The particles are degassed at 130 °C for 24 h in a nitrogen environment prior to analysis.

6. Water desorption using an alternating magnetic field (AMF); Pictures from the AMF heating step



Figure S-4. The pictures from the AMF heating step to desorb water.

7. Evaporation modeling of water – butyric acid (HBU) mixtures using the NRTL activity coefficient model

The NRTL activity coefficient model was employed to study the binary equilibrium of the water-butyric acid (HBU) system, and the residual concentration profiles during evaporation of dilute HBU in water mixtures.

The following assumptions were applied in the aforementioned model:

1. The liquid contains only water and HBU
2. Water and HBU are physically present in the pores of the adsorbent meaning that the adsorption of HBU on the surface of the pores is not taken into account.
3. 1% of the total loaded liquid evaporates in each equilibrium stage.

7.1. Vapor liquid equilibrium diagrams

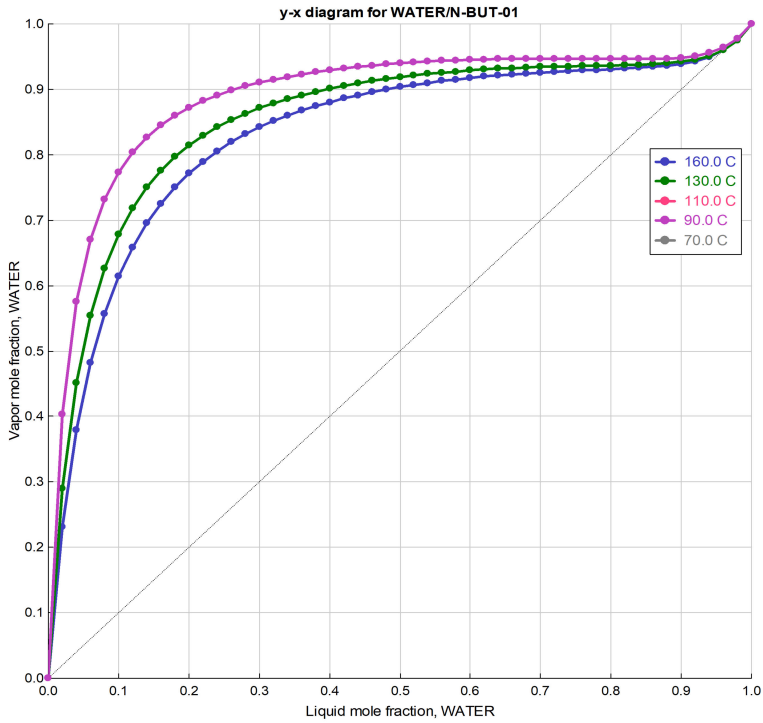


Figure S-5. Vapor-liquid equilibrium (VLE) diagrams for the water-butyric acid system at various applied temperatures.

Table S-2. The applied NRTL binary parameters for the water-butyric acid system.

Component i	Component j	A_{ij}	A_{ji}	B_{ij}	B_{ji}	C_{ij}	Source
Water	HBu	2.6442	-2.1196	90.1091	735.809	0.3	APV110 VLE-IG

7.2. Residual concentration of water during evaporation of dilute HBu in the aqueous mixtures

To study the residual concentration of water and acid during evaporation, we calculated the composition of the residue during the evaporation process, using small steps in which 1% of the total loaded liquid evaporates per step. Figure S-6 and S-7 show the selectivity of water removal as function of the residual concentration of water during evaporation at various applied temperatures for an initial water content higher and lower than 0.96 mole fraction, respectively. The selectivity is defined as the ratio of the activity coefficients multiplied by the ratio of the saturated vapor pressures, according to Eq. (S-2).

$$S = \frac{\gamma_w}{\gamma_{HBu}} \times \frac{P_w^{sat}}{P_{HBu}^{sat}} \quad (S-2)$$

Where S is water selectivity, γ_w activity coefficient of water, γ_{HBu} activity coefficient of HBu, P_w^{sat} vapor pressure of water and P_{HBu}^{sat} vapor pressure of HBu.

At concentrations higher than around 0.96 mole fraction, the selectivity of water is lower than 1 at all applied temperatures, while at concentrations below 0.96 mol fraction water, the selectivity of water is above 1. It indicates that the acid is selectively being removed at high water molar fractions, resulting in an increase in water concentration. For the mixture with initial water content less than 0.96, the opposite trend is observed. Below this water content, as the selectivity of water is higher than 1, water is selectively being evaporated.

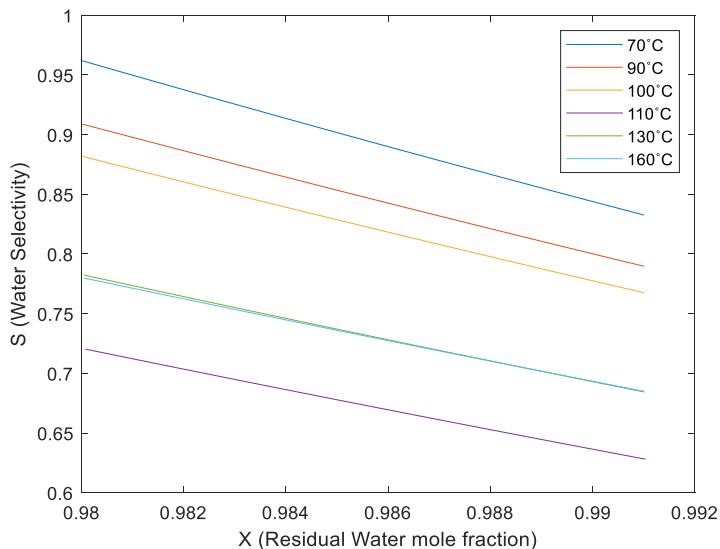


Figure S-6. Selectivity of water removal during evaporation of a highly dilute solution of butyric acid in water with initial water content of 0.98 mole fraction at various applied temperatures.

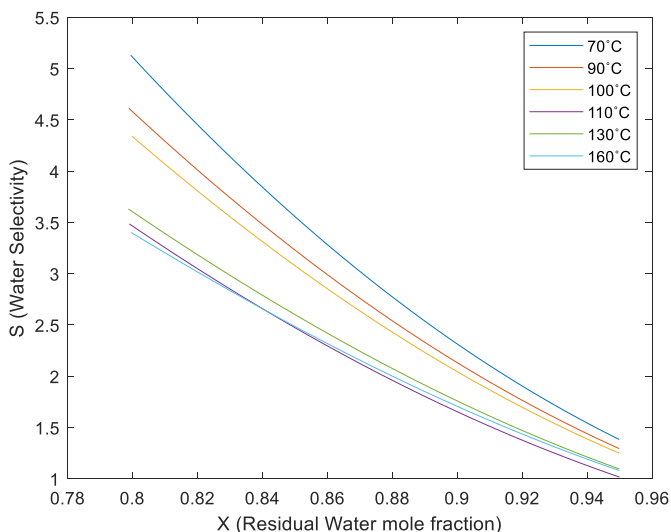


Figure S-7. Selectivity of water removal during evaporation of a highly dilute solution of butyric acid in water with initial water content of 0.95 mole fraction at various applied temperatures.

Appendices

Table S-3. Vapor liquid equilibrium calculation for an aqueous solution of HBU at constant temperatures and various water mole fractions using the NRTL model.

x_{water}	Temp. [°C]	γ_{water}	γ_{HBU}	P_{water}^{sat} [bar]	P_{HBU}^{sat} [bar]	S_{water}	ω	Evaporated water [%]	Evaporated HBU [%]
0.98	100	1	11.90	1.01	1.14	0.89	43	80	85
0.96	100	1	9.46	1.02	0.91	1.12	27	80	74
0.94	100	1.02	7.69	1.03	0.74	1.40	22	80	61
0.9	100	1.05	5.38	1.07	0.52	2.06	19	80	40
0.8	100	1.18	2.83	1.19	0.27	4.39	17	80	19
0.7	100	1.34	1.89	1.36	0.18	7.5	17	80	12
0.6	100	1.54	1.46	1.56	0.14	11.11	17	80	9
0.5	100	1.76	1.24	1.78	0.12	14.90	15	80	8
0.4	100	1.98	1.12	2.01	0.11	18.63	12	80	7
0.3	100	2.22	1.05	2.25	0.10	22.14	9	80	6
0.2	100	2.45	1.02	2.49	0.10	25.33	6	80	6

Table S-4. Vapor liquid equilibrium calculation for an aqueous solution of HBU at various temperatures using the NRTL model.

x_{water}	Temp. [°C]	γ_{water}	γ_{HBU}	P_{water}^{sat} [bar]	P_{HBU}^{sat} [bar]	S_{water}	ω	Evaporated water [%]	Evaporated HBU [%]
0.98	70	1	14.38	0.31	0.32	0.96	47	80	82
0.98	90	1	12.66	0.70	0.77	0.91	45	80	84
0.98	110	1	11.21	1.44	1.66	0.86	42	80	85
0.98	130	1	9.99	2.71	3.29	0.82	40	80	87
0.98	160	1	8.51	6.21	8.09	0.77	38	80	89

Table S-3 presents the modeling results for a system with water mole fraction of 0.98 at different applied temperatures where x is the mole fraction of water in the liquid, γ is the activity coefficient, S is the selectivity and ω is the molar ratio of evaporated water to evaporated HBU. The results indicate that to remove 80% of water content at 70 °C from the mixture which contains 90 wt% water, about 82% of the acid also evaporates.

In the next modelling, the temperature was kept constant while the mole fraction of water differed for the loaded liquid. The results are shown in Table S-4. Overall, it proves that it is impossible to selectively separate water

without losing acid in extremely dilute aqueous mixtures of HBU due to the high activity coefficient of the acid.

8. Calculating the power generated by MNPs in AMF

Table S-5 summarizes the equations used to calculate the power generated by MNPs in AMF which are taken from Suriyanto et al. [2].

Table S-5. The equations used to calculate the heat generation by MNPs in AMF.

Parameter	Equation	Nomenclature
Neel relaxation time τ_N [s]	$\tau_N = \frac{\sqrt{\pi}}{2} \tau_0 \frac{\exp \Gamma}{\Gamma^{1/2}}$	τ_0 time constant [s]
Gamma, Γ	$\Gamma = \frac{KV_M}{k_B T}$	K anisotropy constant [J/m ³] V _M magnetic volume [m ³] k _B Boltzmann constant T absolute temperature [K]
Volumetric power dissipation, P [W/m ³]	$P = \pi \mu_0 \chi_0 H_0^2 f \frac{2\pi f \tau}{1 + (2\pi f \tau)^2}$	μ_0 free space permeability H ₀ magnetic field strength [A/m] f magnetic field frequency [1/s] τ is effective relaxation time [s], $\tau = \tau_N$ (in our case)
Equilibrium susceptibility, χ_0	$\chi_0 = \chi_i \frac{3}{\xi} \left(\coth \xi - \frac{1}{\xi} \right)$	
Initial susceptibility, χ_i	$\chi_i = \frac{\mu_0 \phi M_d^2 V_M}{3 k_B T}$	ϕ nanoparticle volume fraction M _d domain magnetization [A/m]
Langevin parameter, ξ	$\xi = \frac{\mu_0 M_d H_0 V_M}{k_B T}$	
Specific lose power [W/kg]	$SLP = \frac{P}{\rho \phi}$	ρ nanoparticle density [kg/m ³]
Volumetric power dissipation of a polydispersion, \bar{P} [W/m ³]	$\bar{P} = \int_0^\infty P g(D) dD$	D particle diameter (m) LnD ₀ median of lnD
Particle size distribution function g(D)	$g(D) = \frac{1}{\sqrt{2\pi} \sigma D} \exp \left[-\frac{\left(\ln \left(\frac{D}{D_0} \right) \right)^2}{2\sigma^2} \right]$	σ standard deviation of lnD

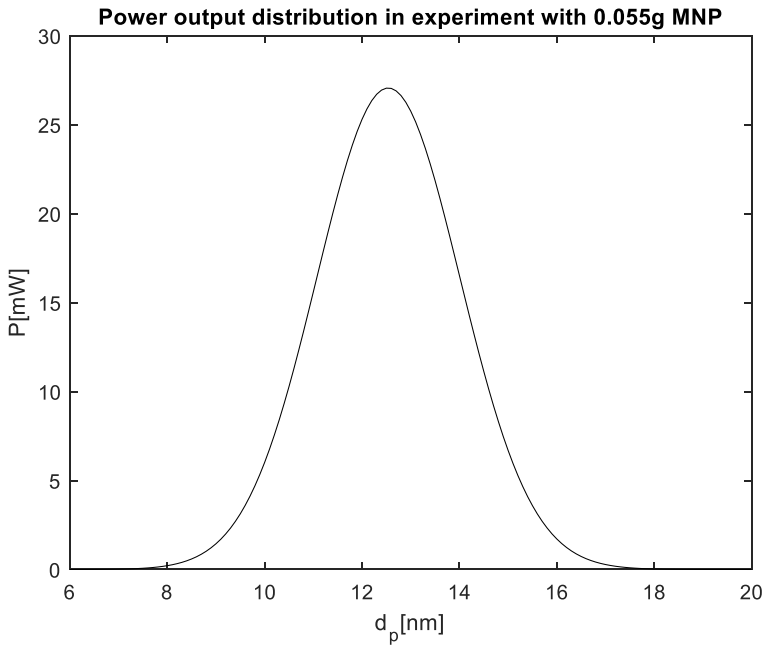


Figure S-8. The experimental power output distribution. The size distribution of MNPs was obtained by TEM analysis. $T = 298$ [K], $K = 30000$ [J/m³], $\rho = 5180$ [kg/m³], $M_d = 4.46e+5$ [A/m], $\phi = 1$, $H_0 = 25$ [mT], $f = 52$ [kHz].

The area of the graph in Figure S-8 is the average produced power in this experiment which is about 100 mW.

9. Thermal gravimetric analysis (TGA) graph of the extracted polymer by 2-MTHF

The TGA graphs of the polymer precipitated by various methods are shown here. The pure PHBV and non-pure PHBV refer to the polymer precipitated by an antisolvent and solvent evaporation, respectively. As can be seen from Figure S-9, there is no residual mass for pure PHBV after ~ 280 °C. Therefore, precipitation by the antisolvent enables the recovery of highly pure PHBV.

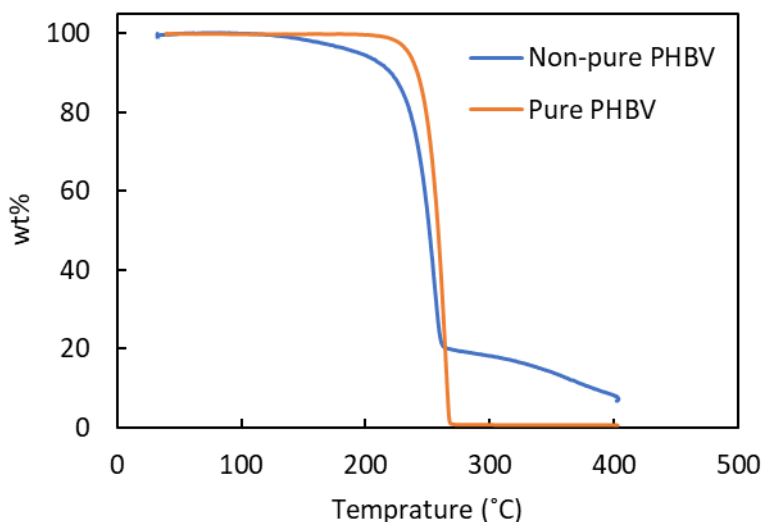


Figure S-9. TGA graph of the PHBV extracted by 2-MTHF (at 80 °C, 1h, 5%[g/mL]) using both *n*-heptane as an antisolvent with a volume ratio of 1:3 at 4 °C for 24h (pure PHBV) and evaporating the solvent to recover the PHBV (non-pure PHBV).

10. Fourier transform infrared (FT-IR) analysis of the extracted polymer by 2-MTHF

The 2-MTHF based extracted PHBV which was either retrieved by solvent evaporation or adding antisolvent was analyzed with FT-IR. As can be seen from Figure S-10, there is no clear peak at around 1536 cm^{-1} for the polymer retrieved by solvent evaporation which is associated with Amide Band I of the cellular protein [3]. However, there is a small peak at around 1650 cm^{-1} only in the spectrum of the polymer which is precipitated by evaporation of the solvent which might be an evidence of cellular proteins being a part of the impurities in the polymer, because the aforementioned peak belongs to the Amide Band II of the cellular proteins.

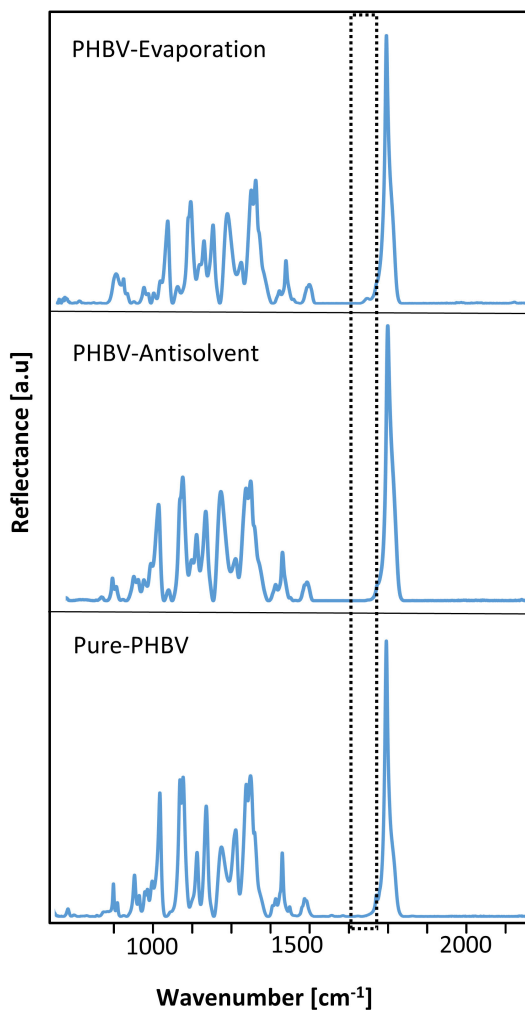


Figure S-10. FT-IR graph of the commercial PHBV (pure PHBV) and the PHBV extracted by 2-MTHF (at 80 °C, 1h, 5%[g/mL]) using both n-heptane as an antisolvent with a volume ratio of 1:3 at 4 °C for 24h (PHBV-Antisolvent) and evaporating the solvent to recover the PHBV (PHBV-Evaporation).

11. Solubility of PHB with high crystallinity in 2-MTHF and Cyrene

PHB is the type of PHA with high crystallinity, limiting its solubility in the solvents. Therefore, we examined the capability of 2-MTHF and cyrene to

Appendices

dissolve a commercial PHB with high crystallinity. The results in Table S-6 indicate that the aforementioned solvents can dissolve a limited amount of the polymer with high crystallinity. However, they are definitely able to dissolve the amorphous MMC based PHBV with low average MW.

Table S-6. Solubility of the PHB with high crystallinity in 2-MTHF and cyrene.

Polymer	MW [kDa]	X _c [%]	Solubility [wt%]	
			2-MTHF 80 °C	Cyrene 120 °C
PHB-Commercial	727	60.8	0.4	0.5
PHBV-extracted from batch 2 by 2-MTHF	122	-	7.1	>7.4 ^a

^a where for 2-MTHF solid residuals were observed, in cyrene we did not observe any solid residuals but ran out of the polymer from the same batch to increase the concentration beyond the reported value.

12. Gc- spectrum of pyrolyzate mixture

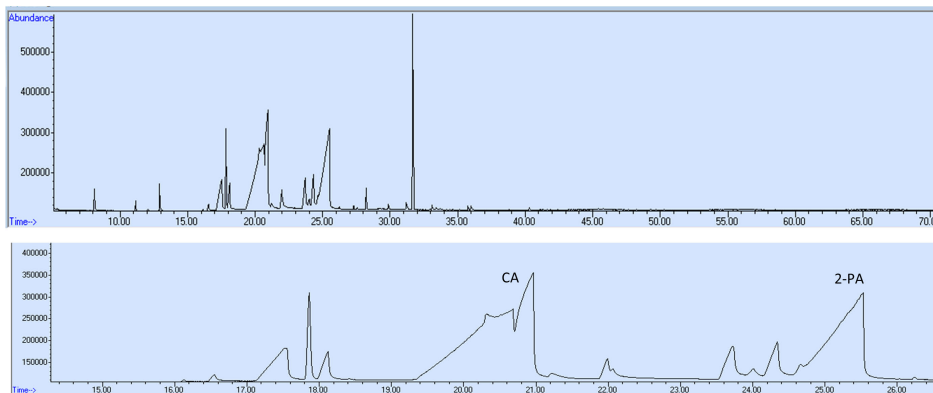


Figure S-11. GC-spectrum of the pyrolyzate mixture obtained by direct pyrolysis of the biomass at 240 °C, 50 mbar and 1h.

13. HPLC spectrum of the pyrolyzate mixture

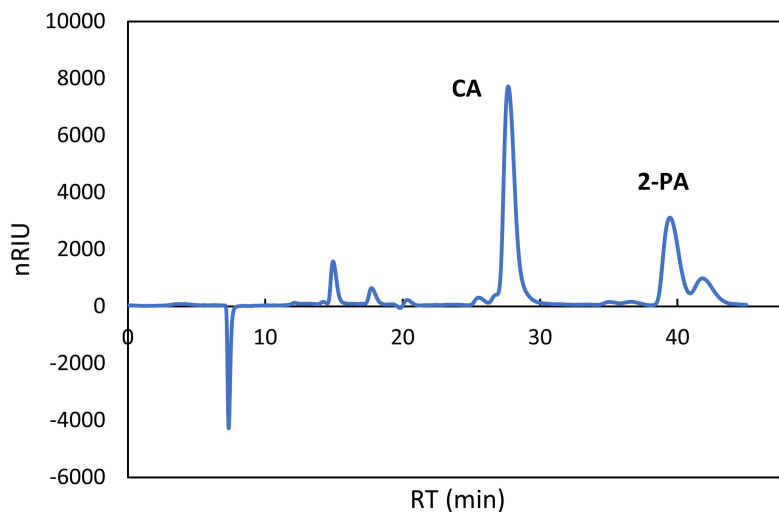


Figure S-12. HPLC spectrum of the pyrolyzate mixture obtained by direct pyrolysis of the biomass at 240 °C, 50 mbar and 1h.

14. Gaussian fit of CA and 2-PA HPLC peaks

As the CA peak in GC analysis was completely overlapped with other side products, HPLC analysis was used to quantify the acids in the pyrolyzate mixture. As shown in Figure S-13 and S-14, the acids peaks in the HPLC analysis are also slightly overlapped with the peaks of the side products. However, the HPLC peaks of the acids are totally symmetric, meaning that a Gaussian fit can be applied to integrate the acid peaks with relatively high accuracy. Therefore, the peaks were fitted with a Gaussian function using OriginPro 2019b.

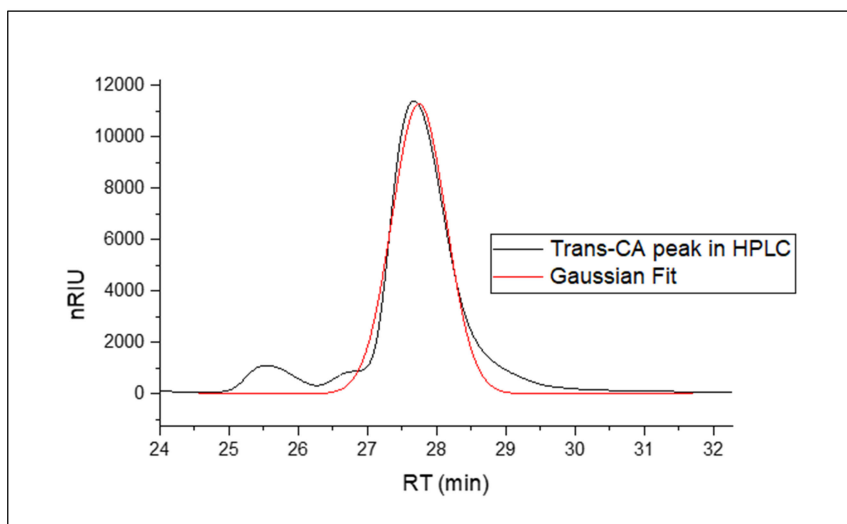


Figure S-13. Gaussian fit of the HPLC peaks for CA in the pyrolyzate mixture obtained by direct pyrolysis of the biomass at 240 °C, 50 mbar and 1h.

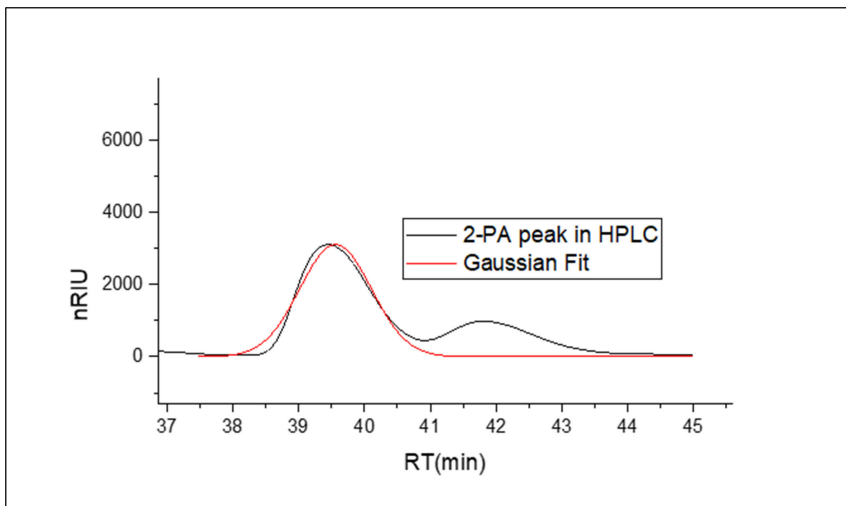


Figure S-14. Gaussian fit of the HPLC peaks for 2-PA in the pyrolyzate mixture obtained by direct pyrolysis of the biomass at 240 °C, 50mbar and 1h.

15. GC-MS spectrum of CA purified by distillation

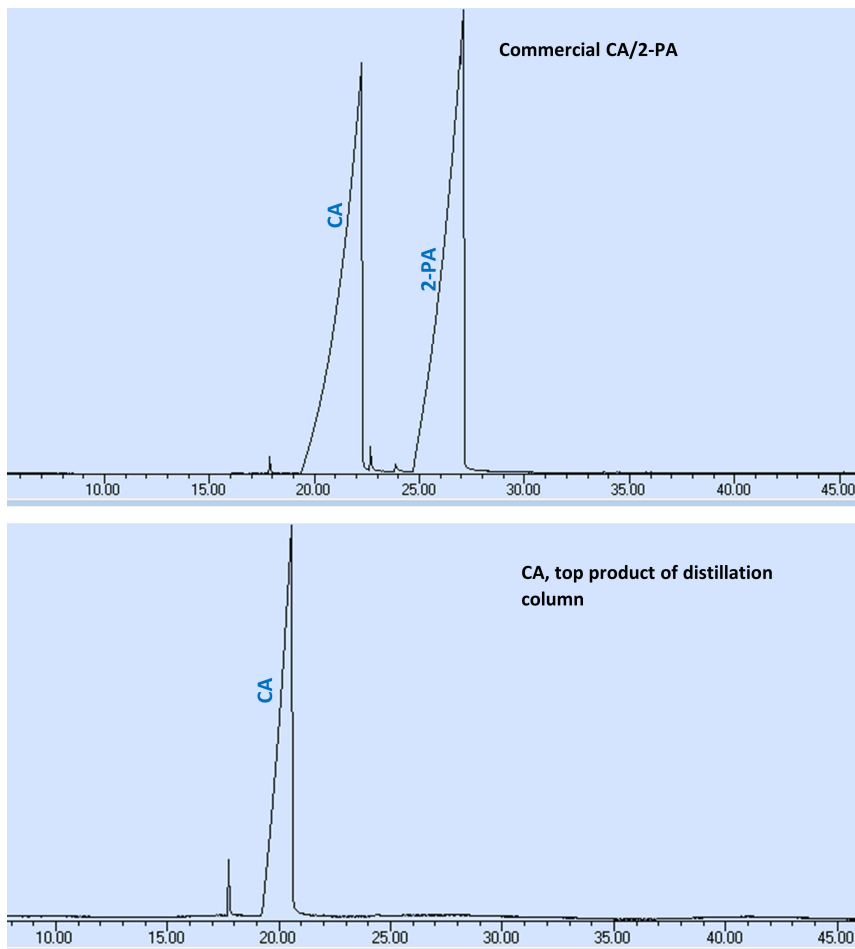


Figure S-15. GC-MS spectrum of CA/2-PA mixture and purified trans-CA by vacuum distillation at 50 mbar, 110 °C.

16. $^1\text{H-NMR}$ spectrum of CA purified by distillation

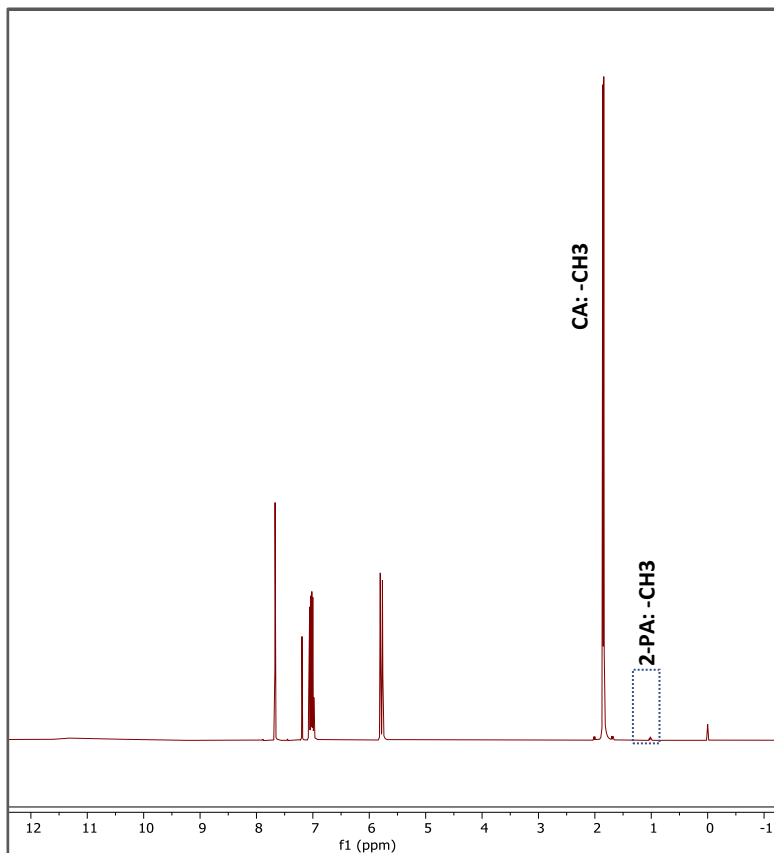


Figure S-16. $^1\text{H-NMR}$ spectrum of CA purified by vacuum distillation at 50 mbar and 110 °C.

17. Calculating dew point for acid mixture in vapor phase, originating from pyrolysis

The vapor phase generated by pyrolysis contains mainly CA and 2-PA. It is extremely diluted by N_2 gas which was used as a carrier gas to

manipulate the mean residence time of the vapor phase in the hot oven-pyrolyzer. The dew point of the vapor phase is calculated as following:

Assumptions:

1. CA is the predominant and most volatile compound in vapor mixture. Therefore, the dew point is calculated for a mixture of CA/N₂ and assuming any condensing CA will be pure CA in the liquid phase, the activity coefficient of CA is set equal to 1.
2. The total pressure is equal to the atmospheric pressure.

Table S-7. The equations used to calculate the dew point of CA/N₂ vapor mixture.

Equations	Formula	Parameters	Units	Ref.
Raoult's law	$y_i P_{tot} = \gamma_i x_i P_i^{sat}$	$\gamma_{CA}=1$	-	
Antoine	$P_i^{sat} = 10^{(A_i - \frac{B_i}{T+C_i})}$	CA: A=8.60269, B=2430.085, C=239.62 N ₂ : A=6.93878, B=330.16, C=277.196	T [°C] P [mmHg]	[4] [5]

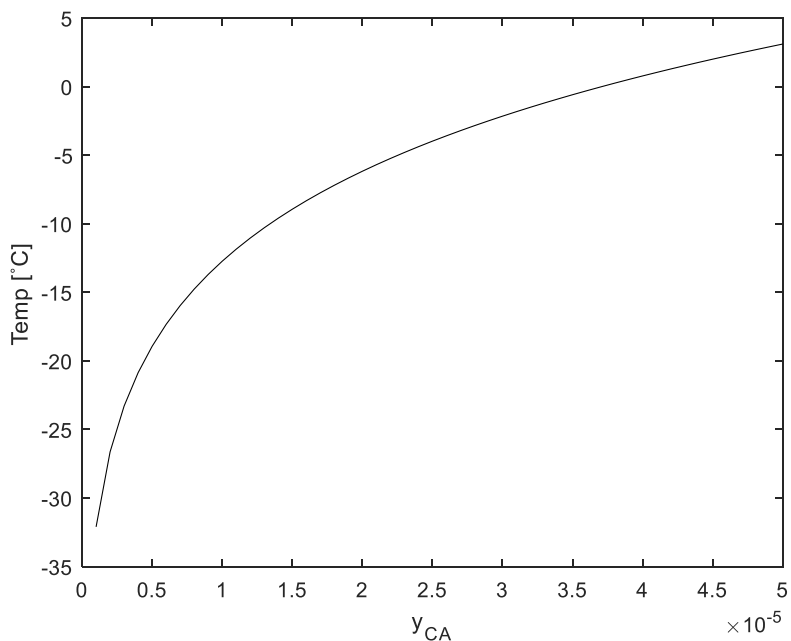


Figure S-17. The dewpoint of CA/N₂ mixture at atmospheric pressure and various composition.

The amount of CA not condensing in the N₂ at -5 °C was calculated using the ideal gas law. At 0.2 L/min, and a mol fraction CA of 2.5×10^{-5} a CA outflow is realized of 2.24×10^{-7} mol/min, which is 1.16×10^{-3} g/h. this corresponds to 0.085% of the potential CA that can be obtained (80 wt% of the 1.7g in the feed).

References

- [1] M. Kokate; K. Garadkar; A. Gole, One pot synthesis of magnetite–silica nanocomposites: applications as tags, entrapment matrix and in water purification. *Journal of Materials Chemistry A*. **2013**, *1*, 2022-2029.
- [2] Suriyanto; E. Ng; D.K. Srinivasan, Physical mechanism and modeling of heat generation and transfer in magnetic fluid hyperthermia through Néelian and Brownian relaxation: a review. *BioMedical Engineering OnLine*. **2017**, *16*,
- [3] M.V. Arcos-Hernandez; N. Gurieff; S. Pratt; P. Magnusson; A. Werker; A. Vargas; P. Lant, Rapid quantification of intracellular PHA using infrared spectroscopy: An application in mixed cultures. *Journal of Biotechnology*. **2010**, *150*, 372-379.
- [4] D.R. Stull, Vapor Pressure of Pure Substances. Organic and Inorganic Compounds. *Industrial & Engineering Chemistry*. **1947**, *39*, 517-540.
- [5] NIST Chemistry Webbook Available online: <https://webbook.nist.gov/cgi/cbook.cgi?ID=C7727379&Mask=4&Type=ANTOINE&Plot=on#> (accessed on 09-12-2022).

List of publications

V. Elhami; N. van de Beek; L. Wang; S.J. Picken; J. Tamis; J.A.B. Sousa; M.A. Hempenius; B. Schuur, Extraction of low molecular weight polyhydroxyalkanoates from mixed microbial cultures using bio-based solvents. *Separation and Purification Technology*. **2022**, 299, 121773.

V. Elhami; M.A. Hempenius; B. Schuur, Crotonic acid production by pyrolysis and vapor fractionation of mixed microbial culture-based Poly(3-hydroxybutyrate-co-3-hydroxyvalerate). *Industrial and Engineering Chemistry Research*. **2022**, 62, 916-923.

V. Elhami; E.C. Antunes; H. Temmink; B. Schuur, Recovery Techniques Enabling Circular Chemistry from Wastewater. *Molecules*. **2022**, 27, 1389.

V. Elhami; L.M. Neuendorf; T. Kock; N. Kockmann; B. Schuur, Separation of crotonic acid and 2-pentenoic acid obtained by pyrolysis of bio-based polyhydroxyalkanoates using a spinning band distillation column. *Sustainable Chemistry and Engineering*, **2023**.

In preparation

V. Elhami; M.A. Hempenius; G.J. Vancso; E.J.G. Krooshoop; L. Alic; X. Qian; M. Jebur; R. Wickramasinghe; B. Schuur, Recovery of Dilute (Bio-Based) Volatile Fatty Acids by Adsorption with Magnetic Hyperthermal Swing Desorption. **2023**.

V. Elhami; S. Ronka; B. Schuur, Methacrylonitrile-based Adsorbents for Recovery of VFAs from Fermentation Broth. **2023**.

Publications prior to PhD thesis:

V. Elhami; A. Karimi; M. Aghbolaghy, Preparation of heterogeneous bio-Fenton catalyst for decolorization of Malachite green. *Journal of the Taiwan Institute of Chemical Engineers*, **2015**, 15, 154-159,

H. R. Khaledian; P. Zolfaghari; **V. Elhami**; M. Aghbolaghy; S. Khorram; A. Khataee; A. Karimi, Modification of Immobilized Titanium Dioxide Nanostructures by Argon Plasma for Photocatalytic Removal of Organic Dyes. *Molecules*, **2019**, 24, 383.

Acknowledgement

Acknowledgement

Almost five years ago, I came to The Netherlands and started a whole new journey of my life in Enschede. I believe that this fantastic journey made me stronger, wiser and more knowledgeable. I have developed so much during the years that I worked at university of Twente. I would like to express my gratitude to all the people who accompanied and supported me through out the years of my PhD.

First I would like to thank **Boelo** for giving me the chance to start this adventurous period. I still remember our first meet in Turkey where you interviewed me. It was a great and successful trip for me as I passed the interview very well. You are a perfect supervisor for a PhD student due to your incredible supervision skills and your knowledge in your field. I was honored to have you also as a “witness” in my wedding on behalf of my family who could not make it. I appreciate all you have done for me so far.

I would like to express my gratitude to the rest of my graduation committee members: **Mark**, thanks a lot for all the fruitful discussions about my project, especially about the polymers. **João** and **Jelmer**, I do appreciate you for helping me to understand the biological fundamentals about how a bacteria can produce a polymer. **Julius**, I was honored to have you as my co-promoter and receive your knowledgeable feedbacks on polymers in my project. **Ranil**, I received a lot help and advice from you and your group about magnetic heating. Thank you all for helping me to understand the fundamental physics on how a magnetic nanoparticle can dissipate heat in an alternating magnetic field. **Meik** and **Rob**, it is my honor to have you in my graduation committee. Thank you for your effort in reviewing this thesis. **Norbert**, Thank you so much for giving us an opportunity to use your innovative spinning band

Acknowledgement

distillation column in your group. It is also a great honor to have you being part of my defense committee.

Sascha, your intelligence in Chemical Engineering is incredible. I really enjoyed supervising the students with you in Lab course. You are also a great company for a trip, I realized it in our SPT group trip 2022. **Wim**, I learnt a lot about CO₂ capturing from you and your team during our group meetings. I was really happy to hear your pilot plants are functioning in various industries. Because the climate change and environmental issues are my concerns as well. That is why I joined SPT to learn how to deal with these challenges. **Jean-Paul**, I delighted to listen to your discussions during our SPT group meeting. After every discussion, I realized that combing the chemistry fundamentals with process engineering skills can help somebody to be a knowledgeable and powerful engineer. I would like to learn chemistry as much as I can along my engineering journey. **Pilar**, although you are bombarded with PhD students these days, you take a good care about group activities such a group trip and New people diner. Thanks a lot for making those fun moments for us and I wish you lots of success in plastic recycling challenges. **Louis**, thanks for your nice supervision and discussions in our group meetings. **Edwin**, I just received your invitation for your inaugural lecture while I was writing this. As I can not attend, I would like to congratulate you here and wish you the best in your process optimization journey.

I would like to thank our staff members whose support is essential to get every project done. **Yvonne**, since I started my PhD, there was too many new systems at UT every year such as HoraFinita, myHR, Unit4 and etc. Thanks for helping me on those moments when I was lost in these applications. **Erna**, I

Acknowledgement

definitely appreciate all your help to solve my analysis problems. I needed various analysis equipment for every part of my broad project. We also had a great collaboration on supervision an ROC student in which you taught me about Dutch Education System. Special thank to our skillful technicians **Benno, Ronald, Johan, Raymond** who easily turn our ideas into a functioning set-up. **Benno**, unfortunately I could not see you during the last months of my PhD. Since you had a serious car accident. I wish you a good recovery and hope to see you in my defense.

Mahsa and **Romolo**, thanks for being my paranymphs. **Mahsa**, you were my paranymph in my wedding as well. I could not have any of my family member there. But you were with me all the time like a sister. Many many thanks for all your support. **Romolo**, you have changed the atmosphere of the group significantly. In my opinion, it has become more friendly and fun group, since you have joined. Thank you!

Sometimes, we complained about our PhD office as it is too busy and has a regular malfunction in its air ventilation system. But I think we should also not underestimate the impact of its “gezellig” atmosphere on our work. I had also so much fun with all my colleagues, working together in that office. **Tim, Michel, Shahab, Eline, Maryam, An, Mario, Helda, Helena, Evelyn, Abhinav, Yordi, Jasper, Peter, Albertus, Hilbert, Kim, Dwiputra, Jayaram, Sterre, Enrico, DooLi, Christian** and **Rick**, thanks for the friendly working atmosphere and our endless discussions during lunch breaks about every subject from traditional dishes of our home countries to semi-political topics.

I would like to also thank my former colleagues with whom I started my PhD journey. **Thomas**, I was supposed to follow up Ehsan’s work. But he was

Acknowledgement

already gone. You helped me how to work with his adsorption set-up and taught me general work regulations in Meander lab. Thank you for all your support mainly in the beginning of my PhD when I definitely needed a hand. **Angelo**, Thanks for all the Swiss chocolates which you brought for me. It took almost a year for me to finish 3kg chocolates, of course with a bit help from Dion. **Tessa**, you analyzed too many TGA samples for me, I do appreciate your help. **Tomas, Juraj, Lisette, Varsha, Surika, Martijn, Thimo, Pushkar, Ehsan, Rick** and **Urmi**, I had a great time with you guys in the NPS, Christmas market in Dortmund and in the PhD defense parties. Thank you guys for all the funs which we had together.

I would like to also thank all my students whose work directly or indirectly contributed in this project. **Koen, Andrea, Frank, Gabriela, Harald, Kuno, Marjolein, Noor, Peter, Sander** and **Ali**, thank you all for your hard work. I was happy to receive these many student with various backgrounds and personalities to supervise them through their assignments. It helped me to improve not only my scientific skills but also my supervision and communication skills. I hope you guys had also nice time in collaborating with me.

Of course, a broad project requires a lot of help from various groups. **Lejla**, I admit that without your support, I would not be able to properly finalize the magnetic heating part of this project. Thank you for your kind help. **Erick**, it is incredible how you make those magnetic devices in magnetic detection and imaging department. Many thanks for designing alternating magnetic field set-up for my project. **Giorgos**, thanks for all TGA and DSC analysis which we ran in your group. **Cindy**, thank you for helping me with DLS and BET analysis. **Laura and Tobias**, I really enjoyed collaborating with you on the last

Acknowledgement

part of my project where I used the spinning band distillation column in Technical University Dortmund. Thanks for your help!

I would like to thank the jochies. **Dennis, Rolf, Maria, Finn, Devi, Raoul, David, Edo, Lionel** and **Jan Niklas**, we had sometimes nice social activities together in the weekend which helped me to be refreshed for the next week. You all attended our wedding and made a fantastic night for us. We will never forgot it. Thank you guys for the nice moments that we had so far and definitely we will have more fun activities again.

Although I am thousands kilometers far from my family, thank to internet and networking. The impact of the virtual help which I got from my family during my PhD was incredible. I admit it was one of the crucial factors to push me forward and keep me on the right track. I would like to thank **my parents** not only for their virtual helps but also for giving me full freedom and letting me follow my wishes in abroad which is still not accepted in every Iranian family. Especial thank to my lovely **sisters** and **brothers** who fully supported me in every situation.

I admit I was lucky to find a nice family in law here where I am far from my family. **Sandra** and **Theo**, you are the best parents in law that I ever wished to have. Thanks for all the love, supports and sympathies which you have given me so far. **Carmen** and **Paul**, thank you for all the fun and “gezellig” time that we had so far.

Dion, You did your best to both scientifically and emotionally support me during my PhD which overlapped with lots of issues in my home country, resulting in hard moments for me. Thanks a lot for all your support. I admit the life style of an engineering couple is much different than I thought. I love

Acknowledgement

our endless scientific and engineering discussions about every thing in our daily routine life, from eddy currents in induction stoves to mechanical issues in our cars, hahaha. BTW, thanks for all the nice foods that you cooked to cheer me up after every frustrating day. I love you so much!